EFFECT OF ANGLE OF INCLINATION AND OF CROSSFLOW ON FLOW, HEAT AND MASS TRANSFER FOR A LAMINAR IMPINGING SLOT JET

by

© Jean-Paul JAUSSAUD

A thesis submitted to the
Faculty of Graduate Studies and Research
of McGill University
in partial fulfilment of the requirements for the
degree of Master of Engineering

Department of Chemical Engineering
McGill University
Montreal
Quebec, Canada

June, 1979

ABSTRACT

The influence of angle of impingement and of presence of a crossflow on the flow, heat and mass transfer of a laminar semi-confined slot jet impinging on an isothermal wet surface was studied numerically. The digital computer simulation model was obtained by solving the governing Navier Stokes equations in their primitive form (velocity and pressure) together with the continuity, energy and species equations using a hybrid upwind and central finite difference scheme based on the control volume integration approach. Fluid property variations with both temperature and composition were taken into account.

The parameters studied include nozzle-to-plate spacing, effect of the presence of a crossflow, ratio of the Reynolds numbers of the crossflow and the jet flow and angle of impingement.

The presence of a crossflow was found to reduce the stagnation point and average heat and mass transfer rates below what would be expected if crossflow were not present. For moderate crossflow magnitude (with respect to the jet) the heat and mass transfer rates on the plate are those of an impinging jet weakened by the crossflow, while for large values of the crossflow magnitude they are those of channel flows along a plate. Impingement exists in the former case but not in the latter. For a given crossflow magnitude and a given nozzle-to-plate spacing there exists an optimum angle (directed slightly against the crossflow direction) for which the heat and mass transfer rates are maximum.

RÉSUMÉ

On a etudié numériquement l'influence de l'angle d'inclinaison et de la présence d'un vent transversal sur les caractéristiques de l'écoulement et des transferts de chaleur et de masse d'un jet d'air laminaire semi-confiné issu d'une buse de section rectangulaire et impactant sur une surface humide maintenue à temperature constante. La simulation du problème sur l'ordinateur fut obtenue en résolvant simultanément les équations de Navier Stokes sous leur forme primitive (vitesse et pression) et les équations de conservation de la masse, de l'énergie et des espèces, tout en tenant compte des modifications des propriétés physiques du fluide dûes aux variations de sa temperature et de sa composition (fraction de vapeur d'eau).

L'étude a porté sur les paramètres suivants: espacement entre la sortie de la buse et la plaque d'impact, effet de la présence d'un vent transversal, rapport des nombres de Reynolds respectifs de l'écoulement transversal et du jet, et angle d'inclinaison de la buse.

Pour les nombreux cas étudiés on a analysé les champs de vitesse et la distribution de la pression, du cisaillement, du transfert de chaleur (nombre de Nusselt) et du transfert de masse (nombre de Sherwood) le long de la plaque.

Les resultats obtenus confirment que la presence d'un vent transversal réduit les taux locaux et moyens de transfert de masse et de chaleur du jet impactant. Pour de faibles écoulements transversaux, les coefficients de transfert sur la plaque sont ceux d'un jet impactant affaibli et dévié; pour de forts écoulements transversaux on obtient par contre des coefficients de transfert du type de ceux que produit un écoulement d'air parallèle à une plaque. Le jet impacte effectivement sur la plaque dans le premier cas, alors qu'il est emporté par le vent transversal et n'impacte pas dans le second.

L'étude de l'influence de l'inclinaison de la buse a montré que pour un écartement donné de cette buse vis-a-vis de la plaque et pour un vent transversal donné, il éxiste un angle d'inclinaison optimum pour lequel les coefficients de transfert de masse et de chaleur sont maximums.

ACKNOWLEDGEMENTS

The author wishes to express his sincere appreciation and gratitude to:

Professor W.J.M. Douglas for his valuable advice and support and for proof-reading this thesis.

Professor A.S. Mujumdar for his helpful suggestions and advice.

Mes remerciements vont aussi au Gouvernement du Québec pour son aide financière apportée sous la forme d'une bourse France-Québec.

Je remercie aussi spécialement Mademoiselle Nancy Oliver pour avoir dactilographié cette thèse dans des délais remarquablement brefs.

TABLE OF CONTENTS

LIST OF FIGURES

LIST OF TABLES

NOMENCLATURE

A	control volume cross sectional area
a_e, a_w, a_n, a_s	see Equation (4.10)
A_p	see Equation (4.19)
C_e, C_w, C_n, C_s	convective flux, ρuA; see Equation (4.8)
C_f	skin friction coefficient, $\tau/\frac{1}{2}\rho_j U^2$
C_p	specific heat capacity of fluid mixture at constant pressure, J/kg.°K
D	jet nozzle width, m
D_e, D_w, D_n, D_s	diffusive flux, $\Gamma A/\Delta x$; see Equation (4.9)
DU_p, DV_p	gradient of velocity w.r.t. pressure change from iteration to iteration; see Equations (4.21) and (4.22)
F	flux at control volume boundaries; see Equations (4.1) to(4.5)
FACTOR	residual normalization factor
g	gravitational acceleration, 9.807 m/s^2
h	heat transfer coefficient, $Q/(T_j - T_p)$, W/m^2.°K
H	nozzle-to-impingement-plate spacing, m
J_i	molar flux of i relative to mass average velocity, mole/m^2.s
j_i	mass flux of i relative to mass average velocity, kg/m^2.s
k	mass transfer coefficient, $W(1-m_p)/(m_j-m_p)$, kg/m^{2}s
l	space coordinate, see Figure 1.1
L	nozzle-to-plate spacing measured on inclined jet axis, H/cos θ, see Figure 2.1
m	mass fraction of water vapour, mass of water vapour/ total mass of mixture
$\underset{\sim}{M}$	ratio of crossflow volumetric flow rate to jet volumetric flow rate; also equal to the ratio of the corresponding mass flow rates, and to the ratio of the Reynolds numbers of the crossflow and the jet.

m_j	mass fraction of water vapour at jet nozzle exit.
m_p	mass fraction of water vapour along impingement plate.
MW	molecular weight
$\overline{MW}$	molecular weight of fluid mixture; $1/\overline{MW} = M_A/MW_A + M_B/MW_B$, kg/kilomole
n_A, n_B	mass fluxes of species A and B respectively along impingement plate, kg./m^2.s
NI,NJ	size of grid mesh in x- and y-direction respectively.
Nu	Nusselt number, hD/λ_j
P	pressure, N/m^2
P_{sat}	saturated vapour pressure of water vapour, N/m^2
ΔP	difference between the local and ambient pressure. In Chapter 4: pressure correction term from iteration to iteration, $P = P' + \Delta P$
Pe	local Peclet number $\rho u \Delta x/\Gamma$
Pr	Prandtl number, $C_p \mu/\lambda$
Q	heat flux along impingement plate in positive x-direction, W/m^2
q	energy flux relative to mass average velocity, J/m^2.s
R	half width of nozzle, D/2, m
r	space coordinate; see Figure 1.1
Re	Reynolds number, $\rho_j UD/\mu_j$
RESID	normalized residual; see Equation (5.6)
S_ϕ	source term
$S_{\phi,vol}$	integral source term; see Table 4.1
S_{false}	false source term; see Equation (4.19)
Sc	Schmidt number, $\mu/(\rho\delta)$
Sh	Sherwood number, $kD/\delta_j\rho_j$

St	Stanton number, $h/(\rho_j C_{p_j} \bar{U})$
Su	component of linearized source term; see Equation (4.20)
T	thermodynamic temperature, °K
U	velocity vector
$\bar{U}$	average velocity at the exit of the jet nozzle, m/s
u	velocity component in the x-direction, m/s
u_{suc}	suction velocity along impingement plate in positive x-direction, m/s
URF	under-relaxation factor; see Section 5.5.1
$\bar{V}$	average velocity at entry of crossflow, m/s
v	velocity component in the y-direction
V	volume of control volume, 1.0 ūv
W	mass flux of water vapour along impingement plate in positive x-direction, $kg/m^2.s$
x_A	molar concentration of water vapour, $mole/m^2.s$
x	space coordinate, m; see Figure 1.1
y	space coordinate, m; see Figure 1.1
y_o	coordinate of jet centerline on exit plane.
$\Delta x, \Delta y, \Delta l$	size of control volume; see Figure 4.1
y_R	half width of nozzle aperture, $R/\cos\theta$

Greek letters

Γ	exchange coefficient; see Table 3.1
δ	mass diffusivity of fluid mixture, m^2/s
λ	thermal conductivity of fluid mixture, W/m.°K

μ	dynamic viscosity of fluid mixture, kg/m.s
ρ	mass density of fluid mixture, kg/m^3
τ	shear stress along impingement plate, $\mu \partial v/\partial y\|_p$, N/m^2
ϕ	variable; see Table 3.1
ϕ_{AB}	weighting factor for fluid properties
θ	angle of impingement (inclination of nozzle)

Subscripts

A	water vapour
B	dry air
j	at nozzle exit
p	along impingement plate
e,w,n,s	east, west, north and south side boundaries of control volume; see Figures (4.1) and (4.2)
E,W,N,S	see Figures (4.1) and (4.2)
P	center of control volume

CHAPTER 1

INTRODUCTION

Impinging air jets of various sizes and geometrical configurations are widely used in a large number of industrial processes involving heating, cooling, and drying of surfaces because of the high heat and mass transfer rates they can yield. Applications include annealing of foil, tempering and toughening of glass, manufacturing of prestressed automobile windshields, cooling of leading edges of turbine blades and electronic components. In the paper industry, for example, some typical applications are: drying of tissue on Yankee dryers, drying of veneer with hot air or superheated steam, drying of newsprint at relatively low moisture content by combining impinging jets with a suction applied through the wet web.

Extensive work has been previously done by many researchers to investigate flow configuration and heat/mass transfer under round and slot jets impinging on permeable or impermeable surfaces. For a long time this work has been concerned with the study of only one single transport process (i.e. either heat or mass transfer), but studies reporting simultaneous heat and mass transfer results have been published recently.

One of the important variables, the effect of which has not yet been studied in the case of a semi-confined laminar impinging jet involving both heat and mass transfer is the angle of impingement. It may be noted that industrial devices seldom entail a single jet, but rather comprise one or several rows of jets with the consequence that each jet impinges in a crossflow created by the neighbouring ones.

The present study is concerned with simultaneous heat and mass transfer under a semi-confined slot jet impinging at a range of angles on an impermeable plate over which a crossflow is also imposed. By "semi-confined" it is intended that the jet is partially confined by a surface parallel to the impingement plate and situated at the level of the nozzle exit.

The computational method presented by Gosman et al. (G7) is employed to develop a digital computer simulation model for a steady, laminar, relatively dry and hot slot air jet discharging into a cross-flowing air stream and impinging on a cooler wet flat plate. The configuration is sketched in Figure 1.1. The simulation is obtained by solving iteratively the governing equations of motion in their primitive form along with the energy and conservation of species equations using a hybrid central and upwind differencing scheme based on the control volume integration approach. A non-uniform grid is imposed on the flow field and a line-by-line method is used to generate a tri-diagonal matrix which is then solved numerically. The entire domain is swept for each variable at a time and then iterated over all variables.

A brief review of the related literature is given in Chapter 2.

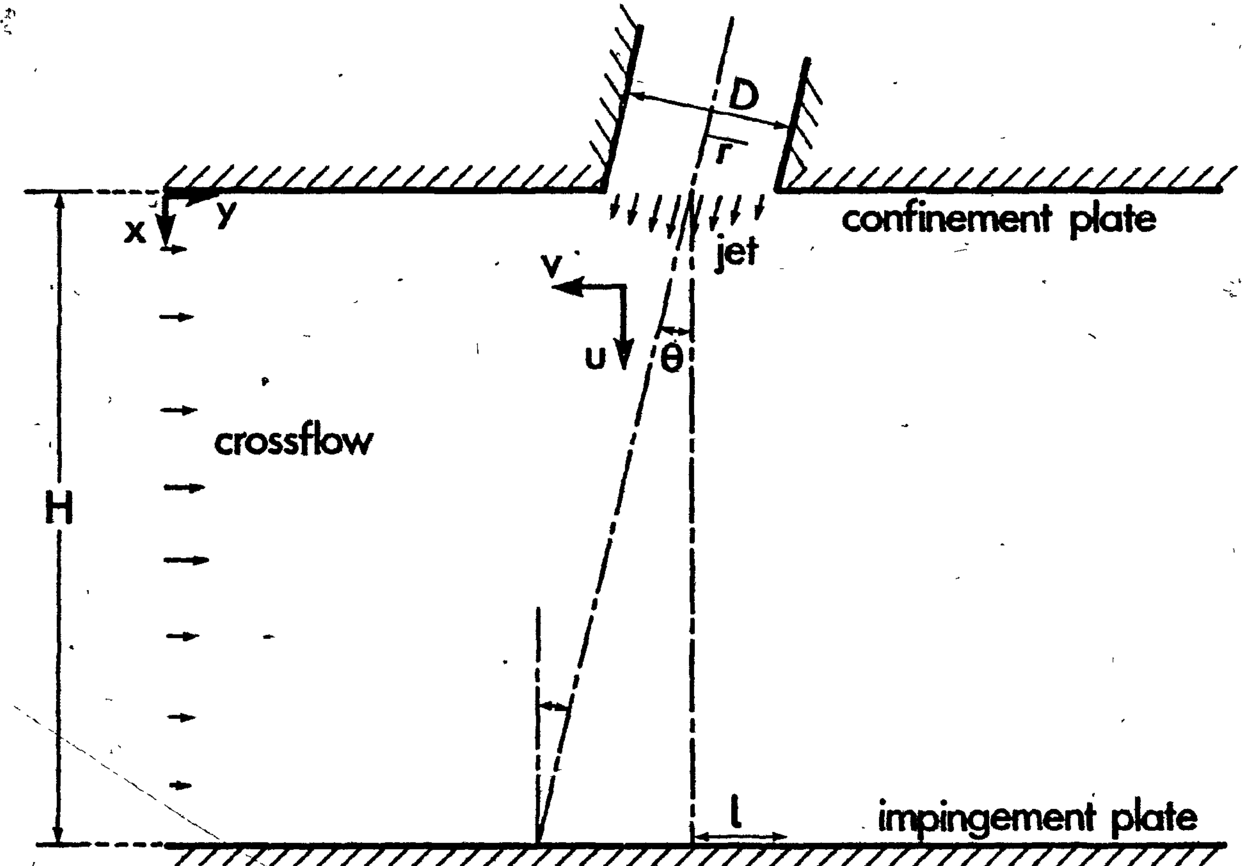

Figure 1.1 : Geometrical configuration of the jet and crossflow system.

The theoretical development which leads to the finite difference equations is presented in Chapter 3 while the numerical and computational procedures are discussed in Chapters 4 and 5 respectively. The numerical results for flow, heat and mass transfer characteristics are discussed in Chapter 6. The parameters which have been studied include nozzle-to-plate spacing, effect of the presence of crossflow (by comparison with cases without crossflow), ratio of the crossflow mass flow-rate to the jet mass flow-rate, and angle of impingement for inclined jets impinging in the crossflow direction (downstream) as well as for jets impinging against the crossflow direction (upstream).

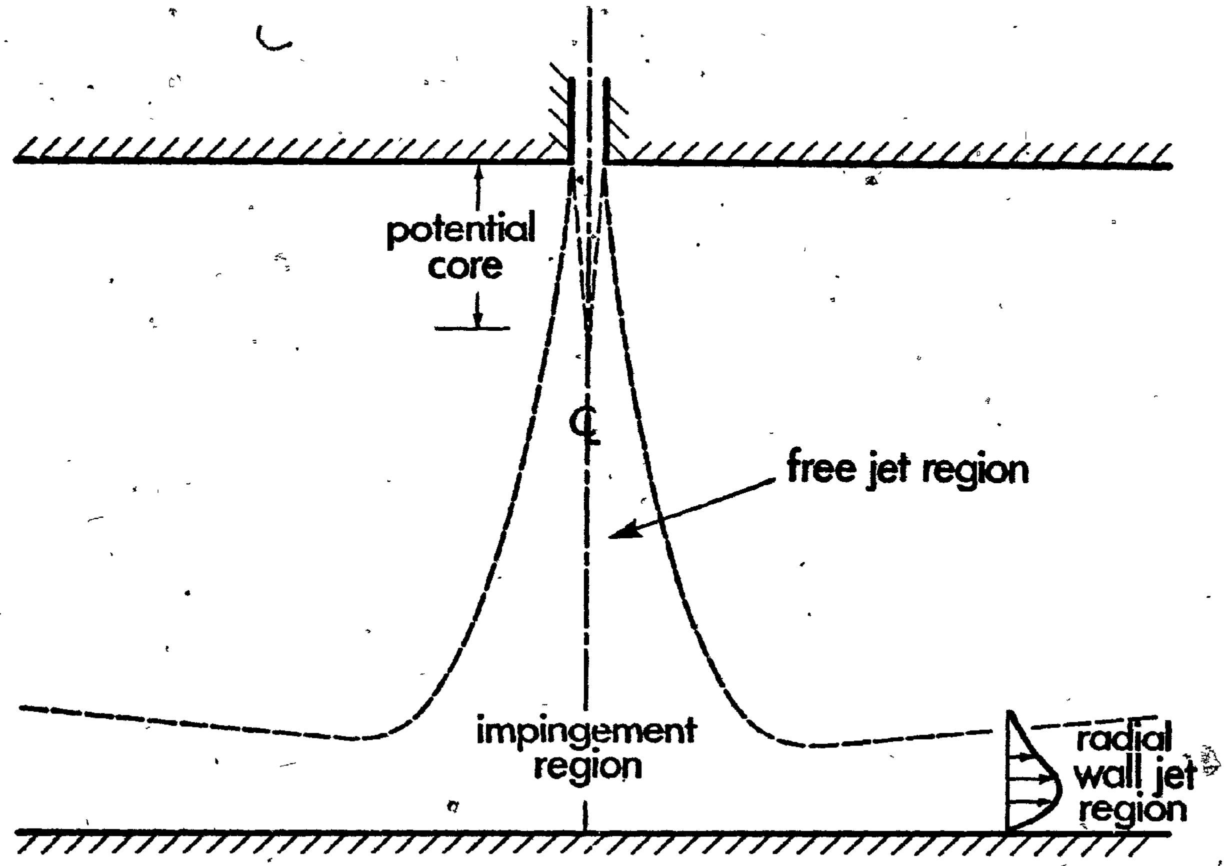

Figure 1.2 : Flow characteristics of an impinging jet.

CHAPTER 2

REVIEW OF RELATED LITERATURE

2.1 INTRODUCTION

Many publications have appeared in recent years on the fluid mechanics and heat and mass transfer aspects of both laminar and turbulent impingement flows. These studies, both numerical and experimental, were concerned with various types of jet velocity profiles and of confinement configurations. A number of publications have also examined the flow and heat transfer characteristics of multiple impinging jets. Parameters such as nozzle-to-plate spacing, presence of confining walls, motion of the impingement surface, temperature dependent properties, presence of swirl, and application of suction or blowing have been considered. A few investigators have studied the effect of non-normal impingement, but they all were only concerned with turbulent flows, and no previous data or results have been found for the case of a laminar impinging jet discharging in a crossflow at various angles. In view of the large number of parameters governing flow, heat and mass transfer under impinging jets, it is not surprising that a serious disparity exists between the results and correlations of various workers. Obot (01) in particular has analyzed the extent of disagreement. A number of extensive reviews on various aspects of impinging jets have appeared in recent years (G1, M1, M3).

The reader is referred to these review articles for general knowledge and comprehension of the phenomena related to impinging jets. Only the more relevant references of direct interest to this study will be mentioned in the present thesis.

It may be noted that most of the numerous publications in impingement transport are concerned with axisymetric round jets. The case of slot jets has been studied to a lesser extent, but, although the behaviours of these two types of jets are not quite identical, the trends of the transport phenomena and the influence of many parameters are similar; consequently, work on round jets as well as slot jets will be cited here.

2.2 IMPINGING JETS

2.2.1 Flow Characteristics

The flow patterns of jets impinging on a solid surface have been discussed by many investigators (G1, M1, D1); four distinct flow regions can be characterized. These are shown on Figure 1.2 and are described as follows:

(1) Region I is the region of flow establishment. It extends from the nozzle exit to the apex of the potential core. The so-called potential core is the central portion of the flow in which velocity remains equal to nozzle exit velocity.

(2) Region II is a region of established flow in the direction of the jet beyond the peak of the potential core; it is characterized by a diminution of the centerline jet velocity and by a spreading of the jet in the transverse direction. This region is often refered to as the free jet region.

(3) Region III is the region where the jet is deflected from the axial

direction due to the presence of the impingement surface. It is usually called the impingement flow region.

(4) Region IV is the region of lateral flow along the impingement surface and outside the stagnation zone. This region is known as the wall jet region, where the flow increases in thickness as the boundary layer builds up along the solid surface.

The preceding characterization of flow regions is generally valid for an unconfined jet. In the present study, as noted in Chapter 1, the flow is confined between two parallel plates (the impingement surface and the upper confining plate of equal size), and this induces a region of recirculating flow between the confining surfaces (H3, S2, V2). Most industrial applications of impinging jets for heating, cooling or drying do involve the presence of a confining wall of some kind.

Of fundamental importance in the study of impinging jets (or any jet) is the distinction between laminar and turbulent jets. For a round jet, for example, Vickers (V1) states that the critical Reynolds number (based on nozzle diameter and nozzle exit velocity) which distinguishes laminar jet flows from turbulent jet flows is about 1000. On the other hand, McNaughton reports four jet patterns for free jets (M2), namely:

(1) The dissipated laminar jet, $Re < 300$. In this case, the viscous forces are large compared to the inertial forces, and the jet diffuses rapidly into the surrounding fluid.

(2) Fully laminar jets, $300 < Re < 1000$. In this case there is no noticeable diffusion of the jet into the surrounding fluid.

(3) A transition or semi-turbulent jet, 1000 < Re < 3000.

(4) A fully turbulent jet, Re > 3000.

These results were confirmed by Cederwell (C1) who also found that jets are turbulent for Re > 3000. Although this discussion relating jet patterns to Re range is based on studies of circular jets, corresponding criteria appear to apply also to jets issuing from slots. Gardon and Akfirat (G6) indicate that slot jets are turbulent for Re = 2000 (where Re is based on the slot width).

A theoretical study reported by Levey (L3) indicated that the effect of the impingement surface was not felt by the jet further than one slot width from the surface; this study was for an idealized case, i.e. incompressible flow with no account for viscous effects or turbulent mixing. Other studies (G1, G2) and particularly the experimental work of Tani and Komatsu (T3) confirmed that no effect of the impingement surface on the jet was observed beyond about two jet diameters from the plate. Consequently, an impinging jet can be considered to behave like a free jet except in the immediate vicinity of the impingement surface.

Results of some previous studies on flow in the four characteristic regions are described below.

Region of flow establishment (Region I)

Near the nozzle exit the jet is decelerated by the tangential shear stress while the surrounding fluid is correspondingly accelerated. This interaction produces a zone of mixing at the jet flow periphery which grows in width in the downstream direction, leaving a potential core within which the fluid properties and the velocity remain relatively unchanged from their values at the nozzle exit. Eventually, at some position downstream, the core is dissipated as a result of the mixing action.

Experimental data reported by Albertson (A1) suggest that the sole force producing deceleration of the jet and acceleration of the surrounding fluid is tangential shear within the mixing region. Then, if viscous action has no influence on the mixing process, the mean flow should be dynamically similar under all conditions. Thus a similar velocity profile must characterize every section in the diffusion zone. As a matter of fact Albertson's experimental data follow the general trend of the Gàussian distribution and he writes for each value of x:

$$\frac{u(y)}{u_c} = \text{EXP}\left(\frac{-y^2}{2s^2}\right) \qquad (2.1)$$

where:

x = distance along the axis

y = transverse distance from the jet axis

u(y) = velocity at distance y from axis

u_c = velocity on the jet centerline

s = standard or root-mean-square deviation (the value of y for which $u = 0.606\ u_c$).

This equation is merely a result of a curve fit and has no theoretical basis. The condition of dynamic similarity requires that at all cross sections, regardless of the efflux velocity,

$$\frac{s}{x} = K \qquad (2.2)$$

where the value of K must be determined experimentally for a slot jet. Combining this analysis of the velocity field in the potential core (Region I) with a similar analysis in Region II and with his experimental data, Albertson states that the potential core length for slot jets extends 5.2 slot widths. He investigated air flowing through slots of widths 0.635, 0.159, and 0.079 cm for a range of Reynolds numbers.

In an appendix to reference (A1), Baines examined the results of Albertson more closely and concluded that the Reynolds number has an effect on the potential core length. For a round jet he recommended values of 5 nozzle diameters for Re = 14 000, and 7 nozzle diameters for Re = 100 000.

The length of this potential core has been measured by several other researchers. Hrycak et al. (H4) found that the length of the potential core is dependent upon jet Reynolds number. He reported lengths of 15 jet diameters at Re = 500 for round jets. This length increases with Reynolds number to a maximum of about 20 diameters for Re = 1000. As Re increases further, small scale turbulence is established and the potential core length decreases sharply, becoming relatively constant at a length of about 6 to 7 diameters for Reynolds numbers larger than 10 000. Other researchers (S1, D1, N1, S7) have reported the length of the potential cores of axisymetric turbulent jets to extend from 4.0 to 7.5 nozzle diameters.

Since from a heat transfer standpoint core length is important, it appears in view of the disparity of these results that additional work in this area is required.

Region of established flow (Region II)

For free slot jets Albertson et al. (A1) showed that the decay of centerline axial velocity is inversely proportional to square root of the dimensionless distance from the jet nozzle exit. With the definition for K given in Equation (2.2), Albertson writes:

$$\frac{u_c(x)}{u_c(0)} = \sqrt{\frac{1}{\sqrt{\pi}\, K}} \left(\frac{x}{D}\right)^{-\frac{1}{2}} \quad \text{or} \quad \frac{u_c(x)}{u_c(0)} = \sqrt{C} \left(\frac{x}{D}\right)^{-\frac{1}{2}}$$

where:

$u_c(x)$ = centerline velocity at distance x from nozzle exit.

D = nozzle width

C = potential core length

For free circular jets Albertson (A1), Gaunter et al. (G1) and Donaldson et al. (D1) found that the decay of the centerline velocity is inversely proportional to dimensionless distance from the nozzle exit. If K' is the value of K — as defined in Equation (2.2) — determined for a round jet, one writes:

$$\frac{u_c(x)}{u_c(0)} = \frac{1}{2K'}\left(\frac{x}{D}\right)^{-1} \qquad \frac{u_c(x)}{u_c(0)} = C'\left(\frac{x}{D}\right)^{-1}$$

where:

D' = nozzle diameter

C' = potential core length

For laminar impinging jets, Saad (S2) and Huang (H2) have observed in their numerical studies that rate of spread and axial velocity decay are dependent on shape of the velocity profile at the nozzle exit. Unlike the case of a parabolic inlet jet profile, there is a strong and immediate interaction between the jet flow and the surrounding fluid for a flat (plug) velocity profile. In this latter case, axial momentum just inside the free streamline is an order of magnitude greater than that in the entrained fluid just outside the free streamline. Accordingly, the high momentum fluid of the jet begins to diffuse immediately into the weaker flow field into which it is discharging, causing a considerably higher rate of spread of the jet. For the same reasons, the axial velocity decay is also faster for a jet issuing with a plug profile than for one issuing with a parabolic velocity profile.

In some applications, and particularly in the present study, the impingement surface is placed inside the potential core region. In this case the free jet region will be vanishingly small.

Region of deflection (Region III)

As the jet flow approaches the impingement surface, it is rapidly decelerated and pressure increases. If the impingement surface is impermeable and non-evaporative, the velocity is zero and the pressure attains a local maximum at the stagnation point. Over the impingement surface, the axial flow is deflected i.e., axial momentum is transformed into transverse momentum. Flow is of the boundary layer type with the influence of viscosity restricted to a thin layer near the impingement surface.

Beltaos et al. (B4) in a study of shear stress along the impingement plate in the case of turbulent axisymetric jets, found that it increases almost linearly with radial distance r from the stagnation point to a maximum value, after which it decreases with further increase in r. Similar results have been found numerically by Saad (S2). Saad (S2) and Li (L2) found that shear stress on the plate, expressed nondimensionally as skin friction coefficient, C_f, does not depend on square root of the Reynolds number as is predicted by boundary layer theory for a flat plate boundary layer. They found, nevertheless, that C_f decreases as jet Reynolds number increases.

Evaporation along the impingement plate increases the mass flow-rate of fluid over the plate. As the evaporation rate increases, the "effective local Reynolds number" increases at constant jet Reynolds number, causing C_f to decrease (L2). In addition to this Re effect, evaporation also decreases the axial gradient of the radial velocities, thereby further lowering C_f. In his computer simulation of axisymetric round jet Li (L2) also found that the application of suction through the plate leads to an increase in C_f.

<u>Wall Jet Region (Region IV)</u>

Glauert (G3) divided this flow region into two parts:

(1) an inner layer where the effect of the wall is felt by the fluid flow.

(2) an outer layer which is characterized by the features of a free flow.

The boundary between these two layers is taken as the position of the maximum velocity.

In the case of round jets, Poreh et al. (P3) and Glauert (G3) showed that this maximum velocity can be expressed as a function of the radial distance r as follows:

$$V_{max} = \frac{\text{Constant}}{r^n}$$

where n ranges from 1.1 to 1.143 according to various investigators.

Martin (M1) and Donaldson et al. (D1) further report that :

$$V_{max} / u_j = B\ r^{-n}$$

where n takes the same values as in the previous equation, and where B is a function of H/D only (S1).

2.2.2 Oblique Impingement

It has been seen in the previous paragraph that the existence of four distinct flow regions have been established in the case of a jet impinging normally on a flat surface, and that a fifth region (region of recirculating flow) also exists when the jet is confined. The same regions can be expected to exist in the case of oblique impingement (B5). However, while for normal impingement the flow is entirely symetric, this is not so for oblique impingement.

Beltaos (B6) measured the wall pressure distributions in the impingement zone (Region III) for slot turbulent jets impinging with various angles. Operating at L/D ratios ranging from 45.5 to 68.2, he found that the stagnation point, which corresponds to the location of maximum wall pressure, does not coincide with the intersection of the wall and the jet centerline but is shifted by a distance, s,(see Figure 2.1). This shift is caused by the tendency of the stagnation streamline to intersect the wall at right angles. With their experimental data obtained for L/D = 20,30 and 40, Schauer and Eustis (S10) evaluated the eccentricity of the stagnation point and proposed the equation,

$$\frac{S}{L} = 0.154 \tan \theta$$

with notations as indicated on Figure 2.1.

For the case, $\theta = 60°$, Beltaos (B6) reports that the pressure excess with respect to ambient mean pressure is seen to take negative values on the side of negative x (Figure 2.1). This occurence has also been observed by other investigators (K1, S10) and is believed to be the result of a vortex formation in the entrainment field. When θ becomes sufficiently large, the boundaries of the free jet and of the wall jet get so close to each other on the side of negative x that some of the fluid in the upper layers of the wall jet is entrained in the free jet, thus completing a circulatory motion and forming a vortex. At the same time, the vortex is located sufficiently close to the wall so as to impress some low pressures on it (B6).

2.2.3 Deflection by a crossflow

Although several investigators have studied various aspects of

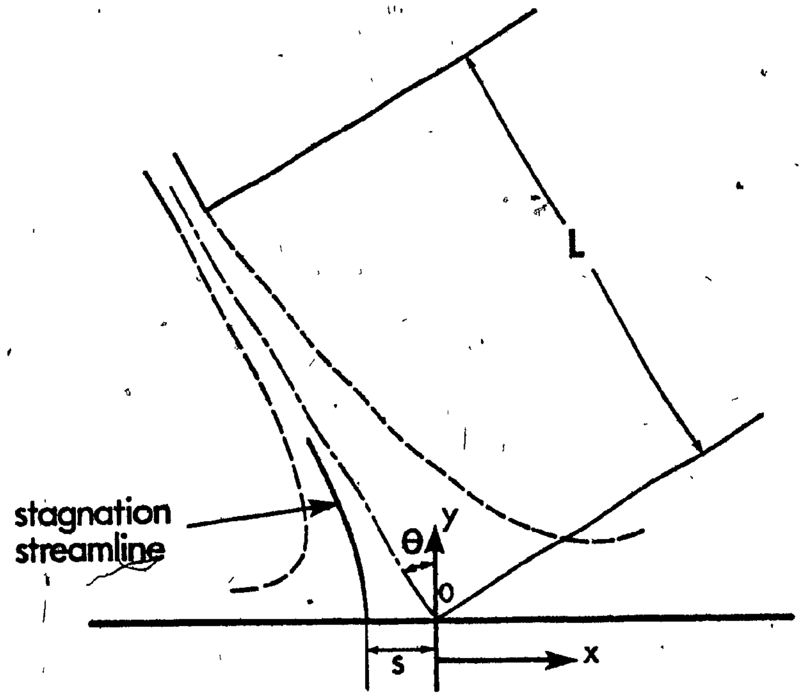

Figure 2.1 : Definition sketch for oblique impingement.

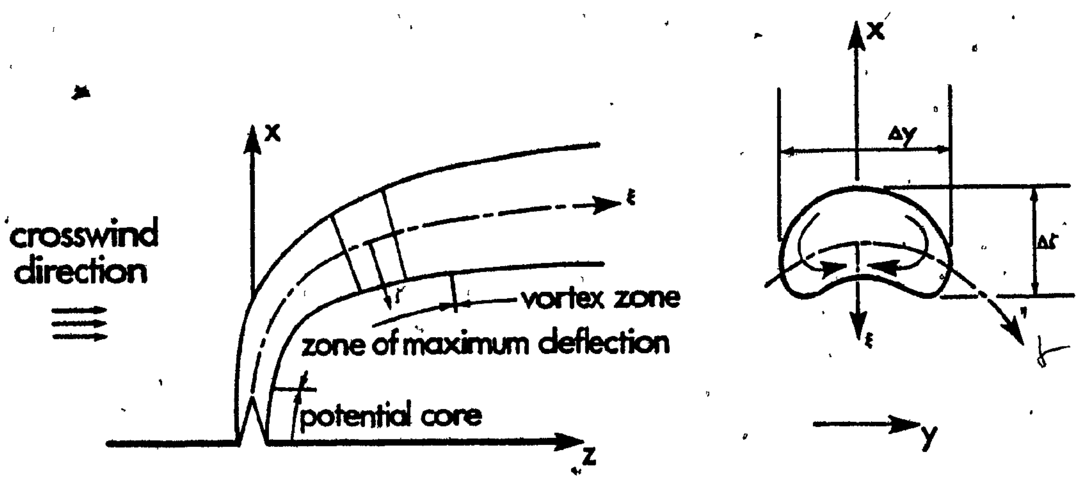

Figure 2.2 : Pattern of a free jet deflected by a crosswind.

impingement heat transfer for a turbulent jet in a cross flow, only one publication (B3), as will be seen further, reports observations of the flow pattern characteristics for such impinging jets. However, because of the applications of free jets in the areas of fluid waste disposal, dispersion of effluents from chimney stacks, and fan and wing combinations used by V/STOL aircraft, many researchers have studied the flow of turbulent jet flows deflected by a crosswind. Since their conclusions are of interest to the present study, they will be briefly summed up here.

Careful observation made by Pratte and Baines (P4) of a jet of nonbuoyant smoke discharging normal to a crossflow, lead to the delineation of three flow zones (see Figure 2.2):

(1) The potential core still exists. In this potential zone the streamlines are essentially parallel to the jet direction, and the crossflow is affected in the same manner as if a solid cylinder were present. The small entrainment velocity moves fluid toward the jet at the sides and a separation occurs just behind the maximum width. In the wake, the mean velocity is much smaller than in either jet or crossflow and two attached vortices can be seen, exactly as found in flow around a cylinder at low Reynolds number. At the end of the potential zone the eddies are of comparable size to the jet and appear to be strong enough to add to the jet entrainment. Downstream of the jet and attached eddies, the crossflow recloses, forming a decelerated but relatively steady motion.

(2) Zone of maximum deflection: this zone is characterized by the deflection of the jet and by a rapid decrease of mean velocity. Just

beyond the potential zone the cross and jet flows mix rapidly because the volume of fluid entrained increases with the effective jet diameter. The action of the crossflow momentum causes the jet to bend over. Turbulent shear acts as in the simple jet (i.e. without crossflow) to entrain the surrounding air, as do the attached eddies which grow and intensify to occupy a large part of the jet cross-section as a pair of vortices. The mean velocity decreases much more rapidly than in the case of a simple jet (K2). In a relatively short length the jet is moving in a direction only a few degrees different from the crossflow direction (see Figure 2.2), and no longitudinal relative motion between the two flows can be detected.

(3) In the third region, referred to by Pratte and Douglas as the vortex zone, the two turbulent vortices are carried along at the crossflow velocity. The profile continues to rise at a slow and decreasing rate, the vortices increasing in size along with the jet cross section, but decreasing in angular velocity. It would be expected that in an infinite crossflow, the turbulent and vortex motions would be dissipated by viscosity, so that the jet would approach the conditions of its surroundings. An indication of the length of the vortex zone is given by observation of its continued existence 1000 jet diameters downstream of the source in a wind tunnel.

Pratte's results are in good accordance with what has also been found by Keffer and Baines (K2) and by Platten and Keffer (P5) who plotted the loci of maximum velocity obtained for a jet discharging at right angles into the main stream. They report that the most marked result of increasing the velocity ratio (i.e. the ratio of the jet velocity to the crossflow velocity) is that the trajectories experience a less abrupt deflection upon entering the crossflow. One would expect the absolute jet penetration to depend upon the initial momentum flux of the jet relative to the cross-wind, and this is confirmed by the higher values of x/D reached by the high velocity ratios within the curvilinear zone in Platten's experiments (P5).

The only study of the flow pattern of an impinging jet in a cross-flow that this literature research could uncover is the one published by Bouchez and Goldstein (B3). Flow visualization has been performed for turbulent jets in a wind tunnel using a fog generated by dropping carbon dioxide pellets (dry ice) into a pressure vessel filled with hot water. The authors show interesting pictures for H/D = 6 and 12. They found that when the jet impinges violently on the opposite wall, there is a strong turbulent recirculation zone upstream of the impingement area. This vortex is associated with a noticeable underpressure in this area. Just downstream of this underpressure, an overpressure is present and is in effect the signature of the stagnation point. Due to rapid lateral spreading of this zone, there is a sidewall effect when the tunnel walls interfere with the flow. This occurs only a few diameters downstream of the stagnation point and causes an uplift of this area of the jet. As the blowing rate mass flux ratio (of the jet to crossflow) decreases, the recirculation zone diminishes and finally disappears as does the underpressure.

It may be noted here that all the publications reported in this section are concerned with turbulent jets. An extensive litterature research failed to uncover any previous study of the flow field characteristics of an impinging laminar jet in a crossflow.

2.3 IMPINGEMENT HEAT AND MASS TRANSFER

2.3.1 Analytical Studies

2.3.1.1 Various theoretical approaches

Two categories of theoretical approaches have been adopted by most researchers to predict the laminar impinging jet heat or mass transfer characteristics: (1) inviscid flow - boundary layer solution matching schemes, and (2) iterative finite difference procedures to solve the full elliptic governing equations.

(1) Inviscid flow - boundary layer solution matching schemes: This approach is used near the stagnation region, based on the assumption that in the free jet region (as defined in paragraph 2.2.1) the flow is inviscid and can be represented by an appropriate potential flow solution, and that in the stagnation region a laminar flow exists. The potential flow solution is used to provide the free stream velocity for computation of the wall boundary layer flow. The governing boundary layer equations are transformed into convenient forms by using suitable similarity variables, and the resulting differential equations can be solved by finite difference methods, hence allowing prediction of the stagnation region heat transfer. The main drawback of this method, besides its inability to predict the effect of turbulence, is the uncertainty as to the size of the laminar boundary layer flow. Measured values were found to exceed predicted values, sometimes by a large amount, both for circular and slot jets (H5).

Wall jet heat transfer predictions, although mostly limited to slot jets, have been found to agree with experimental results (H5). The theoretical approaches employ consideration of two flow layers: an inner layer along the wall and an outer layer assumed to behave as a free jet. Both integral and finite difference solutions, often complicated, have been obtained by various investigators.

(2) Iterative finite difference procedure: The full elliptic partial differential equations of conservation of mass, momentum, and energy are transformed into sets of finite difference equations which are then solved iteratively. This method, like the previous one, is not satisfactory to handle turbulent flow problems. For laminar jet flows, however, this approach provides solutions which are in excellent agreement with experimental measurements, as has been shown by Saad et al. (S11) and by van Heiningen et al. (V2)

2.3.1.2 <u>Parameters governing heat and mass transfer</u>

(i) Jet velocity profile at nozzle exit: Sparrow and Lee (S7) studied the effect of jet exit conditions and showed that, for a non-uniform initial velocity profile of the jet, the streamwise velocity gradient at the stagnation point was relatively constant over a large range of nozzle-to-plate spacings. For a uniform (flat) initial velocity profile, however, there were significant changes in velocity gradient for different spacings. From the relationship between stagnation point heat or mass transfer and streamwise velocity gradient, the behaviour of the stagnation point heat transfer can be inferred. Scholtz and Trass (S4, S5) derived a potential flow solution for the impinging region and then used it as the boundary condition for the boundary layer along the wall. They found that, for equal Reynolds number, mass transfer at the stagnation point in the case of a uniform initial velocity is less than half that for the non-uniform jet under the conditions tested: $0.5<H/D<6$ and $570<Re<1970$.

Similar results were also found by van Heiningen et al. (V2) who solved numerically the full Navier - Stokes equations, in their stream function-vorticity formulation, coupled with the energy equation for an impinging slot jet. They found that for H/D = 4 and Reynolds number between 100 and 950, the stagnation heat transfer rate for an initially parabolic velocity was 1.5 to 2 times the value for an initially flat velocity profile. Van Heiningen explained his results by noting that the jet contracts slightly below the nozzle for a parabolic profile, while for a flat profile the jet expands continuously. Consequently the free streamline is significantly closer to the impingement plate for the parabolic velocity profile owing to its higher momentum and lower rate of spreading, leading thereby to steeper velocity and temperature gradients near the impingement plate.

Saad (S2) in his simulation of flow and heat transfer characteristics of a laminar semi-confined impinging round jet further confirmed these results.

(ii) Nozzle-to-plate spacing: Although the rate of heat transfer must decrease for sufficiently large values of nozzle-to-plate spacings, for small values of H/D heat transfer has been reported by several researchers to be insensitive to nozzle-to-plate spacing. Sparrow and Lee (S7), for example, formulated this conclusion for H/D around 0.25 and 1.5. Saad (S11) in his simulation of an axisymmetric round jet found that, over the range $1.5 < H/D < 12$, there is no perceptible decrease at Re = 950 and only 15% decrease at Re = 450.

In his simulation of simultaneous heat and mass transfer for a round axisymmetric impinging jet, Li (L2) found that transfer rates decreased with increasing nozzle-to-plate spacing for $H/D > 6$. He associated this result with a decrease in the limiting radial velocity gradient.

(iii) Jet confinement: When the impingement and confinement surfaces are sufficiently large, a complete recirculation bubble attached to the confinement plate is established. Such a recirculation bubble influences the spreading of the jet and the flow pattern of the deflected jet. As is reported by van Heiningen et al. (V2), this feature of the flow influences the heat transfer rate distribution along the impingement surface. As for just the stagnation zone however, by comparing his own results for semi-confined jets with the experimental results for unconfined jets of Scholtz and Trass (S4) and Gardon and Akfirat (G4), Saad (S2) showed that the presence of a confinement plate has only a minor influence on the stagnation point heat transfer for $2<H/D<4$ and $450<Re<2500$, regardless of the shape of the initial jet velocity profile. Van Heiningen's results for the stagnation region are consistent with Saad's conclusion.

This observation is in good agreement with the statement of Giralt et al. (G2) that the stagnation flow region can be considered to start at a distance around one nozzle diameter from the impingement plate. It is the velocity profile at this particular location that determines transfer rates in the stagnation zone. Hence, provided that the effect of the confinement plate - induced recirculation flow is not sufficiently strong to affect the free streamlines (i.e. region II of the flow field), the effect of partial confinement is not felt in the impingement region.

(iv) Temperature - sensitive fluid properties: Van Heiningen et al. (V2) presented the influence of variable properties (viscosity, thermal conductivity, etc.) on the Stanton number. They allowed viscosity to vary with temperature according to the Van Driest interpolation formula. It was found that the non-dimensional temperature gradient at the wall was affected by the change from constant to variable fluid properties. However, away from the stagnation point the heat transfer coefficient in form of Stanton number based on properties at the nozzle was found to be hardly affected by the change in variable properties. Van Heiningen noted that this was in agreement with the theoretical solutions of the influence of variable properties on two-dimensional stagnation flow and laminar boundary-layer flow over a flat plate without a pressure gradient.

(v) Suction and blowing: Saad (S2), van Heiningen (V2) and Huang (H2) investigated the effect of suction on impingement heat transfer for round and slot jets; in Saad's case, for example, the suction velocity was 1% of the jet velocity. They all found that suction enhances the transfer rates by about a constant absolute increment over the entire region from the stagnation point out to the wall jet region. Skin friction was like-wise found to increase with the application of suction.

On the other hand blowing leads to a lowering in local heat transfer coefficients over the entire impingement surface by an equivalent constant absolute increment. The enhancement of the heat transfer rate due to suction has been observed experimentally by Obot (O1) for a turbulent round jet.

(vi) Presence of evaporative mass flux: This is the case of simultaneous heat and mass transfer. No computer simulation of this case was available until the recent study of Li (L2). He found that the presence of an evaporative mass flux increases the various boundary layer thicknesses and reduces both heat and mass transfer rates. He observed that this reduction was almost independent of the jet Reynolds number, but was dependent on the magnitude of the axial velocities over the impingement surface.

(vii) Presence of a swirl: The study of Huang (H2) seems to have been the only attempt to investigate numerically the effect of swirl on laminar impingement transfer rates. Huang solved the full Navier-Stokes equations together with the energy equation in their primitive form using a hybrid central and upwind difference scheme. He observed that swirl enhances the rate of spread of the jet causing, under certain conditions, development of a toroidal recirculation region next to the impingement plate. This closed recirculation flow in the stagnation region effectively insulates the plate from the jet flow, causing a substantial decrease in stagnation region heat transfer. Furthermore, the stagnation point Stanton number was found to be insensitive to variation in the nozzle-to-plate spacing for $1.5<H/D<4$. Since introduction of a swirl generally results in lowered average heat transfer rates (H2), it is evident that swirl should be avoided in all practical applications except when a less peaked transfer rate profile is desired.

(viii) Reynolds Number: Initial attempts to predict heat transfer from an impinging jet to a plane surface analytically were limited to the neighbourhood of the stagnation point. Most investigators assumed laminar conditions to exist in the impingement region, even for turbulent jets. This assumption is suported by Gardon and Akfirat (G4, G6) who observed experimentally the existence of secondary peaks in the local heat transfer distribution along the plate for small H/D ratios, and who ascribed these secondary peaks to a transition from laminar to turbulent boundary layers. With this laminar flow assumption, a $Re^{\frac{1}{2}}$ dependence for the Nusselt number was found by most researchers. Kezios (K3), for example, reports the following expression for the stagnation point heat transfer:

$$Nu_0 = 0.475\sqrt{Re_{D/2}}$$

where the characteristic length is D/2 (nozzle radius).

It is however appropriate to remark here that Wolfstein (W1) noted that the observed dependence of Nusselt number on Reynolds number, as indicated by the exponent on the latter varying from 0.56 to 0.87, suggests existence of turbulence even near the stagnation point. The effect of free-stream turbulence should therefore be considered, and one of the major reasons for the disagreement between theory and measurements may be neglect of this influence.

(ix) Fluid properties (Schmidt or Prandtl number): Many heat and mass transfer correlations in terms of Reynolds, Prandtl and Schmidt numbers have been established. Waltz (W2), using the results originally derived by Eckert, obtained the expression:

$$Nu = 0.44\ Pr^{0.36}\ Re_r^{0.5}$$

for the local values in the axisymetric flow, where Re_r is the local Reynolds number at distance r from the stagnation point. For the average values he found:

$$\overline{Nu} = 0.88\ Pr^{0.36}\ Re_r^{0.5}$$

Metzger (M4), using Eckert's wedge flow solution, obtained for slot jets the following equation for local values of Nusselt number based on distance from the stagnation point:

$$Nu = 0.57\ Pr^{0.37}\ Re_r^{0.5}$$

and for the average values of Nusselt number he found:

$$Nu = 1.14 \, Pr^{0.37} \, Re_r^{0.5} .$$

Wolfstein (W1) found a $Pr^{0.333}$ dependence for the stagnation Nusselt number, in the range $0.7 \leq Pr \leq 10$.

The inability of such formulas to account directly for the effect of the nozzle-to-plate spacing must be considered their principal weakness (H5).

The problem of mass transfer in laminar radial wall jets has been studied analytically by Scholtz and Trass (T6) using the von Karman - Polhausen approach which assumes polynomial forms for the velocity and concentration profiles. Assuming $Sc > 1$ they found that the mass transfer coefficient for the laminar wall jet was dependent on $(x/R)^{-1.25}$ and $Re^{0.75}$. These results received experimental confirmation by the work of Kapur and McLeod (K4) who used a laser holography technique to measure local sublimation rates. Scholtz and Trass (S4, S5) later obtained a solution for mass transfer in the stagnation region. For a non-uniform laminar round jet with $1 < Sc \leq 10$, they gave the following correlation for the stagnation point Sherwood number:

$$Sh = 1.6484 \, Re^{\frac{1}{2}} \, Sc^{0.361} .$$

This correlation has been found to be in good agreement with experimental results for the mass transfer coefficients in the case of sublimation of naphthalene into air ($Sc = 2.45$) (S5).

2.3.2 Experimental Studies

2.3.2.1 Introduction: Whereas numerical investigations on impinging jets were mostly concerned with laminar jets, almost all experimental investigations have been for turbulent jets.

Hrycak et al. (H5) surveyed the correlations proposed by various researchers and noted that a comparison between results of heated jets impinging on room-temperature surfaces and room-temperature jets impinging on heated surfaces is difficult because of fundamentally different boundary conditions. In addition heat transfer rates were measured in different ways by the many researchers. The various methods include use of metal rod calorimeters, steam calorimeters, thermocouples, and heat transfer gages. The areas over which these measurements were made varied in size, and what some investigators called local values were in fact at best average values (H5). As for mass transfer rates measurements, methods such as laser holographic interferometry, weight loss determination of humid materials, and sublimation of naphthalene were used.

In a critical review of the many different analytical and experimental studies, Obot (O1) has found large quantitative differences between the results. However, the experiments reported in the present review of more limited scope reveal in general the same trends.

2.3.2.2 Parameters governing heat and mass transfer

(i) Nozzle-to-plate spacing: Huang (H1) investigated both stagnation and average heat transfer from a hot turbulent jet to a surface normal to the jet flow with various nozzle diameters and nozzle-to-plate spacings.

In his investigation the heat transfer coefficient was found to be independent of spacing for H/D < 6. In contrast, major changes were found by Gardon and Cobonpue (G5) who present results of tests of cool air impinging from a circular jet onto an isothermal hot surface. These authors provide results for variation of heat transfer rates with radial distance from the stagnation point, for a nozzle exit Reynolds number of 28 000. They obtained, for large nozzle-to-plate spacings, smooth bell shaped profiles with the maximum at the stagnation point. As nozzle-to-plate spacing was reduced, they obtained secondary peaks in the heat transfer rate profiles. At H/D = 6 an anular hump begins to develop and grows into a well defined secondary peak as H/D decreases further. When nozzle-to-plate spacing is less than the potential core length, they found that, at the stagnation point, the central peak was replaced by a central minimum in heat transfer. For values of H/D < 0.5, the impingement of a free jet gives way to a wall jet and the heat transfer-rate increases again.

Chia et al. (G2), who studied mass transfer under turbulent axisymetric impinging jets at Re = 34 000, report the same type of radial distribution of mass transfer-rate at various nozzle-to-plate spacings. The radial variation at H/D = 1.2, in particular, shows two pairs of peaks at values of x/R of 1.2 and 3.9, in contrast with the bell shaped distribution found at H/D = 8.0. Similar peaks were also observed by Gardon et Akfirat (G4). The inner peaks were attributed to a thinning of the accelerating boundary layer flow when the nozzle-to-plate spacings are small; the formation of the outer peaks was attributed to flow turbulence, specifically to transition from laminar to turbulent flow.

The experimental investigations mentioned above have been carried out with relatively high Reynolds numbers. Of great importance for the present study are the results of Kapur and McLeod (K4) whose Reynolds number is of the same order of magnitude as that used in the present computer simulation. They report that the mass transfer coefficients near the impingement point for Re = 1340 and nozzle-to-plate distances of 0.5, 1 and 1.5 diameters, are found to be independent of H/D, both at the stagnation point and in the region close to it, as are those in the wall jet region more remote from that point. These results are in agreement with those of Gardon and Akfirat (G6) who found that for Re less than 2000 and nozzle-to-plate distances of 0.5 to 5.0 diameters, the stagnation point Nusselt numbers depend on the Reynolds number only.

The large variety of experimental conditions chosen by the various researchers, as well as the complexity of the problem, make it difficult to draw precise quantitative conclusions as to the effect of the nozzle-to-plate spacing on heat and mass transfer. However, the general trends have been established clearly enough and could be summed up as follows: For very small H/D ratios (up to 2 or 3) some researchers find no effect whereas other investigators find a small diminution of the stagnation point heat transfer when H/D increases. For larger values of H/D, the local heat transfer coefficient at the stagnation region increases with spacing, reaches a maximum value for a spacing corresponding to the potential core length (usually between 6.0 and 8.0), and then decreases for higher spacings.

Among the many published correlations, the one of Gardon and Akfirat (G6) could be cited. They report St to be proportional to $(H/D)^{-0.62}$ for $H/D > 16$. For a round jet, Gardon and Cobonpue (G5) found St to be proportional to $(H/D)^{-1}$ for $H/D > 20$.

(ii) Nozzle design: The nozzle shape influences the impingement heat or mass transfer because it determines the jet velocity profile at the nozzle exit, the turbulence level and the length of the potential core. Metzger (M4), who compared heat transfer for a slot jet and a circular jet when the same target area, flow rate , and nozzle area were considered, found that the round jet gave a heat transfer rate 8 percent higher than the slot jet. It was noted however that the shapes of the areas cooled were quite different, and it was concluded that the shape of the area to be cooled (or dried) is of primary importance in deciding which type of jet to use.

(iii) Fluid properties (Schmidt and Prandtl number): Chamberlain (C2) used room-temperature turbulent air jets impinging on a segmented, Invar, steam-heated surface. Nozzle exit Reynolds numbers to 67 000, and nozzle-to-plate spacings to 50 nozzle diameters were investigated. He reported the following correlation for the local stagnation point Nusselt number:

$$Nu_0 = 1.16\, Re_D^{0.447}\, Pr^{0.333} \qquad \text{for } H/D \leqslant 7$$

$$Nu_0 = 0.384\, Re_a^{0.569}\, Pr^{0.333} \qquad \text{for } H/D \geqslant 7$$

where Re_a is the Reynolds number based on arrival velocity. For locations along the plate away from the stagnation point, the correlation

$$\frac{h_r}{h_0} = \text{EXP}\left[-1.56\left(\frac{r}{H}\right)^{0.75}\right]$$

was suggested; here h_r is the local coefficient at a distance r from the stagnation point.

Nakatogowa et al. (N1) found good agreement between the correlation

$$Nu_D = 0.535 \ Re_D^{0.5} \ Pr^{0.4}$$

and their experimental values for heat transfer at the stagnation point for various Reynolds numbers (from Re = 10^4 to Re = 10^5) for spacings lower than the potential core.

(iv) Angle of impingement: Very few investigators have studied the problem of heat and mass transfer under an oblique impinging jet. In 1954, Perry (P1) investigated heat transfer from a hot round oblique jet to a plane surface. The impingement plate was water cooled and he measured the heat flux with a calorimeter of 0.65 inch diameter placed at its center, from the temperature rise of a metered flow of water. The calorimeter diameter was used as the characteristic length in Nu and Re for all the correlated results. This was so because the heat flow was measured only over the area of the calorimeter and also temperature and velocity values for the correlations were obtained as mean figures over the area ofthis instrument. Perry found that changing the angle of jet impingement from 15 to 90 degrees increased the stagnation heat transfer coefficient by nearly 100 percent for any temperature and velocity.

The nozzle-to-plate spacing was at least 8 nozzle diameters, and his test results were correlated by :

$$Nu = K\ Re^{0.7}\ Pr^{0.33}$$

where the value of K is dependent on the angle as follows:

Angle of Impingement (deg.)	$K = Nu\ Re^{-0.7}\ Pr^{-0.33}$
90	0.1810
75	0.1745
60	0.1579
45	0.1422
30	0.1224
15	0.1037

Nothing else seems to have appeared on this matter until 1972 when Korger and Krizek (K5) published results for mass transfer under an oblique impinging round turbulent jet. Their investigation technique was based on sublimation of naphthalene. They found that the maximum mass transfer location is displaced in the direction of the jet nozzle for an inclined jet (i.e. away from the intersection between the jet axis and the plate) by an amount ε

$$\varepsilon = (14 + 0.15\ L)\ \tan\alpha$$

where L (nozzle-to-plate separation along axis of the jet) and ε are expressed in mm, and where α is the angle of impingement. This formula was found to be independent of the jet velocity for $10 < u_j < 40$ m/sec.

From the potential flow analysis of Schah (S8) it is found by Kroger and Krizek that the stagnation point for inclined round jets coincides closely with the maximum mass trasnfer point.

The authors also give the mass ratio of the two dividing air streams after impingement:

$$\frac{q_1}{q_2} = \frac{1 + \cos \alpha}{1 - \cos \alpha}$$

This equation has also been reported by Beltaos assuming that the ratio behaves as that of a potential jet (B6).

Korger and Krizek reported that the maximum mass transfer value decreases when the angle is decreased under 90°. Studying the mass transfer distribution along the plate, they found that when the jet comes from the left side, for example, the values on the right side of the maximum transfer point are higher than on the left side. This is because most of the jet stream flows on the right side.

Figures for the average mass transfer coefficients are shown, and the results indicate that for $30° < \alpha < 90°$ the average mass transfer values are sensibly the same as the one for normal impingement ($\alpha = 90°$). It is interesting to note that Perry (P1) made the same type of conclusion concerning the average heat transfer coefficient for round jets impinging at angles between 15 and 90 degrees.

(v) Presence of crossflow: Metzger and Korstad (M5) studied experimentally the effects of a cross-flowing air stream on the heat transfer characteristics of a single line of circular air jets. The crossflow, perpendicular to the line of jets, is characterized by the ratio of the crossflow to jet mass flow-rates, M. The general effect of H/D in the downstream region is found to be similar to the behaviour previously reported for jet flow alone, but the crossflow increases and complicates it. The upstream propagation distance of the jets is relatively short, even for moderate crossflow rates. As a consequence, the heat transfer-rates immediately upstream of the nozzle exit plane are reduced significantly below what would be expected if crossflow were not present. Correspondingly, the average heat transfer-rates, over regions immediately downstream are increased significantly above what would be expected if crossflow were not present, despite the fact that the impingement angle for the deflected jet must be less than 90 degrees. Further, they found that on an overall basis for a symetrical region extending ten nozzle diameters both upstream and downstream of the nozzle exit plane, the presence of crossflow always reduces the average heat transfer below what would be expected without crossflow.

Sparrow et al. (s9) report measurements of the local heat transfer coefficients resulting from impingement of a turbulent round jet which interacts with a crossflow. H/D ratios were between 3 and 12, and the ratio of the jet to crossflow mass velocity ($M' = (\rho u)_j / (\rho u)_\infty$) was varied from 4 to 12. The deflection of the jet by the crossflow was found to be small for mass velocity ratios $M' > 8$, and for these mass velocities the impingement point heat transfer coefficient achieves a maximum value at separation distances H/D = 5 or 6. Again, this result is comparable to what has been found by prior researchers in the absence of crossflow. For a mass velocity ratio $M' = 4$, the maximum is attained at smaller separation distances owing to the substantial deflections experienced by the jet at larger H/D. The influence of the presence of a semi-confinement plate was limited to cases where H/D >4 with the largest effects at the lowest mass velocity ratio.

Bouchez and Goldstein (B3), who studied experimemtally the impingement cooling from a circular jet in a crossflow, found that heat transfer coefficients are lower than those reported in the literature for an impinging jet in the absence of crossflow.

Nagpal (N2) studied experimentally the effect of spent-flow in perforated-plate air impingement heat transfer. The spent-flow is in fact the crossflow coming from neighbouring jets and interfering with any particular jet. Nagpal correlated the magnitude of the local heat transfer rates with the geometry of the perforated plate and the air flow rate. From his results and analysis he provided a basis for engineering design of multi-jet air - impingement cooling or heating devices. Most of his results concerning heat transfer rates are highly conditioned by the particular configuration of the perforated plates he used (free flow area ratio, etc.). The mean heat transfer rates, for example, are averaged over areas containing several plate perforations and thus several jets and could therefore not be compared with the ones obtained in the present study. However it is of importance that his results on the mean heat transfer conclude that there exists an optimum plate spacing at which the average heat transfer is maximum. This optimum value of H/D is a function of the plate configuration (dimension and number of orifices, free-flow area ratio) among other things.

CHAPTER 3

MATHEMATICAL FORMULATION

3.1 INTRODUCTION

The governing equations for the flow of a variable-property binary mixture issuing from a rectangular jet are presented in Section 3.2. In Section 3.3 all these equations are converted to a unique standard form so that a single solution algorithm can be applied to all. The boundary conditions associated with this set of elliptic partial differential equations are established in Section 3.4. Finally, the regression equations to account for variation with temperature and composition of physical properties of the binary air-water vapour mixture are presented in Section 3.5.

3.2 GOVERNING EQUATIONS

Application of the laws of conservation of mass, momentum, energy and species to multicomponent Newtonian fluid flows yield the following vector equations (B2):

$$\underline{\text{mass}}: \quad \frac{D}{Dt} \rho + \rho \, (\nabla \cdot U) = 0$$

$$\underline{\text{momentum}}: \quad \rho \frac{D}{Dt} U = - \nabla P - \nabla \cdot \underline{\tau} + \rho g \qquad (3.1)$$

$$\underline{\text{energy}}: \quad \rho C_p \frac{DT}{Dt} = - \nabla \cdot q - \underline{\tau} : \nabla U + \sum_{i=1}^{n} (j_i \cdot q_i)$$

$$+ \left(\frac{\partial \ln \rho}{\partial \ln T} \right)_{P, x_i} \frac{DP}{Dt} + \sum_{i=1}^{n} \overline{H}_i \, (\nabla \cdot J_i - R_i)$$

$$\underline{\text{species } i}: \quad \frac{D}{Dt} \rho_i + \rho_i (\nabla \cdot U) = - \nabla \cdot j_i + r_i \qquad (3.2)$$

where: ρ = bulk density of the fluid

ρ_i = mass of i per unit volume

P = hydrodynamic pressure

$\underline{\tau}$ = viscous stress tensor

J_i = molar flux of i relative to mass average velocity

j_i = mass flux of i relative to mass average velocity

q = energy flux per unit area, relative to mass average velocity

$\overline{H}_i$ = partial molar enthalpy of i

R_i = molar rate of production of species i

n_i = mass flux with respect to stationary coordinates

r_i = mass rate of production of species i.

The above equations, which are general for the description of Newtonian fluids, constitute the set of governing equations in the present study.

Because of the particular geometry of the system, these equations will be used in two-dimensional cartesian coordinates. The fluid flow is assumed to be Newtonian and steady. All $\partial/\partial t$ terms are then eliminated.

Further simplifications and assumptions made in individual equations are listed below.

Momentum Equations

Gravity is supposed to be acting in the positive x-direction.

Energy Equation

(i) The gas flow velocities involved in this study are low. Consequently, the pressure work $\left(\frac{\partial \ln \rho}{\partial \ln T}\right)_{P,x_i} \frac{DP}{Dt}$, and the viscous dissipation $\underline{\tau}:U$ are very small with respect to the other terms in the energy equation, and hence are neglected.

(ii) The diffusion-thermo effect is assumed to be negligible, and therefore the heat flux vector for a multicomponent fluid is given by:

$$q = -\lambda \nabla T + \sum_{i=1}^{n} \bar{H}_i J_i \qquad (3.3)$$

Species Equation

(i) The fluid is chemically inert and is an ideal mixture of water vapor (A) and dry air (B). Thus, $R_i = 0$.

(ii) The thermal-diffusion effect is assumed to be negligible, and therefore the mass flux formulation reduces to Fick's first law:

$$j_i = -\rho \delta_{AB} \nabla m_i \qquad (3.4)$$

where m_i is the mass fraction of species i, defined as mass of i per unit mass of the mixture.

Since the fluid properties are temperature dependent, it is more convenient to choose temperature as the dependent variable in the energy equation. Applying the caloric equation of state, enthalpy terms in the energy equation can be expressed in terms of temperature, T, as:

$$J_i \cdot \nabla \bar{H}_i = j_i \cdot \nabla h_i$$

and $$h_i = h_{i,ref} + \int_{T_{ref}}^{T} C_{p_i} \, dT \qquad (3.5)$$

where $h_{i,ref}$ is the reference enthalpy, and the integral term in Equation (3.5) represents the sensible enthalpy per unit mass.

Further, for a two-component system of A and B, the diffusion coefficients are equal, i.e. $\delta_{AB} = \delta_{BA} = \delta$, and thus $j_A = - j_B$. (3.6)

By substituting the flux equations (3.3) and (3.4) into the governing equations (3.2), and by using equations (3.5) and (3.6), one obtains the following set of simplified conservation equations:

<u>mass:</u>

$$\frac{\partial}{\partial x}(\rho u) + \frac{\partial}{\partial y}(\rho v) = 0$$

<u>momentum:</u>

x - component: $$\rho\left(u \frac{\partial u}{\partial x} + v \frac{\partial u}{\partial y} \right) = - \frac{\partial P}{\partial x} - \left(\frac{\partial \tau_{xx}}{\partial x} + \frac{\partial \tau_{yx}}{\partial y} \right) + \rho g_x$$

y - component: $\rho \left(u \frac{\partial v}{\partial x} + v \frac{\partial v}{\partial y} \right) = - \frac{\partial P}{\partial y} - \left(\frac{\partial \tau_{xy}}{\partial x} + \frac{\partial \tau_{yy}}{\partial y} \right)$

energy:

$$\rho C_p \left(u \frac{\partial T}{\partial x} + v \frac{\partial T}{\partial y} \right) = \frac{\partial}{\partial x} \left(\lambda \frac{\partial T}{\partial x} \right) + \frac{\partial}{\partial y} \left(\lambda \frac{\partial T}{\partial y} \right)$$

$$+ \delta \rho \left\{ \frac{\partial m_A}{\partial x} \frac{\partial}{\partial x} \left[(Cp_A - Cp_B) T \right] + \frac{\partial m_A}{\partial y} \frac{\partial}{\partial y} \left[(Cp_A - Cp_B) T \right] \right\}$$

species:

$$\frac{\partial}{\partial x} (\rho m_A u) + \frac{\partial}{\partial y} (\rho m_A v) = \frac{\partial}{\partial x} \left(\rho \delta \frac{\partial m_A}{\partial x} \right) + \frac{\partial}{\partial y} \left(\rho \delta \frac{\partial m_A}{\partial y} \right) \qquad (3.7)$$

The viscous stress tensor for a Newtonian fluid can be expressed as follows (B2)::

$$\tau_{xx} = - \mu \left\{ 2 \frac{\partial u}{\partial x} - \frac{2}{3} (\nabla \cdot U) \right\}$$

$$\tau_{yy} = - \mu \left\{ 2 \frac{\partial v}{\partial y} - \frac{2}{3} (\nabla \cdot U) \right\} \qquad (3.8)$$

$$\tau_{xy} = \tau_{yx} = - \mu \left\{ \frac{\partial u}{\partial y} + \frac{\partial v}{\partial x} \right\}$$

where

$$\nabla \cdot U = \frac{\partial u}{\partial x} + \frac{\partial v}{\partial y}$$

which, by using the conservation of mass equation, yields:

$$\nabla \cdot U = -\frac{1}{\rho} \{ u \frac{\partial \rho}{\partial x} + v \frac{\partial \rho}{\partial y} \}$$

3.3 GENERAL TRANSPORT EQUATION

The set of five conservation equations (3.7) is the set of governing equations to be solved numerically. Following the method of Gosman et al. (G7, C5) we transform these five equations into one standard form so that they can all be treated by the same solution algorithm.

This standard form, also called "general transport equation", is given by equation (3.10) in rectangular coordinates:

$$\frac{\partial}{\partial x} (\rho u \phi) + \frac{\partial}{\partial y} (\rho v \phi) - \frac{\partial}{\partial x} (\Gamma \frac{\partial \phi}{\partial x}) - \frac{\partial}{\partial y} (\Gamma \frac{\partial \phi}{\partial y}) = S_\phi \qquad (3.10)$$

|← convection terms →| |← diffusion terms →| ↑ source term

Equation (3.10) describes the transport of a quantity represented as the variable ϕ. The first two terms account for convective transport of ϕ due to bulk motion of fluid. The following two terms represent diffusional transport of ϕ. The term on the right hand side, the "source term", accounts for any sources of transport of ϕ other than by convection and diffusion.

Conservation of Mass:

The equation of conservation of mass can be written in the form of the general transport equation where $\phi = 1$, $\Gamma = 0$ and $S_\phi = 0$. However this equation will not be solved directly but will be used to generate an equation for pressure, as will be shown further.

Conservation of Momentum:

x - component: Substitution of the viscous stress equation into the x - component conservation of momentum equation gives:

$$\rho\left[u\frac{\partial u}{\partial x} + v\frac{\partial u}{\partial y}\right] = -\frac{\partial P}{\partial x} + \frac{4}{3}\mu\frac{\partial^2 u}{\partial x^2} + \frac{1}{3}\mu\frac{\partial^2 v}{\partial x\partial y} + \mu\frac{\partial^2 u}{\partial y^2} + \rho g_x \qquad (3.11)$$

The continuity equation multiplied by u gives:

$$u\frac{\partial}{\partial x}(\rho u) + u\frac{\partial}{\partial y}(\rho v) = 0 \qquad (3.12)$$

Adding equations (3.11) and (3.12):

$$\rho u\frac{\partial u}{\partial x} + u\frac{\partial}{\partial x}(\rho u) + v\frac{\partial u}{\partial y} + u\frac{\partial}{\partial y}(\rho v) = -\frac{\partial P}{\partial x} + \frac{4}{3}\mu\frac{\partial^2 u}{\partial x^2} + \frac{1}{3}\mu\frac{\partial^2 v}{\partial x\partial y} + \mu\frac{\partial^2 u}{\partial y^2} + \rho g_x$$

and rearranging:

$$\frac{\partial}{\partial x}(\rho uu) + \frac{\partial}{\partial y}(\rho vu) - \frac{\partial}{\partial x}\left[\mu \frac{\partial u}{\partial x}\right] - \frac{\partial}{\partial y}\left[\mu \frac{\partial u}{\partial y}\right] = -\frac{\partial P}{\partial x} + \frac{1}{3}\mu \frac{\partial^2 u}{\partial x^2} + \frac{1}{3}\mu \frac{\partial^2 v}{\partial x \partial y} + \rho g_x$$

which is in the form of the general transport equation with:

$$\begin{cases} \phi = u \\ \Gamma = \mu \\ S_\phi = -\frac{\partial P}{\partial x} + \frac{1}{3}\mu \frac{\partial}{\partial x}(\nabla \cdot U) + \rho g_x \end{cases}$$

<u>y - component</u>: Substitution of the viscous stress equations into the y - component of the momentum equation gives:

$$\rho \left[u \frac{\partial v}{\partial x} + v \frac{\partial v}{\partial y} \right] = -\frac{\partial P}{\partial y} + \mu \frac{\partial^2 v}{\partial x^2} + \frac{1}{3}\mu \frac{\partial^2 u}{\partial y \partial x} + \frac{4}{3}\mu \frac{\partial^2 v}{\partial y^2} \qquad (3.13)$$

The continuity equation multiplied by v is:

$$v \frac{\partial}{\partial x}(\rho u) + v \frac{\partial}{\partial y}(\rho v) = 0 \qquad (3.14)$$

Adding equations (3.13) and (3.14) gives:

$$\rho u \frac{\partial v}{\partial x} + v \frac{\partial}{\partial x}(\rho u) + \rho v \frac{\partial v}{\partial y} + v \frac{\partial}{\partial y}(\rho v) = -\frac{\partial P}{\partial y} + \mu \frac{\partial^2 v}{\partial x^2} + \frac{1}{3}\mu \frac{\partial^2 u}{\partial y \partial x} + \frac{4}{3}\mu \frac{\partial^2 v}{\partial y^2}$$

and by rearranging:

$$\frac{\partial}{\partial x}(\rho uv) + \frac{\partial}{\partial y}(\rho vv) - \frac{\partial}{\partial x}\left[\mu \frac{\partial v}{\partial x}\right] - \frac{\partial}{\partial y}\left[\mu \frac{\partial v}{\partial y}\right] = -\frac{\partial P}{\partial y} + \frac{1}{3}\mu \frac{\partial}{\partial y}\left[\frac{\partial u}{\partial x} + \frac{\partial v}{\partial y}\right]$$

which is in the form of the general transport equation with:

$$\begin{cases} \phi = v \\ \Gamma = \mu \\ S_\phi = -\dfrac{\partial P}{\partial y} + \dfrac{1}{3}\mu \dfrac{\partial}{\partial y}(\nabla \cdot U) \end{cases}$$

Conservation of Energy:

Since specific heat capacities of dry air and water vapour are only weak functions of temperature, their variation within a small control volume is negligible. This simplification eliminates the ∂C_p terms in the equation of energy conservation (3.7) and gives:

$$\rho u \frac{\partial T}{\partial x} + \rho v \frac{\partial T}{\partial y} = \frac{1}{C_p}\frac{\partial}{\partial x}\left(\lambda \frac{\partial T}{\partial x}\right) + \frac{1}{C_p}\frac{\partial}{\partial y}\left(\lambda \frac{\partial T}{\partial y}\right) + \delta\rho \frac{C_{pA} - C_{pB}}{C_p}\left[\frac{\partial m_A}{\partial x}\frac{\partial T}{\partial x} + \frac{\partial m_A}{\partial y}\frac{\partial T}{\partial y}\right] \qquad (3.15)$$

Multiplying the continuity equation by T gives:

$$T\frac{\partial}{\partial x}(\rho u) + T\frac{\partial}{\partial y}(\rho v) = 0 \qquad (3.16)$$

Adding Equations (3.15) and (3.16) yields:

$$\rho u \frac{\partial T}{\partial x} + T \frac{\partial}{\partial x} (\rho u) + \rho v \frac{\partial T}{\partial y} + T \frac{\partial}{\partial y} (\rho v) = \frac{1}{C_p} \frac{\partial}{\partial x} (\lambda \frac{\partial T}{\partial x}) + \frac{1}{C_p} \frac{\partial}{\partial y} (\lambda \frac{\partial T}{\partial y})$$

$$+ \delta\rho \frac{Cp_A - Cp_B}{C_p} \left[\frac{\partial m_A}{\partial x} \frac{\partial T}{\partial x} \quad \frac{\partial m_A}{\partial y} \frac{\partial T}{\partial y} \right] \qquad (3.17)$$

Combining the terms of the left hand side, and noting that:

$$\begin{cases} \frac{1}{C_p} \frac{\partial}{\partial x}\left(\lambda \frac{\partial T}{\partial x}\right) = \frac{\partial}{\partial x}\left(\frac{\lambda}{C_p} \frac{\partial T}{\partial x}\right) - \lambda \frac{\partial T}{\partial x} \frac{\partial}{\partial x}\left(\frac{1}{C_p}\right) \\ \frac{1}{C_p} \frac{\partial}{\partial y}\left(\lambda \frac{\partial T}{\partial y}\right) = \frac{\partial}{\partial y}\left(\frac{\lambda}{C_p} \frac{\partial T}{\partial y}\right) - \lambda \frac{\partial T}{\partial y} \frac{\partial}{\partial y}\left(\frac{1}{C_p}\right) \end{cases}$$

enables us to rewrite Equation (3.17) in the following form:

$$\frac{\partial}{\partial x} (\rho u T) + \frac{\partial}{\partial y} (\rho v T) - \frac{\partial}{\partial x} \left[\frac{\lambda}{C_p} \frac{\partial T}{\partial x} \right] - \frac{\partial}{\partial y} \left[\frac{\lambda}{C_p} \frac{\partial T}{\partial y} \right] = - \lambda \frac{\partial T}{\partial x} \frac{\partial}{\partial x} (\frac{1}{C_p})$$

$$- \lambda \frac{\partial T}{\partial y} \frac{\partial}{\partial y} (\frac{1}{C_p}) + \delta\rho \frac{Cp_A - Cp_B}{C_p} \left[\frac{\partial m_A}{\partial x} \frac{\partial T}{\partial x} + \frac{\partial m_A}{\partial y} \frac{\partial T}{\partial y} \right]$$

which is in the form of the general transport equation with:

$$\begin{cases} \phi = T \\ \Gamma = \lambda/C_p \\ S_\phi = \delta\rho \dfrac{Cp_A - Cp_B}{C_p} \left[\dfrac{\partial m_A}{\partial x} \dfrac{\partial T}{\partial x} + \dfrac{\partial m_A}{\partial y} \dfrac{\partial T}{\partial y} \right] - \lambda \left[\dfrac{\partial T}{\partial x} \dfrac{\partial}{\partial x} \left(\dfrac{1}{C_p}\right) + \dfrac{\partial T}{\partial y} \dfrac{\partial}{\partial y} \left(\dfrac{1}{C_p}\right) \right] \end{cases}$$

Conservation of Species:

Rearranging the terms of the species equation transforms it into the general form of the transport equation:

$$\frac{\partial}{\partial x} (\rho u m_A) + \frac{\partial}{\partial y} (\rho v m_A) - \frac{\partial}{\partial x} \left[\rho\delta \frac{\partial m_A}{\partial x} \right] - \frac{\partial}{\partial y} \left[\rho\delta \frac{\partial m_A}{\partial y} \right] = 0$$

with
$$\begin{cases} \phi = m_A \\ \Gamma = \delta\rho \\ S_\phi = 0 \end{cases}$$

A summary of all the governing equations in the standard form is given in Table 3.1.

3.4 BOUNDARY CONDITIONS

With the four governing equations, listed on Table 3.1, must be associated the boundary conditions at the five boundaries of the flow field, indicated on Figure (3.1). The conditions at these five boundaries are detailed below.

Table 3.1

<u>General Form of the Transport Equation</u>

$$\frac{\partial}{\partial x}(\rho u \phi) + \frac{\partial}{\partial y}(\rho v \phi) - \frac{\partial}{\partial x}\left(\Gamma \frac{\partial \phi}{\partial x}\right) - \frac{\partial}{\partial y}\left(\Gamma \frac{\partial \phi}{\partial y}\right) = S_\phi$$

Equation	ϕ	Γ	S_ϕ
x-momentum	u	μ	$-\frac{\partial P}{\partial x} + \frac{1}{3}\mu \frac{\partial}{\partial x}(\nabla \cdot U) + \rho g_x$
y momentum	v	μ	$-\frac{\partial P}{\partial y} + \frac{1}{3}\mu \frac{\partial}{\partial y}(\nabla \cdot U)$
Energy	T	λ/C_p	$\delta\rho \frac{C_{p_A} - C_{p_B}}{C_p}\left[\frac{\partial m_A}{\partial x}\frac{\partial T}{\partial x} + \frac{\partial m_A}{\partial y}\frac{\partial T}{\partial y}\right] - \lambda\left[\frac{\partial T}{\partial x}\frac{\partial}{\partial x}\left(\frac{1}{C_p}\right) + \frac{\partial T}{\partial y}\frac{\partial}{\partial y}\left(\frac{1}{C_p}\right)\right]$
Species	m_A	$\delta\rho$	0

Boundary I

Nozzle exit: Fully developed parabolic profile

$$U = \frac{3}{2}\,\overline{U}\left[1 - \left(\frac{r}{R}\right)^2\right]$$

where the mean velocity U is fixed by the choice of the Reynolds number: $\overline{U} = \mu Re/\rho D$, and since for $x = 0$ we have $r = |\, y-y_0 \,| \cos\theta$ (see Figure 3.1) where

y_0 = ordinate of jet centerline on exit plane

and $y_R = R/\cos\theta$

the velocity at the nozzle exit can also be written:

$$U = \frac{3}{2}\,\overline{U}\left[1 - \left(\frac{|\, y-y_0 \,| \cos\theta}{y_R \cos\theta}\right)^2\right]$$

so that the boundary conditions are finally:

$$\begin{cases} u = \frac{3}{2}\,\overline{U}\left[1 - \left(\frac{y-y_0}{y_R}\right)^2\right]\cos\theta \\ v = \frac{3}{2}\,\overline{U}\left[1 - \left(\frac{y-y_0}{y_R}\right)^2\right]\sin\theta \\ T = \text{prescribed value } T_j \\ m_A = \text{prescribed value } m_j \end{cases}$$

Boundary II

Plate confinement: no-slip, non-evaporative, impermeable, isothermal wall at the temperature of the inlet jet, i.e.

$$u = 0; \quad v = 0; \quad T = T_j; \quad \partial m_A/\partial x = 0$$

Boundary III

Impingement plate: evaporative, permeable, isothermal wall with a thin film of liquid water (i.e. free unbound moisture) at the surface, where uniform suction may be applied.

The y-component of the velocity along this plate is v = 0.

For the normal component an analysis of the mass transport phenomena in the vicinity of the plate is required. The resultant velocity along the impingement plate is a vector sum of the evaporation velocity and of the prescribed suction velocity which is superimposed on it.

Assuming negligible solubility of dry air in water, the evaporation velocity can be derived starting from Fick's first law in terms of n_A, the mass flux relative to stationary coordinates:

$$n_A = - m_A \left(n_A + n_B \right) - \rho \delta_{AB} \nabla m_A \qquad (3.18)$$

where δ_{AB} is the mass diffusivity in $m^2 s^{-1}$

m_A is the mass fraction of A $\quad (m_A = \rho_A/\rho)$

n_A and n_B are the mass fluxes of species A and B, respectively, in $kg.m^{-2}.s^{-1}$.

This equation shows that the diffusion flux n_A relative to stationary coordinates is the resultant of two vector quantities: the vector

$$m_A \left(n_A + n_B \right)$$

which is the mass flux of A resulting from bulk motion of the fluid, and the vector

$$j_A = -\rho\delta_{AB}\nabla m_A$$

which is the molar flux of A resulting from diffusion superimposed on the bulk flow.

In our case, where the evaporating system has attained a steady state, there is a net motion of A away from the evaporating surface. In the vicinity of this surface the bulk flow can be neglected since there is no tangential slip ($v = 0$) and since the present calculation of the evaporation velocity does not involve suction, which will be accounted for subsequently by adding the term u_{suc} to the velocity. As the flux of the non-evaporating component B at evaporating surface is zero, Equation (3.18) with $n_B = 0$ gives:

$$n_A = -\frac{\rho\delta}{1 - m_A}\nabla m_A$$

According to our assumptions the evaporation is normal to the plate, so that we can solve for $n_{A,x}$:

$$n_{A,x} = -\frac{\rho\delta}{1 - m_A}\frac{\partial m_A}{\partial x}$$

and since $n_{A,x} = \rho_A u_A$ where u_A is the velocity of species A, noting that $\rho/\rho_A = 1/m_A$ we can write:

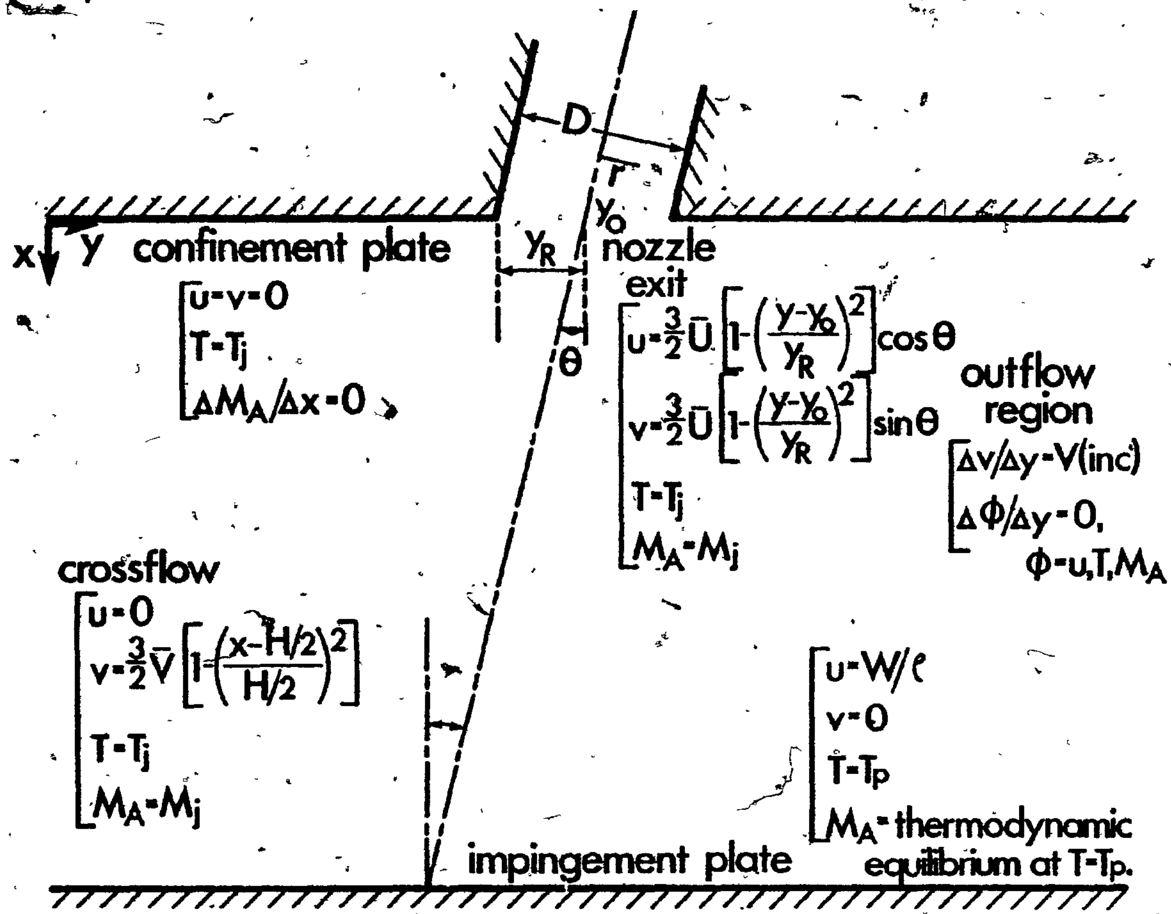

Figure 3.1 : Boundary conditions.

$$u = \frac{-\delta}{\dot{m}_A\,(1 - m_A)}\,\frac{\partial m_A}{\partial x}$$

Noting that $u = m_A u_A + m_B u_B$, but with $u_B = 0$ in the present case, and adding the term for suction finally yields the following boundary condition for the velocity in this region:

$$u = -\frac{\delta}{(1 - m_A)}\,\frac{\partial m_A}{\partial x} + u_{suc}$$

Note that since the mass transfer rate is unknown before the problem is solved, being part of the solution to the problem, the u component boundary condition along the impingement plate is of an iterative nature.

Although provision has been made in the last equation to incorporate the influence of suction, this parameter has not been investigated because of time limitations. Therefore for the present study $u_{suc} = 0$.

The boundary condition for the mass fraction of water vapour along the plate is:

$$m_A = \frac{P_{sat}\,MW_A}{(P_{sat})MW_A + (P-P_{sat})MW_B}$$

This boundary condition is derived by assuming existence of thermodynamic equilibrium between liquid water and water vapour. Also Raoult's law which assumes ideal solution and no differences between fugacities and pressures, is used. These are reasonable assumptions in the present case because the solubility of air in water under the temperature range investigated is negligible (H1), and because the operating pressure is low.

Boundary IV:

Outflow region.

The two different cases of impingement in the absence and in the presence of crossflow must be examined separately.

(i) In the absence of crossflow: In this case there are of course two outflow regions, situated at the open extremities of the impingement flow field (see Figure 1.2). Because of entrainment of fluid by the confined jet, a recirculation zone is formed between the confinement and impingement plates. Two flow patterns are possible at this boundary. Depending on the size of the impingement and confining plates (the two being in all cases of the same size) this recirculation bubble may either be completely enclosed, for wide plates, or cut by the outflow boundary in the case of narrow plates. In the first case, fluid flows out at all points across this boundary. In the second case, however, there are regions of inflow and outflow adjacent, respectively, to the confinement and impingement surfaces.

The manner in which the y-direction velocity, v, is specified is valid for both the above cases. Before a converged solution is obtained, the mass residues for each control volume can be relatively large. Within each iterative cycle, as the computation marches towards the boundary, the resulting v-velocity profile generally leads to an overall mass accumulation inside the physical system. In order to fulfill the overall mass balance, a correction must be made at each iteration so that the overall mass inflow equals the overall mass outflow. This can be done by writing:

$$v(J=1) = v(J=2) + \frac{1}{2}v_{inc}$$

$$v(J=NJ) = v(J=NJ-1) + \frac{1}{2}v_{inc} \quad (3.19)$$

In these equations, $v(J=1)$ and $v(J=2)$ are the v-components of the velocity along and immediately inside the outflow boundary respectively for the left side. And $v(J=NJ)$ and $v(J=NJ-1)$ are the v-components of the velocity along and immediately inside the outflow boundary respectively for the right side. The term v_{inc} is the correction term determined by:

$$v_{inc}\int_{\text{Bound. IV}} \rho dA = \int_{\text{Bound. I,III}} \rho u dA - \int_{\text{Bound. IV}} \rho v^* dA$$

where v^* is taken one grid point inside Boundary IV, i.e. stands for $v(J=2)$ and $v(J=NJ-1)$ on the left and right hand side of the flow field respectively.

Note that the right hand side of this equation represents the net mass accumulation inside the physical boundaries. Equations (3.19) mean that the shape of the velocity profile calculated in each iteration is retained, but scaled to satisfy the overall mass balance. The corrected value of v at Boundary IV will affect the adjacent points and the effect, in general, carries into the entire flow field. This correction is applicable regardless of wether or not an inflow occurs at this boundary.

The boundary conditions for u, T, and m_A are established by specifying no more variation in the y-direction for these variables at Boundary IV, i.e. $\partial/\partial y = 0$. This boundary condition is correct when there is only outflow at this boundary, but in the regions where inflow occurs it is somehow paradoxical as it implies determination of upstream conditions from downstream conditions. Van Heiningen (V2) who studied various possible boundary conditions at the outflow boundary for a semi-confined laminar slot jet came to the conclusion that the impingement region flow field and heat transfer are insensitive to variations in specifications of boundary conditions at the outflow, provided that this flow boundary is sufficiently distant from the impingement region. Saad (S2) and Huang (H2) have used succesfully the equivalent condition of zero radial variation at this boundary in their numerical studies of round jet impingement. Li (L2) also used this formulation for the outflow boundary condition in his laminar round jet simulation with an impingement plate significantly smaller than that of the present study. He showed that using a larger impingement plate (i.e. having the outflow boundary conditions specified further from the impingement region) has a noticeable effect only over the outer part of the plate, whereas the impingement region results are unaffected.

In view of this analysis, the $\partial/\partial y = 0$ boundary condition was adopted over the entire Boundary IV.

(ii) <u>In the presence of crossflow</u>: In this case the outflow region is located on the right hand side of the domain of interest, whereas the left hand side, the source of the crossflow, constitutes Boundary V (see Figure 3.1)

As in subsection (i), two flow patterns are possible, i.e. with the recirculation being totally or only partially enclosed. Again, a correction must be made at each iteration in order to fulfill the overall mass balance. This is done by writing:

$$v(J=NJ) = v(J=NJ-1) + v_{inc}$$

where the correction term v_{inc} is determined by:

$$v_{inc}\int_{\text{Bound.IV}} \rho dA = \int_{\text{Bound.I,III}} \rho u dA + \int_{\text{Bound.V}} \rho v dA - \int_{\text{Bound.IV}} \rho v^* dA$$

Following the discussion given in subsection (i), the same boundary condition is taken for u, T, and m_A, namely $\frac{\partial}{\partial y} = 0$.

Boundary V:

Crossflow entry.

The crossflow, of temperature and water vapour content identical to that of the inlet jet, enters parallel to the confinement and impingement plates.

The crossflow is specified to have a fully developed velocity profile:

$$V = \frac{3}{2}\overline{V}\left[1 - \left(\frac{|x - H/2|}{H/2}\right)^2\right]$$

The magnitude of the crossflow is defined by the ratio, M, of the crossflow volumetric flow rate to the jet volumetric flow rate:

$$M = \frac{\overline{V}\,H}{\overline{U}\,D}$$

where $\bar{V}$ is the mean velocity of the crossflow at its entry. As the crossflow and the jet flow are of the same fluid (air in this case) at the same temperature, and at essentially the same pressure, the density and viscosity are also effectively the same. Thus M may also be regarded as the mass flow rate ratio between the crossflow and the jet flow, or as the corresponding ratio of the Reynolds numbers of the crossflow and the jet flow.

Hence Boundary V is defined by:

$$\left[\begin{array}{l} u = 0 \\ v = \frac{3}{2}\bar{V}\left[1 - \left(\frac{x - H/2}{H/2}\right)^2\right] \\ T = T_j \\ m_A = m_j \end{array}\right.$$

Note that Boundary V does not exist in the limiting case, included in this study, where there is no crossflow.

3.5 FLUID PROPERTY EQUATIONS

The fluid throughout the flow field is assumed to be an ideal mixture of water vapour (species A) and dry air (species B).

The effect of variable temperature and composition on all fluid properties is considered. Because the pressure variations encountered in the present study are small, the effect of pressure on all fluid properties, except density and mass diffusivity, is assumed to be negligible. Second order polynomials were derived from available data to express the dependance of each fluid property of interest on temperature. These polynomials were used by Li (L2) and gave satisfactory results.

3.5.1 Density

Within the temperature range of 300°K to 600°K and approximately 10^5 N/m^2 pressure (1 atm), the compressibility factor for air is sufficiently close to one that the ideal gas law is applicable, giving:

$$\rho = P\,\overline{MW}/RT$$

where R = gas constant = 8 314.2 J/kilo-gmole °K

$\overline{MW}$ = the mixture molecular weight, expressed as (B2)

$$1/\overline{MW} = m_A/MW_A + m_B/MW_B$$

3.5.2 Viscosity

(i) Water Vapour

Based on their own experimental data, Thomas and Jackson (T1) proposed the following equation for the dynamic viscosity of water vapour:

$$\mu_A = (0.99354\ E\text{-}6) + (0.27067\ E\text{-}7)T + (0.88906\ E\text{-}11)T^2$$

where μ = dynamic viscosity, kg/m.s

T = temperature, °K

All their data were taken between 500°K and 800°K, and the average deviation of data from the equation is 1.88%. Comparison of results from the equation with other existing data (H6, B1) for temperatures as low as 273°K is also satisfactory.

(ii) Dry Air

Data for viscosity of dry air reported in reference (H6) are fitted to a second degree function of temperature using the least squares method. The resulting equation is:

$$\mu_B = (0.25641\ E{-}5) + (0.60198\ E{-}7)T - (0.23723)T^2$$

Comparison of results with data from other sources (B1) is satisfactory (L2); the average deviation being only 1.4% over the temperature range 350°K to 450°K.

(iii) Mixtures

The variation of viscosity of binary mixtures with composition is usually not linear, and mixture viscosities are often larger than the values predicted by mole-fraction average. At low pressures, Reid and Sherwood (R2) recommend use of Wilke (W3) estimation method for mixtures. For binary mixtures of dry air and water vapour, the Wilke formulation is:

$$\mu = \mu_A / [\ 1 + (x_B/x_A)\ \phi_{AB}]\ \ + \mu_B / [\ 1 + (x_A/x_B)\ \phi_{BA}\ ]$$

where x = mole-fraction

$$\phi_{AB} = [\ 1 + 1.126\ \sqrt{\mu_A/\mu_B}\ ]^2 / 3.6022$$

$$\phi_{BA} = [\ 1 + 0.888\ \sqrt{\mu_B/\mu_A}\ ]^2 / 4.5674$$

For reduced temperature of approximately 2, which is within the temperature range under investigation, viscosities of dry air and water vapour are independent of pressure up to about 10^6 N/m^2 (B1).

3.5.3 Specific Heat Capacity

(i) Water Vapour

Crotogino (C3) recommends the following regression equation for the specific heat of water vapour:

$$C_{pA} = (0.18241\ E{-}4) + (0.21976)T + (0.23487\ E{-}3)T^2$$

where C_p = specific heat capacity J/kg.°K

(ii) Dry Air

A least squares fit of the data given in reference (H6) for the specific heat of dry air between 300°K and 600°K gives:

$$C_{pB} = (0.10256\ E{-}4) - (0.17317)T + (0.36146\ E{-}3)T^2$$

Comparison of the results with those tabulated in the CRC Handbook (B1) shows negligible difference between the experimental data and the least squares equation.

(iii) Mixture

The specific heat of the binary mixture is assumed to be a mass-fraction average of the individual species (B2):

$$C_p = C_{pA}\, m_A + C_{pB}\, m_B$$

3.5.4 Thermal Conductivity

(i) Water Vapour

A least squares fit of the tabulated data in the CRC Handbook (B1) to a second degree function of temperature, gives:

$$\lambda_A = (0.86868\ E\text{-}2) + (0.11318\ E\text{-}4)T + (0.85793\ E\text{-}7)T^2$$

where λ = thermal conductivity, W/m °K

Comparison with data from other sources (H6) in the temperature range of 373°K to 600°K shows average and maximum deviation of approximately 2% and 4% respectively (L2).

(ii) Dry Air

Thermal conductivity data for dry air is reported in reference (B1). A least squares fit of these data gives:

$$\lambda_B = (0.38793\ E\text{-}3) + (0.95425\ E\text{-}4)T - (0.30699\ E\text{-}7)T^2$$

(iii) Mixture

Reid and Sherwood (R2) recommend the Lindsay and Bromley (L1) equation for the thermal conductivity of a mixture of polar and non-polar gases:

$$\lambda = \lambda_A / \{1 + (x_B/x_A)\Phi_{AB}\} + \lambda_B / \{1 + (x_A/x_B)\Phi_{BA}\}$$

where

$$\Phi_{AB} = \frac{1}{4}\left[1 + \sqrt{1.428\,\frac{\mu_A}{\mu_B}\,\frac{1 + 410/T}{1 + 120/T}}\right]^2 \frac{1 + 155/T}{1 + 410/T}$$

$$\Phi_{BA} = \frac{1}{4}\left[1 + \sqrt{\frac{1}{1.428}\,\frac{\mu_B}{\mu_A}\,\frac{1 + 120/T}{1 + 410/T}}\right]^2 \frac{1 + 155/T}{1 + 120/T}$$

The Lindsay-Bromley equation is estimated by Cheung to have an average error of 2.1% with a maximum error of 6.9% (R2).

3.5.5 Mass Diffusivity

The variation of mass diffusivity of a mixture of air and water vapour with temperature and pressure can be estimated by using the following well known equation:

$$P\delta = CT^n$$

where δ = mass diffusivity, m^2/s.

Various researchers suggest different values for n, which range from 1.5 to 2.3 in the literature (B2, T2). Careful review of the literature shows that n is calculated using experimental data for low temperature ranges only (L4). Little experimental work on diffusivity has been reported for even moderately elevated temperatures. The only notable high temperature study measurements of the diffusivity of the air-water vapour system was made by Klibanov (K6). The temperature covered ranges from 300°K to over 1500°K. The experimental data were correlated by Crotogino (C3) giving:

$$\delta = 0.2794\ E\text{-}4 - 0.1306\ E\text{-}6T + 0.4016\ E\text{-}9T^2 \quad \text{for } T \leq 521°K$$

$$\delta = -\ 0.1057\ E\text{-}3 + 0.335\ E\text{-}6T \quad \text{for } T \geq 521°K$$

3.5.6 Auxilliary Equations and Data

Saturated Vapour Pressure of Water Vapour

Its evaluation is necessary in order to specify the boundary condition for m_A along the impingement plate. Data tabulated in steam tables (B1) are fitted to an Antoine type of equation giving:

$$\ln P_{sat} = 23.365 - \frac{3919.9}{T + 42.062}$$

with P_{sat} = saturated vapour pressure of water vapour, N/m^2

<u>Molecular Weights</u>

The molecular weight of water vapour and of dry air, MW_A and MW_B respectively, are taken to be 18.02 and 28.97 g/gmole (T2).

CHAPTER 4

NUMERICAL FORMULATION

4.1 FINITE DIFFERENCE EQUATIONS

In this chapter the finite difference form of the general transport equation is established. There are many ways in which sets of algebraic equations can be constructed so as to simulate, in major respects, the behaviour of partial differential equations; but some ways are better than others in accuracy of simulation, convenience in use, and tendency to promote convergence in iterative solution procedures, Huang (H2) reviewed the various solution procedures which could be applied to solve problems of the present type and gave an extensive review of the literature. In the present study the finite difference equations are derived using the control volume integration technique (G7). Thus the general transport equation is integrated over a control volume.

The field of interest will be covered by a rectangular grid network. At each nodal point (intersection of the grid lines) the properties of the fluid (density, viscosity) are defined. Since these properties depend on the temperature, pressure and composition of the fluid, these variables (T, P, m_A) are also defined at the same point. Because all scalar quantities are calculated at grid line intersections, this type of grid is referred to as the scalar grid. The remaining variables are the two components of the velocity vector. It would also be possible to define them at the same grid points, but since the velocity is a result of pressure gradient, it is highly preferable to calculate velocity components at locations between the nodal points used for pressure. These velocity components are then calculated at points midway between the scalar nodes; these points are on the boundaries of the scalar control volumes.

One of the advantages of using such a "staggered" grid system is that it simplifies computation of mass flux into and out of the scalar grid control volume, as the velocity vectors u and v are located at the control volume boundary itself (Figure 4.1). The control volume of a node is the space which surrounds the node and is bounded midway between neighbouring nodes. It is important to note that, if the control volume is defined for ϕ, then ϕ should be at the center of the control volume. Hence, the control volumes for u and v are not the same as those for the scalar variables.

Two different approaches may be used to specify the physical boundaries, i.e. for the physical boundaries to coincide with the scalar grid lines or with the boundaries of the scalar grid control volumes. Since the boundary conditions for velocity are usually well specified at the physical boundaries, and since the specification of the physical properties at the wall boundaries is difficult and ambiguous, the physical boundaries are therefore chosen to coincide with the scalar control volume boundaries.

Having specified the variables and the control volume, one can integrate the transport equation over the corresponding volume, inside which the scalar properties are assumed constant. Thus:

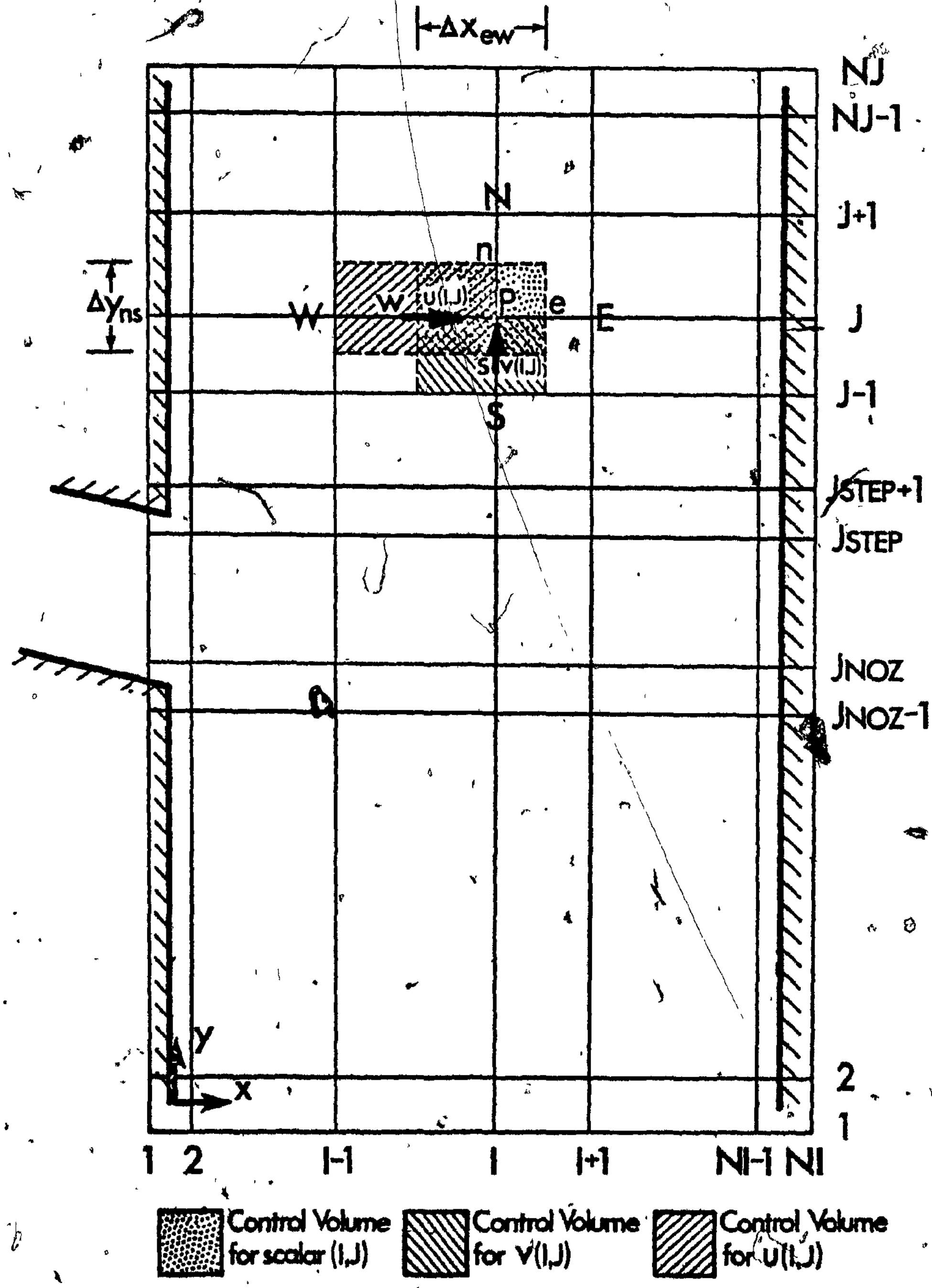

Figure 4.1 : Finite difference mesh.

$$\iint_V \left[\frac{\partial}{\partial x}(\rho u \phi) + \frac{\partial}{\partial y}(\rho v \phi) - \frac{\partial}{\partial x}\left(\Gamma \frac{\partial \phi}{\partial x}\right) - \frac{\partial}{\partial y}\left(\Gamma \frac{\partial \phi}{\partial y}\right)\right] dV = \iint_V S_\phi dV$$

using Gauss' theorem gives then:

$$\int_s^n \left[\rho u \phi - \Gamma \frac{\partial \phi}{\partial x}\right]\Bigg|_{\substack{\text{boundary}\\\text{surface}}} dy + \int_w^e \left[\rho v \phi - \Gamma \frac{\partial \phi}{\partial y}\right]\Bigg|_{\substack{\text{boundary}\\\text{surface}}} dx - \iint_V S_\phi dV = 0$$

that is:

$$\int_s^n \left[\left(\rho u \phi - \Gamma \frac{\partial \phi}{\partial x}\right)_e - \left(\rho u \phi - \Gamma \frac{\partial \phi}{\partial x}\right)_w\right] dy$$

$$+ \int_w^e \left[\left(\rho v \phi - \Gamma \frac{\partial \phi}{\partial y}\right)_n - \left(\rho v \phi - \Gamma \frac{\partial \phi}{\partial y}\right)_s\right] dx - \iint_V S_\phi dV = 0$$

or in short:

$$F_e - F_w + F_n - F_s - \iint_V S_\phi dV = 0 \qquad (4.1)$$

where the subscripts e, w, n, s indicate that the corresponding quantities are evaluated at the east, west, north and south boundaries respectively, and:

$$F_e = \int_s^n \left(\rho u \phi - \Gamma \frac{\partial \phi}{\partial x}\right)_e dy \qquad (4.2)$$

$$F_w = \int_s^n \left(\rho u \phi - \Gamma \frac{\partial \phi}{\partial x}\right)_w dy \qquad (4.3)$$

$$F_n = \int_w^e \left(\rho v \phi - \Gamma \frac{\partial \phi}{\partial y}\right)_n dx \qquad (4.4)$$

$$F_s = \int_w^e (\rho v\phi - \Gamma \frac{\partial\phi}{\partial y})_s \; dx \qquad (4.5)$$

$(F_e - F_w)$ represents the net flux of ϕ in the x-direction through the control volume, and $(F_n - F_s)$ represents the net flux in the y-direction. All geometric quantities and locations relative to an arbitrary scalar control volume are shown on Figure 4.1.

Equation (4.1) can be re-written under the more compact form

$$\sum_i F_i = S_{\phi,vol} \qquad (4.6)$$

where $\sum_i$ denotes summing over n, s, e, and w with appropriate signs,

and $S_{\phi,vol} = \iint_V S_\phi dV$

By assuming that transport across the control volume boundary is one-dimensional, flux expressions derived from one-dimensional flow theory can be used (C5), and approximate solutions for the F terms can be obtained (C5, S12). For the particular case of F_w this solution takes the following form:

$$F_w = \rho_w u_w A_w \left[f_w \phi_W + (1 - f_w)\, \phi_P \right] \qquad (4.7)$$

where $f_w = EXP(Pe)_w \,/\, \left[EXP(Pe)_w - 1\right]$

$(Pe)_w = \rho_w u_w \Delta x_{ew} \,/\, \Gamma_w$

$A_w = \Delta y_{ns}$ 1.0 (area of the boundary perpendicular to x-direction)

$\rho_w = (\rho_W + \rho_P) / 2$

$\Gamma_w = (\Gamma_W + \Gamma_P) / 2$

Note that the points P and W, and the intervals Δx_{ew} and Δy_{ns} as shown on Figure 4.1 correspond to the particular case of transport of a scalar variable; thus, when ϕ is a scalar (temperature, T, for example) the subscripts of Equation (4.7) correspond to points indicated on Figure 4.1. But if ϕ is a vector quantity, the figure will not be the same. For $\phi = u$, for example, the control volume to be considered is translated to the west since control volumes for vector and scalar variables do not coincide. Hence, when Equation (4.7) applies to the u-velocity, the subscripts represent points indicated on Figure 4.2. Similarly, when $\phi = v$ the domain of interest is shifted to the south and the points corresponding to the subscripts of Equation (4.7) have to be determined with respect to the v-velocity control volume of integration.

The calculation of exponentials by digital computers is relatively slow. However, by using Spalding's method (S12) to express exponentials in a simple algebraic form, computer time can be reduced. For any x,

$$\frac{e^x}{e^x - 1} \simeq \begin{cases} \frac{1}{2}\left(1 + \frac{2}{x}\right) & \text{if } |x| < 2 \\ 1 & \text{if } x > 2 \\ 0 & \text{if } x < -2 \end{cases}$$

Using this approximation and letting $a_W = \rho_W u_W A_W f_W$, and $C_W = \rho_W u_W A_W$ Equation (4.7) becomes:

$$F_W = a_W\,(\phi_W - \phi_P) + C_W \phi_P \tag{4.8}$$

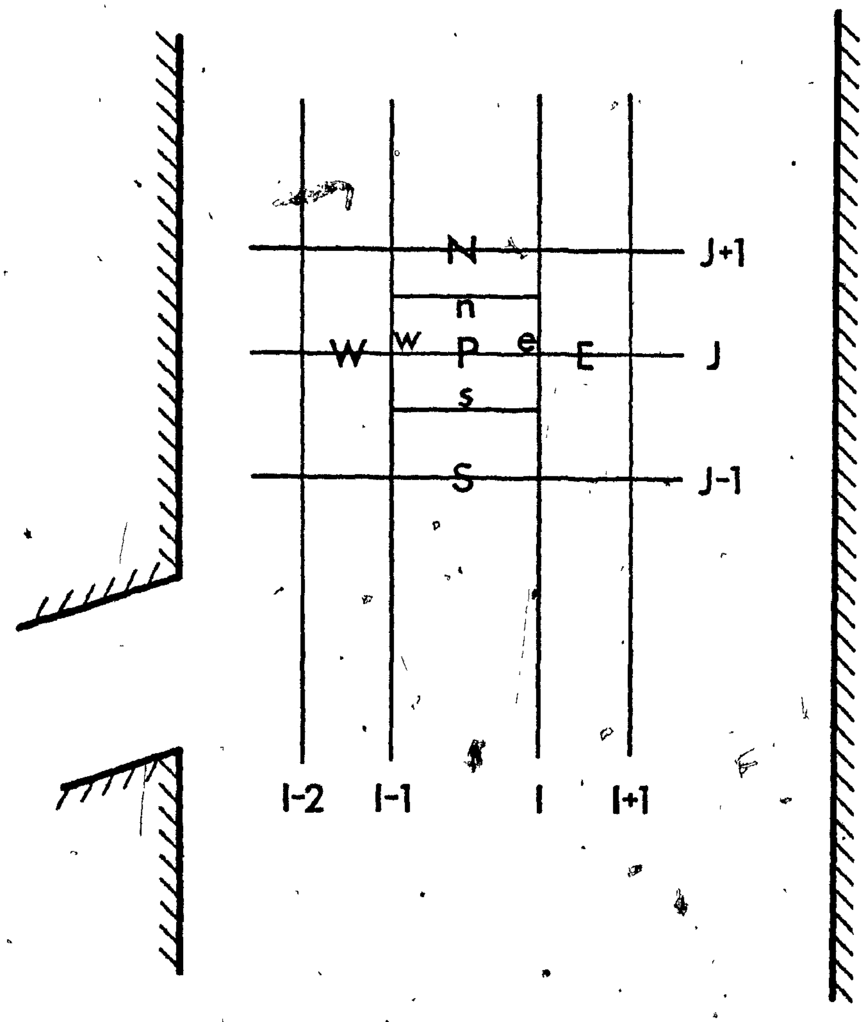

Figure 4.2 : Geometrical subscripts for a u-velocity control volume.

where

$$a_w \simeq \begin{cases} C_w \left(\frac{1}{2} + (Pe)_w^{-1} \right) & \text{when } |(Pe)_w| < 2 \\ C_w & \text{when } (Pe)_w > 2 \\ 0 & \text{when } (Pe)_w < -2 \end{cases}$$

Further, letting $D_w = \Gamma_w A_w / \Delta x_{ew}$, $(Pe)_w$ becomes C_w/D_w and the coefficient a_w becomes:

$$a_w \simeq \begin{cases} C_w/2 + D_w & \text{when } |C_w/2| < D_w \\ C_w & \text{when } C_w/2 > D_w \\ 0 & \text{when } C_w/2 < -D_w \end{cases} \tag{4.9}$$

The various expressions of a_w in Equation (4.9) can be expressed conveniently as:

$$a_w = \max \left(|C_w/2|, D_w \right) + \tfrac{1}{2} C_w \tag{4.10}$$

It should be recalled that, by definition, the C and D terms represent convective transfer and transfer due to diffusion, respectively. The parameter Pe, the local Peclet number is the ratio of convective to diffusive transfer rates. One can then see that, according to Equation (4.8) the total flux across the boundaries into or out of the control volume is a weighted sum of the convective and diffusive fluxes. For a local Peclet number between -2 and 2 both convective and diffusive transfers are of comparable magnitude. However, as the convective transfer increases and becomes dominant, the diffusive transfer can be neglected. Thus, for large $|C_w|$, the flux F_w across the west side boundary of the control volume becomes either $C_w\phi_W$ or $C_w\phi_P$ depending on the direction of the flow.

Equations (4.8) and (4.9) may be regarded as a hybrid of central and upwind-difference schemes (C5) in that they reduce to the former when $|Pe|$ is less than 2 but yield the latter for large values of $|Pe|$. Recalling the conclusion of Spalding (S12) that the upwind-difference scheme is preferable to the central-difference scheme when $|Pe|$ is greater than 2, it can be seen that the present hybrid scheme has the advantages of being more accurate over a wide range of Peclet numbers than either of its components (R3), and of yielding a diagonally-dominant matrix of coefficients for all Pe.

Applying the same principle for the other F terms and summing over n, s, e and w yields:

$$\sum_i F_i = \sum_i a_i\phi_i + \phi_P\sum_i C_i - \phi_P\sum_i a_i \qquad (4.11)$$

from definition of the C terms, it appears that the term $\sum_i C_i$ on the right hand side of Equation (4.11) represents the total mass accumulation in the control volume. From the continuity equation it can be equated to zero. Therefore:

$$\sum_i F_i = \sum_i a_i\phi_i - \phi_P\sum_i a_i \qquad (4.12)$$

Substituting into the original transport equation (in the form of Equation (4.6)) yields the following equation:

$$\sum_i a_i \phi_i - \phi_P \sum_i a_i = S_{\phi,vol}$$

where the subscript i stands for e, n, w and s, and $S_{\phi,vol} = \iint_V S_\phi dV$ is the integral of the source term over the control volume.

4.2 CALCULATION OF THE SOURCE TERMS

The evaluation of $S_{\phi,vol}$ for u, v, m and T is necessary. Each of them are obtained by integrating the corresponding S_ϕ's over the control volume, and the final form is expressed in a finite difference form.

4.2.1 x-component of velocity vector, u

$$S^u_{\phi,vol} = \iint_V S_u dxdy \; 1.0$$

$$S^u_{\phi,vol} = 1.0 \left\{ \iint \left[-\frac{\partial P}{\partial x} + \frac{1}{3} \mu \frac{\partial}{\partial x} \left(\frac{\partial u}{\partial x} + \frac{\partial v}{\partial y} \right) + \rho g \right] dxdy \right\}$$

and with the equation of conservation of mass:

$$S^u_{\phi,vol} = 1.0 \left\{ \iint \left[-\frac{\partial P}{\partial x} - \frac{1}{3} \frac{\mu}{\rho} \frac{\partial}{\partial x} \left(u \frac{\partial \rho}{\partial x} + v \frac{\partial \rho}{\partial y} \right) + \rho g \right] dxdy \right\}$$

$$S^{u}_{\phi,vol} = 1.0\left\{\iint\left[\int -\frac{\partial P}{\partial x}\,dx\right]dy - \frac{1}{3}\frac{\mu}{\rho}\int\left[\int\frac{\partial}{\partial x}\left(u\,\frac{\partial\rho}{\partial x}\right)dx\right]dy\right.$$

$$\left. + \frac{1}{3}\frac{\mu}{\rho}\int\left[\int\frac{\partial}{\partial x}\left(v\,\frac{\partial\rho}{\partial y}\right)dx\right]dy + \iint\rho g\,dxdy\right.$$

$$S^{u}_{\phi,vol} = \int\left(P\Big|_{e}^{w}\right)dy + \frac{1}{3}\frac{\mu}{\rho}\int\left(u\,\frac{\partial\rho}{\partial x}\right)\Big|_{e}^{w}dy - \frac{1}{3}\frac{\mu}{\rho}\int\left(v\,\frac{\partial\rho}{\partial y}\right)\Big|_{e}^{w}dy$$

$$+ (\rho g)\Big|_{p}\iint dxdy \quad 1.0$$

$$S^{u}_{\phi,vol} = 1.0\left\{P\Big|_{e}^{w}\Delta y_{ns} + \frac{1}{3}\left[\frac{\mu}{\rho}\left(u\,\frac{\Delta\rho}{\Delta x} + v\,\frac{\Delta\rho}{\Delta y}\right)\right]\Big|_{e}^{w}\Delta y_{ns} + (\rho g)\Big|_{p}\Delta x_{ew}\Delta y_{ns}\right\} \tag{4.14}$$

note that the subscripts e, w, n, s and P are relative to the control volume of u.

4.2.2 y-component of velocity vector, v.

$$S^{v}_{\phi,vol} = 1.0 \iint_{V} S_{v}\,dxdy$$

$$S^{v}_{\phi,vol} = 1.0\iint\left\{-\frac{\partial P}{\partial y} - \frac{1}{3}\,\mu\,\frac{\partial}{\partial y}\left[\frac{1}{\rho}\left(u\,\frac{\partial\rho}{\partial x} + v\,\frac{\partial\rho}{\partial y}\right)\right]\right\}dxdy$$

$$S^{v}_{\phi,vol} = 1.0\left\{\int\left[\int -\frac{\partial P}{\partial y}\,dy\right]dx - \int\left[\int\frac{1}{3}\,\mu\,\frac{\partial}{\partial y}\left(\frac{1}{\rho}\,u\,\frac{\partial\rho}{\partial x} + \frac{1}{\rho}\,v\,\frac{\partial\rho}{\partial y}\right)dy\right]dx\right\}$$

$$S^{v}_{\phi,vol} = 1.0 \left\{ \int P\Big|_n^s dx + \int \left[\frac{1}{3} \mu \left(\frac{1}{\rho} u \frac{\partial\rho}{\partial x} + \frac{1}{\rho} v \frac{\partial\rho}{\partial y} \right)\Big|_n^s \right] dx \right.$$

$$S^{v}_{\phi,vol} = 1.0 \left\{ P\Big|_n^s \Delta x_{ew} + \frac{1}{3} \left(\frac{\mu}{\rho} \left(u \frac{\Delta\rho}{\Delta x} + v \frac{\Delta\rho}{\Delta y} \right) \right)\Big|_n^s \Delta x_{ew} \right\} \quad (4.15)$$

note that the subscripts e, w, n, s are relative to the control volume of v.

4.2.3 Energy equation

$$S^{T}_{\phi,vol} = 1.0 \iint_V S_T dxdy$$

$$S^{T}_{\phi,vol} = 1.0 \iint \left\{ \delta\rho \frac{C_{p_A} - C_{p_B}}{C_p} \left[\frac{\partial m_A}{\partial x} \frac{\partial T}{\partial x} + \frac{\partial m_A}{\partial y} \frac{\partial T}{\partial y} \right] - \lambda \left[\frac{\partial T}{\partial x} \frac{\partial}{\partial x} \left(\frac{1}{C_p} \right) + \frac{\partial T}{\partial y} \frac{\partial}{\partial y} \left(\frac{1}{C_p} \right) \right] \right\} dxdy$$

$$S^{T}_{\phi,vol} = 1.0 \left\{ \delta\rho \frac{C_{p_A} - C_{p_B}}{C_p} \left[\frac{\Delta m_A}{\Delta x} \frac{\Delta T}{\Delta x} + \frac{\Delta m_A}{\Delta y} \frac{\Delta T}{\Delta y} \right] - \lambda \left[\frac{\Delta T}{\Delta x} \frac{\Delta}{\Delta x} \left(\frac{1}{C_p} \right) + \frac{\Delta T}{\Delta y} \frac{\Delta}{\Delta y} \left(\frac{1}{C_p} \right) \right] \right\} \Delta x \Delta y \quad (4.16)$$

4.2.4 Species Equation

$$S^{m_A}_{\phi,vol} = \iint_V S_m dydx = 0 \qquad (4.17)$$

4.2.5 Modification of source term for stability

The finite difference equations derived in the previous section constitute a set of non-linear algebraic equations to be solved iteratively. The stability of the iterative solution scheme must then be examined.

Consider a set of algebraic equations of the form

$$x_i = \sum_{j \neq i} (a_{ij} x_j) + b_i$$

where the x's are any unknown variable vectors. If the equations are linear, i.e. a's and b's are constants, the use of algebraic equations as substitution formulae in iterative procedures is stable and yields convergent solutions when

$$\left\{ \begin{array}{ll} \sum_{j \neq i} |a_{ij}| \leq 1 & \text{for each } i \\ \text{and } \sum_{j \neq i} |a_{ij}| < 1 & \text{for at least one } i \end{array} \right. \qquad (4.18)$$

For non-linear equations, these conditions are often sufficient, although they may not be the necessary condition for convergence (C5).

In order that our system of equations satisfies these conditions, and also to avoid numerical problems when the coupling coefficients are zero during an iteration, we will introduce a false source term, S_{false}, into Equation (4.13) as follows:

$$S_{false} = \max\,(\text{net mass outflow from control volume}, 0.0)\,(\phi_P' - \phi_P)$$

or $$S_{false} = \max\,(\sum_i C_i, 0.0)\,(\phi_P' - \phi_P)$$

where the superscript prime indicates values from the previous iteration. Note that S_{false} will not affect the final results for converged solutions.

$$\phi_P \sum_i a_i = \sum_i a_i \phi_i - S_{\phi,vol} + \max(\sum_i C_i, 0.0)\,(\phi_P' - \phi_P)$$

or $$\phi_P \left\{ \sum_i a_i + \max(\sum_i C_i, 0.0) \right\} = \sum_i a_i \phi_i - S_{\phi,vol} + \phi_P' \max\,(\sum_i C_i, 0.0)$$

or $$\phi_P A_P = \sum_i a_i \phi_i + Su \qquad (4.19)$$

where $$A_P = \sum_i a_i + \max(\sum_i C_i, 0.0)$$

$$Su = -S_{\phi,vol} + \max\,(\sum_i C_i, 0.0)\,\phi_P' \qquad (4.20)$$

and since $\max\,(\sum_i C_i, 0.0)$ can be only positive or equal to zero, the conditions in (4.18) are satisfied.

The finite difference form of Su for the variables are summarized in Table 4.1.

4.3 PRESSURE CALCULATION

Although there is no simple means of estimating the pressure terms required for solution of the momentum equations, this difficulty may be overcome by making use of the continuity equation. The net accumulation of mass inside each control volume is calculated and the local pressure is adjusted at successive iterations so that velocities are consistent with conservation of mass in that control volume. This procedure is carried out by: (1), defining a new dependent variable ΔP, the pressure correction term, such that $P = P' + \Delta P$ where P' is an estimated value of pressure resulting from the previous iteration, and P is the actual local pressure. (2), substituting $(P' + \Delta P)$ for P' in the source term of the u-momentum equation. (3), subtracting the u-equation from the u'-equation. This u'-equation, although it belongs to the same iteration as the u-equation, results from the value of pressure of the previous iteration, i.e. P'.

$$a_p(u_p - u_p') = \sum_i a_i(u_i - u_i') + 1.0\ (\Delta P_w - \Delta P_e)\ \Delta y_{ns}$$

For approximately converged results, $u_i \simeq u_i'$ for $i = e, w, s, n$, one can for simplicity assume $u_i - u_i' = 0$. Hence:

$$a_p\ (u_p - u_p') = 1.0\ \Delta y_{ns}(\Delta P_w - \Delta P_e)$$

or $$u_p = u_p' + (\Delta P_w - \Delta P_e)\ DU_p \qquad (4.21)$$

where $DU_p = 1.0\ (\Delta y_{ns})\ /\ a_p$

From its definition, DU_P can be visualised as the derivative of velocity with respect to the pressure change from iteration to iteration.

In a similar manner one obtains:

$$v_P = v_P' + (\Delta P_s - \Delta P_n) \, DV_P \tag{4.22}$$

where $DV_P = 1.0 \, (\Delta x_{ew}) \, / \, a_P$

Similar expressions could be obtained for all surrounding nodes, and noting that the nodal points for pressure lie on the control volume boundaries of u and v:

$$\begin{aligned} u_E &= u_E' + (\Delta P_P - \Delta P_E) \, DU_E \\ u_W &= u_W' + (\Delta P_W - \Delta P_P) \, DU_W \\ v_N &= v_N' + (\Delta P_P - \Delta P_N) \, DV_N \\ v_S &= v_S' + (\Delta P_S - \Delta P_P) \, DV_S \end{aligned} \tag{4.23}$$

Now, from continuity equation:

$$(\rho uA)_W + (\rho uA)_S - (\rho uA)_E - (\rho uA)_N = 0 \tag{4.24}$$

where A stands for the cross sectional areas of the control volume boundaries. Substitution of Equation (4.23) into Equation (4.24) gives:

$$(\rho u'A)_W + (\rho v'A)_S - (\rho u'A)_E - (\rho v'A)_N$$
$$+ (\rho A\ DU)_W (\Delta P_W - \Delta P_P) + (\rho A\ DV)_S (\Delta P_S - \Delta P_P)$$
$$+ (\rho A\ DU)_E (\Delta P_E - \Delta P_P) + (\rho A\ DV)_N (\Delta P_N - \Delta P_P) = 0$$

Rearranging,

$$\left[(\rho A\ DU)_E + (\rho A\ DU)_W + (\rho A\ DV)_N + (\rho A\ DV)_S\right]\Delta P_P$$
$$= (\rho A\ DU)_E\ \Delta P_E + (\rho A\ DU)_W\ \Delta P_W + (\rho A\ DV)_N\ \Delta P_N + (\rho A\ DV)_S\ \Delta P_S - \sum_i C_i$$

where $\sum_i C_i$ is the net accumulation of mass.

At this point one can see that this equation for ΔP also fits the general form of the algebraic Equation (4.19):

$$\phi_P\ (A_P) = \sum_i a_i \phi_i + Su$$

where $\phi = \Delta P$, $a = \rho A\ DU$, $A_p = \sum_i a_i$, and $Su = -\Sigma_i C_i$

This enables determination of ΔP using the same solution algorithm as the one used for the other variables. After solving for ΔP, one can then update the velocity components by Equations (4.21) and (4.22). In the present simulation study it is rather the pressure difference that is of interest; this pressure difference is calculated with reference to the jet nozzle pressure.

Table 4.1

Definition of Su

$$\phi_P \left\{ \sum_i a_i + \max\left(\sum_i C_i,\ 0.0\right) \right\} = \sum_i a_i \phi_i + Su$$

where $$Su = \phi_P' \max\left(\sum_i C_i,\ 0.0\right) - S_{\phi,vol}$$

ϕ	$S_{\phi,vol}$
u	$P\Big\|_e^w \Delta y_{ns} + \frac{1}{3}\left[\frac{\mu}{\rho}\left(u\frac{\Delta\rho}{\Delta x} + v\frac{\Delta\rho}{\Delta y}\right)\right]\Big\|_e^w \Delta y_{ns} + (\rho g)\Big\|_P \Delta x_{ew}\Delta y_{ns}$
v	$P\Big\|_n^s \Delta x_{ew} + \frac{1}{3}\left[\frac{\mu}{\rho}\left(u\frac{\Delta\rho}{\Delta x} + v\frac{\Delta\rho}{\Delta y}\right)\right]\Big\|_n^s \Delta x_{ew}$
T	$\delta\rho\,\frac{C_{p_A} - C_{p_B}}{C_p}\left[\frac{\Delta m_A}{\Delta x}\frac{\Delta T}{\Delta x} + \frac{\Delta m_A}{\Delta y}\frac{\Delta T}{\Delta y}\right]\Delta x\Delta y - \lambda\left[\frac{\Delta T}{\Delta x}\frac{\Delta}{\Delta x}\left(\frac{1}{C_p}\right) + \frac{\Delta T}{\Delta y}\frac{\Delta}{\Delta y}\left(\frac{1}{C_p}\right)\right]\Delta x\Delta y$
m_A	0

4.4 CLOSURE

The computational procedure used for solving the set of algebraic equations derived in this chapter is described and discussed in Chapter 5.

CHAPTER 5

COMPUTATIONAL PROCEDURE

5.1 INTRODUCTION

Implementation of a finite difference scheme requires discretization of the domain of interest. This discretization is achieved by selection of a grid which covers the whole domain. This grid distribution and its effect on accuracy of the solution are described in Section 5.2.

Finite difference methods always result in sets of algebraic equations, and when these are tridiagonal in nature, as in the present problem, solution is simpler than for a general set of algebraic equations. It will be seen in Section 5.3 that the iterative solution procedure used in the present study is based on the tridiagonal matrix algorithm (TDMA). The TDMA is described in Section 5.4. Section 5.5 is a discussion of convergence criteria and of the use of under-relaxation factors, while an outline of the computer program completes the chapter as Section 5.6.

5.2 GRID DESIGN

Size and distribution of the grid are of fundamental importance in influencing not only accuracy of solution but also the convergence characteristics. In the present simulation the grids used are non-uniform, i.e. the spacing between grid lines is not constant. Thus the grid is finer in areas where gradients of the variables are large, and vice versa. Although the grid distribution is not the same for all runs, it is fixed at some predetermined pattern throughout each computation. Due to large differences in the flow field between the various cases studied, use of a single grid pattern throughout the present study would have been inappropriate and inefficient . As gradients of the flow field variables and of heat and mass transfer coefficients are high in the impingement region, a fine grid distribution is required here. Since location of the impingiment region is a function of angle of impingement and strength of the crossflow, the grids used were adjusted according to these variables. Consequently, more than ten different grids were employed in the present study. However these grids are all of the same type, differencing only by shifting the finer grid spacing zone to follow the impingement region.

Velocity, temperature and composition boundary layers build up along the impingement and confinement surfaces. Here the relatively large gradients of these variables require use of fine grid spacing. This is particularly important for the impingement plate along which heat and mass transfer are to be calculated. For example, the equation used for the case of heat transfer is

$$h\,A\,(T_j - T_p) = A\,k\left(\frac{dT_p}{dx}\right)_{x=x_p}$$

where A represents the area under consideration. And it is clear that the quantity $(dT/dx)_{x=x_p}$ cannot be determined properly if the grid line adjacent to the plate is not placed sufficiently close. Numerical tests were made to ensure that further increases in fineness of the grid spacings adjacent to the impingement plate have no effect on the computed transfer rates. The grid spacing in the x-direction is thus small near the plate and larger in the central region. It may be mentioned here that the crossflow entrance velocity profile would be more accurately defined if the grid were also small in the central region, but multiplication of the grid points leads to a tremendous increase in computer time; there is a tradeoff between these two considerations. In view of the small nozzle-to-plate spacings considered here, the x-direction resolution chosen for the present study is however sufficient to define adequately the crossflow parabolic entrance velocity profile.

As to the grid spacing in the y-direction, it must be small in the area covering the nozzle so that the inlet jet profile is adequately defined, and in the impingement region to ensure accurate calculation of the stagnation point transfer rates. In the upstream region occupied by the crossflow, as well as in the downstream region near the outflow boundary, rates of change of the variables are small and a wider resolution has consequently been used.

A 20 x 40 grid system was used in the case of a jet without crossflow, and 20 x 50 grids were used in all computer runs involving the effect of a crossflow. A typical grid spacing distribution is listed in Appendix B as part of the program output.

It has been mentioned earlier that better accuracy can be obtained through higher resolution, i.e. by using smaller grid line spacings. It is appropriate to recall here that this statement is subject to the following limitation: when a numerical scheme such as the one considered here is used on a digital computer, reducing the grid spacing will improve accuracy only up to a certain point after which smaller spacing yet will in fact reduce accuracy. This limitation is due to the fact that digital computers have a finite word length, i.e. that the resolution of numbers by the computer is finite. In computation of derivatives of a function, two numbers corresponding to the values of the function on two successive grid lines are subtracted and the result is divided by the grid spacing. Hence it is clear that in the case of small gradients and of very small spacing between the grid lines, a fixed round-off error eventually causes an increased error in the results.

Another factor, also related to the grid distribution, which affects solution accuracy is control volume size. As discussed in Section 4.1, the hybrid central and upwind differences method is based on the value of the Peclet number, Pe, which is computed locally at each grid point as follows:

$$Pe = \frac{\rho u \delta l}{\Gamma}$$

where δl is the length of the control volume. Hence the value of Pe depends not only on local fluid properties, but also on the size δl of the control volume, which in turn depends on grid spacing.

Clearly, it is possible to design a grid pattern such that the diffusion terms are neglected in the whole flow field, thus leading to unacceptable solutions. Since the velocity field is not known before computation, it is not possible to determine the local Peclet number and then design the grid distribution accordingly. A trial and error method must be used.

The grid spacing distribution used in the present study and shown in Appendix B is the result of taking all factors discussed above into consideration.

5.3 SOLUTION PROCEDURE

The finite difference equations derived in Chapter 4 constitute a set of strongly coupled non-linear algebraic equations. Basically the solution to these equations is obtained by determining values of the variables at each grid point from values at neighbouring points by means of an iterative procedure.

For a NI x NJ grid mesh where NI and NJ are the numbers of grid lines in the x- and y-directions respectively, there are (NI-2)·(NJ-2) algebraic equations for each of the five variables u, v, ΔP, T, m_A, making a total of 5 (NI-2)·(NJ-2) simultaneous equations aside from the equations for the physical properties of the fluid which are functions of T and m_A. In the case of the present 20 x 50 grid this makes 4320 equations, and if one were to solve for the unknowns using a classical matrix inversion method, the size of the matrix would be enormous and a tremendous amount of computer time would be required.

In the present case it is possible to simplify the problem by reducing the number of simultaneous equations to be solved from 5(NI-2) (NJ-2) to (NI-2) (NJ-2). This is done by solving separately for each of the five variables using the iterative cycle of steps listed below:

1. Guess the values of all variables, u, v, P, T, m_A.
2. Calculate the corresponding properties of the fluid (density, viscosity, etc.)
3. Assemble the coefficients of the u-momentum equation according to the guessed values, then solve for u.
4. Assemble the coefficients of the v-momentum equation according to the guessed values, then solve for v.
5. Calculate ΔP, then P and update the u and v according to Equations (4.21) and (4.22).
6. Assemble the coefficients of the energy equation according to the guessed values, then solve for T.
7. Similarly for m_A.
8. Treat the modified variables as improved guesses and repeat steps 2 to 8 until the specified convergence criteria are satisfied.

Steps 2 to 7 constitute an iteration. In steps 3, 4, 5, 6, and 7, only the equations for individual ϕ's need be solved simultaneously. The method chosen to solve each time this set of (NI-2)$\cdot$(NJ-2) simultaneous equations uses the tridiagonal matrix algorithm (TDMA), whereby a set of equations each with exactly three unknowns in a particular order (except the first and last ones which have only two unknowns) may be solved sequentially.

In the present study the marching direction goes from confinement plate to impingement plate. This marching procedure is clearly preferable when crossflow is not present as information on the jet inflow to the flow field is provided at the begining of the computation. In the case where a crossflow is present an alternative marching procedure (from crossflow entry to outflow boundary) could be used since it is the main-flow direction, but trials with this procedure did not result in any substantial computer time saving.

Values at grid nodes along a grid line J are taken to be unknown (values at W, P and E for each point P), but values at each N and S neighbour, i.e. variable along grid lines J-1 and J+1 are taken as known using the most recent values. The TDMA is then applied to this grid line by recasting the algebraic equations as presented in Equation (4.19) into the following form:

$$a_P \underline{\phi_P} = (a_n \phi_N + a_s \phi_S + Su) + a_w \underline{\phi_W} + a_e \underline{\phi_E}.$$

with the underlined quantities assumed unknown. This results in equations with three unknowns, except for nodes adjacent to boundaries where only two unknowns remain after specification of boundary conditions. Hence for each grid line there is (NI-2) equations with (NI-2) unknowns which can be solved by the TDMA as described in the next section.

It may be noted here that it is not necessary to obtain a fully converged solution for the matrix since the other variables have only approximate values. Therefore a limited number of sweeps from south to north is sufficient. Following the recommendation of Gosman et al. (G7), only three sweeps were performed at each iteration for u, v, T and m_A, while five sweeps were used for ΔP.

5.4 TRIDIAGONAL MATRIX

The problem having been transformed into one represented by a tridiagonal matrix, the solution is obtained by iterating over the entire flow field and over the several variables. The TDMA will be rapidly presented here and the reader is referred to reference (C4) for more details relative to its practical application.

As seen in Section (5.3), the equations at hand are of the form:

$$a_P\phi_P = (a_n\phi_N + a_s\phi_S + Su) + a_w\phi_W + a_e\phi_E \tag{5.1}$$

where ϕ_P, ϕ_W and ϕ_E are the dependent variables while all other terms are assumed constant.

Letting
$$a = a_e$$
$$b = a_w$$
$$c = a_n\phi_N + a_s\phi_S + Su$$
$$d = a_P$$

Equation (5.1) can be rewritten for each control volume as:

$$-b\phi_W + d\phi_P - a\phi_E = c$$

And for all control volumes in the same line one gets:

$$
\begin{aligned}
- b_2 \phi_1 + d_2 \phi_2 - a_2 \phi_3 &= C_2 \\
- b_3 \phi_2 + d_3 \phi_3 - a_3 \phi_4 &= C_3 \\
- b_i \phi_{i-1} + d_i \phi_i - a_i \phi_{i+1} &= C_i \\
- b_{NI-1} \phi_{NI-2} + d_{NI-1} \phi_{NI-1} - a_{NI-1} \phi_{NI} &= C_{NI-1}
\end{aligned}
\qquad (5.3)
$$

or in matrix form:

$$
\begin{bmatrix}
d_2 & -a_2 & & & & & \\
-b_3 & d_3 & -a_3 & & & & \\
 & -b_4 & d_4 & -a_4 & & & \\
 & & & & & & \\
 & & -b_i & d_i & -a_i & & \\
 & & & & & & \\
 & & & & -b_{NI-2} & d_{NI-2} & -a_{NI-2} \\
 & & & & & -b_{NI-1} & d_{NI-1}
\end{bmatrix}
\begin{bmatrix}
\phi_2 \\ \phi_3 \\ \phi_4 \\ \\ \phi_i \\ \\ \phi_{NI-2} \\ \phi_{NI-1}
\end{bmatrix}
=
\begin{bmatrix}
C_2 + b_2 \phi_1 \\ C_3 \\ C_4 \\ \\ C_i \\ \\ C_{NI-2} \\ C_{NI-1} + a_{NI-1} \phi_{NI}
\end{bmatrix}
$$

which can be abreviated as: $\left[A\right]\left[\phi\right] = \left[C\right]$

We know that A can be factored into two (NI-1)·(NI-1) matrices, L and U, such that L and U are unique. So:

$$\left[A\right] = \left[L\right]\left[U\right]$$

and $[A][\phi] = [L][U][\phi]$

Recalling that $[A][\phi] = [C]$

and letting $[U][\phi] = [C']$ (5.4)

where C' is a column matrix with elements C_2, C_3, ... C_{NI-1}, yields:

$$[L][C'] = [C] \quad (5.5)$$

Defining $C_1 = \phi_1$, all the C_i's are given by Equation (5.5) and one can solve for the ϕ's using Equation (5.4).

5.5 UNDER-RELAXATION FACTORS AND CONVERGENCE CRITERIA

5.5.1 Under- relaxation factors

Large changes in the tridiagonal matrix coefficients from iteration to iteration might lead to divergence. To cope with this drawback the so-called under-relaxation method is used. If $\phi_{P,k-1}$ and $\phi_{P,k}$ are the values of ϕ_P computed in the (k-1)-th and in the k-th iteration respectively, then the value actually used in the following iteration, say $\phi_{P,k'}$, is given by:

$$\phi_{P,k'} = URF\ \phi_{P,k} + (1-URF)\ \phi_{P,k-1}$$

where URF is the under-relaxation factor which is a real number between 0 and 1.

5.5.2 Convergence Criteria

As seen earlier the numerical procedure entails two iterative loops. The first one scans the seven dependent variables, the second one repeatedly treats the flow field for individual variables. It has been seen that the second iteration loop does not require a converged solution. Therefore only the criterion for the first iteration loop need be defined.

The iterative procedure is considered a converged solution if the absolute normalized residuals (Equation 5.6) for u, v, ΔP, T and m_A are all less than a prescribed small number CC, the convergence criterion. Thus:

$$RESID = \sum_{\substack{all \\ nodes}} \left|\sum_i a_i \phi_i + Su - A_P \phi_P\right| / FACTOR \leq CC \qquad (5.6)$$

where FACTOR, the normalization factor, will be interpreted later in this section. The term RESID as defined in Equation (5.6) is the difference between the left and right hand sides of the governing equations (4.19); hence for exact solutions RESID = 0. For the equations for u and v, FACTOR equals the total inflow of jet and crossflow momentum; physically this means that the convergence criterion implies that the total accumulation of momentum inside the physical system has to be less than a prescribed percentage of the momentum inflow. Similarly, for ΔP, FACTOR represents the total inflow of mass through the jet and crossflow. For T and m_A, FACTOR represents the product of total volumetric inflow and a characteristic difference in T or m_A, respectively

After testing the effect of a range of values of convergence criterion, CC, the value of this important computational parameter was set at 0.015. Figure (5.1) shows the values taken by velocity at a monitoring point in the flow field (I=18, J=20) along the iterative computation process. It is clearly evident that a large value for CC would give quite inaccurate results, while a lower value would result in an increase in computing time without yielding a discernable improvement in the velocity results. The transfer rate values are subject to the same behaviour. Choice of CC = 0.015 was therefore clearly a good choice for the convergence criterion.

5.6 OUTLINE OF THE COMPUTER PROGRAM

Figure (5.2) is a flow diagram showing the computational procedure. Figure (5.3) describes Subroutine CALCU which solves for the u-momentum equation; solution of all other equations follows identical steps, and Subroutines CALCV, CALCP, CALCT and CALCW are similar to Subroutine CALCU.

The grid distribution is set up by Subroutine GRID. Subroutine INIT computes subsequently all the geometric quantities relative to each control volume and stores them in arrays for subsequent refernce. All variables are then initialized, and fluid properties (ρ, μ, C_p, λ and δ) are calculated by Subroutine PROPS and stored in arrays. The non-iterative boundary conditions are then prescribed, and a first output is printed describing the flow field as initialized.

One complete iteration is then performed by calling sequentially the subprograms CALCU, CALCV, CALCP, CALCT and CALCW which update u, v, ΔP, T and m_A values throughout the grid. Based on these updated values, the arrays containing the fluid properties are then modified by Subroutine PROPS. After each of these iterations several tests are performed: if either the computer time spent or the number of iterations performed exceeds the prescribed values, the iteration procedure terminates automatically. Also the residuals RESID are checked for convergence after each iteration. If the RESID for the five equations (u, v, ΔP, T and m_A) are all less than the convergence criterion, CC, the program is assumed to have reached the converged solution. The local transport coefficients are then calculated along the impingement plate from gradients at the wall of the v, T and m_A distributions.

The line-by-line solution of the u-equation is performed in subprogram CALCU which contains loops for the computation of the convective terms C and of the diffusive terms D; from these terms CALCU establishes the TDMA coefficients, a, according to Equation (4.10), and finally computes the source terms Su for all nodes. Iterative boundary conditions are prescribed in subprogram MODU. After calculation of the u-residual, CALCU applies the under-relaxation factors and calls subroutine LISOLV. LISOLV performs the line-by-line solution procedure using the TDMA. The maximum number of sweeps (traverses) to be performed is designated by NSWPU in the flow diagram of Figure 5.3.

The complete program is listed in Appendix A, while a typical output listing will be found in Appendix B. Additional information on some aspects of this program can be found in reference (G7).

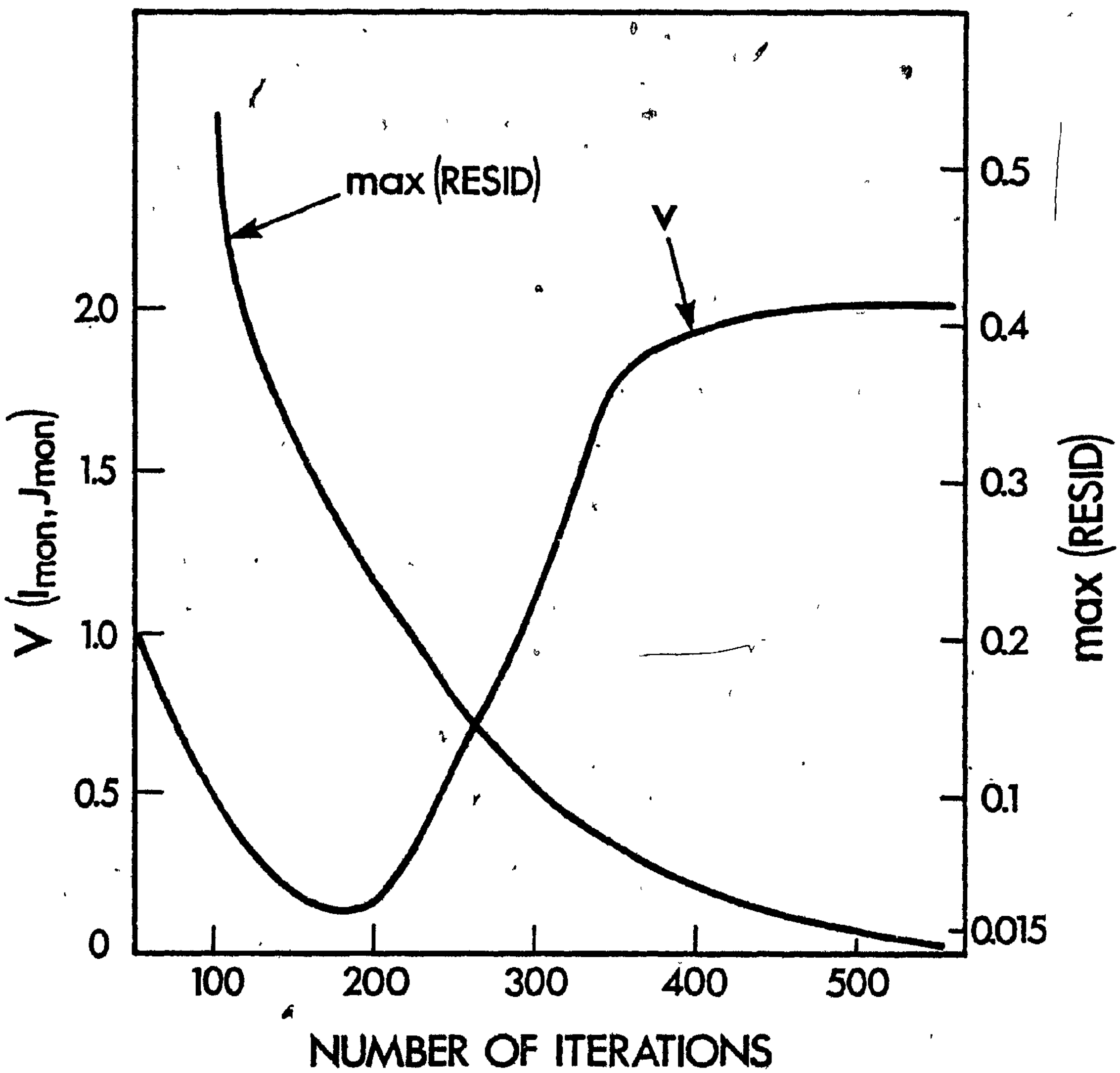

Figure 5.1 : Numerical variation of v-velocity result at monitoring point throughout the iteration cycle.

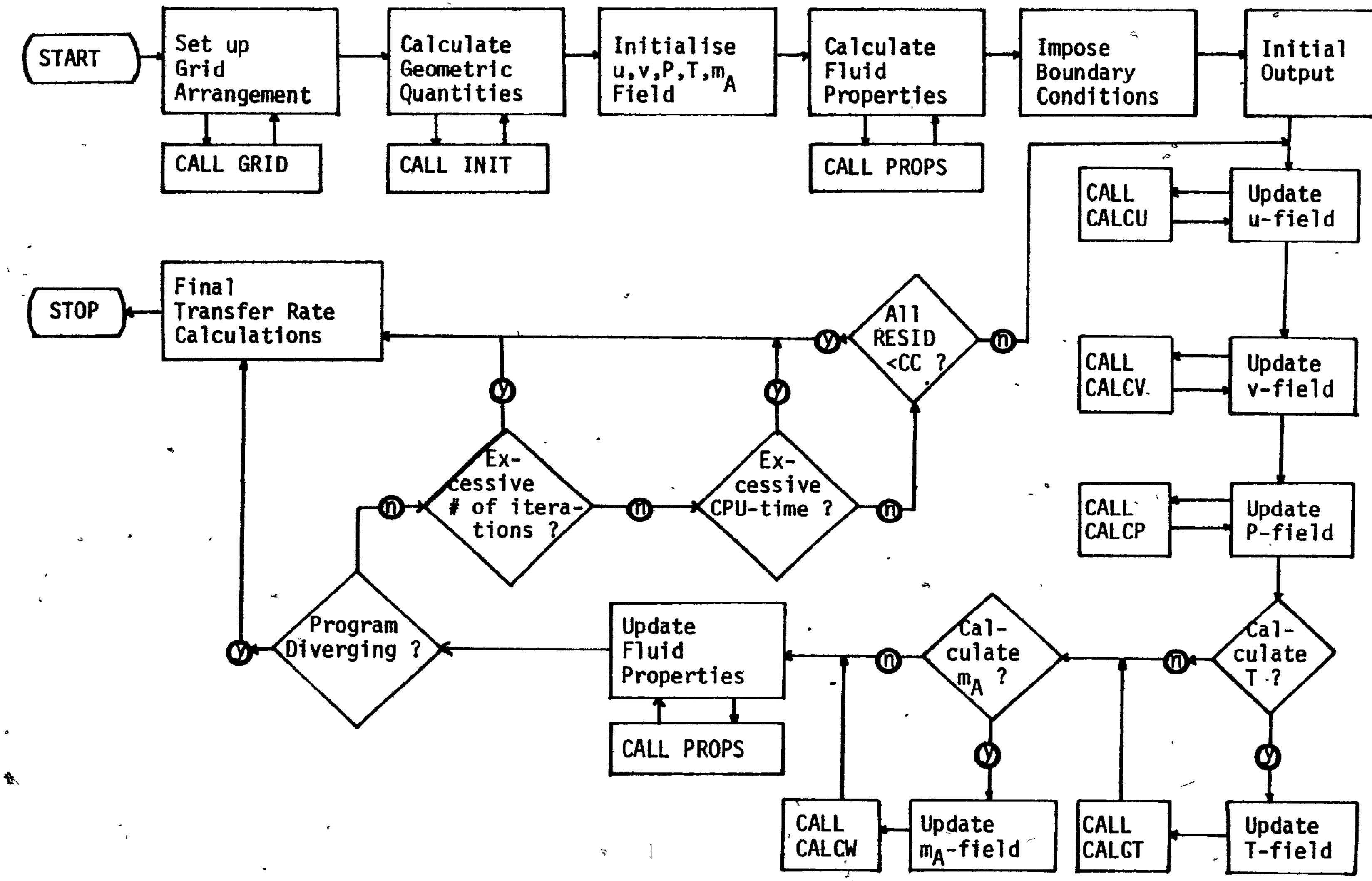

FIGURE 5.2 Computational Flow Diagram: Main Program

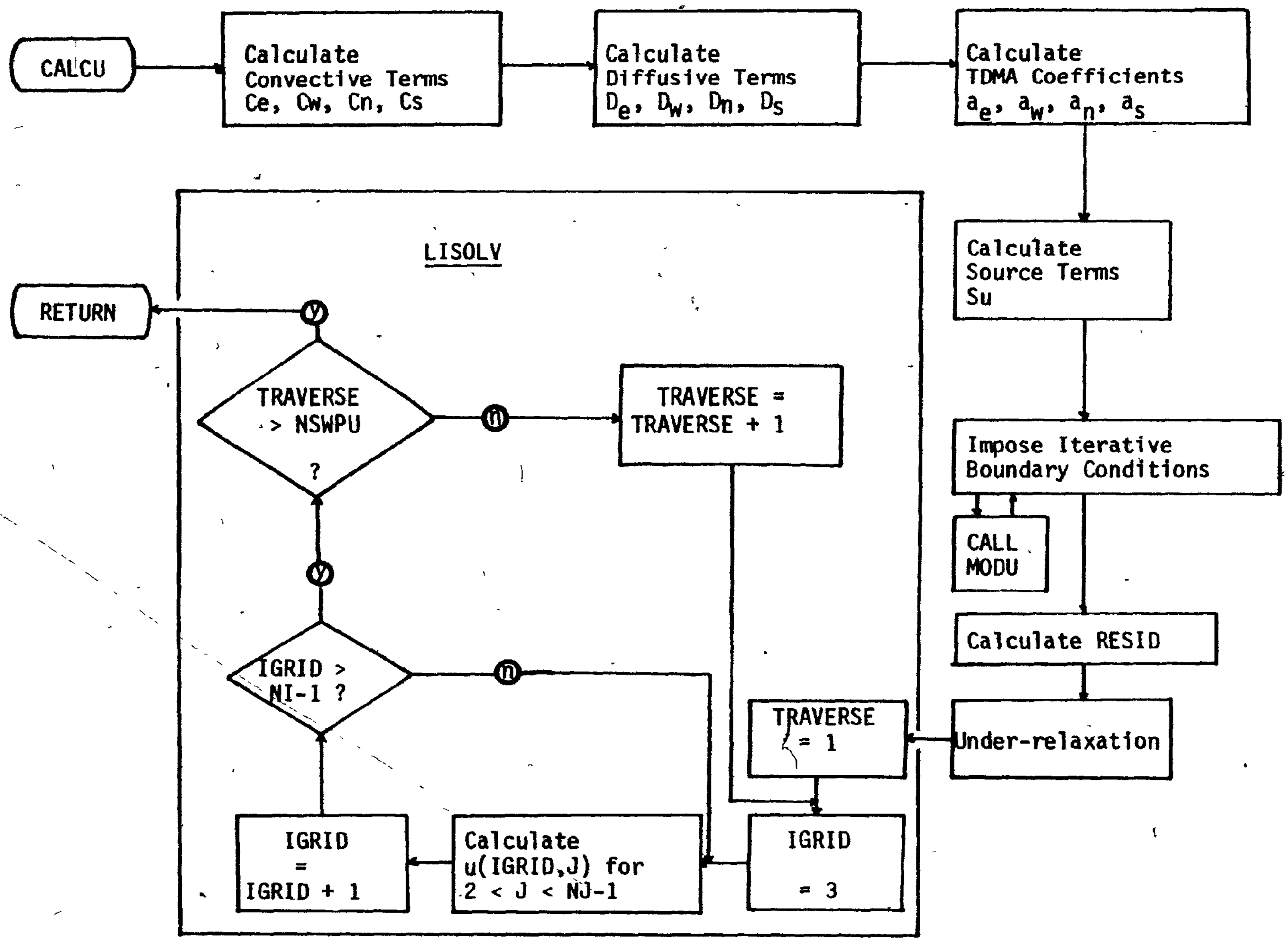

FIGURE 5.3 Computational Flow Diagram: CALCU

CHAPTER 6

RESULTS AND DISCUSSION

6.1 RANGE OF PARAMETERS

Using the finite difference equations derived in Chapter 4 and the numerical procedures described in Chapter 5, a simulation of the flow, heat transfer and mass transfer characteristics was performed for a laminar semi-confined rectangular jet discharging perpendicularly or with an inclination in a crossflow and impinging on an isothermal wetted surface. Simulation runs of an identical jet impinging normally but without crossflow provide comparison between crossflow and non-crossflow cases. The results presented in this chapter include parameters of nozzle-to-plate spacing, effect of presence of a crossflow, ratio of crossflow to jet Reynolds numbers, and angle of impingement. For the latter variable the range of variation included jets inclined towards both the crossflow upstream and downstream direction (negative and positive angles, respectively).

The ranges of the parameters used in the present study are given in Table 6.1. A serial listing of all computer runs is given in Appendix C. A nozzle width of 3.2 mm and a fully developed parabolic velocity profile were selected as the base case for the numerical study. The Reynolds number of the jet at the nozzle exit is 1000, based on nozzle width, and is constant throughout. For all runs the impingement surface

Table 6.1

Values of Parameters used in the Numerical Experiments

Ratio of Reynolds numbers of cross-flow to jet	Nozzle-to-plate spacing	Angle of inclination of nozzle
M	H/D	θ
0.01	2	-45°
0.1	3	-30°
0.167	4	-10°
0.25		- 5°
0.4		0°
0.5		5°
0.7		10°
1.0		30°
2.0		

was maintained at a temperature of 350°K, while the jet and the crossflow temperature was 450°K. The confinement plate temperature was also 450°K. The impingement surface temperature gives a mass fraction of water vapour along the plate, m_p, equal to 0.302. This value varies slightly between 0.3020 and 0.3023 from run to run due to its dependence on the local pressure which varies very slightly. The jet pressure at the nozzle exit is 1.013 E05 N/m^2 (1 atm) and its water content for all runs is 0.1 mass fraction water. The crossflow enters parallel to the confinement and impingement plates with a fully developed velocity profile, but its entrance temperature and humidity are constant (flat temperature and humidity profiles). The crossflow entry (or southern edge of the plate) is situated at a distance 6.4 D from the center of the nozzle aperture.

The magnitude of the crossflow is defined by the ratio, M, of the crossflow volumetric flow-rate to the jet volumetric flow-rate: $M = \bar{V}H/\bar{U}D$. Figure (6.21) on which the pressure difference between the crossflow entry pressure and the ambient pressure (or nozzle pressure) is plotted versus M shows that the overpressure due to the crossflow on this side is negligible with respect to the ambient pressure the order of magnitude of which is 10^5. As the crossflow and the jet flow are of the same fluid (air) at the same temperature and water vapour content, and essentially the same pressure, the density and viscosity are also effectively the same. Thus M may also be regarded as the mass flow-rate ratio between the crossflow and the jet flow, or as the corresponding ratio of the Reynolds numbers of the crossflow to the jet flow.

The length of the plates on the outflow side was varied between 6.1 D and 8 D in order to have longer plates when the nozzle inclination angle has a large positive value ($\theta = 30°$ e.g.) and when the crossflow magnitude is high (e.g. M = 1.0 or 2.0). This was done so that the transfer rate peaks would not be too close to the edge of the plates, which could have introduced an undesired interaction with the outflow boundary conditions. In retrospect this provision was in fact not necessary for the small H/D ratios studied here, but would be needed for study of larger values of H/D.

For cases without crossflow, the conclusions of Li (L2) concerning influence of plate lengths on transfer rates were used to reduce computer time. Li found that the effect of extending plate length from 4.7 D to 18 D is felt only over the outer parts of the plate, whereas the impingement region results are unaffected. Thus a length of 4.75 D was chosen in the present study for runs without crossflow. Only a few additional runs have been done with a larger plate (total length of 12.5 D) in order to compare the average value of the transfer coefficients with results obtained with crossflow.

Results in the literature are generally presented in non-dimensional form. In fact the governing equations themselves are commonly transformed into appropriate non-dimensional form by using suitable characteristic parameter values (e.g. Saad (S2), van Heiningen et al. (V2)). But choosing correct scaling parameters is difficult or even impossible when temperature and composition dependent physical property variation is allowed. Consequently, in the present study the governing equations have been solved in their dimensional form, and the dimensional results have been converted subsequently into a non-dimensional form for presentation. Thus the lengths and distances are normalized with respect to the nozzle width , the jet flow conditions are expressed in terms of Reynolds number, while the heat and mass transfer results are presented in terms of Nusselt and Sherwood numbers respectively.

6.2 FLOW CHARACTERISTICS

6.2.1 Centerline Velocity Profile

6.2.1.1 Without Crossflow:

In the case of the runs performed without crossflow we can state, in view of the results recorded in Section 2.2.1 for the potential core length, that for the close nozzle-to-plate spacings of the present study we are dealing with potential core type of flow up to the stagnation region adjacent to the impingement surface. This expectation is confirmed by the results of the present investigation presented in Figure 6.1 as decay of centerline axial velocity . The three solid lines show this velocity profile for the case without crossflow, for values of H/D = 2 , 3 , and 4. As is typical for this type of flow, the u-velocity decreases only slightly with axial distance from the nozzle exit until the flow is about one nozzle width from the evaporating surface. Thereafter, axial velocity decreases rapidly to reach the value of the evaporation velocity at the impingement surface, which is not discernably different from zero on the scale of Figure 6.1. This evaporation velocity is directed away from the impingement surface and

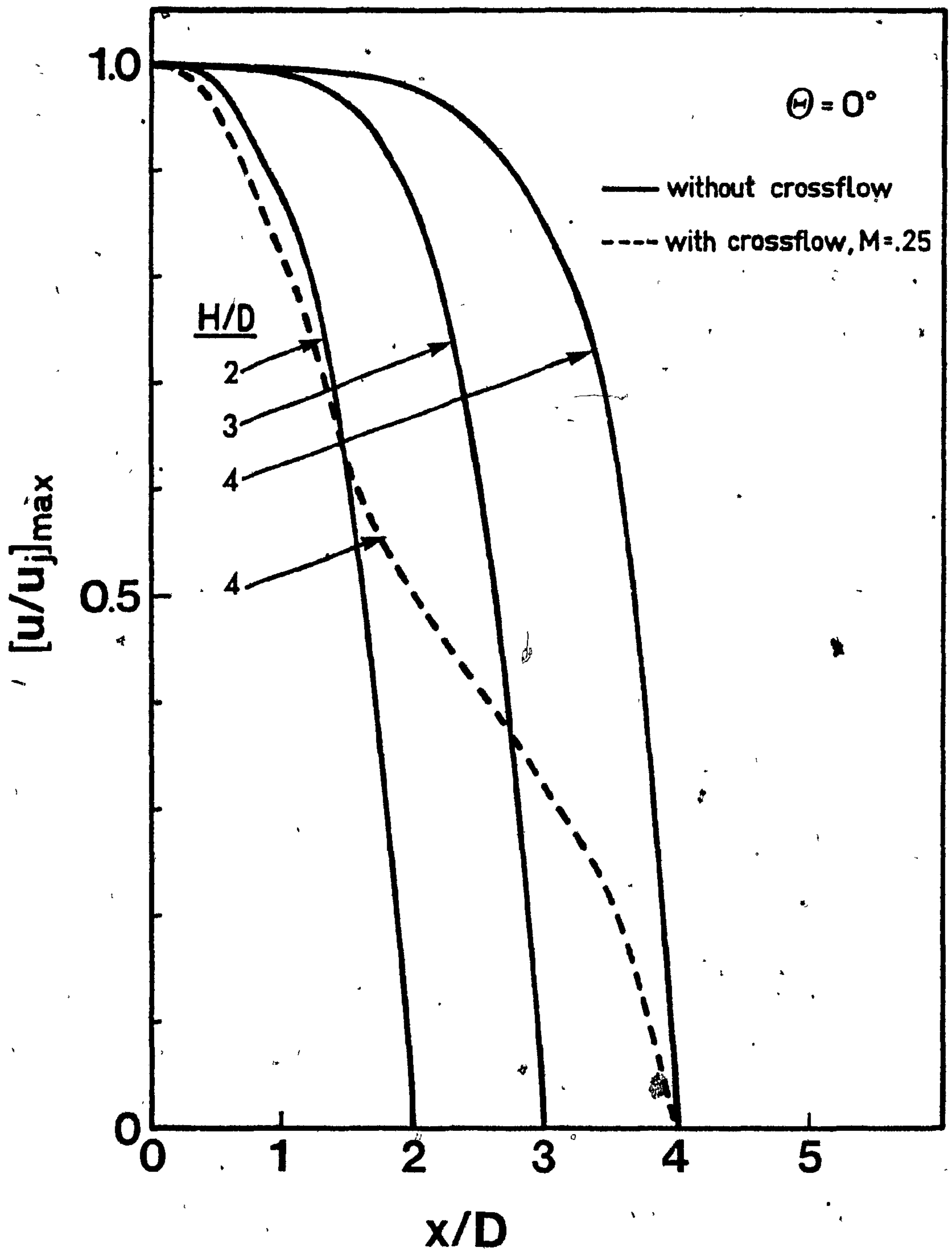

Figure 6.1 : Centerline axial velocity decay.

is thus negative with the sign conventions taken here. However, as this evaporation velocity is three orders of magnitude smaller than the jet velocity, $(u/u_j)_{max}$ seems on Figure 6.1 to reach zero, as it would were the plate non-evaporative. Negative values for u-velocity in the vicinity of the plate are of course printed on the computer outputs.

The axial velocity decay behaviour is consistent with the findings of previous investigators, including Giralt (G2), Saad (S2), Huang (H2) and Li (L2), who showed that, over a wide range of nozzle-to-plate spacing and Reynolds number, the centerline axial velocity of a round jet (both semi-confined and unconfined) is affected by the presence of the impingement plate at only about one nozzle diameter from the plate. This fact is further confirmed by the observation that the three curves for H/D = 2 , 3 , and 4 collapse effectively into a single curve before the effect of the impingement plate is sensed. This sudden decrease of centerline axial velocity near the impingement region is of course associated with the correspondingly large transformation of x-direction momentum into y-direction momentum.

6.2.1.2 With Crossflow:

As it is the u-component of velocity which produces the desirable impingement characteristics of the flow field, it is of interest to note the effect of crossflow on the u-velocity. Comparison on Figure 6.1 of the axial decay profiles of u_{max} for H/D = 4, with and without crossflow, indicates that the u_{max} velocity profile is altered drastically by a crossflow of Reynolds number only 25% of that of the jet.

Since the jet trajectory is now deflected by the crossflow, the loci of maximum velocity are no longer on the nozzle centerline as is the case without crossflow. Thus the values of $(u/u_j)_{max}$ on this and subsequent graphs in the presence of crossflow represent the decay of the maximum u-component velocity situated along the central streamline of the deflected jet.

Because of the large change in the profile caused by a value of M as small as 0.25, a set of such profiles for a range of 4 values of M is shown on Figure 6.2. Although it might appear from Figure 6.2 that there is an anomalously abrupt change in profile between M=10% and the comparative profile shown without crossflow, it should be realised that a profile for the case of crossflow with M = 0 (not shown on Figure 6.2) would be a curve located much closer to that for M = 10% than to the profile shown without crossflow. This effect of crossflow is due to interaction between the jet and crossflow starting right from the point where the jet discharges into the crossflow. Consequently, whereas u_{max} decreases scarcely perceptibly (by ca. 1%) one nozzle width from the nozzle exit in the absence of crossflow, u_{max} decreases by 15-20% over the same distance for M in the range 10-25%. Likewise, only 35-40% of the drop in u_{max} occurs over the last one nozzle width distance above the evaporating surface, as compared to 85% of the drop in u_{max} over this same region in the absence of crossflow.

Figure 6.2 shows that the greater the crossflow, the more rapidly the u_{max} velocity decreases. The direction of this trend was to be expected since it is apparent that for very large values of M, the profile of Figure 6.2 would approach the limit of a vertical line; i.e. u_{max} dropping almost to zero for a small value of x approaching zero.

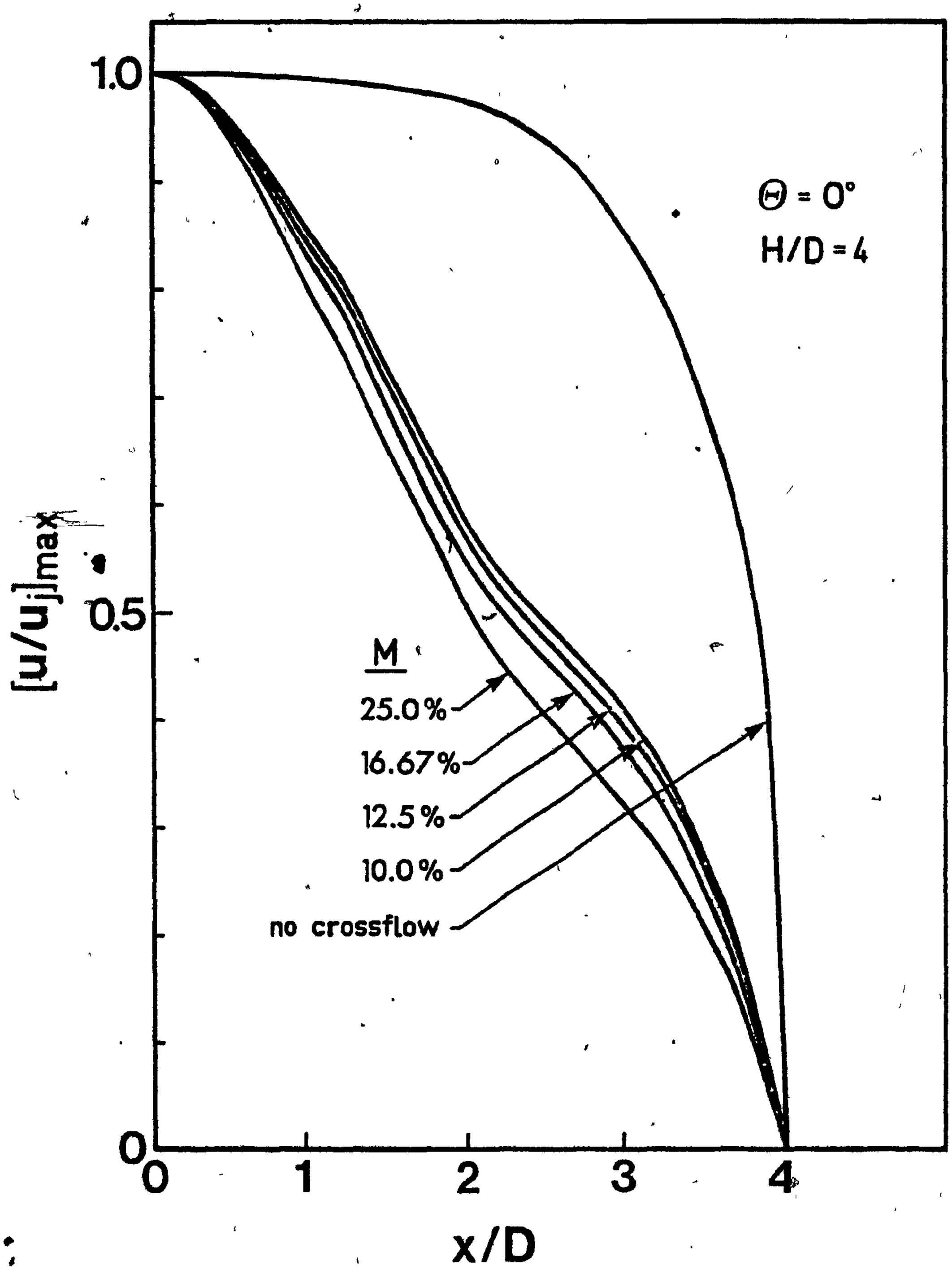

Figure 6.2 : Decay of jet maximum u-velocity for various crossflow magnitudes.

This limiting case corresponds to a strong crossflow affected imperceptibly by a negligible jet flow.

In view of the evidence from the flow field results that the effect of crossflow is to cause a sharp decrease of the u-velocity component which is the essence of the impingement process, one could already anticipate that the heat and mass transfer rates at the evaporating surface would be lower when a crossflow is present.

On Figure 6.3 velocity decay profiles are shown for the cases of an orthogonal nozzle and of a nozzle inclined at an angle of -10° (i.e. directed slightly against the crossflow direction). In both cases a crossflow of M = 10% is present. Since -10° is a rather small inclination angle, the two profiles of u_{max} are not greatly different. However, by reference to the curves for u_{max} it is none the less clear that for $\theta=-10°$ the u_{max} velocity decays less sharply than for $\theta = 0°$. In other words, at a constant crossflow (M = 10%), a change in θ from 0° to -10° shifts the u-velocity profile somewhat closer to the profile without crossflow. Such a trend in the flow field would be expected to be accompanied by an increase in transfer rates at the impingement surface, as will indeed be confirmed subsequently. Decay of the u-velocity is due to transformation of the jet u-momentum into positive y-momentum by action of the crossflow. This transformation is seen as deflection of the jet towards the positive y-direction, and the onset of this deflection will obviously be retarded and less significant if the jet leaves the nozzle with a negative inclination angle.

Figure 6.3 also shows the decay of the total velocity im terms of

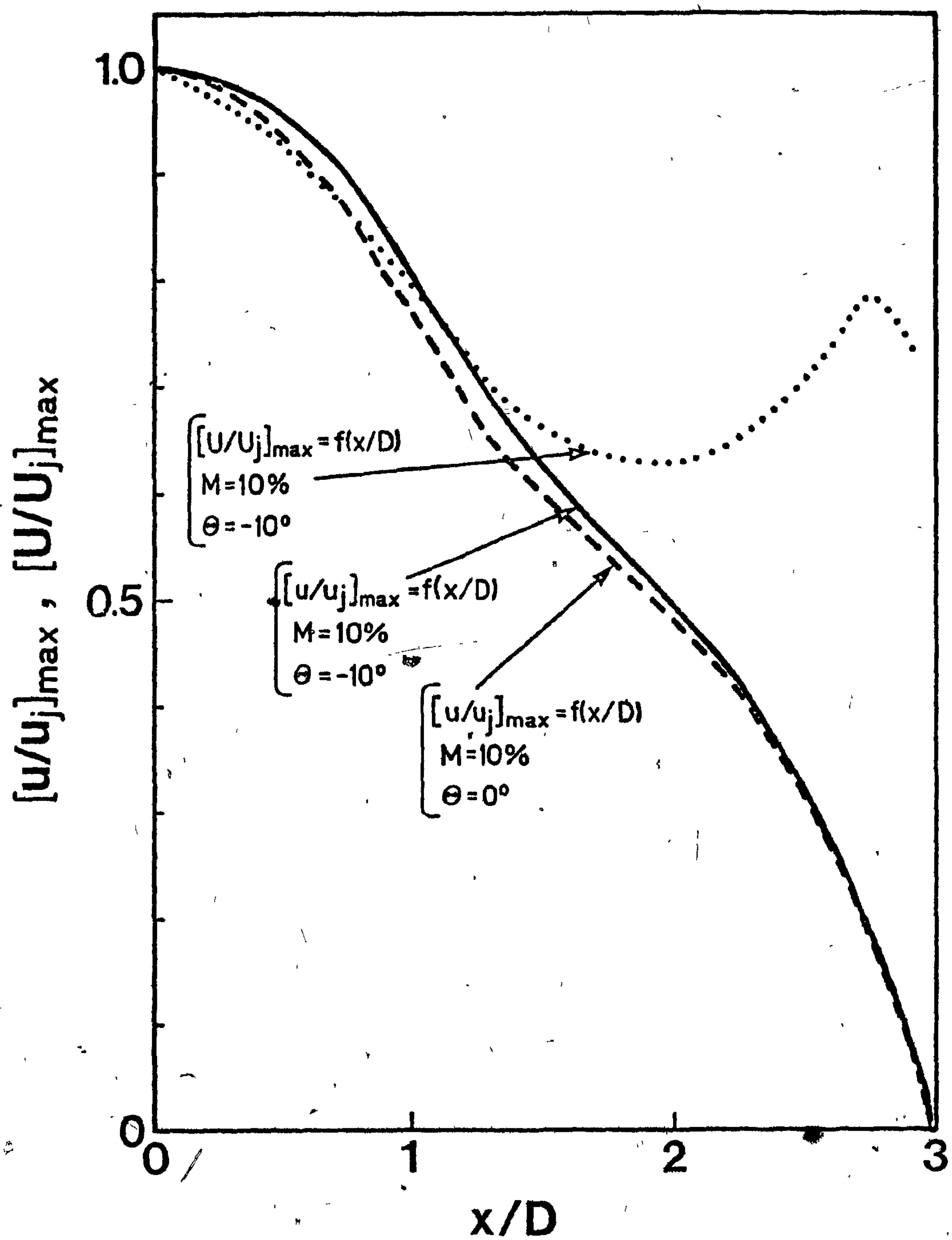

Figure 6.3 : Decay of maximum velocity for jets discharging in a crossflow at different angles.

the ratio $(U/U_j)_{max}$. One can see that, for small distances away from the nozzle aperture, the decay of the total velocity normalized with the jet inlet total velocity is greater than the decay of the u-component. This is due to the fact that U also entails the v-component of velocity which, at the begining, is directed against the crossflow direction and which will be affected more than all other flow characteristics by the crossflow since the first crossflow effect felt by the jet is the impediment of the jet stream progression in the negative y-direction. This total velocity, U, is not as relevant to the impingement process as is the u-component because it is not directed perpendicular to the plate. Up to halfway to the impingement surface the profile for decay of U is similar to that for u_{max}. Thereafter the profile for U rises to a maximum quite close to the impingement surface. This maximum is of course that of the wall jet. Beyond the wall jet maximum, the U velocity profile drops very sharply as the impingement surface is approached.

6.2.2 Flow Field Analysis:

The complete flow field, from impingement to confinement plate, and from crossflow inlet to total flow outlet was mapped for two cases of inclined impingement into a crossflow. This was done through an additional subroutine, SPEED, which calculated total velocity, U, and its angle with the x-axis at all grid nodes. The results of this computation for H/D = 3 and for a crossflow magnitude M = 0.1 for jets impinging at inclination angles of $-10°$ and $+30°$ are as presented on Figures 6.4 and 6.5. On these figures the velocity vector is represented

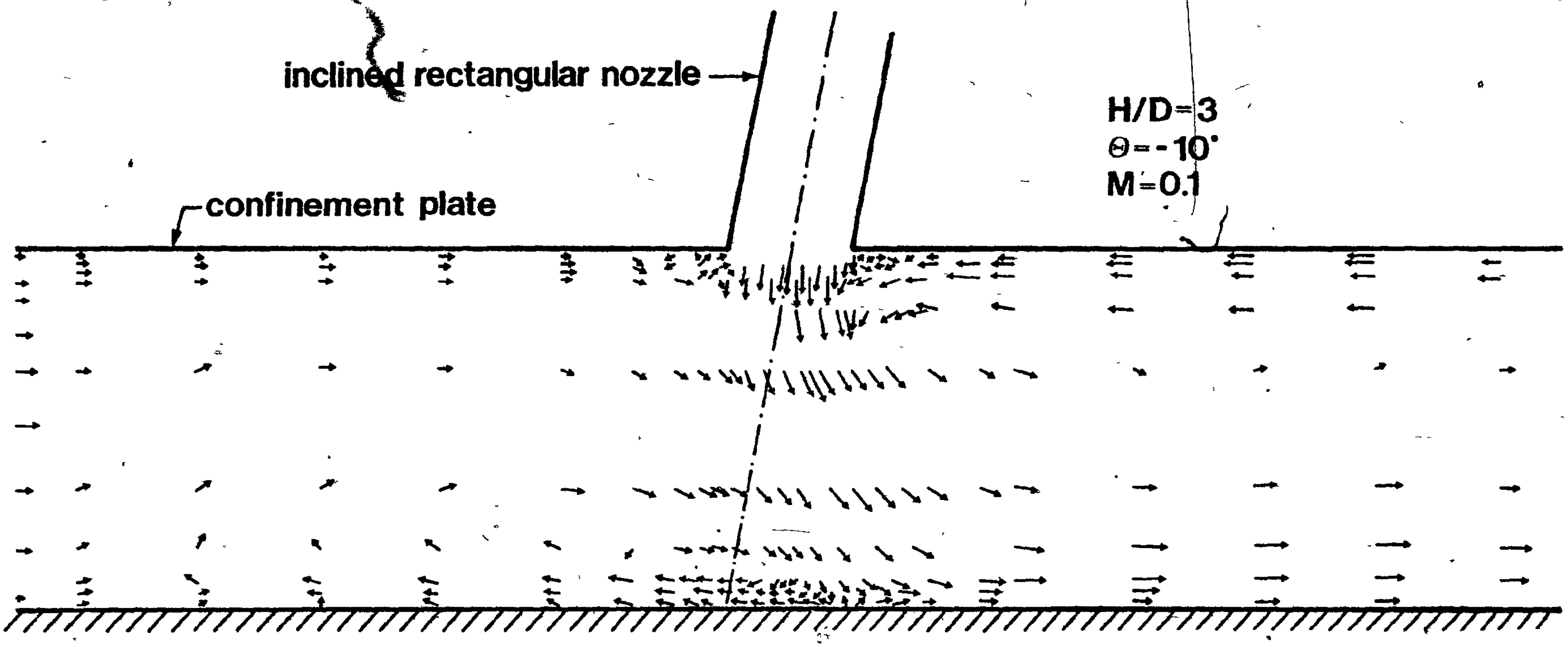

Figure 6.4 : Velocity field for an impinging jet discharging in a crossflow at an angle θ = -10°.

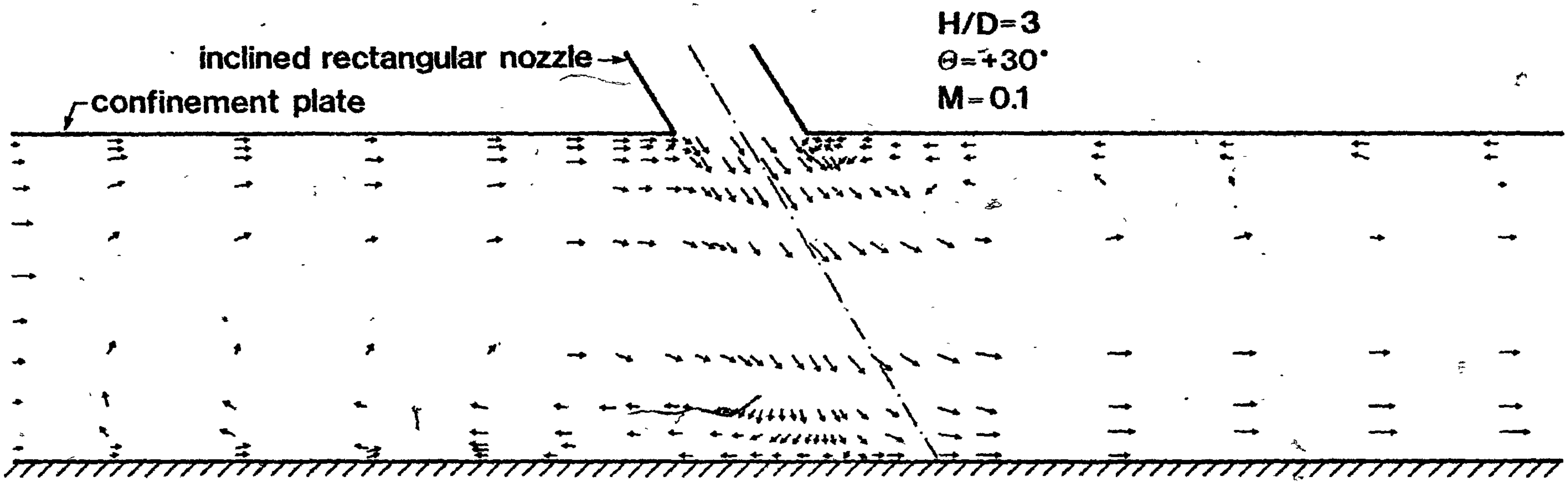

Figure 6.5 : Velocity field for an impinging jet discharging in a crossflow at an angle θ = 30°.

by arrows drawn with the appropriate angle, and of length approximating the actual magnitude of velocity.

Figure 6.4 (for $\theta = -10°$) shows clearly the deflection of the jet from the nozzle centerline by interaction with the crossflow. At impingement the jet is split into two large recirculating flows. The bulk of the jet goes in the downstream direction of the crossflow, while the smaller part forms a wall-jet, about 1D thick, in the direction opposing the crossflow. With the relatively low intensity of crossflow for the case shown on Figure 6.4, i.e. M = 0.1, the recirculation bubble on this side can be seen to extend about 3/4 the way to the crossflow entry. Such a recirculation bubble on the crossflow inlet side was also observed by Bouchez and Goldstein (B7) in their flow visualization for turbulent jets in a wind tunnel. They found a strong turbulent recirculation zone upstream of the impingement area. They also observed that as the flow rate ratio, jet to crossflow, decreases, the recirculation zone diminishes and finally disappears Although the flow fields for M = 1.0 and 2.0, have not been plotted, this last observation of Bouchez is none the less confirmed as values of v-velocity in this region of the flow field in the present study show only positive values when M = 1.0 or 2.0. It is also of interest to note that on this side of the flow field, just adjacent to the nozzle, there is another recirculation bubble, but a very small one, due to the fact that the jet at the nozzle exit is directed somewhat against the crossflow stream direction.

The outflow side of the flow field is filled with a large recirculation bubble of the type discussed in Section 3.4. This recirculating flow, is cut by the outflow boundary (Boundary IV) so that there is actually outflow over most of this flow boundary but with inflow for a region about 1D wide adjacent to the confinement plate. This inflow is a reflection of the pumping or entrainment power of the jet. This inflow stream flows along the confinement plate in the negative y-direction to a point near the nozzle aperture where it becomes entrained by the jet; the junction of these two streams creates a pair of small vortices near the confinement plate.

The stagnation point is carried downstream by the crossflow. For the conditions of Figure 6.4 the stagnation point can be seen to be about 0.5D downstream from the point on the impingement surface which is directly beneath the nozzle centerline.

Figure 6.5 shows the same general type of velocity pattern for $\theta = +30°$. One difference from Figure 6.4 is that the stagnation point is of course shifted further downstream than for the case of $\theta = -10°$, being located now about 1D down from the point directly beneath the nozzle centerline. Intuition might have suggested that, with the jet inclined at an angle of 30° towards the crossflow direction, a recirculation bubble on the crossflow entry side might not have been formed. However, even though the fraction of the jet flow which recirculates upstream against the crossflow is greatly reduced with $\theta = +30°$, it is still sufficiently strong to produce a recirculating flow extending most of the distance to the crossflow entry region. On the other hand, the recirculation bubble observed near the nozzle aperture on the crossflow entry side of the flow field for $\theta = -10°$ is not present when $\theta = +30°$ due to the smooth merging of the crossflow and the jet.

Because of the evaporation occuring at the impingement surface in the present study, the velocity at this surface must in all cases be a vector directed perpendicularly into the flow field. However, within the limits of scale necessary for the representations of Figures 6.4 and 6.5, the closest velocity vectors to the impingement surface are still sufficiently far into the flow that their direction reflects the air flow field rather than the evaporative boundary condition. It has been mentioned in Subsection 6.2.1.1 that this evaporation velocity is three orders of magnitude smaller than the jet velocity.

6.2.3 Shear Stress Analysis:

It is instructive to analyse the effect of θ and M on the lateral distribution of shear stress along the impingement surface by reference first to the case without crossflow and for $\theta = 0°$.

When there is no crossflow and $\theta = 0°$, the flow field is symetric with respect to the nozzle axis. Starting from this axis ($l = 0.0$) the v-component velocity is zero at the stagnation point, but increases very sharply with $|l|$ under the influence of the pressure gradient, then falls off because of viscous action and of the increase of the cross-sectional area occupied by the spreading stream. This flow pattern results in the shear stress distribution along the impingement surface shown on Figure 6.6. For negative values of l, the fluid flows in the negative y-direction, which leads to negative values for τ, so for convenience $|\tau|$ has been plotted. As expected in view of the findings of previous researchers, the influence of nozzle-to-plate spacing is very little for the range of small values of H/D studied here, which

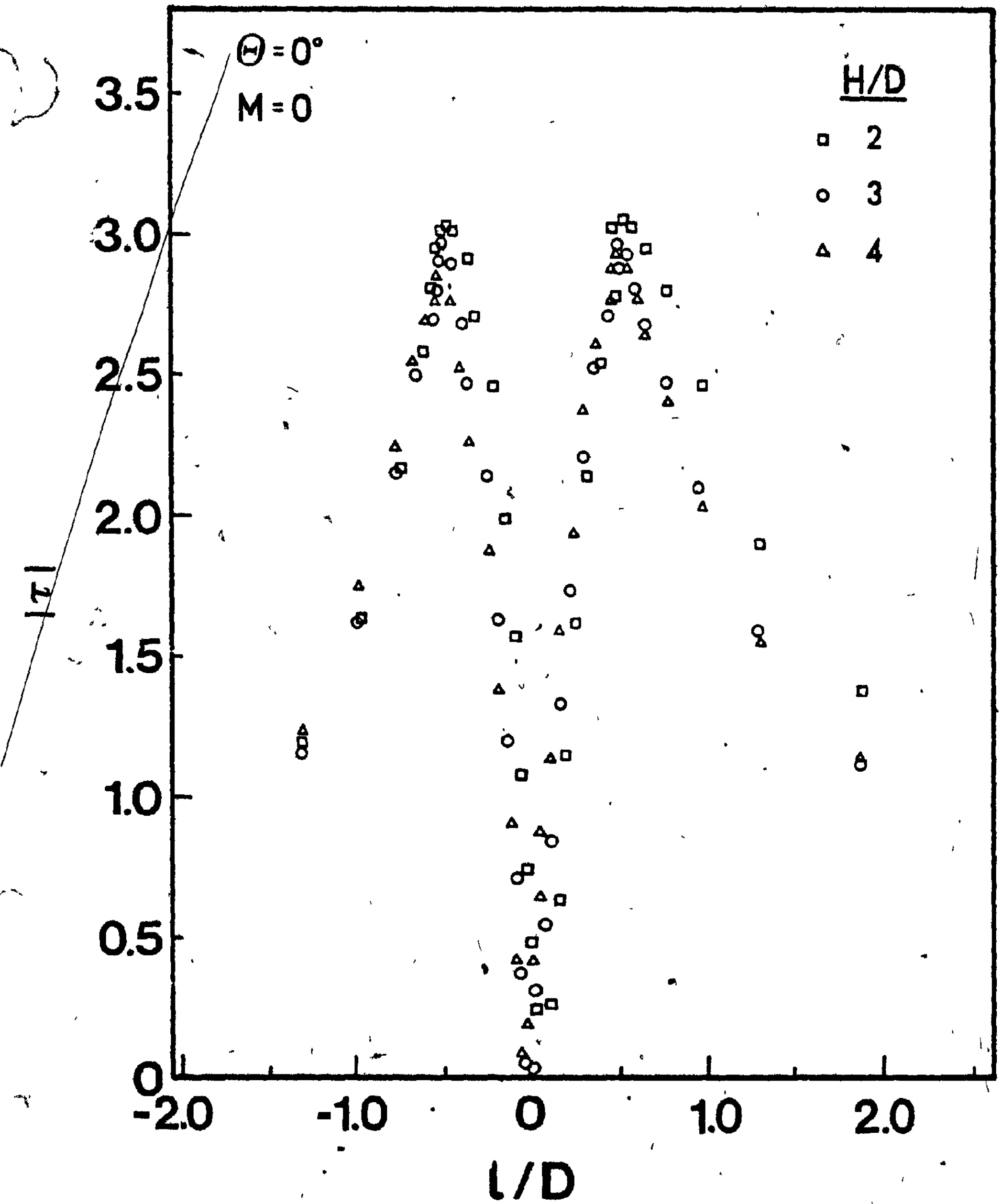

Figure 6.6 : Shear stress along the plate for impingement without crossflow at various H/D ratios.

correspond to location of the impingement surface within the potential core of the jet. Thus over the range from H/D = 2 to H/D = 4 there is a reduction in the maximum value of shear stress of only 6.6%.

Figure 6.7 shows the difference in the shear stress distribution between the case without crossflow and that of a jet discharging into a crossflow of magnitude M = 0.1. The presence of even this small amount of crossflow sharply reduces the shear stress on the impingement surface. The maximum value of τ is reduced by two thirds. This result which shows that the crosswind general tendency is to smother the jet properties and characteristics by reducing all gradients at the impingement surface will be further confirmed by the results obtained for transfer rates. This effect for shear stress as shown by Figure 6.7 is consistent with that shown on Figure 6.2 for the u-component velocity. Figure 6.7 shows also clearly the existence of a stagnation point (where the shear stress becomes zero)in the case where M = 0.1 and H/D = 4; it is shifted downstream by the action of the crossflow, as was already noted in the flow field plots, Figures 6.4 and 6.5. The stagnation point corresponds also to a maximum of the pressure along the plate; such a maximum for P is shown on Figure 6.10 for a similar case (M = 0.1 and H/D = 3).

As the crossflow of Figure 6.7 is quite small (M=0.1), the shear stress distribution along the impingement surface for a jet impinging normally has been plotted on Figure 6.8 for larger values of crossflow. The two quite different types of flow behaviour, depending on the magnitude of the crossflow, are evident on Figure 6.8. For small

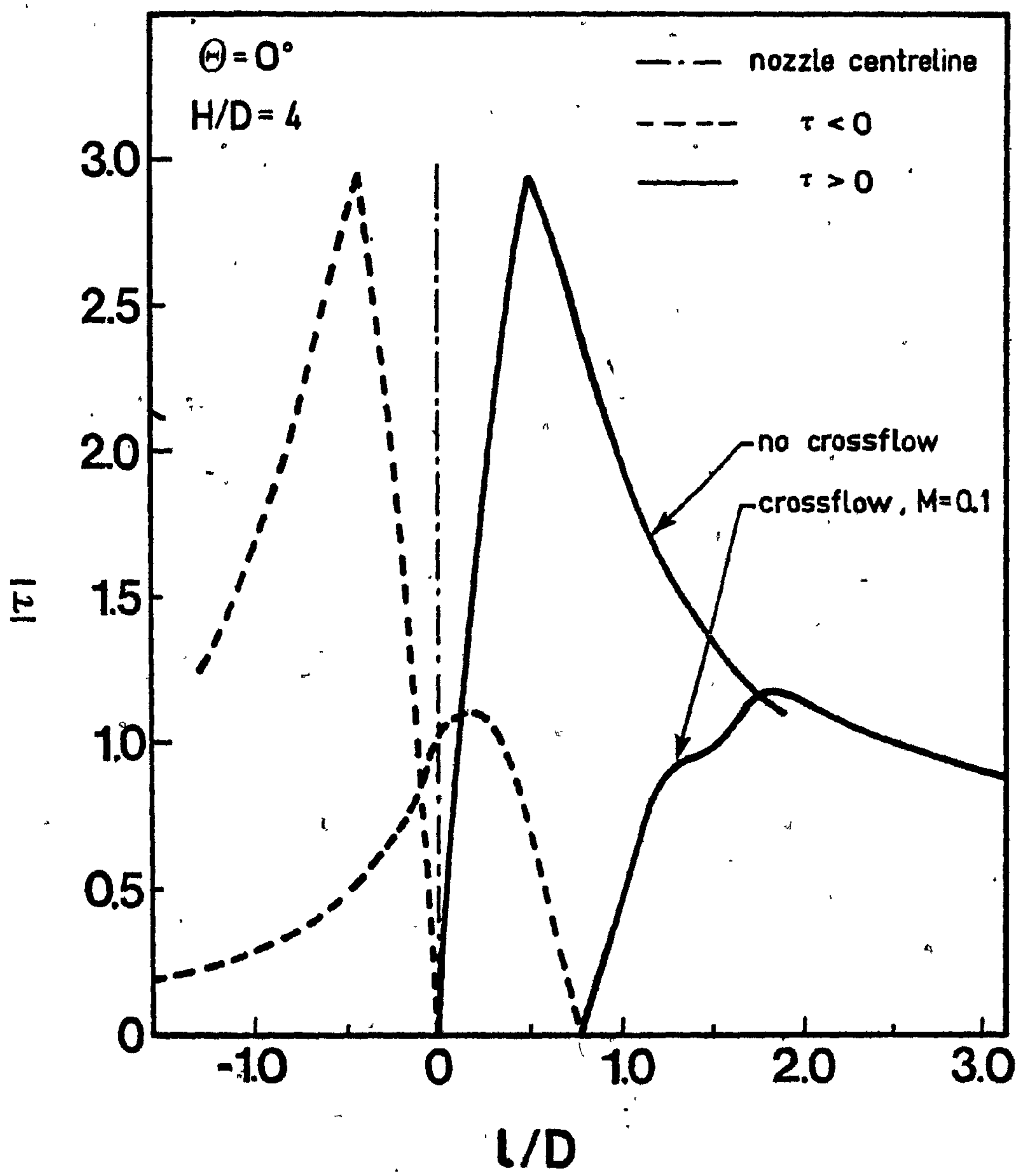

Figure 6.7 : Comparison of shear stress distribution along the plate for impingement with and without crossflow.

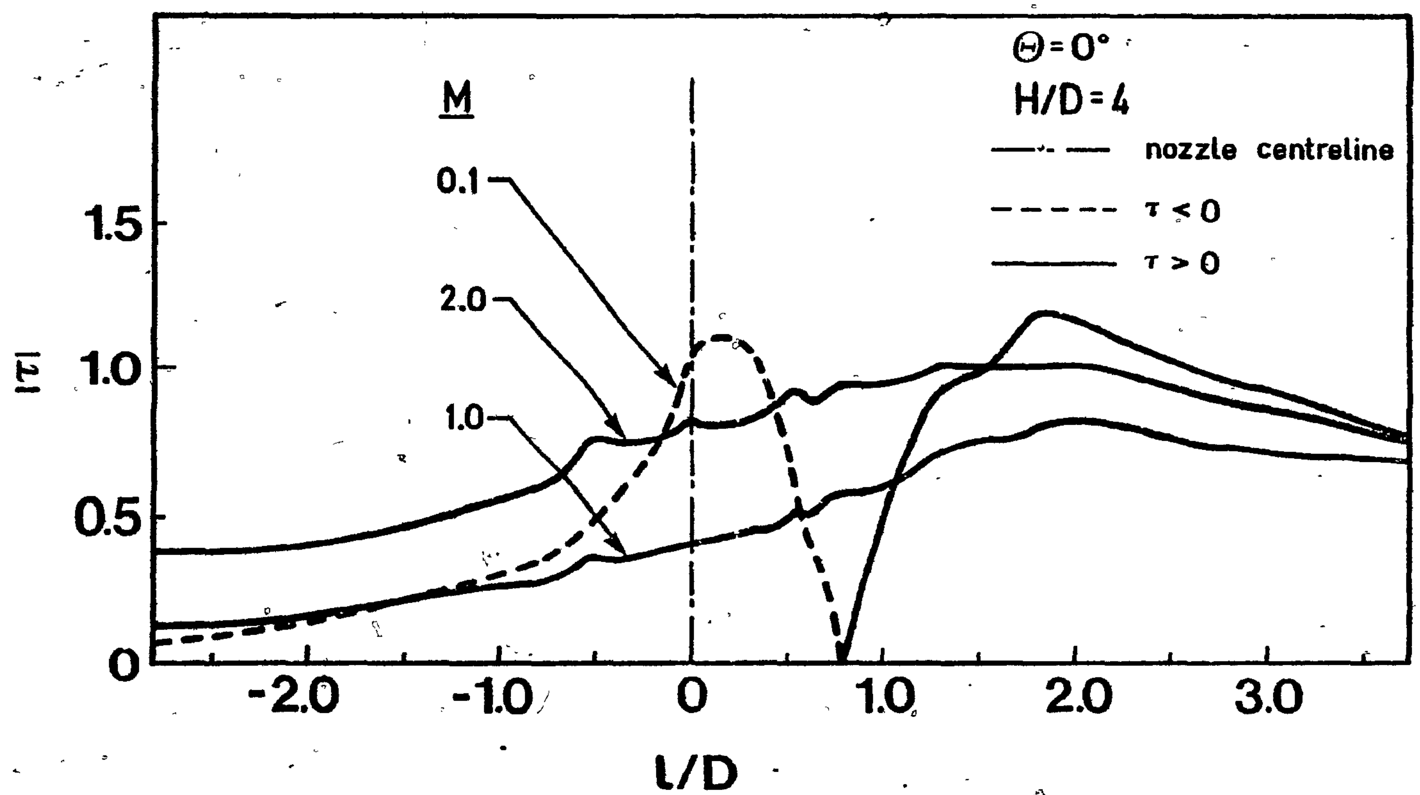

Figure 6.8 : Influence of crossflow magnitude on shear stress along impingement plate.

values of M, as represented by M = 0.1, the jet effectively impinges on the plate, there is a stagnation point, and the flow field, although strongly affected by the presence of the crossflow, is still dominated by the jet. But for large values of M, represented by M = 1.0 and 2.0, the shear stress at the evaporating surface is always positive, i.e. there is no stagnation point. The profile of τ near the crossflow entry approaches that for pure channel flow. However, from about l/D = -2.0 the shear stress increases significantly due to the additional flow provided by the jet. Shear stress reaches a maximum on the downstream side of the jet inlet at about l/D = 2, i.e. at about the same position as for the case of M = 0.1, although the maximum τ is now less even though the total flow is significantly larger. Clearly, no impingement occurs in this case. This absence of impingement is confirmed by the absence of a peak in pressure profile along the evaporating surface when M = 1.0 or 2.0. This pressure profile is similar to that shown on Figure 6.10 for M = 2.0 and $\theta = +30°$. Thus one may say that for large values of M the flow field is dominated by the crossflow, with the crossflow sweeping away the jet and preventing it from even impinging on the transfer surface. With such a flow behaviour the system is expected to yield very poor transfer rates for large values of M, as will be confirmed by the heat and mass transfer results presented subsequently.

The effect on shear stress profile of varying angle of inclination of the jet nozzle for a flow field which is crossflow-dominated (M = 2.0) is shown on Figure 6.9. Moreover, comparison of the curves for $\theta = 0°$ and M = 2.0 on Figure 6.9 (H/D = 3) and on Figure 6.8 (H/D = 4) also indicates the magnitude of the effect of H/D on shear stress in the range of close nozzle-to-plate spacing. Shear stress must of course

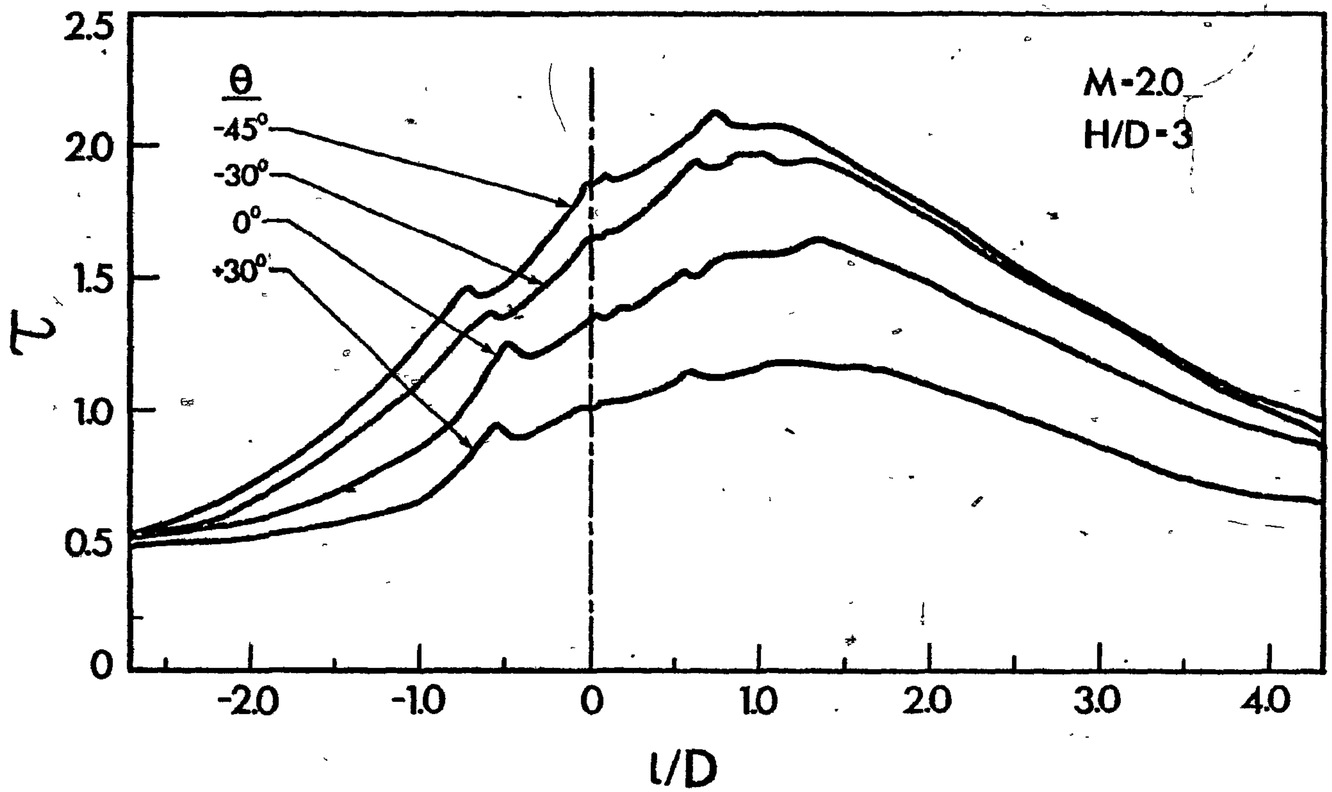

Figure 6.9 : Influence of nozzle inclination angle on shear stress along impingement plate in the case of strong crossflow.

increase as H/D decreases. In this connection it is useful to recall the definition of crossflow magnitude, i.e. $M = H\bar{V}/D\bar{U}$. As $\bar{U}$ and D are held constant, the crossflow mean velocity will be increased if the H/D ratio is decreased for a constant value of M. With the no-slip boundary condition for the v-component velocity at the evaporative surface, the velocity gradient here will also be higher when H/D is smaller, resulting in a higher shear stress at the surface. Comparison of the curves for M = 2.0, $\theta = 0°$ on Figures 6.8 and 6.9 indicates that the peak in shear stress, which is the signature of the influence of the jet on the crossflow is increased by about 60% (i.e. from 1.0 to 1.6) as H/D is decreased from 4.0 to 3.0. These calculations quantify the intuitive conclusion that the further the jet nozzle is spaced from the evaporating surface, the more the system is crossflow-dominated.

Comparison of the various curves on Figure 6.9 indicates the significant fact that the shear stress is steadily increased as the jet nozzle is rotated in the direction from positive through negative angles of inclination. As can be seen by reference to the plots of the flow field for $\theta = -10°$ and $\theta = +30°$, Figures 6.4 and 6.5, the more the nozzle is rotated in the direction of negative angles, the more of the jet flow which is directed upstream against the crossflow and towards the impingement surface, and hence the larger the v-component velocities subsequently in the region beneath and immediately downstream from the nozzle. The result is a higher gradient in v-velocity near the plate, causing higher shear stress.

The small secondary peaks evident on these curves have their origin in the computational procedure, and seem to be associated with the relatively fine computational grid near the nozzle edges (around gridlines JNOZ and JSTEP) which is required for an accurate definition of these edges. Indeed, these small computational maxima correspond exactly to $|1/D| = 0.5$ when $\theta = 0°$ and go slightly further away from this point as θ is increased to +30° and +45°, corresponding to the slight shift in the location of the nozzle edges which are located at $1 = \pm D/\cos\theta$.

The pressure profiles along the evaporative surface, shown as Figure 6.10, have already been referred to in connection with discussion of the shear stress profiles. The three typical profiles shown illustrate the progression from the condition without crossflow, to a small crossflow (M = 0.1) for which there is still impingement and a stagnation point at the pressure maximum, to the case of a totally crossflow-dominated system (M = 2.0) in which there is no pressure maximum or stagnation point, but instead a continuous pressure loss in the direction of the controlling crossflow.

6.3 HEAT TRANSFER RESULTS

6.3.I Without Crossflow

Profiles of heat transfer coefficient at the impingement surface are plotted in terms of local Nusselt number on Figure 6.II for H/D ratios of 2, 3 and 4. These curves, bell shaped around the stagnation point as expected show clearly that, within this range of H/D ratios, nozzle-to-plate spacing has negligible influence on the local Nusselt number as the variation at the peak is only 3%. This confirms the conclusion of Huang (HI) for turbulent jets and of Kapur and McLeod (K4)

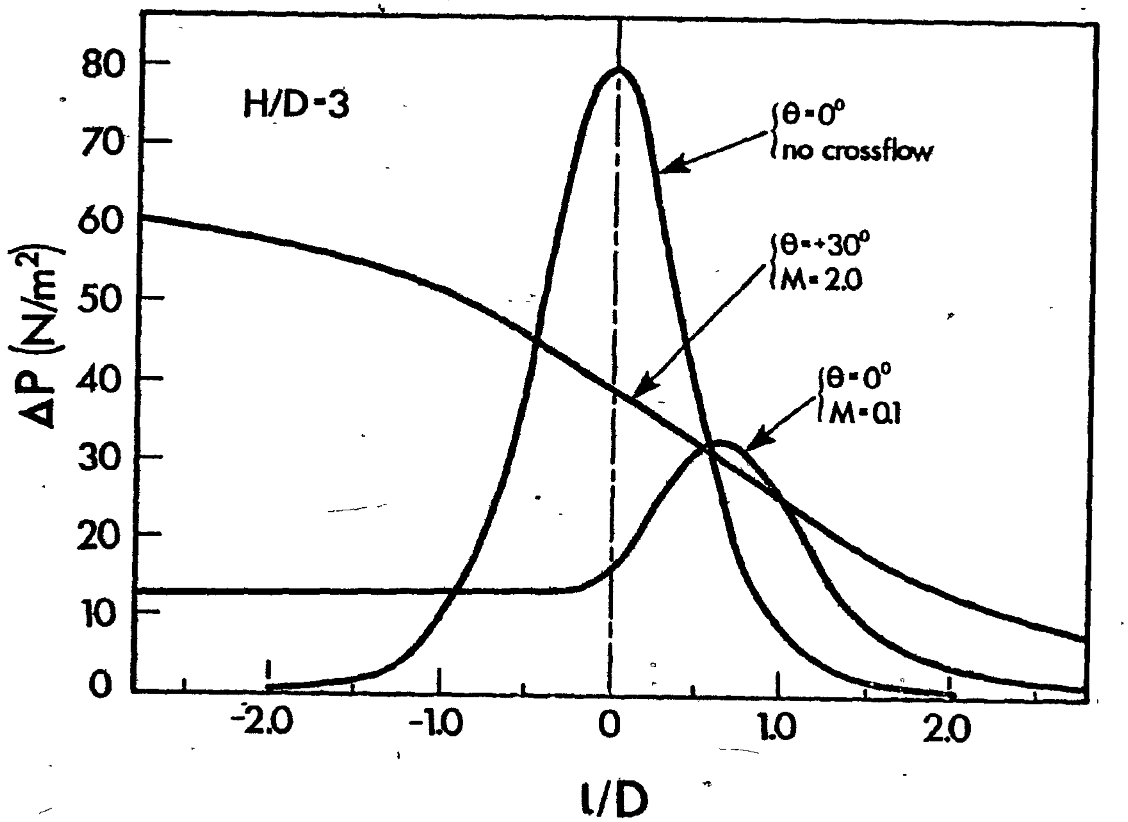

Figure 6.10 : Pressure distribution along impingement plate.

and Gardon and Akfirat (G6) who operated with Reynolds numbers of comparable magnitude to the one chosen here. This finding with respect to heat transfer is consistent also with the small variation in shear stress noted in Section 6.2.3.

The stagnation point Nusselt numbers are somewhat lower than those found by van Heiningen (V2) who also studied heat transfer under a rectangular impinging jet. His results, expressed dimensionlessly as $Nu/\sqrt{Re}$, gave $Nu/\sqrt{Re} = 0.81$ at the stagnation point for Re = 950 and H/D = 4 in the case of a parabolic velocity profile for the jet at the nozzle exit. For H/D = 4 and Re = 1000 the value found in the present study is $Nu/\sqrt{Re} = 0.7$ at the stagnation point. This difference is accounted for by the simultaneous mass transfer which takes place here but not in van Heiningen's study. The reduction in heat transfer caused by linkage with a mass transfer flux in the opposing direction was studied numerically by Li (L2) for the case of a round axisymetric impinging jet.

6.3.2 Effect of Crossflow

As the domain of interest of the present study is evaporation under impinging jets, most of the curves presented in the following sections are limited, for convenience of format, to the central area of the flowfield where interaction between jet and crossflow is felt. Consequently it is important to note that the extent of the region shown in the remaining figures of Chapter 6 is less than the total extent of the flow system. Thus results are usually shown over the prime interest range of H/D of about ± 3, although the crossflow entry is at H/D = -6.4 and the flow exits at a value of H/D in the range from 6.1 to 8. However, for completeness, one profile is presented which covers the entire system, from crossflow inlet to the flow exit. As this complete profile is for mass transfer rate (Figure 6.26), it is discussed

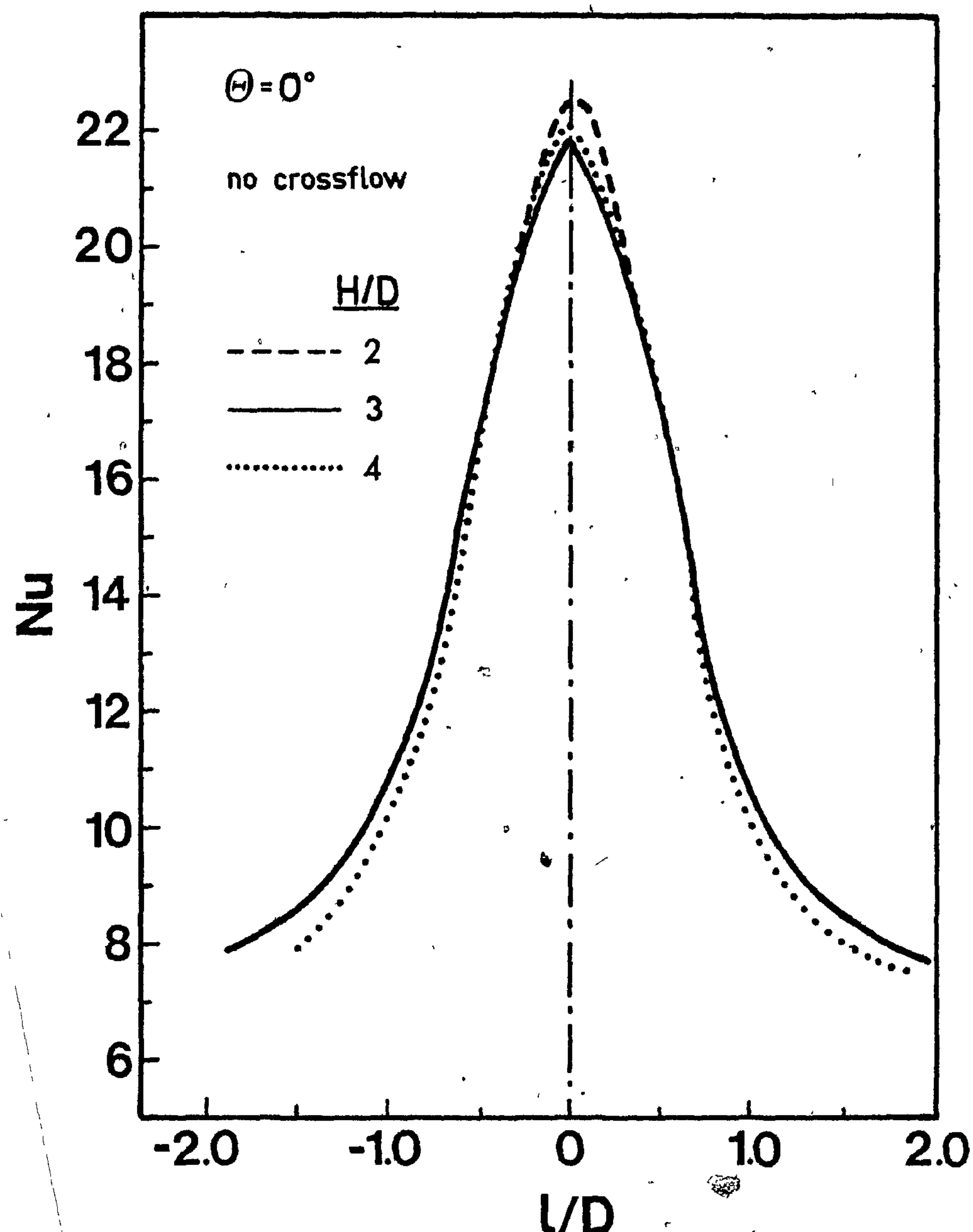

Figure 6.11 : Influence of H/D on heat transfer for a jet impinging normally without crossflow.

subsequently. The trends noted there for mass transfer would by analogy apply also to heat transfer.

6.3.2.1 Influence of Crossflow Ratio

On Figure 6.12 the local Nusselt number distribution is shown for a wide range of crossflow ratios, M, covering both the jet-dominated and crossflow-dominated regimes. The basic difference in the heat transfer profiles between flow regimes of these types as illustrated by Figure 6.12 parallels the corresponding differences in shear stress profiles already noted on Figure 6.8. For the spacing of H/D = 4 on Figures 6.12 and 6.13, the profiles for values of M of 0.01, 0.1, 0.167 and 0.25 are for jet-dominated flow, while the profiles for M = 1.0 and 2.0 clearly correspond to crossflow-dominated flow. These profiles with crossflow may be compared to those of Figure 6.11 without crossflow, as the fact that the plate widths are not the same does not have a significant effect in the central region of interest. Such a comparison indicates that the stagnation point heat transfer is sharply decreased by the crossflow, i.e. it is reduced by 36% for only M = 0.01, and by 50% when M = 0.25. As expected the stagnation point is shifted in the downstream direction by crossflow, and this shift increases for increasing values of M. The curves with crossflow are of course not symetric with respect to the stagnation point, as the mass flow-rate is greater on the downstream than on the upstream side of the stagnation point.

Metzger and Korstad (M5) claimed that the upstream propagation distance of a jet along the impingement surface is relatively short and that, as a consequence, the heat transfer rates immediately upstream of the nozzle exit plane are reduced significantly below what would be expected if crossflow were not present. However, this effect on the upstream side may be viewed simply as a consequence of the simultaneous reduction

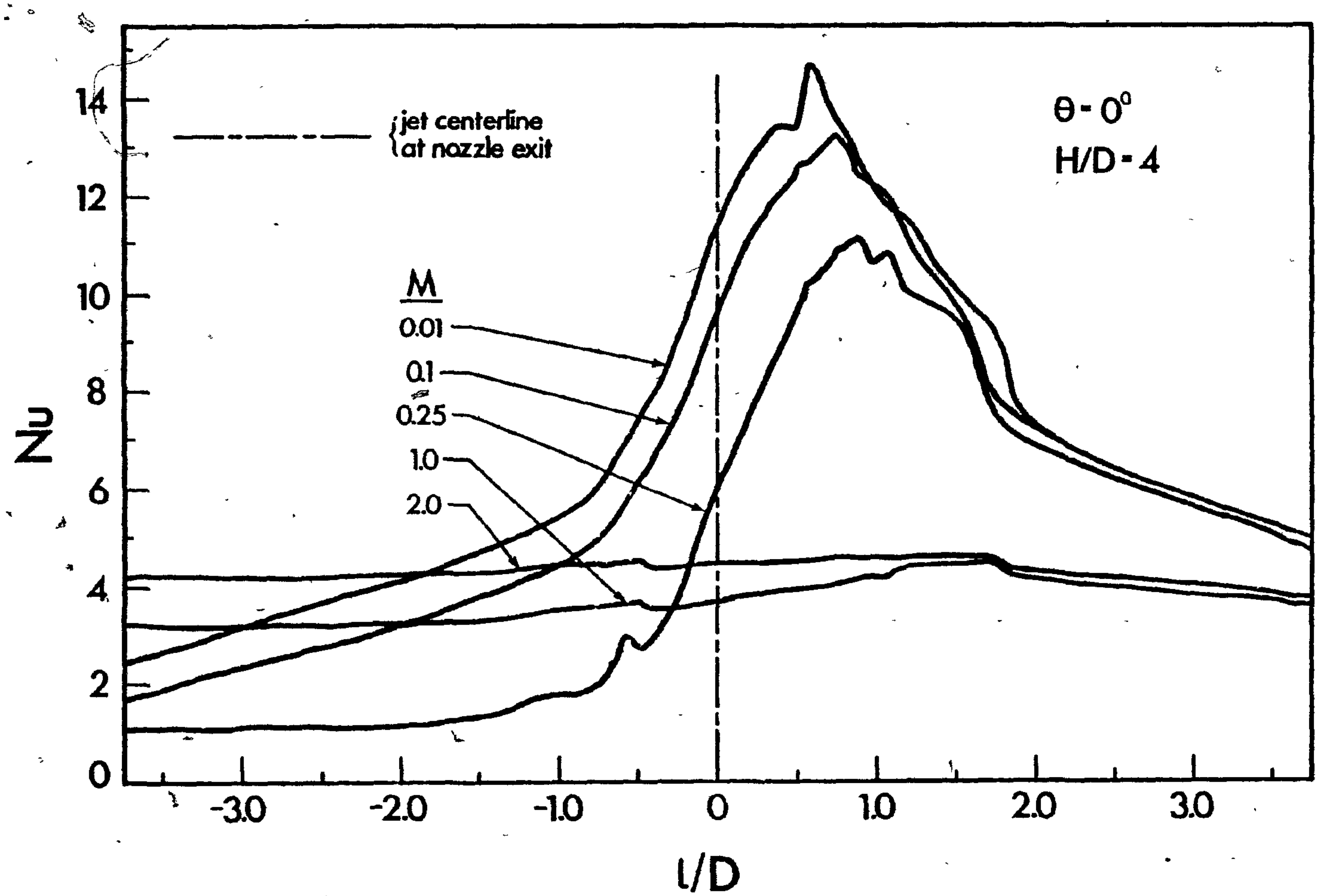

Figure 6.12 : Comparison of the Nusselt number distribution along the plate between jet-dominated and crossflow-dominated systems for a perpendicular nozzle.

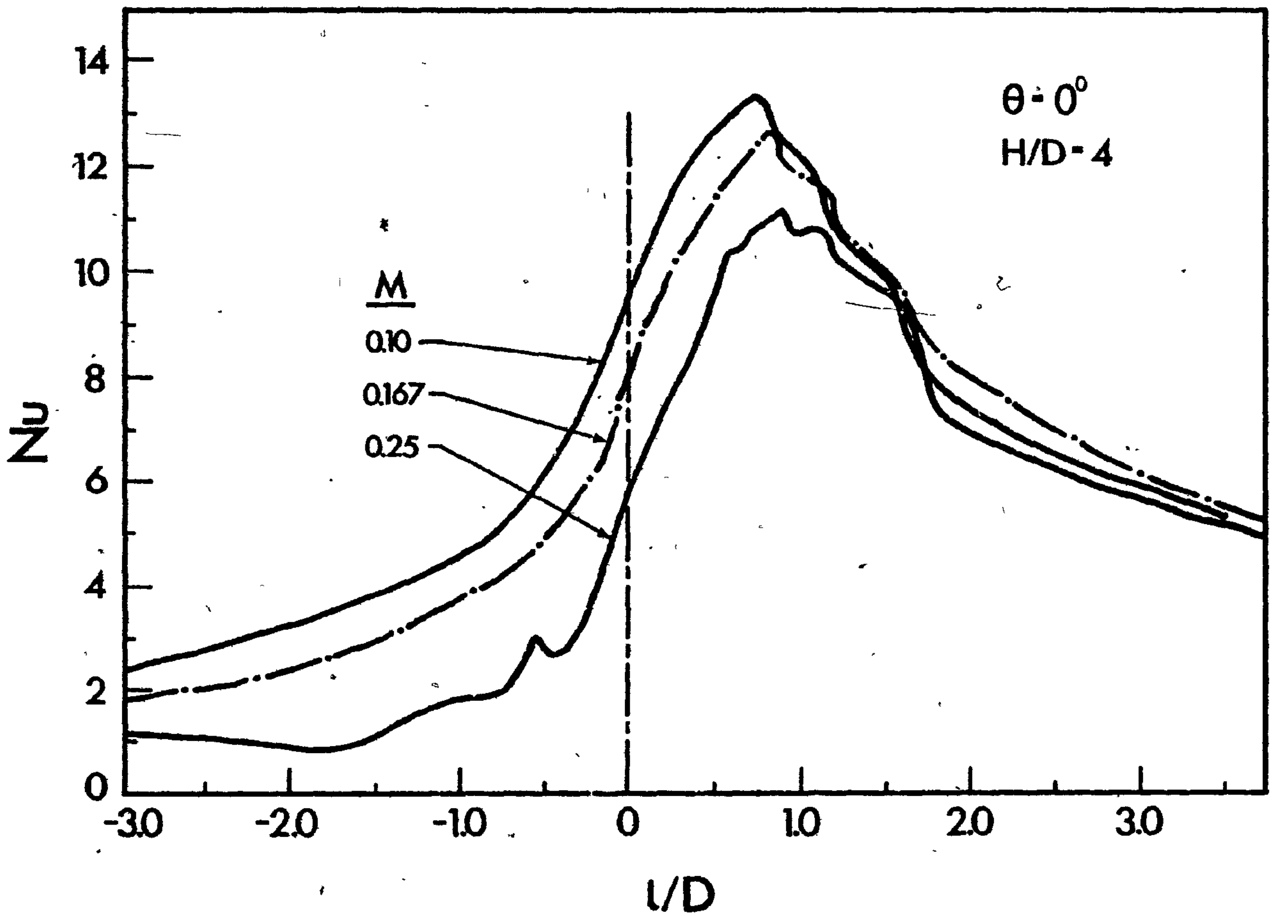

Figure 6.13 : Heat transfer for jet-dominated systems.

in the entire profile and its shift downstream which appear clearly when comparing Figures 6.11 and 6.12. On the other hand, the present results disagree with Metzger's further conclusion that average heat transfer over regions immediately downstream is increased above that without crossflow. The average Nusselt number calculated over different regions of the impingement plate are presented on Table 6.2. It appears clearly that for all the regions considered on Table 6.2 the average heat transfer rate with crossflow is less than that without crossflow. It seems more logical anyway to speak in terms of Nusselt numbers averaged over regions starting from the stagnation point (instead of the nozzle exit plane) or extending on both sides of the stagnation point (see Nu_4 and Nu_5 on Table 6.2). With such definitions it appears clearly that the effect of the crossflow is to reduce the average heat transfer coefficients. On an overall basis for a symetrical region extending ten nozzle widths both upstream and downstream of the nozzle exit plane, Metzger did however conclude that the presence of crossflow always reduces the average heat transfer below that without crossflow (M5). Although the results of the present study contradict Metzger's statement concerning heat transfer in the near downstream region, they nonetheless confirm the latter conclusion of Metzger et al.

For large values of M, (M 1.0 or M 2.0), Figure 6.12 shows that the heat transfer profiles are totally different, as could be expected from the shear stress profiles for large and small crossflow ratios shown on Figure 6.8. For this range of M and H/D ratios we are no longer dealing with impinging jets, as the shear stress results showed that for these conditions there is no stagnation point. Thus the local Nusselt number distribution corresponds to that for channel flow but modified somewhat by the addition of the jet flow. The maxima of the curves are not due to impingement, but only to the increase in flow-rate through the channel that is associated

M	Nu_1	Nu_2	Nu_3	Nu_4	Nu_5
0.01	13.3	11.7	9.8	8.2	6.6
0.1	12.0	11.0	9.3	7.5	6.0
0.25	9.2	9.3	8.2	6.7	4.5
no crossflow	16.8	12.5	10.7	10.7	9.3

Nu_1 : Nusselt number averaged on the region of the impingement plate extending on a one nozzle width-length downstream of the nozzle exit plane.

Nu_2 : Nusselt number averaged on the region of the impingement plate extending on a two nozzle width-length downstream of the nozzle exit plane.

Nu_3 : Nusselt number averaged on a region of the impingement plate extending on a three nozzle width-length downstream of the nozzle exit plane

Nu_4 : Nusselt number averaged on the region of the plate extending on a three nozzle width-length downstream of the stagnation point plane.

Nu_5 : Nusselt number averaged over a symetrical region extending four nozzle widths both upstream and downstream of the nozzle exit plane.

Table 6.2 : Average Nusselt numbers.

with the fluid added from the jet nozzle.

Although heat transfer decreased sharply with increasing crossflow in the low range of M (i.e. at least up to M = 0.25 for H/D =4), it is useful to note that in the high range of M (i.e. from 1.0 to 2.0), heat transfer increases with M. The initial decrease of Nu with increasing M corresponds to destruction of the beneficial impingement flow pattern by crossflow, while the later increase of Nu with M simply corresponds to normal channel flow behaviour. This reversal of the effect of M on Nu is illustrated on Figure 6.14 for one value of H/D and θ. The value of M which marks the transition between jet-dominated and crossflow-dominated flow could be taken as the value of M which gives the minimum value of Nu_{max} on Figure 6.14. This limiting value of M would decrease as H/D increases, and would as well be a function of the nozzle inclination angle.

6.3.2.2 Influence of H/D

The influence of nozzle-to-plate spacing over the small range of H/D investigated is shown on Figure 6.15. The influence of H/D on heat transfer profile, very small without crossflow, becomes quite noticeable with even a small crossflow. For θ = 0°, the stagnation point heat transfer coefficient is reduced by 19% by an increase in H/D from 2 to 4 with M =0.1, whereas the corresponding reduction without crossflow was only 3%. The increased sensitivity of heat transfer profile to H/D is a natural consequence as H/D measures the distance over which the crossflow acts on the jet. For the same reason the maximum Nu at the stagnation point is also deflected increasingly downstream. At any value of M, increasing H/D will eventually lead to a crossflow-dominated flow.

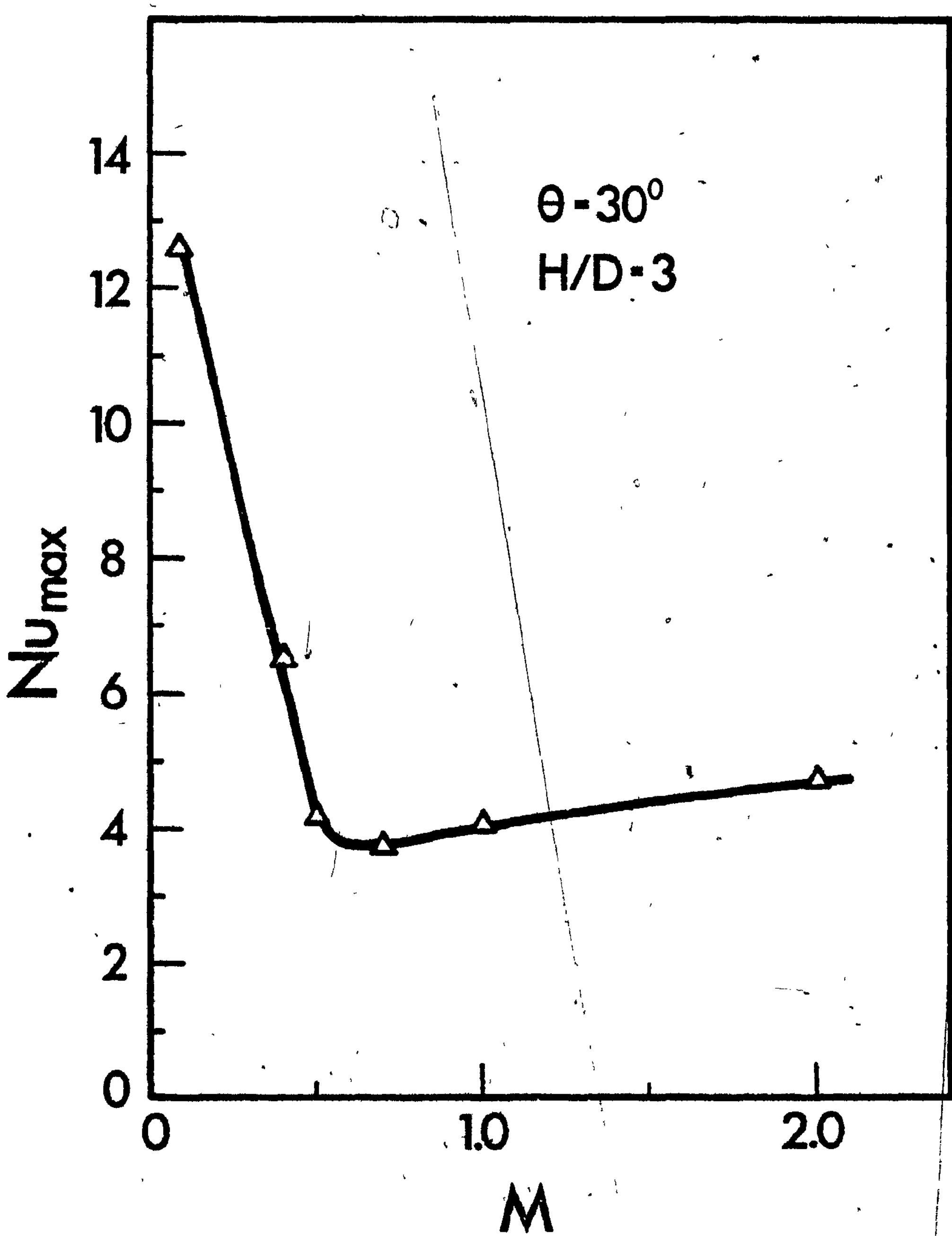

Figure 6.14 : Maximum local Nusselt number as a function of M.

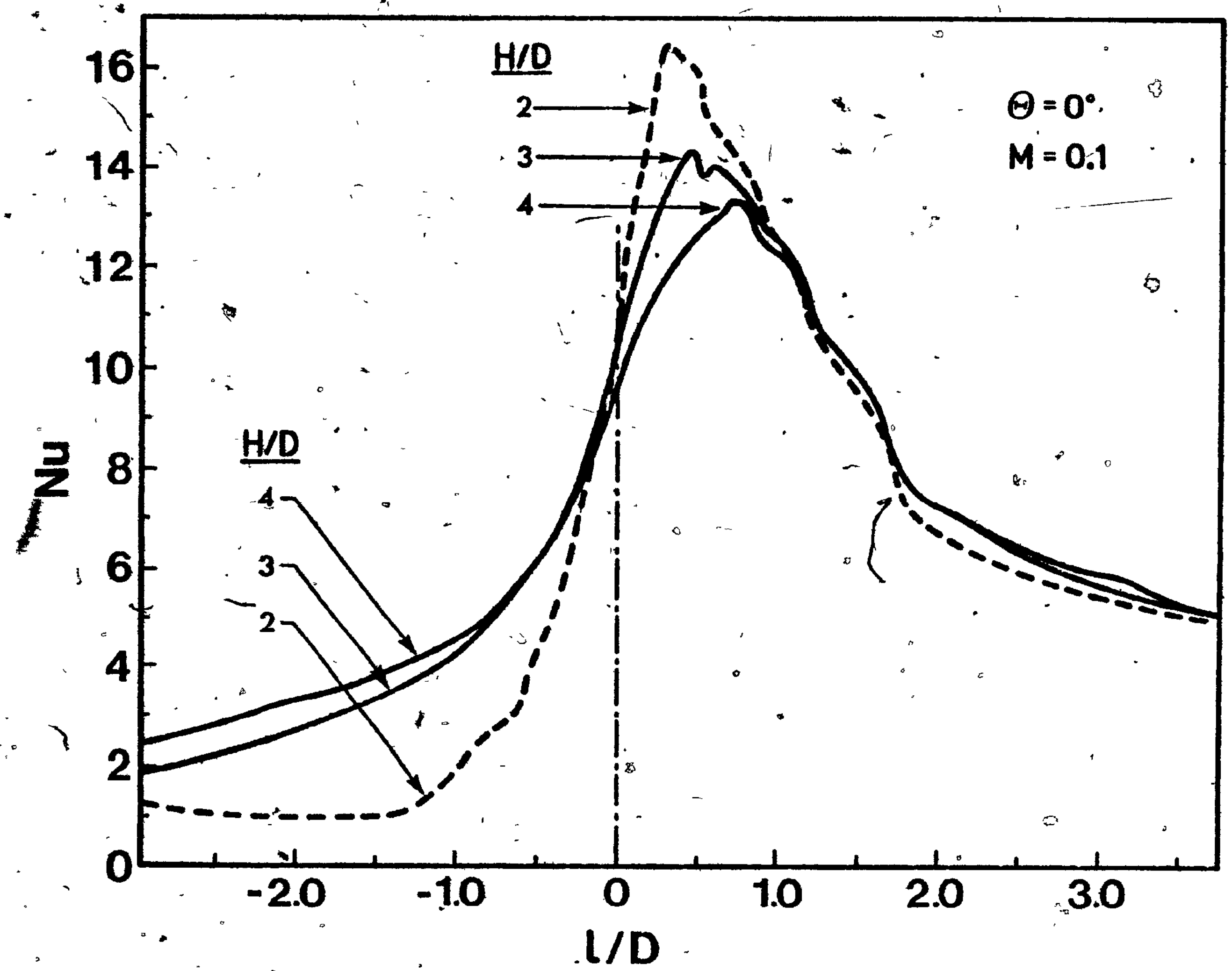

Figure 6.15 : Influence of H/D on local heat transfer for a jet in a crossflow.

6.3.3 Effect of Angle of Inclination

Since it has been established in the previous sections that for a particular nozzle-to-plate spacing two quite different types of flow behaviour can be encountered depending on the value of M, it is useful to review the influence of angle of impingement separately for each case. Subsections 6.3.3.1 and 6.3.3.2 deal, respectively, with small and large values of the ratio M.

6.3.3.1 Effect of Angle for moderate M ratios

Angles varying from -45° to 30° have been investigated for M = 0.1 and H/D = 3. From the curve for M = 0.1 it may be seen on Figure 6.16 that a dinstinct maximum in Nu_{max} occurs at a negative angle situated between -30° and -15°. To interpret this fact it is convenient to start from large positive angles (i.e. jet directed in the same direction as the crossflow) and to see how the flowfield is modified as the angle decreases, takes the value zero (right angle jet) and finally increases in the direction opposed to the crossflow.

Figure 6.17 shows the local Nusselt number distribution obtained along the plate for $\theta = 30°$, $\theta = 0°$ and $\theta = -10°$. For $\theta = 30°$ the jet is more easily taken away by the crossflow because of the compatibility of nozzle inclination with crossflow direction. The jet is thus strongly deflected (as shown by the shifting of the peak in local Nusselt number). As the nozzle is inclined more in the direction of the crossflow, the conversion of x-momentum into y-momentum occurs further from the impingement surface, hence the resulting reduction in heat transfer rates. However, the shear stress results obtained for this run show that there is still a stagnation point where $\tau = 0$, and that the position of the heat transfer maximum is at the stagnation point. As θ decreases from 30° to 0° and to -10° it is clear from Figure 6.17 that the deflection of the jet is smaller and that higher values of maximum heat transfer rates result from

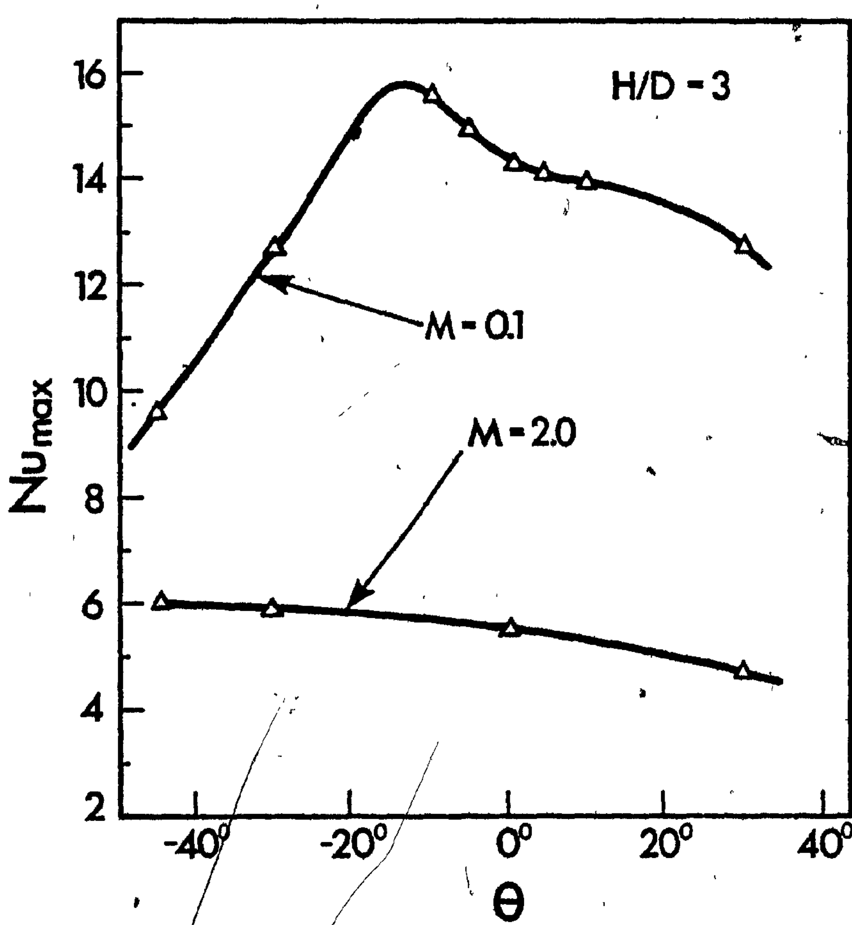

Figure 6.16 : Maximum local Nusselt number as a function of nozzle inclination angle.

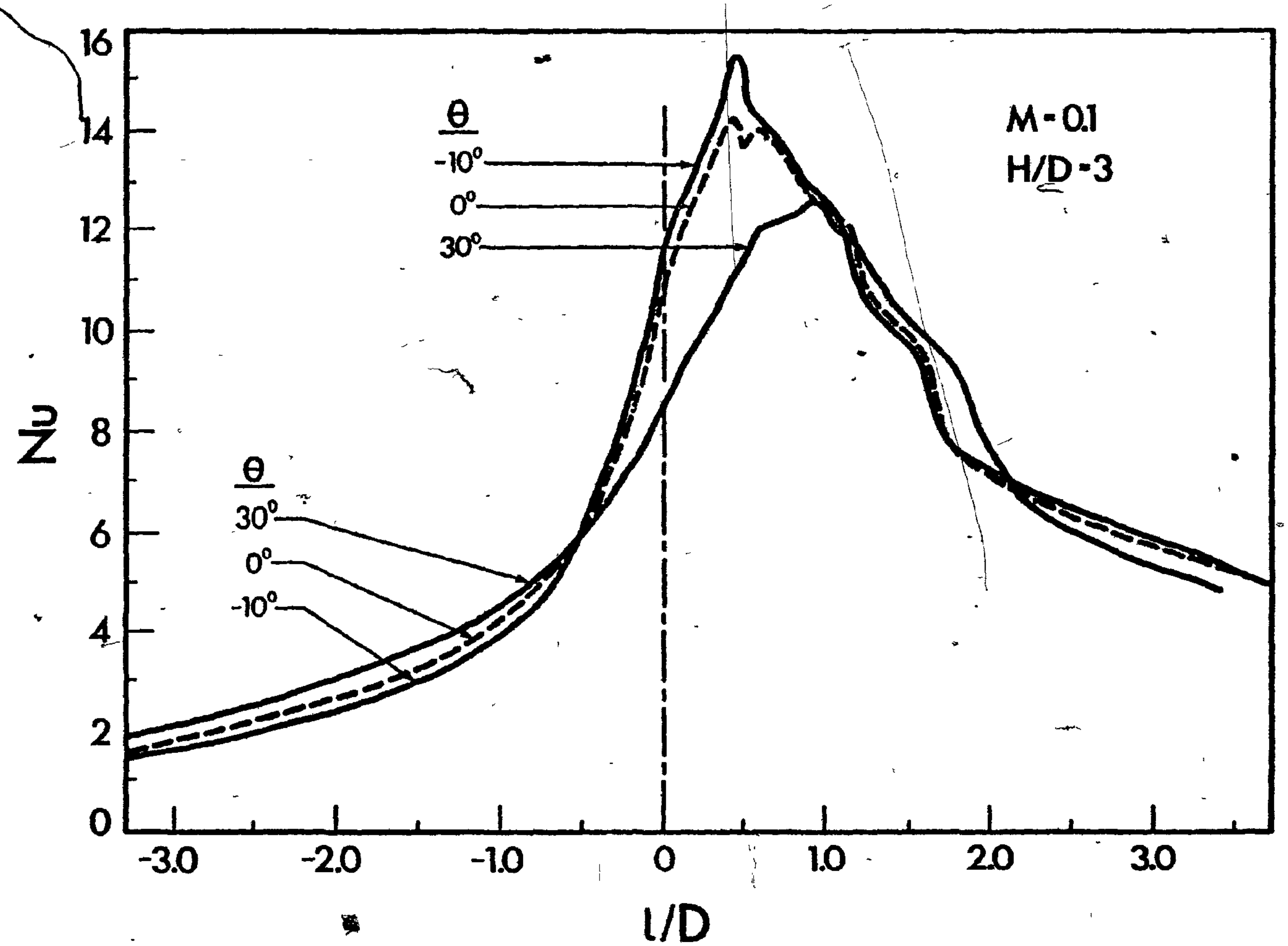

Figure 6.17 : Influence of angle of inclination on local Nusselt number for small values of M.

the increasingly vigourous impingement on the plate.

If the nozzle is inclined more strongly yet against the crossflow, e.g. for $\theta = -30^\circ$ or -45°, then the dominant effect becomes a loss of momentum of the jet in this collision-type process where the two flows are directed against one another. From Figure 6.18 it can be seen that both the maximum and the average values of heat transfer decrease sharply for increasingly negative angles of inclination from -10° to -30° to -45°.

As a conclusion it appears that, for a given crossflow magnitude and nozzle-to-plate spacing, there exists an optimum angle (directed slightly against the crossflow direction) for which heat transfer is maximum. It will be seen in Section 6.4 that this conclusion is also valid for the mass tranfer rates. This observation can be important in industrial practise where a crossflow (caused for example by a neighbouring nozzle) cannot be eliminated, since it appears that the decrease in transfer coefficients caused by the crossflow can be reduced by choice of the optimum nozzle angle.

6.3.3.2 Effect of the Angle for large M ratios

In this case, as seen earlier, there is no stagnation point and hence no real impingement. Figure 6.19 shows that the heat transfer distribution is quite flat for all inclination angles. The heat transfer rates do increase significantly as the angle of inclination is changed from 30° to 0°, and continues to increase slightly as the angle is changed to -30° and -45°. As there is no impingement, this increase is simply due to the augmentation of the crossflow by the nozzle flow in the region beneath and downstream from the location of the nozzle. This behaviour is consistant with the discussion of Section 6.2.3 and with the shear stress results presented on Figure 6.9.

For a fixed angle, $\theta = 30^\circ$, and for a nozzle-to-plate spacing

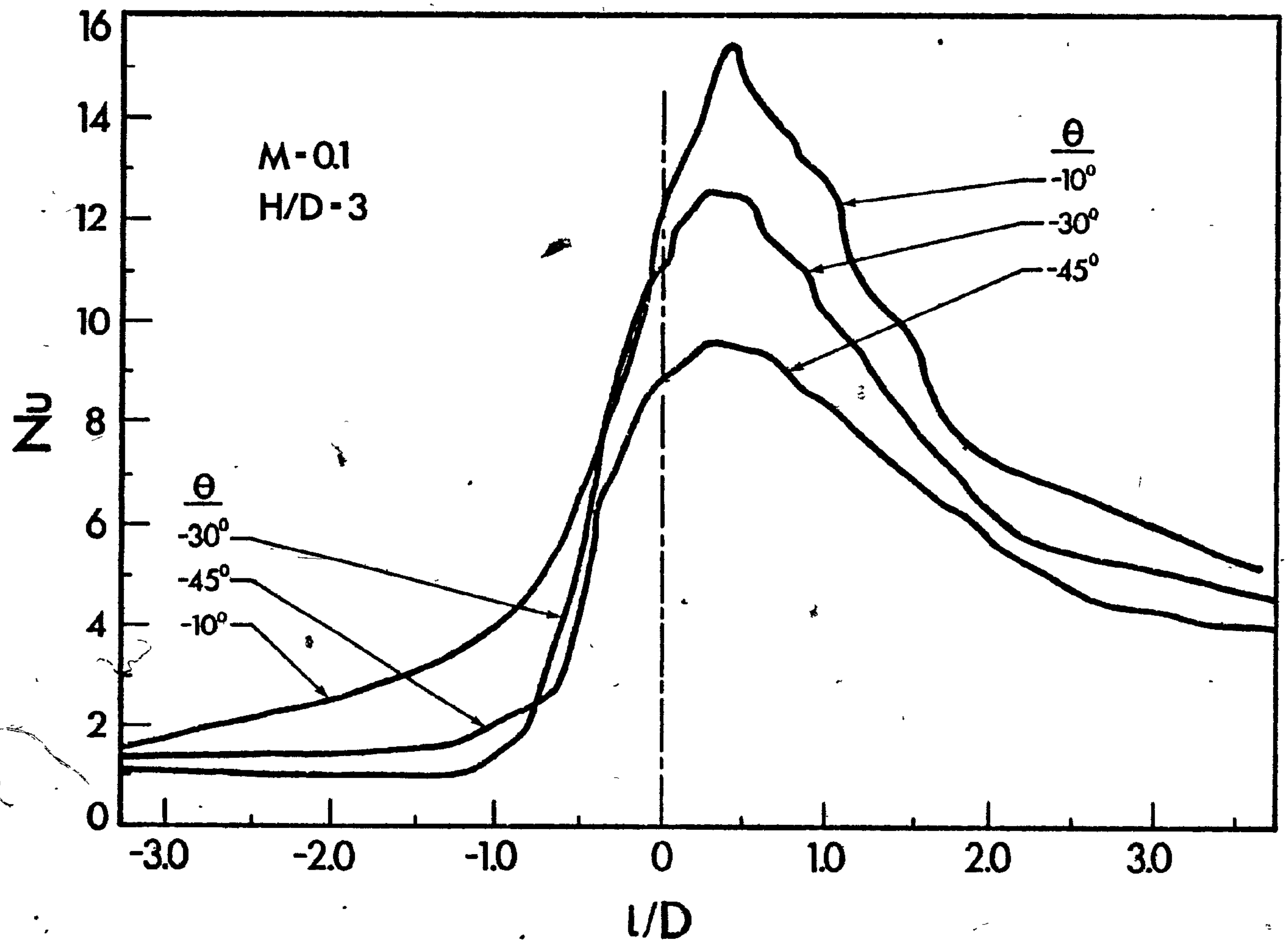

Figure 6.18 : Influence of θ on local Nusselt number for small values of M.

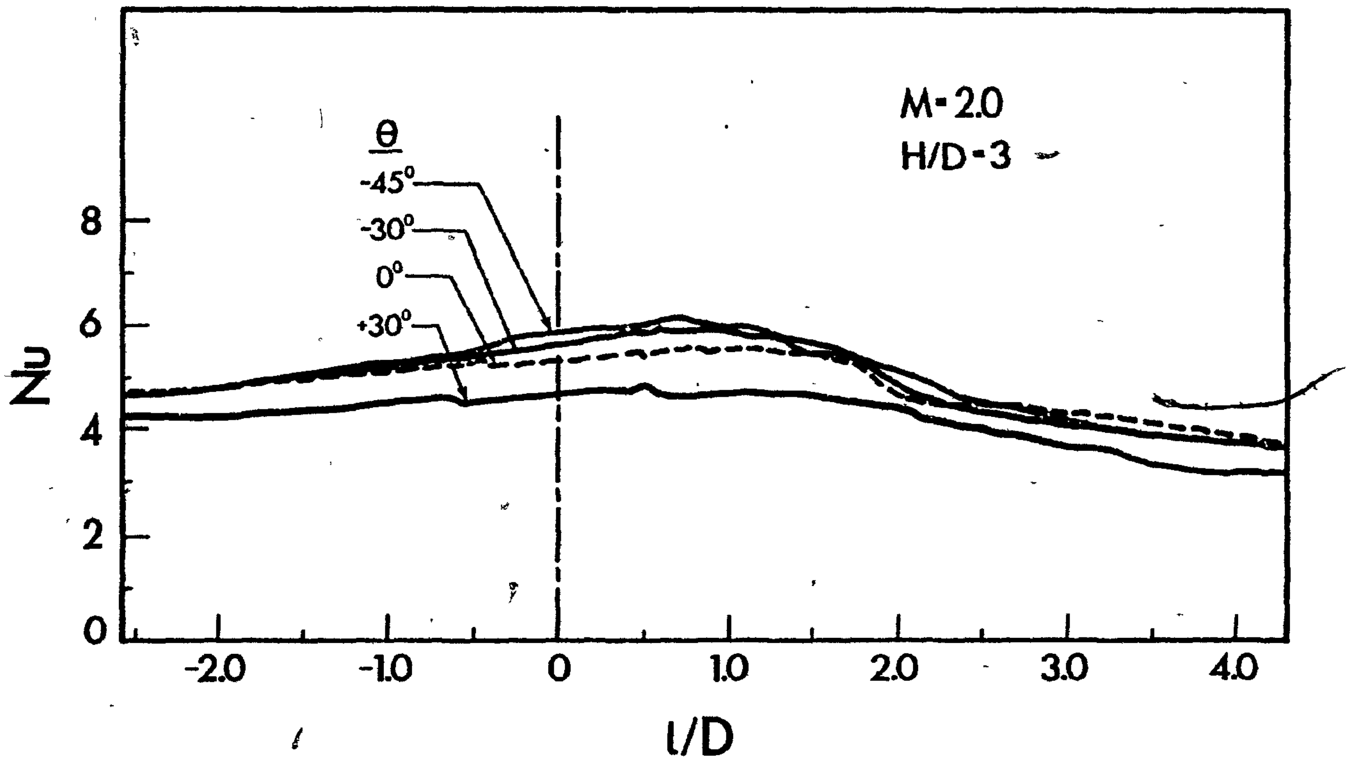

Figure 6.19 : Influence of θ on local Nusselt number for large values of M.

of 3, several crossflow magnitudes were tested and the representation of these results on Figure 6.20 again indicates the transition between jet-dominated systems and crossflow-dominated systems. It appears that for M = 2.0, 1.0 and 0.7 the system is dominated by the crossflow wheras it is dominated by the jet for M = 0.1 and M = 0.4. The case for M = 0.5 appears intermediate. As the existence of a stagnation point where $\tau = 0$ could be taken as a criterion for terming a system as a jet-dominated impingement flow, it is of interest to note that there is a stagnation point for the cases of M = 0.1, 0.4, and 0.5, but not for M = 0.7, 1.0 and 2.0.

6.4 MASS TRANSFER RESULTS

Figures 6.22 through 6.24 show that mass transfer is affected in exactly the same manner as heat transfer by the presence of a crossflow. As in Section 6.3, it appears here that, depending on the value of M, the mass transfer can be dominated by the jet or by the crossflow. The variation of maximum local Sherwood number as a function of M, shown on Figure 6.25, parallels exactly what was observed for local Nusselt number on Figure 6.14, i.e. the stagnation point Sherwood number decreases very sharply with M for jet-dominated flows, whereas the maximum Sherwood number increases slightly with M for large crossflow magnitudes simply because of the augmentation of crossflow by the nozzle flow.

Figure 6.26 shows the influence of H/D on the mass transfer coefficient but shown this time on the entire impingement plate from crossflow entry to the outflow boundary. The central portion parallels the results obtained for heat transfer (Figure 6.15). On Figure 6.26 the dimensional mass transfer coefficient, k, was represented instead of the dimensionless Sherwood number, as this choice permits the case for pure

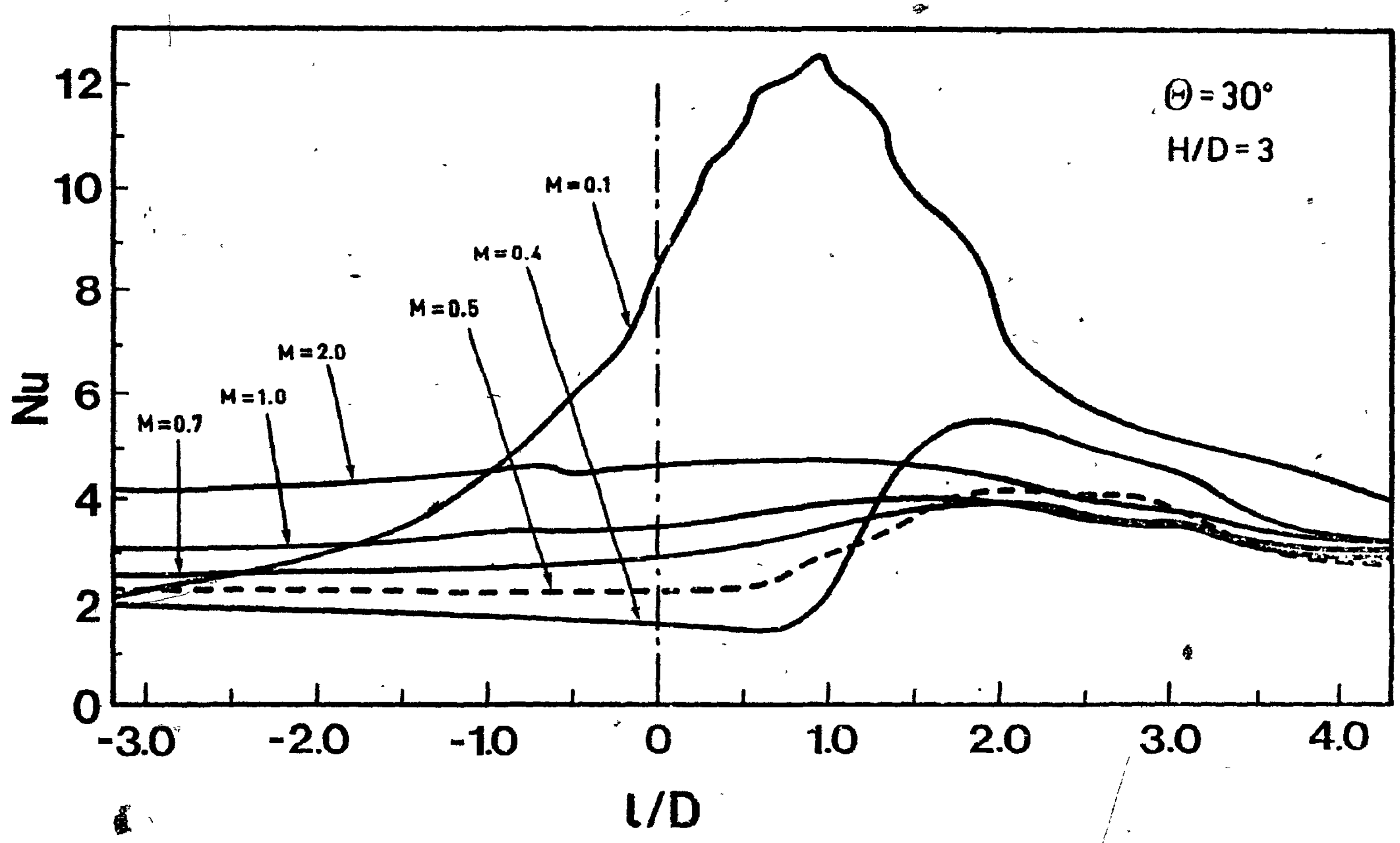

Figure 6.20 : Influence of M on local Nusselt number for θ = 30
and H/D = 3.

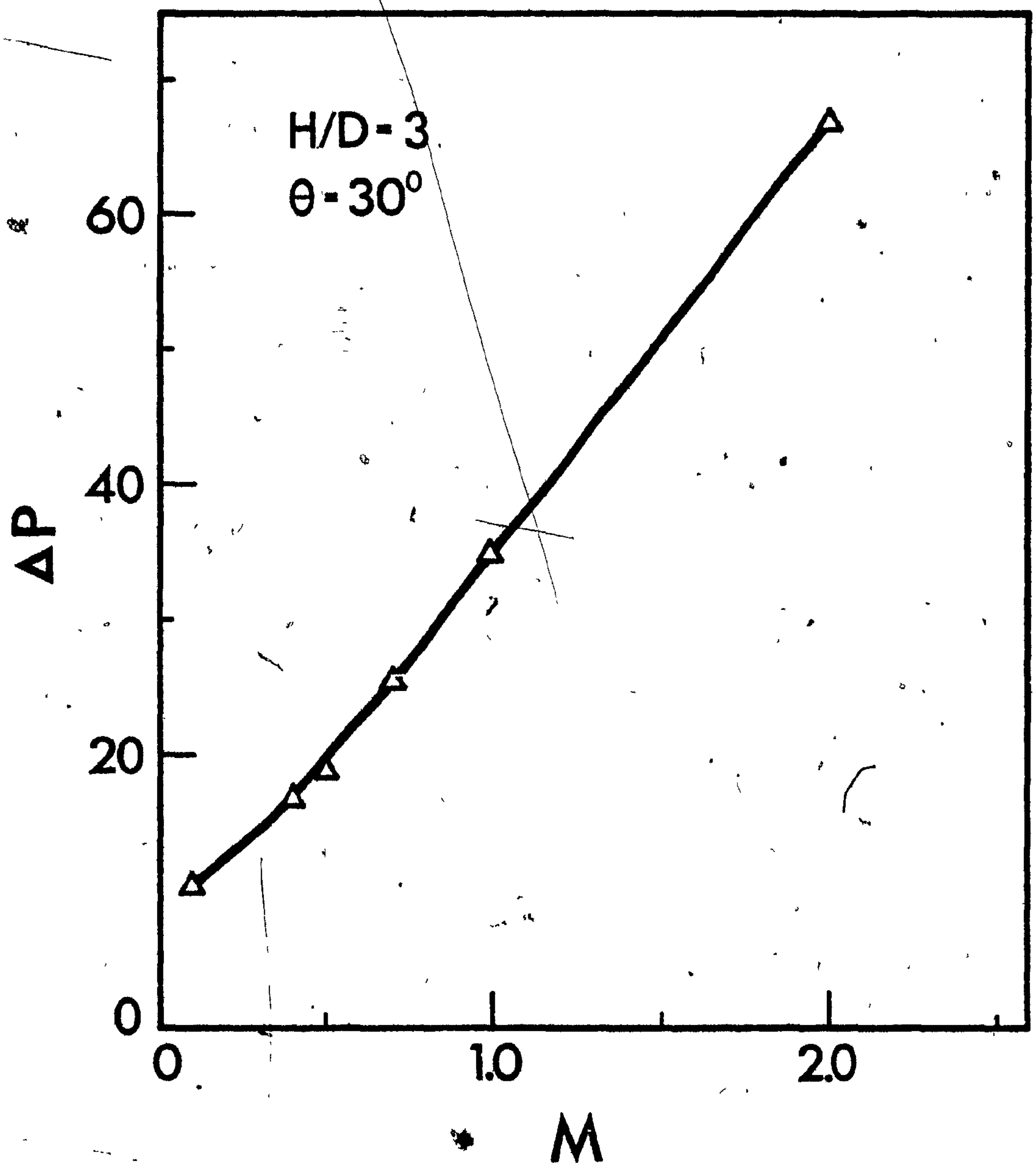

Figure 6.21 : Crossflow entry pressure versus crossflow magnitude, M.

crossflow to be included for comparison. As Sherwood and Nusselt number require use of a characteristic dimension, and as for impingement flows D is the appropriate dimension, it is evident that representation of the limiting case of pure crossflow cannot be in terms of such a dimensionless parameter. Equally, while H is appropriate as a characteristic dimension for crossflow-dominated flows, it would not be for approaching the other limiting case of pure jet flow.

The dashed line curve, representing pure crossflow, is typical of channel flows, i.e. k steadily decreases from its entrance maximum value corresponding to the absence of thermal and concentration boundary layers at the entrance. It may be recalled that in the present study the temperature and humidity profiles at the crossflow entry are flat, but that the flow enters with a fully developed laminar velocity profile. The thermal and concentration boundary layers build up rapidly downstream of the crossflow entry, leading to stabilization of k at a slowly decreasing value around 0.01 kg/m^2s. From the edge of the plate up to 1/D ≃ -4 it is clear that the jet does not influence the mass transfer as these curves are all close to the pure crossflow case. For the same value of M, the smaller the plate spacing, the higher the crossflow velocity, and hence the further the flow proceeds from the crossflow entry before feeling the presence of the jet flow. Thus the position at which the mass transfer coefficient begins to be affected by the jet moves progressively back from values of 1/D of about -1.5 to -3.5 to -4.5 as H/D is increased, respectively, from 2 to 3 to 4. Figure 6.15 showed that the trends were similar for local heat transfer distribution, but the location of the curves is clarified by the inclusion on Figure 6.26 of the pure crossflow case. As noted at the begining of Section 6.3.2.1, these conclusions concerning entrance effect

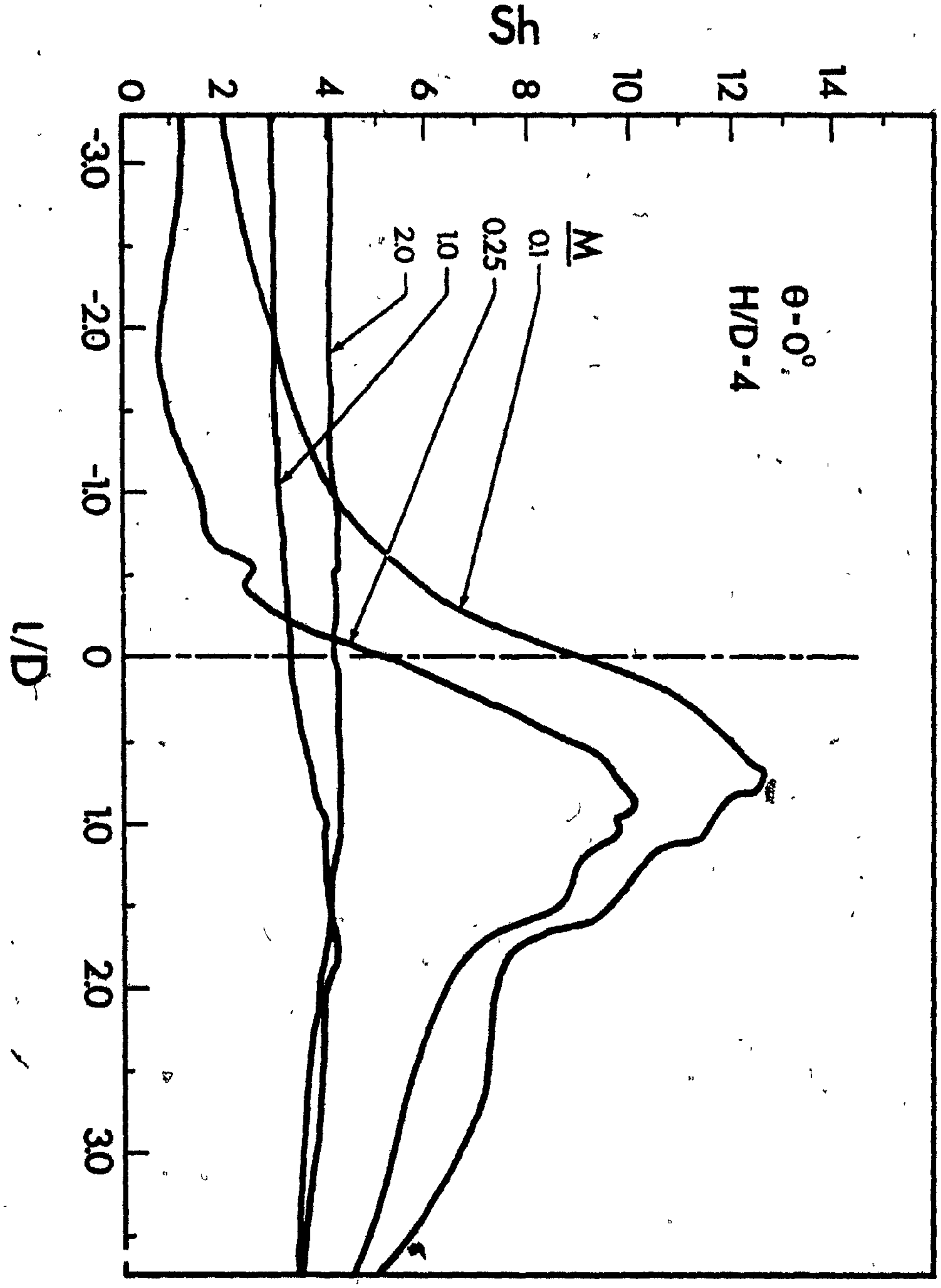

Figure 6.22 : Influence of crossflow magnirude, M, on local mass transfer.

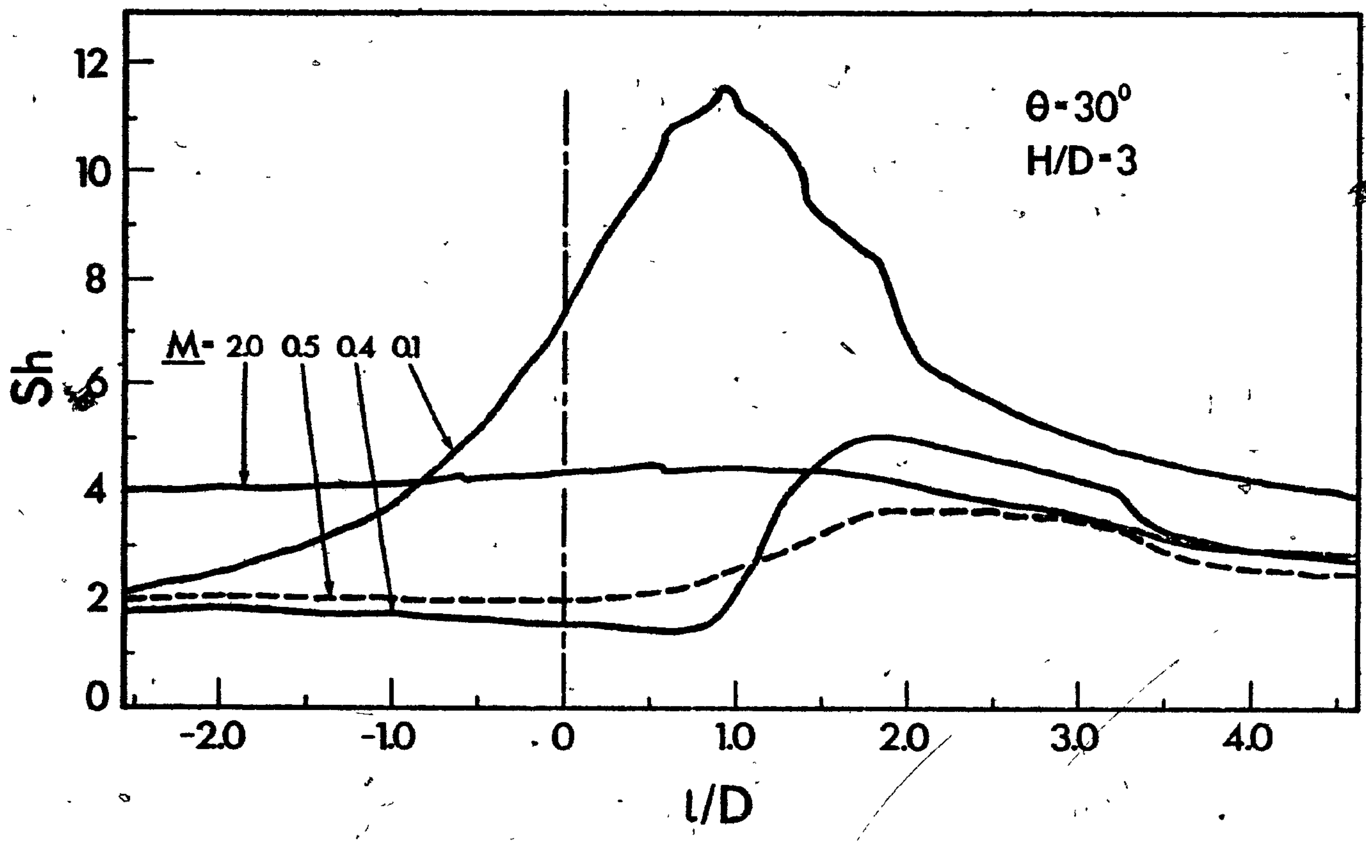

Figure 6.23 : Influence of crossflow magnitude, M, on local mass transfer.

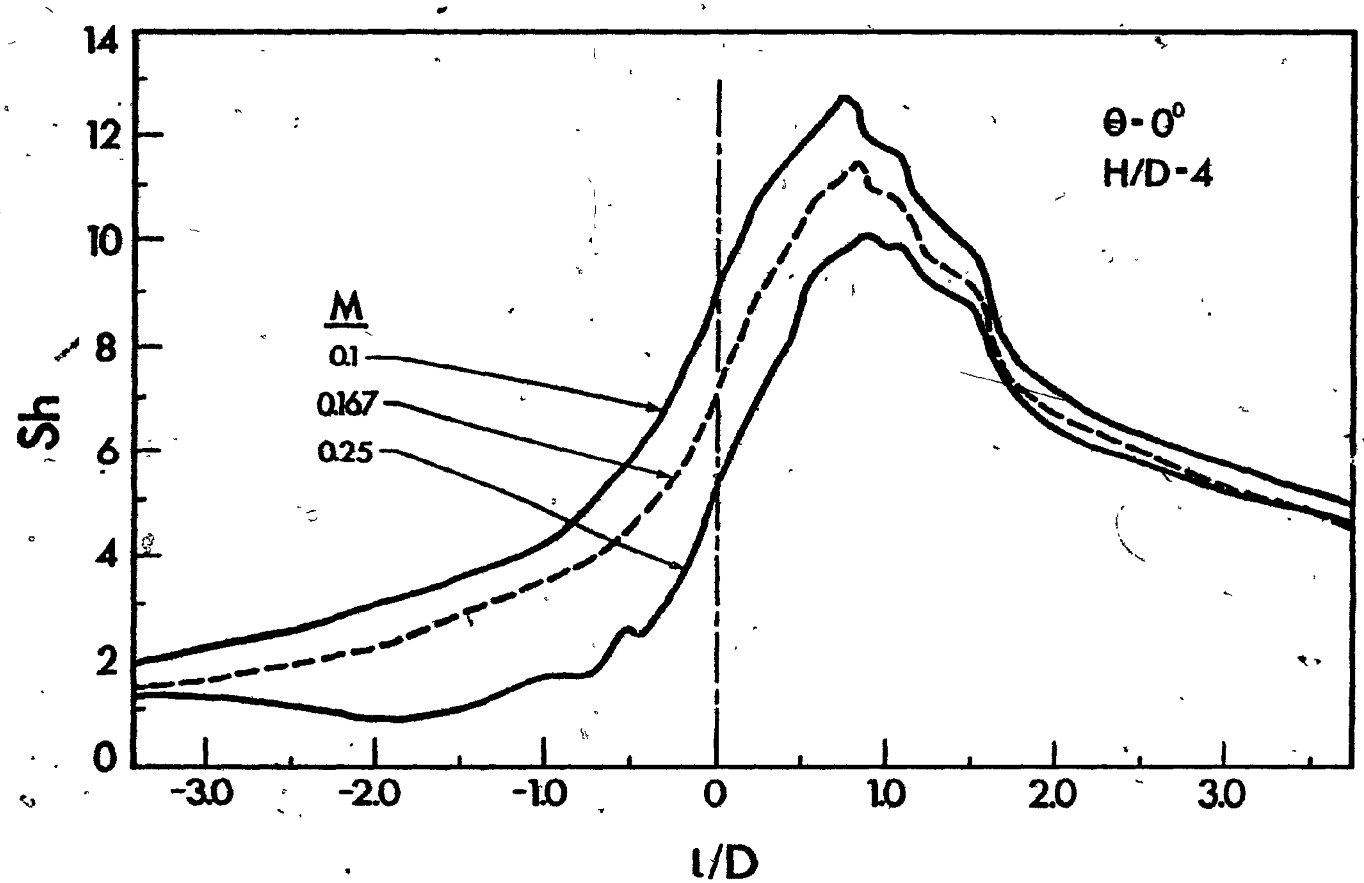

Figure 6.24 : Local mass transfer for jet-dominated systems.

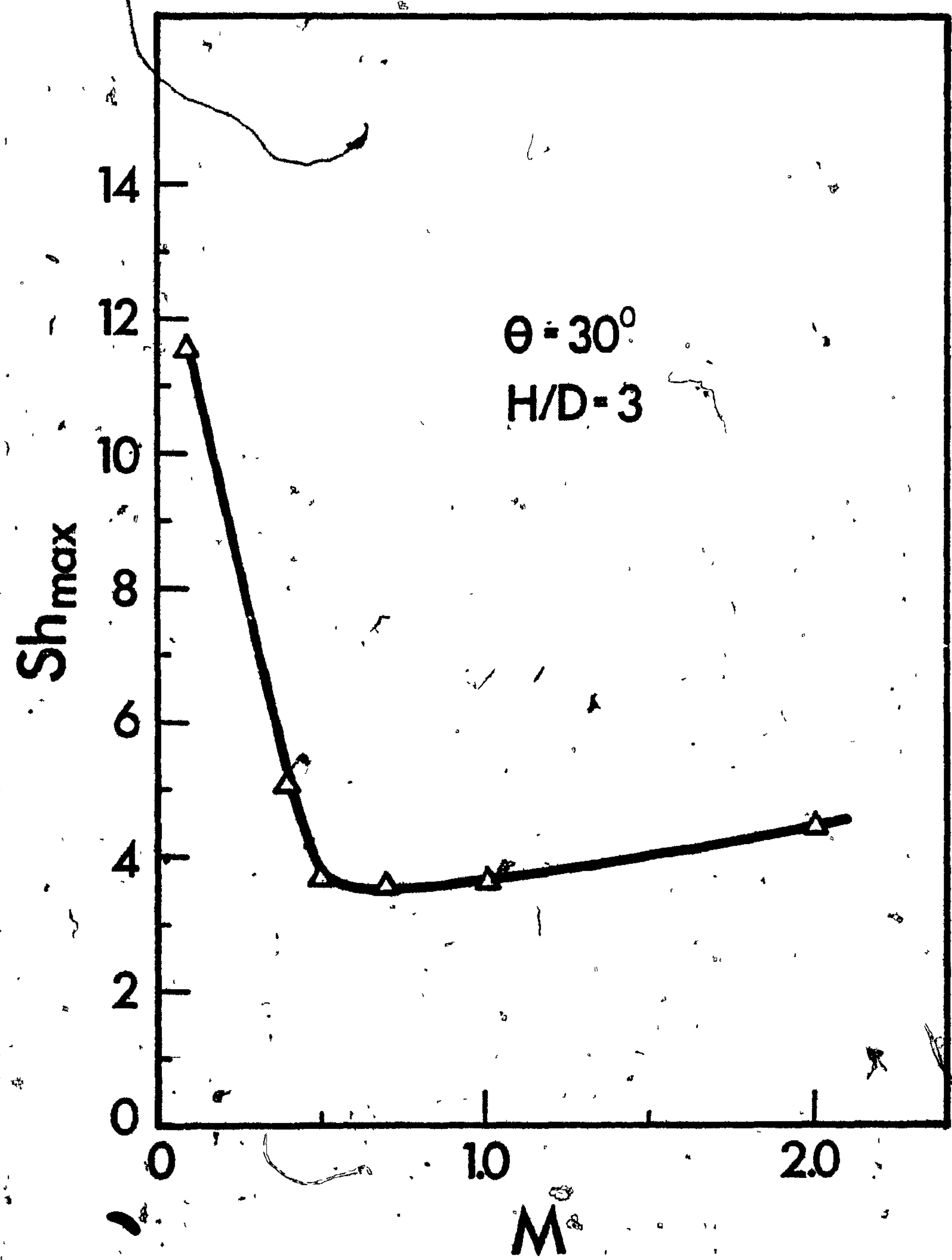

Figure 6.25 : Maximum local Sherwood number as a function of M.

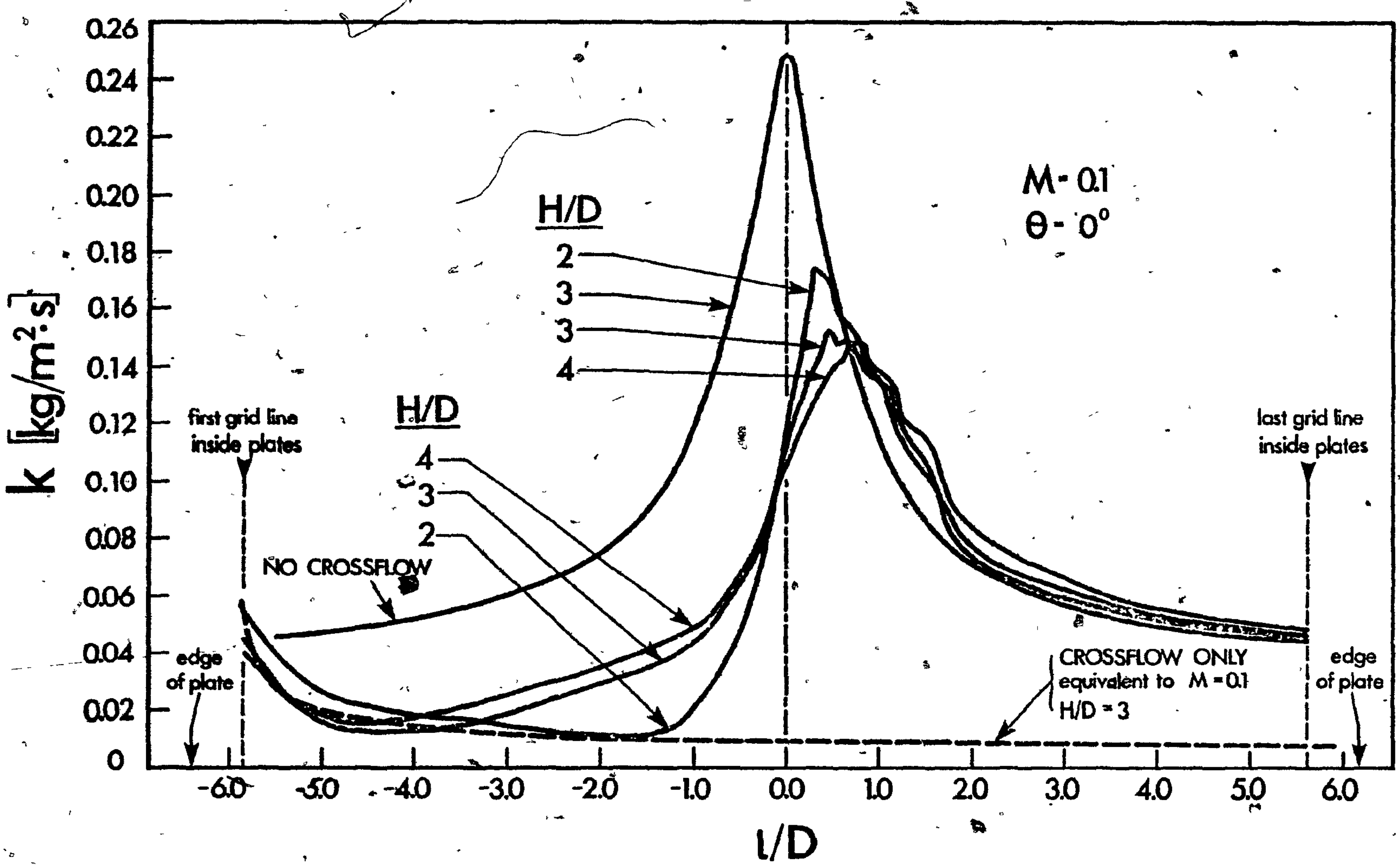

Figure 6.26 : Effect of H/D on local mass transfer for jets in a crossflow. Comparison with non-crossflow case.

on transfer rates at the impingement surface are equally applicable to both mass and heat transfer.

As to the influence of nozzle inclination on mass transfer, Figures 6.27, 6.28 and 6.29 suggest exactly the same comments as for heat transfer, i.e. for a given crossflow magnitude and nozzle-to-plate spacing there exists an optimum angle for which the mass transfer is maximum, and this optimum angle is for the nozzle inclined slightly against the crossflow.

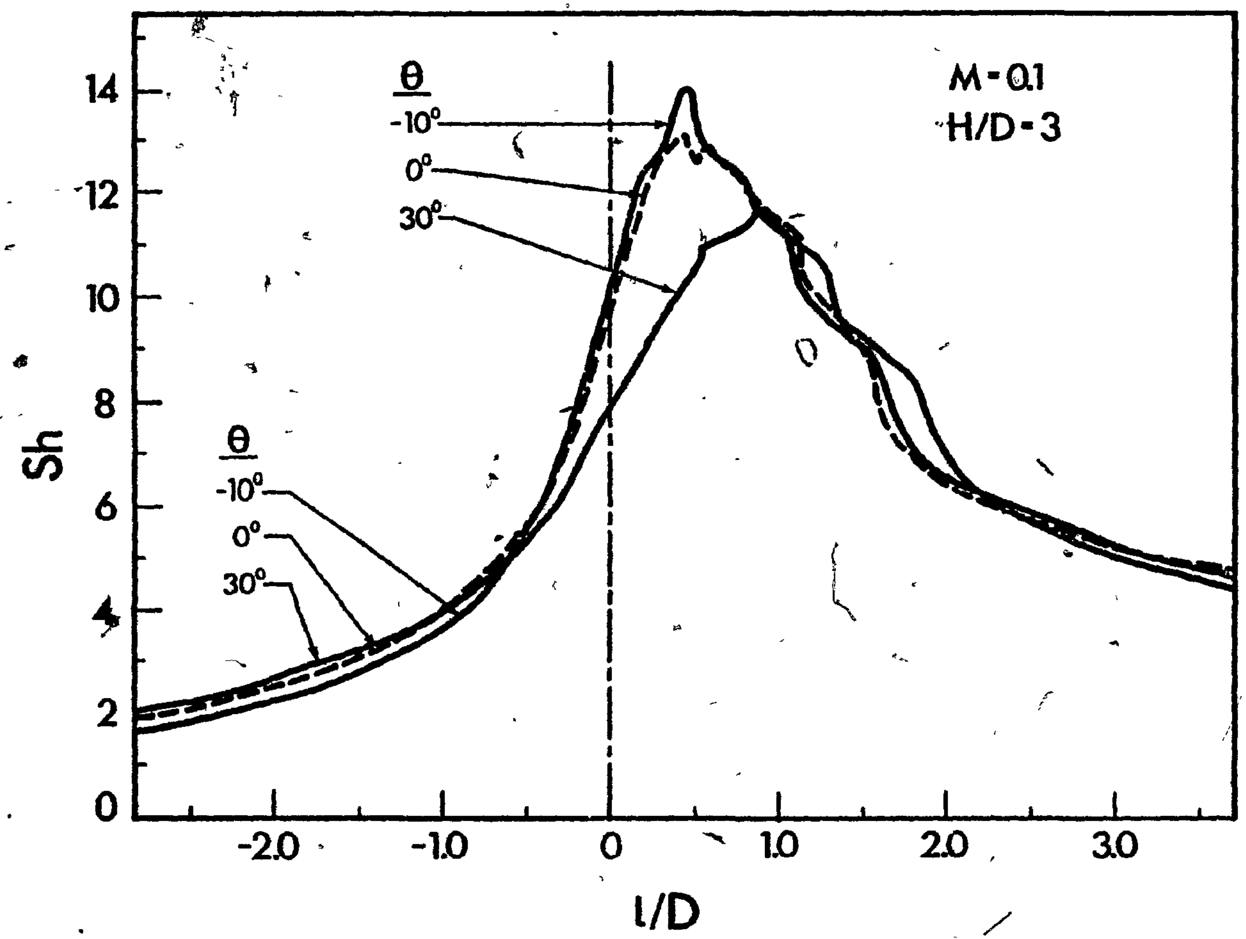

Figure 6.27 : Influence of θ on local Sherwood number for small values of M.

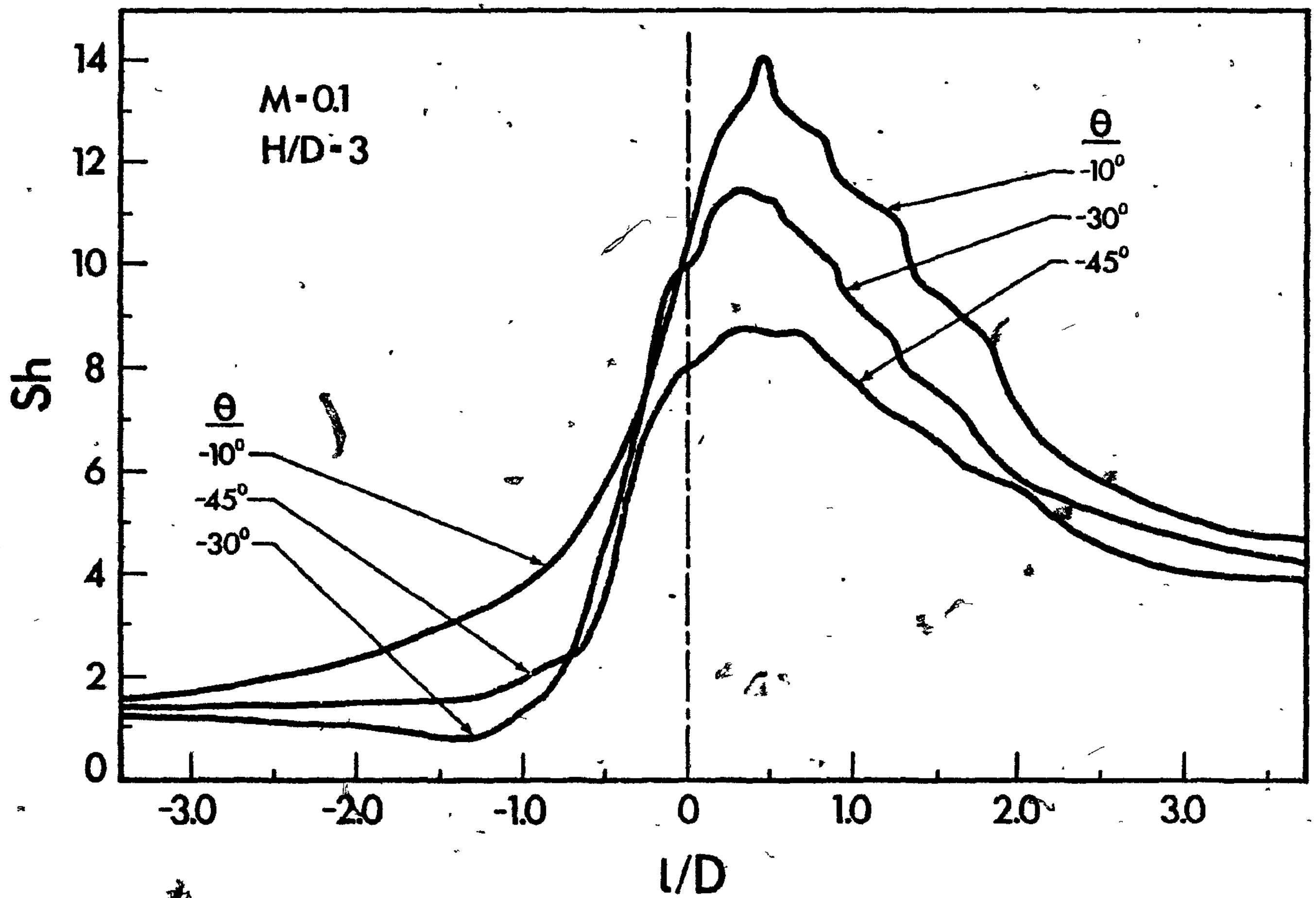

Figure 6.28 : Influence of θ on local Sherwood number for small values of M.

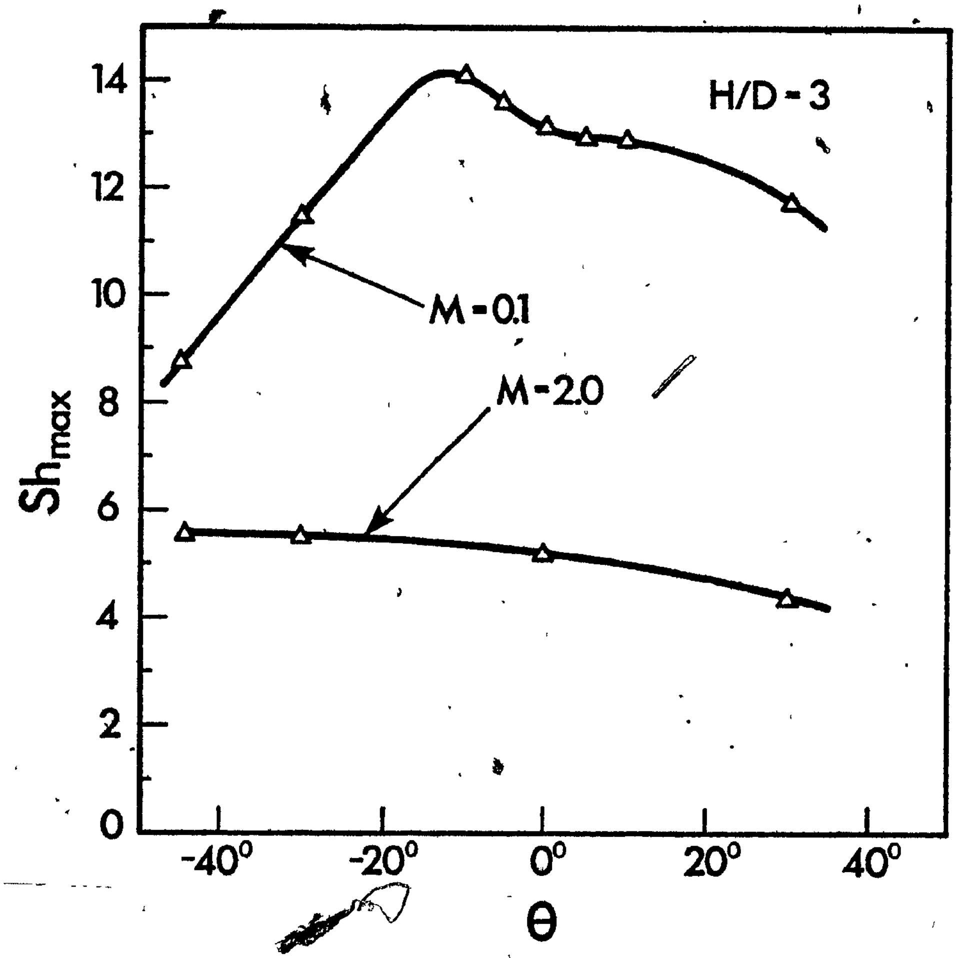

Figure 6.29 : Maximum local Sherwood number as a function of θ .

CHAPTER 7

SUMMARY AND CONCLUSIONS

(i) Numerical solutions for the effect of crossflow and of nozzle inclination on the flow, heat and mass transfer characteristics of a semi-confined rectangular laminar jet impinging on a wetted isothermal flat surface have been obtained by solving iteratively the full governing equations. These equations are the Navier Stokes Equations coupled with the continuity, energy and species equations. The primitive variables are the velocity components, the pressure, the temperature and the mass fraction of water vapour. Allowance is made in the computer program for temperature and composition dependent fluid property variations. The crossflow magnitude is defined by the ratio M of the crossflow volumetric flow-rate to the jet volumetric flow-rate. The nozzle inclination angle θ is counted negative when the jet is directed against the crossflow and positive when it is directed in the crossflow direction. The ranges of the parameters investigated are:

$$2 < H_o/D < 4$$

$$0.01 < M < 2.0$$

$$-45° < \theta < 30°$$

The nozzle width is 0.0032 m ; the jet characteristics at the exit of the nozzle are:

$T_j = 450°K$

$m_j = 0.1$

$Re = 1000$

The impingement plate was maintained at a temperature $T_p = 350$ K $(m_p = 0.302)$.

The present results compare favourably with the experimental data of Bouchez and Goldstein (B7) and of Metzger and Korstad (M5).

(ii) For an orthogonal nozzle the velocity field analysis showed that for moderate values of M the jet is split into two parts at impingement: the main part of the jet flows in the crossflow direction whereas the second stream flows in the opposite direction along the plate. The interaction of this secondary stream with the crossflow creates a recirculation zone upstream of the impingement. As the crossflow magnitude, M, increases this recirculation zone diminishes and finally disapears.

(iii) In accordance with these observations the shear stress analysis along the plate shows that for small values of M the jet actually impinges on the plate whereas it is taken away by the crossflow and does not impinge for large values of M. The value of M which delimitates these two behaviours is a function of H/D and of the nozzle inclination.

(iv) The presence of a crossflow always reduces the stagnation point and average heat transfer rates below what would be expected if crossflow were not present.

(v) The influence of nozzle-to-plate spacing, which is negligible within the range $2 < H/D < 4$ when there is no crossflow, becomes significant in presence of crossflow since H/D measures the distance over which the crossflow acts on the jet. Increasing the nozzle-to-plate spacing leads to more significant deflection of the jet and lower stagnation point transfer rates.

(vi) For moderate values of M, the heat and mass transfer rates on the plate are the ones of an impinging jet deflected and weakened by a crossflow. The larger the crossflow, the more effect on the jet; consequently the transfer rates are decreased as M increases within a range of values which permit impingement.

(vii) For large values of M, the heat and mass transfer rates on the plate are the ones of a channel flow (although influenced by the jet). Consequently the higher the crossflow, the higher the transfer rates. But, due to the absence of impingement, these transfer rates are much lower than in the case of moderate crossflow.

(viii) For a given crossflow magnitude and a given nozzle-to-plate spacing there exists an optimum angle (directed slightly against the crossflow direction) for which the heat and mass transfers are maximum. It appears hence that in practical cases where the presence of a crossflow cannot be eliminated, the decay in transfer coefficients caused by this crossflow can be limited by the choice of the appropriate impingement angle.

REFERENCES

A1 M.L.Albertson, Y.B.Dai and R.A. Jensen, "Diffusion of Submerged Jets", ASCE Trans., 115, 639-697, (1950).

B1 R.E. Bolz and G.L. Tuve, Handbook of Tables for Applied Engng. Science", CRC Handbook Series, (1973)

B2 R.B.Bird, W.E.Stewart and E.N.Lightfoot, "Transport Phenomena" John Wiley and Sons Inc., N.Y. (1960).

B3 J.-P.Bouchez and R.J. Goldstein, "Impingement Cooling from a Circular Jet in a Cross Flow", Int.J.Heat Mass Transfer, vol 13, 719-730, (1975).

B4 S.Beltaos and N.Rajaratnam, "Impinging Circular Turbulent Jets", J. of the Hydraulics Division of American Society for Civil Engineering, 100, 1313-1328, (1974).

B5 S.Beltaos, "Oblique Impingement of Circular Jets", J. of Hydraulic Research, Int. Assoc. for Hydraulic Research, vol 14, #1, 17-36 (1976).

B6 S.Beltaos, "Oblique Impingement of Plane Turbulent Jets", J. of the Hydraulic Division, ASCE, vol 102, No.HY9 1177-1191, (1976).

C1 Cederwell, K., "The Initial Mixing on Jet Disposal into a Recipient", Publ. No.s 14 and 15, Division of Hydraulics, Chalmers U. of Technology, Goteborg, Sweden, (1963).

C2 J.E.Chamberlain, "Heat Transfer between a Turbulent Round Jet and a Segmented Plate perpendicular to it", M.S. Thesis, Newark College of Engineering, (1966).

C3 R.H.Crotogino, "Stoffwerte fur feuchte Luft", pf-Bericht No.1. 83-439, PPRIC.

C4 S.D. Conte, "Elementary Numerical Analysis", McGraw Hill, N.Y.

C5 L.S.Caretto, A.D.Gosman, S.V.Patanker and D.B.Spalding, "Two Calculation Procedures for Steady, Three Dimensional Flows with Recirculation", Proc. 3rd Int'l Conf. on Numerical Method in Fluid Mechanics, published by Springer Verleg, 60-68, (1972).

D1 C.D.Donaldson and R.S.Snedeker, "A Study of Free Jet Impingement, Part I. Mean Properties of Free and Impinging Jets", J. Fluid Mech., 45, 2, 281-319, (1971).

G1 J.W.Guanter, J.N.B.Livingood and P.Hrycak, "Survey of Literature on Flow Characteristics of a Single Turbulent Jet Impinging on a Flat Plate", NASA TN D-5652, Feb., (1970).

G2 F.Giralt, C.J.Chia and O.Trass, "Characterisation of the Impingement Region in an Axisymmetric Turbulent Jet", Ind. Eng. Chem., Fundam., 16, 1, 21-28, (1977).

G3 M.B.Glauert, "The Wall Jet", J.Fluid Mech., vol 1, pt.6, Dec., (1956).

G4 R.Gardon and J.C.Akfirat, "The Role of Turbulence in Determining the Heat Transfer Characteristics of Impinging Jets", Int. J. Heat Transfer, 8, 1261-1272, (1965).

G5 R.Gardon and J.Cobonpue, "Heat Transfer Between a Flat Plate and Jets of Air Impinging on It", International Developments in Heat Transfer, ASME, 454-460, (1963).

G6 R.Gardon and J.C.Akfirat, "Heat Transfer Characteristics of Impinging Two-Dimensional Air-Jets", J. Heat Transfer, vol 88 , no.1,101-108 Feb., (1966).

G7 A.D.Gosman, B.E.Launder and J.H.Whitelaw, "Heat and Mass Transfer in Turbulent Recirculating Flows - Prediction and Measurements", Short Course Notes, McGill Univ., Chem. Engng. Dept., August, (1976).

H1 G.C.Huang, "Investigation of Heat Transfer Coefficients for Air Flow thru Round Jets Impinging Normal to a Heat Transfer Surface", J. Heat Transfer, 85, #3, 237-245, Aug., (1963).

H2 B.Huang, "Prediction of Flow and Heat Transfer Under a Laminar Swirling Impinging Jet", M. Eng. Thesis, Dept. Chem. Eng., McGill University, (1977).

H3 S.Hayashi, T.Matsui and T.Ito, "Study of Flow and Thrust in Nozzle-Flapper Valves", J. Fluid Eng., Trans ASME, 39-50, March, (1975).

H4 P.Hrycak, D.T.Lee, J.W.Gaunter and J.N.B.Livingood, "Experimental Flow Characteristics of a Single Turbulent Jet Impinging on a Flat Plat", NASA TN D-5690, (1970).

H5 P.Hrycak and N.B.Livingood, "Impingement Heat Transfer from Turbulent Air Jets to Flat Plates, a Literature Survey", NASA TM X-2778, May, (1973).

H6 A.L.Horvath, "Physical Properties of Inorganic Compounds", Edward Arnold Ltd., London, (1975).

K1 A.Kamoi and H.Tanaka, "Measurements of Wall Shear Stress, Wall Pressure and Fluctuations in the Stagnation Region Produced by Oblique Jet Impingement", Fluid Dynamic Measurements, Conference Papers, Leicester University Press, Vol.1, 217-227, (1972).

K2 J.F.Keffer and W.D.Baines, "Tre Round Turbulent Jet in a Crosswind", J. of Fluid Mechanics, London vol. 15 , 481, (1963).

K3 S.P.Kezios, "Heat Transfer in the Flow of a Cylindrical Air Jet Normal to an Infinite Plate", Ph.D. Thesis, Illinois Int. Tech. (1956).

K4 D.N.Kapur and N.Macleod, "The Determination of Local Mass Transfer Coefficients by Holographic Interferometry - I.General Principles: Their Application and Verification for Mass-Transfer Measurements at a Flat Plate Exposed to a Laminar Round Air Jet", Int. J. Heat Mass Transfer, 17 , 1151-1162, (1974).

K5 M.Korger and F.Krizek, "Die Stoffubergangszahlen beim Aufprall schrager Flachstrahlen auf eine Platte", Verfahrenstechnik 6, Nr.7, (1972).

K6 T.M.Klibanov, V.V.Pomerantsev and D.A.Frank-Kamenentsky, J.Tech. Phys. USSR- 12, 14, (1942).

L1 Lindsay and Bromley, "Thermal Conductivity of Gas Mixtures", Ind. Eng. Chem., 42, 1508, (1950).

L2 Y.-K.Li, "Heat and Mass Transfer Under a Laminar Impinging Jet", M. Eng. Thesis, Dept. Chem. Eng., McGill University, (1977).

L3 Levey, H.C. "The Back Effect of a Wall on a Jet", geit.f. Angew. Math. Phys., 11 , #2, 152-157, (1960).

L4 P.E.Liley, "Survey of Recent Work on the Viscosity, Thermal Conductivity and Diffusion of Gases and Gas Mixtures", Thermodynamic Conductivity and Transport Properties of Gases, Liquids and Solids", McGraw-Hill, N.Y., (1959).

M1 H.Martin, "Heat and Mass Transfer Between Impinging Gas Jets and Solid Surfaces", Advances in Heat Transfer, 13, (1977).

M2 K.J.McNaughton and C.G.Sinclair, "Submerged Jets in Short Cylindrical Flow Vessels", J. Fluid Mech., 25, 2, 367-375, June, (1966).

M3 A.S.Mujumdar and W.J.M.Douglas, "Impingement Heat Transfer: a Literature Survey", Paper presented at TAPPI Meeting, New Orleans, LA., Ocotober 3-5, (1972).

M4 D.E.Metzger,"Spot Cooling and Heating of Surface with High Velocity Impinging Air Jets, Part 1 - Slot Jets on Plane Surface, TR no 52 Stanford University (1962).

N1 T.Nakatogawa and N.Nishiwaki, "Heat Transfer of Round Turbulent Jet Impinging Normally on Flat Plate", Proc. 4th Int. Heat Transfer Conf., Preprint FC5.2, (1970).

N2 S.Nagpal, "Analysis of the Spent Flow Effect in Air-Impingement Heat Transfer", Ph.D. Thesis, Mech. Eng. Dept. Colorado State University, March, (1974).

P1 K.P.Perry, "Heat Transfer by Convection from a Hot Gas Jet to a Plane Surface", Proc. Inst. Mech. Eng., 168, 775-780 , N230 (a954).

P2 M.Poreh, and J.E.Cermak, "Flow Characteristics of a Circular Submerged Jet Impinging Normally on a Smooth Boundary", Sixth Midwestern Conference on Fluid Mechanics, Univ. Texas, 198-212, (1959).

P3 M.Poreh, Y.G.Tsuei and J.E.Cermak, "Investigation of a Turbulent Radial Wall Jet", J. Appl. Mech. , 34, #2, 457-463, June, (1967).

P4 D.Pratte, and W.D. Baines, "Profiles of the Round Turbulent Jet in a Crossflow"; J. Hydraulics Division, ASCE, 53-64, May (1968).

P5 J.L.Platten and J.F.Keffer, "Deflected Turbulent Jet Flows", J. of Applied Mechanics, Trans ASME, 756-758, Dec., (1971).

R1 W.E.Ranz and P.F.Dickson, "Mass and Heat Transfer Rates for Large Gradients of Concentration and Temperature", Ind.Eng.Chem. (Fundamental), 4, 3; 345-353, (1965).

R2 R.C.Reid and T.S.Sherwood, "The Properties of Gases and Liquids", 2nd Ed., McGraw-Hill, N.Y., (1966).

R3 A.K.Runchal, "Convergence and Accuracy of Three Finite Difference Schemes for a Two-Dimensional Conduction and Convection Problem", Int. J. Num. Meth. Engng, 4, 541-550, (1972).

S1 H.Schrader, VDI-Forshungsheft, 484, (1961).

S2 N.R.Saad, "Simulation of Flow and Heat Transfer Under a Laminar Impinging Round Jet", M.Eng. Thesis, Dept. Chem. Eng., McGill University, (1975).

S3 H.Schlichting, "Boundary Layer Theory", 6th Ed., McGraw-Hill,(1968).

S4 M.T.Scholtz and O.Trass, "Mass Transfer in a Non-uniform Impinging Jet, Part I. Stagnation Flow-Velocity and Pressure Distribution", AIChE Journal, 16, 82-90, (1970).

S5 M.T.Scholtz and O.Trass, "Mass Transfer in a Non-Uniform Impinging Jet, Part II. Boundary Layer Flow-Mass Transfer", AIChE Journal, 16 , 90-96, (1970).

S6 M.T.Scholtz and O.Trass, "Mass Transfer in the Laminar Radial Wall Jet', AIChE J., 9 , 548-554, (1963).

S7 E.M. Sparrow and L.Lee, "Analysis of Flow Field and Impingement Heat / Mass Transfer Due to a Non-Uniform Slot Jet", J. Heat Transfer, Trans ASME, 191-197, (1975).

S8 W.Schach, "Umlenkung eines freien Flussigkeitsstrahls an einer ebenen Platte", Ingenieur Archiv., 4, 245-265, (1934).

S9 E.M.Sparrow, R.J.Goldstein, and M.A.Rouf, "Effect of Nozzle-Surface Separation Distance on Impingement Heat Transfer for a Jet in a Crossflow", J. of Heat Transfer, Trans ASME, 528-533, Nov., (1975).

S10 J.J.Schauer and R.H.Eustis, "The Flow Developement and Heat Transfer Characteristics of Plane Turbulent Impinging Jets", Tchn Report 3 Dept. of Mech. Eng., Stanford University, Calif., (1963).

S11 N.Saad, W.J.M.Douglas and A.S.Mujumdar, "Prediction of Heat Transfer Under an Axisymmetric Laminar Impinging Jet", Ind. Eng. Chem., Fundam., 16 , 148-154, (1977).

S12 D.B.Spalding, "A Novel Finite Difference Formulation for Differential Expressions Involving Both 1st and 2nd Derivatives", Int. J. Numerical Methods in Engng., 4 , 551-559, (1972).

T1 F.A.Thomas and T.W.Jackson, "the Viscosity of Steam", "Thermodynamic and Transport Properties of Gases, Liquid and Solids", McGraw-Hill N.Y., (1959) (ENGNG TP 242 S9)

T2 R.E.Treybal, "Mass Transfer Operation", 2nd Ed., McGraw-Hill, N.Y., (1968).

T3 I.Tani and Y.Komatsu, "Impingement of a Round Jet on a Flat Surface", Proceedings, 11th International Congress of Applied Mechanics, Munich, 672-676, (1964).

V1 J.M.F.Vickers, "Heat Transfer Coefficients Between Fluid Jets and Normal Surfaces", Ind. Eng. Chem., 51, 8, 967-972, August, (1959).

V2 A.R.P.van Heiningen, A.S.Mujumdar and W.J.M. Douglas, "Numerical Prediction of the Flow Field and Impingement Heat Transfer Caused by a Laminar Slot Jet", J. Heat Transfer, Trans ASME, 654-658, November, (1976).

W1 M.Wolfstein, "Convection Process in Turbulent Impinging Jets", London University, Ph.D dissertation, (1968).

W2 D.R.Walz, "Spot Cooling and Heating of Surfaces with High Velocity Impinging Air Jets, Part 2, Circular Jets on Plane and Curved Surfaces, Slot Jets on Curved Surfaces", Th. no 61, Stanford University, (AD607 727) July (1964).

W3 C.R.Wilke, "A Viscosity Equation for Gas Mixtures", J. Chem. Phys., 18 , 517-519, (1950).

O1 N.T.Obot, "An Apparatus for the Study of the Effect of Suction on Heat Transfer for Impinging Round Jets", M. Eng. Thesis, Dept. Chem. Eng., McGill University, August, (1975).

APPENDIX A

LISTING OF COMPUTER PROGRAM

```
FORTRAN IV G1  RELEASE 2.0          MAIN              DATE = 79037          23/48/10              PAGE 0001
                 C      SUBROUTINE CONTRO                                                          MAIN0001
                 C                                                                                 MAIN0002
                 C                                                                                 MAIN0003
                 C*******************************************************************************CMAIN0004
                 C                                                                                CMAIN0005
                 C             PROGRAMME D'ORDINATEUR POUR LE CALCUL DES
                 C             TRANSFERTS DE MASSE ET DE CHALEUR SOUS UN
                 C             JET RECTANGULAIRE IMPACTANT AVEC DIFFERENTS
                 C                   ANGLES SUR UNE PLAQUE HUMIDE
                 C                                                                                CMAIN0008
                 C             A COMPUTER PROGRAM FOR THE CALCULATION OF                          CMAIN0009
                 C               HEAT AND MASS TRANSFER OF SLOT JETS
                 C                    IMPINGING ON A WET PLATE
                 C                                                                                CMAIN0012
                 C                                                                                CMAIN0013
                 C*******************************************************************************CMAIN0014
                 C                                                                                 MAIN0015
 0001                   COMMON NITER
 0002                   COMMON SPLIT(200)
 0003                   COMMON CNIV(200)
 0004                   COMMON HEDU(9),HEDV(9),HEDP(9),HEDT(9),HEDW(9),HEDVIS(9),
                       1      HEDDEN(9),HEDCP(9),HEDDIF(9),HEDCON(9)
 0005                   DIMENSION HPUNCH(9)                                                        MAIN0019
 0006                   REAL NU                                                                    MAIN0020
 0007                   LOGICAL PUNIN,PUNOUT                                                       MAIN0021
 0008                   LOGICAL CALW,CALT,FLAT                                                     MAIN0022
 0009                   COMMON                                                                     MAIN0023
                       1/UVEL/RESORU,NSWPU,URFU,DXEPU(22),DXPWU(22),SEWU(22)
                       1/VVEL/RESORV,NSWPV,URFV,DYNPV(22),DYPSV(22),SNSV(22),YCV(22)
                       1/PCOR/RESORM,NSWPP,URFP,DU(20,20),DV(20,20),IPREF,JPREF
                       1/TEMP/RESORT,NSWPT,URFT                                                    MAIN0027
                       1/SPEC/RESORW,NSWPW,URFW                                                    MAIN0028
 0010                   COMMON                                                                     MAIN0029
                       1/ALL/IT,JT,NI,NJ,NIM1,NJM1,GREAT                                           MAIN0030
                       1/VAR/U(20,20),V(20,20),P(20,20),PP(20,20),T(20,20),W(20,20)
                       1/GEOM/X(22),Y(22),DXEP(22),DXPW(22),DYNP(22),
                       2      DYPS(22),SNS(22),SEW(22),XU(22),YV(22)
                       1/PGM/PUNIN,PUNOUT,TIMAX,MAXIT,SORMAX,INOPRI                                MAIN0034
 0011                   COMMON                                                                     MAIN0035
                       1/FLUPR/RHOA,RHOB,RATIO,CPA,CPB,CPDE,                                       MAIN0036
                       2       DEN(20,20),VIS(20,20),CPP(20,20),DIFF(20,20),COND(20,20)
                       1/FLUPR2/CONDA1,CONDA2,CONDA3,CONDB1,CONDB2,CONDB3,                         MAIN0038
                       2VISA1,VISA2,VISA3,VISB1,VISB2,VISB3,DIFFU,                                 MAIN0039
                       3CPA1,CPA2,CPA3,CPB1,CPB2,CPB3                                              MAIN0040
 0012                   COMMON /MOLEWT/WTA,WTB                                                     MAIN0041
                       1/PROB1/RE,TIN,PIN,TWALL,WIN,FLOWIN,FLOWEV,                                 MAIN0042
                       2       ISTEP,JSTEP,ISTP1,JSTP1,ISTM1,JSTM1                                 MAIN0043
                       3       ,JNOZ,JNOZP1,JNOZM1
                       1/COEF/AP(20,20),AN(20,20),AS(20,20),AE(20,20),AW(20,20),
                       2       SU(20,20),SP(20,20)
 0013                   COMMON /SUCTON/USUC,SUCR                                                   MAIN0046
 0014                   COMMON/ANGLE/THETA
 0015                   COMMON/CROSS/PCNTCR,DELTIN,DELWIN
                 CHAPTER  0  0  0  0  0  0  0  0  PRELIMINARIES  0  0  0  0  0  0  0  0           MAIN0047
```

```
C                                                                       MAIN0048
C-----DEPENDENT VARIABLE SELECTION                                       MAIN0049
C                                                                       MAIN0050
      CALL CLOCK1                                                       MAIN0051
      READ(5,010)HEDU,HEDV,HEDP,HEDT,HEDW,HEDVIS,HEDDEN,HEDCP,HEDDIF     MAIN0052
     1   ,                .HEDCON                                       MAIN0053
  010 FORMAT(9A4)                                                       MAIN0054
CHAPTER  1  1  1  1  1  PARAMETERS AND CONTROL INDICES  1  1  1  1  1  1MAIN0055
C                                                                       MAIN0056
      NITER=0
      FLAT=.FALSE.                                                      MAIN0058
      CALT=.TRUE.                                                       MAIN0059
      CALW=.TRUE.                                                       MAIN0060
      INPROP=2                                                          MAIN0062
      CALL GRID(JNOZ,JSTEP,RSMALL,HDRATO)
      NIM1=NI-1                                                         MAIN0064
      NJM1=NJ-1                                                         MAIN0065
      ISTP1=ISTEP+1                                                     MAIN0066
      ISTM1=ISTEP-1                                                     MAIN0067
      JSTP1=JSTEP+1                                                     MAIN0068
      JSTM1=JSTEP-1                                                     MAIN0069
      JNOZP1 = JNOZ+1
      JNOZM1 = JNOZ-1
      CALL INIT                                                         MAIN0070
      IMON=NIM1-1                                                       MAIN0071
      JMON=10
CHAPTER  2  2  2  2  2  2  INITIAL OPERATIONS  2  2  2  2  2  2  2  2  2MAIN0073
C                                                                       MAIN0074
C     GAS CONSTANT, R = 8.3142E+3  J/KILO-GMOLE-K                       MAIN0075
      GAS=8.3142E+3                                                     MAIN0076
      ATEMP=(TIN+TWALL)*0.5                                             MAIN0077
      CPB=CPB1+CPB2*ATEMP+CPB3*ATEMP*ATEMP                              MAIN0078
      RATIO=WTB/WTA                                                     MAIN0079
      RHOA=WTA/GAS                                                      MAIN0080
      RHOB=WTB/GAS                                                      MAIN0081
      RENO = SQRT(RE)
      XAJ=WIN/(WIN+(1.-WIN)/RATIO)                                      MAIN0082
      DJET=2.*RSMALL                                                    MAIN0083
      DJP=HDRATO*DJET                                                   MAIN0084
C                                                                       MAIN0085
      IF(.NOT.PUNIN) GOTO 208                                           MAIN0086
C                                                                       MAIN0087
C-----FIELD INITIALIZATION                                              MAIN0088
      READ (5,10) HPUNCH                                                MAIN0089
      READ(5,600) ((U(I,J),I=1,NI),J=1,NJ)
      READ(5,600) ((V(I,J),I=1,NI),J=2,NJ)
      READ(5,600) ((P(I,J),I=1,NI),J=1,NJ)
      READ(5,600) ((T(I,J),I=1,NI),J=1,NJ)
      READ(5,600) ((W(I,J),I=1,NI),J=1,NJ)
      GOTO 210                                                          MAIN0095
  208 CONTINUE                                                          MAIN0096
      DO 200 I=1,NI                                                     MAIN0097
      DO 200 J=1,NJ                                                     MAIN0098
      U(I,J)=0.0                                                        MAIN0099
```

```
                V(I,J)=0.0                                                     MAIN0100
                P(I,J)=0.0                                                     MAIN0101
                W(I,J)=WIN                                                     MAIN0102
                T(I,J)=TIN                                                     MAIN0103
    200 CONTINUE                                                               MAIN0104
    211 CONTINUE                                                               MAIN0105
        DO 206 I=1,NI                                                          MAIN0106
        DO 206 J=1,NJ                                                          MAIN0107
        IF(.NOT.CALT) T(I,J)=ATEMP                                             MAIN0108
        IF(.NOT.CALW) W(I,J)=WIN                                               MAIN0109
        PP(I,J)=0.0                                                            MAIN0110
        DU(I,J)=0.0                                                            MAIN0111
        DV(I,J)=0.0                                                            MAIN0112
        SU(I,J)=0.0                                                            MAIN0113
        SP(I,J)=0.0                                                            MAIN0114
    206 CONTINUE                                                               MAIN0115
C-----FLUID PROPERTIES - DEN,VIS,DIFF,CPP,COND - CALCULATIONS                   MAIN0116
        CALL PROPS                                                             MAIN0117
C                                                                              MAIN0118
C-----CROSS FLOW DEFINITION
        UIN=VIS(1,1)*RE/DEN(1,1)/RSMALL*0.5
        VIN=PCNTCR*UIN/HDRATO
        DO 212 I=2,NIM1
        U(I,1)=0.0
        HRATIO=ABS(X(I)-DJP/2.)/DJP/2.
        V(I,2)=3./2.*VIN*(1.-HRATIO*HRATIO)
        P(I,1)=0.0
        T(I,1)=TIN-DELTIN
        W(I,1)=WIN-DELWIN
    212 CONTINUE
C-----SPECIFY CONFINEMENT PLATE CONDITIONS                                      MAIN0131
        DO 201 J=1,NJ
        T(1,J) = TIN
        U(2,J) = 0.0
        IF(J.EQ.1) GO TO 201
        V(1,J)=0.0
    201 CONTINUE
C-----SPECIFY IMPINGMENT PLATE CONDITIONS                                       MAIN0136
        PSTT=PST(TWALL)                                                        MAIN0137
        WWALL=PSTT/(PSTT+(PIN-PSTT)*RATIO)                                     MAIN0138
        IF(.NOT.CALW) WWALL=WIN                                                MAIN0139
        DO 207 J=1,NJ                                                          MAIN0140
        T(NI,J)=TWALL                                                          MAIN0141
C-----INITIAL GUESSING OF W-WALL                                                MAIN0142
        W(NI,J)=WWALL                                                          MAIN0143
        IF(J.EQ.1) GO TO 207
        V(NI,J)=0.0
    207 CONTINUE
C-----------CALCULATE RESIDUAL SOURCE-NORMALIZATION FACTORS-------------        MAIN0145
        FLOJET=0.0
        XMOJET=0.0
        YMOJET=0.0
        FLOCRS=0.0
        YMOCRS=0.0
```

```
          DO 258 I=2,NIM1
          ARDE1 = 0.5*(DEN(I,1)+DEN(I,2))*SEW(I)*0.01
          FLOCRS=FLOCRS+ARDE1*V(I,2)
          YMOCRS=YMOCRS+ARDE1*V(I,2)*V(I,2)
      258 CONTINUE
          CNTR=PCNTCR*100.
          FLOWIN=FLOJET+FLOCRS
          XMONIN=XMOJET
          YMONIN=YMOJET+YMOCRS
          RECRS=V(10,2)*DEN(10,2)*HDRATO*2.*RSMALL/VIS(10,2)
          SNORMT=FLOWIN*ABS(TIN-TWALL)                                  MAIN0153
          SNORMW=FLOWIN*WWALL                                           MAIN0154
          IF(ABS(TIN-TWALL).LE.1.E-6) SNORMT=1.                         MAIN0155
          IF(ABS(SNORMW-0.0).LE.1.E-6) SNORMW=1.0                       MAIN0156
C-----INITIAL OUTPUT                                                    MAIN0157
          WRITE(6,210)                                                  MAIN0158
          WRITE (6,280) (X(I),I=1,NI)                                   MAIN0159
          WRITE (6,280) (Y(J),J=1,NJ)                                   MAIN0160
          WRITE (6,220) RE,UIN,TIN,PIN,WIN,XAJ                          MAIN0163
          WRITE (6,221) PRANDL,SCHMIT                                   MAIN0164
          WRITE(6,222) RECRS,V(10,2),T(10,1),P(10,1),W(10,1)
          WRITE(6,223) CNTR
          WRITE (6,230) TWALL,SUCR                                      MAIN0165
          WRITE(6,232) RSMALL,HDRATO,JNOZ,JSTEP,THETA
          WRITE (6,250) MAXIT,TIMAX,SORMAX                              MAIN0167
          WRITE(6,260) FLOJET,XMOJET,YMOJET
          WRITE(6,261) FLOCRS,YMOCRS
          IF(PUNIN) WRITE (6,602) HPUNCH                                MAIN0169
                    CALL PRINT(1,1,NI,NJ,IT,JT,XU,Y,U,HEDU)             MAIN0171
                    CALL PRINT(1,2,NI,NJ,IT,JT,X,YV,V,HEDV)             MAIN0172
                    CALL PRINT(1,1,NI,NJ,IT,JT,X,Y,P,HEDP)              MAIN0173
                    CALL PRINT(1,1,NI,NJ,IT,JT,X,Y,T,HEDT)              MAIN0174
                    CALL PRINT(1,1,NI,NJ,IT,JT,X,Y,W,HEDW)              MAIN0175
C                                                                       MAIN0177
CHAPTER  3  3  3  3  3  3  3  ITERATION LOOP  3  3  3  3  3  3  3  3  3 MAIN0178
C                                                                       MAIN0179
          RESORW=0.                                                     MAIN0180
          RESORT=0.                                                     MAIN0181
          WRITE(6,310) IMON,JMON                                        MAIN0182
      300 NITER=NITER+1                                                 MAIN0183
C-----UPDATE MAIN DEPENDENT VARIABLES                                   MAIN0184
                    CALL CALCU                                          MAIN0185
                    CALL CALCV                                          MAIN0186
                    CALL CALCP                                          MAIN0187
          IF(CALT) CALL CALCT                                           MAIN0188
          IF(CALW) CALL CALCW                                           MAIN0189
C-----UPDATE FLUID PROPERITIES                                          MAIN0190
          IF(NITER.GT.30) INPROP=3                                      MAIN0191
          IF(NITER.GE.60) INPROP=5                                      MAIN0192
          IF(MOD(NITER,INPROP).EQ.1) CALL PROPS                         MAIN0193
C-----INTERMEDIATE OUTPUT                                               MAIN0194
          RESORM=RESORM/FLOWIN                                          MAIN0195
          RESORU=RESORU/(XMONIN+YMONIN)
          RESORV=RESORV/(XMONIN+YMONIN)
```

```
0152            IF(CALW) RESORW=RESORW/SNORMW                               MAIN0198
0153            IF(CALT) RESORT=RESORT/SNORMT                               MAIN0199
0154            WRITE(6,311) NITER,RESORU,RESORV,RESORM,RESORT,RESORW       MAIN0200
               1         ,U(IMON,JMON),V(IMON,JMON),P(IMON,JMON),T(IMON,JMON) MAIN0201
               2         ,W(IMON,JMON),SPLIT(NITER),CNIV(NITER)
0155            IF(MOD(NITER,INDPRI).NE.0) GO TO 301                        MAIN0203
0156                      CALL PRINT(1,1,NI,NJ,IT,JT,XU,Y,U,HEDU)           MAIN0204
0157                      CALL PRINT(1,2,NI,NJ,IT,JT,X,YV,V,HEDV)           MAIN0205
0158                      CALL PRINT(1,1,NI,NJ,IT,JT,X,Y,P,HEDP)            MAIN0206
0159                      CALL PRINT(1,1,NI,NJ,IT,JT,X,Y,T,HEDT)            MAIN0207
0160                      CALL PRINT(1,1,NI,NJ,IT,JT,X,Y,W,HEDW)            MAIN0208
0161            WRITE(6,310) IMON,JMON                                      MAIN0209
0162        301 CONTINUE                                                    MAIN0210
          C-----TERMINATION TESTS                                           MAIN0211
0163            SORCE=AMAX1(RESORM,RESORU,RESORV,RESORT,RESORW)             MAIN0212
0164            IF(NITER.EQ.MAXIT) GO TO 302                                MAIN0213
          C-----TIMER                                                       MAIN0214
0165            CALL CLOCK2(ITIME)                                          MAIN0215
0166            IF(ITIME/60..GT.TIMAX) GO TO 302                            MAIN0216
          C                                                                 MAIN0217
0167            IF(RESORT.LT.SORMAX) GO TO 303
0168            GO TO 304
0169        303 CALT=.TRUE.
0170            IF(MOD(NITER,10).NE.1) CALT=.FALSE.
0171        304 IF(RESORW.LT.SORMAX) GO TO 305
0172            GO TO 306
0173        305 CALW=.TRUE.
0174            IF(MOD(NITER,10).NE.1) CALW=.FALSE.
0175        306 CONTINUE
0176            IF(SORCE.GT.SORMAX) GO TO 300                               MAIN0218
0177            IF(NITER.LE.10) GOTO 300                                    MAIN0219
0178        302 CONTINUE                                                    MAIN0220
          C                                                                 MAIN0221
          CHAPTER  4  4  4  4  4  4  FINAL OPERATIONS AND OUTPUT  4  4  4  4  4  4MAIN0222
          C                                                                 MAIN0223
0179            FLOUT=0.0                                                   MAIN0224
0180            DO 421 I=2,NIM1                                             MAIN0225
0181            ARDENJ=0.5*(DEN(I,NJ)+DEN(I,NJM1))*SEW(I)*0.01
0182            FLOUT=FLOUT+ARDENJ*V(I,NJ)
0183        421 CONTINUE                                                    MAIN0228
0184            ACCUM=FLOWEV+FLOWIN-FLOUT                                   MAIN0229
0185            WRITE (6,420) FLOWEV,FLOUT,ACCUM,PUNOUT                     MAIN0230
          C                                                                 MAIN0231
0186                      CALL PRINT(1,1,NI,NJ,IT,JT,XU,Y,U,HEDU)           MAIN0232
0187                      CALL PRINT(1,2,NI,NJ,IT,JT,X,YV,V,HEDV)           MAIN0233
0188                      CALL PRINT(1,1,NI,NJ,IT,JT,X,Y,P,HEDP)            MAIN0234
0189                      CALL PRINT(1,1,NI,NJ,IT,JT,X,Y,T,HEDT)            MAIN0235
0190                      CALL PRINT(1,1,NI,NJ,IT,JT,X,Y,W,HEDW)            MAIN0236
0191                      CALL PRINT(1,1,NI,NJ,IT,JT,X,Y,VIS,HEDVIS)        MAIN0237
0192                      CALL PRINT(1,1,NI,NJ,IT,JT,X,Y,DEN,HEDDEN)        MAIN0238
0193                      CALL PRINT(1,1,NI,NJ,IT,JT,X,Y,CPP,HEDCP)         MAIN0239
0194                      CALL PRINT(1,1,NI,NJ,IT,JT,X,Y,DIFF,HEDDIF)       MAIN0240
0195                      CALL PRINT(1,1,NI,NJ,IT,JT,X,Y,COND,HEDCON)       MAIN0241
0196            IF(.NOT.PUNOUT) GOTO 410                                    MAIN0242
```

30

```
      WRITE(7,600) ((U(I,J),I=1,NI),J=1,NJ)                           MAIN0243
      WRITE(7,600) ((V(I,J),I=1,NI),J=2,NJ)                           MAIN0244
      WRITE(7,600) ((P(I,J),I=1,NI),J=1,NJ)                           MAIN0245
      WRITE(7,600) ((T(I,J),I=1,NI),J=1,NJ)                           MAIN0246
      WRITE(7,600) ((W(I,J),I=1,NI),J=1,NJ)                           MAIN0247
  410 CONTINUE                                                        MAIN0248
C                                                                     MAIN0249
C-----CALCULATIONS OF SHEAR-STRESS COEFF, NUSSELT NO, STANTON NO, SHERWOMAIN0250
      DZN=XU(NI)-X(NIM1)                                              MAIN0251
      DDZN=XU(NI)-X(NI-2)                                             MAIN0252
      DELT=TWALL-TIN                                                  MAIN0253
      IF(ABS(DELT-0.).LE.1.E-8) DELT=1.                               MAIN0254
      ATEMP=0.5*(TIN+TWALL)                                           MAIN0255
      CPA=CPA1+CPA2*ATEMP+CPA3*ATEMP*ATEMP                            MAIN0256
      IF(ABS(DELT-0.).LE.1.E-8) TERM=1.                               MAIN0257
      WRITE (6,402)                                                   MAIN0258
      DO 401 J=2,NJM1                                                 MAIN0259
      ACPP=0.5*(CPP(2,2)+CPP(NI,J))                                   MAIN0260
      ADEN=0.5*(DEN(2,2)+DEN(NI,J))                                   MAIN0261
      ADIFF=0.5*(DIFF(NI,J)+DIFF(2,2))                                MAIN0262
      ACOND=0.5*(COND(2,2)+COND(NI,J))                                MAIN0263
      APRESS=0.5*P(NI,J)+PIN                                          MAIN0264
C-----MASS TRANSFER CALCULATIONS                                      MAIN0265
      WP=W(NI,J)                                                      MAIN0266
      XAP=WP/(WP+(1.-WP)/RATIO)                                       MAIN0267
      WDIFF=ALOG((1.-XAJ)/(1.-XAP))                                   MAIN0268
      IF(ABS(WDIFF-0.0).CE.1.E-8) WDIFF=1.0                           MAIN0269
      WFLUX=U(NI,J)*DEN(NI,J)                                         MAIN0270
      HM1=-WFLUX/WDIFF/WTA                                            MAIN0271
      SH1=HM1*DJET/ADIFF*(GAS*ATEMP/APRESS)                           MAIN0272
      HM=-WFLUX*(1.-W(NI,J))/(W(NI,J)-W(2,2))                         MAIN0273
      SH=HM*DJET/DIFF(2,2)/DEN(2,2)                                   MAIN0274
C-----HEAT TRANSFER CALCULATIONS                                      MAIN0275
      IF(.NOT.CALW) WFLUX=1.E-4                                       MAIN0276
      HFLUX=(T(NI-2,J)-TWALL)/DDZN                                    MAIN0277
      HFLUX=COND(NI,J)*HFLUX                                          MAIN0278
      H=-HFLUX/DELT                                                   MAIN0279
      NU=H*DJET/COND(2,2)                                             MAIN0280
      ST=H/(DEN(2,2)*CPP(2,2)*UIN)                                    MAIN0281
      YI = Y(M)-DJP*TAN(THETA)
      YY = (Y(J)-YI)/DJET
      WRITE (6,403) J,YY,WDIFF,WFLUX,HM1,SH1,HM,SH,HFLUX,H,NU,ST      MAIN0283
      IF((J-1)/5*5.EQ.(J-1)) WRITE (6,422)                            MAIN0284
  401 CONTINUE                                                        MAIN0285
C-----SHEAR STRESS CALCULATIONS                                       MAIN0286
      WRITE (6,425)                                                   MAIN0287
      DO 407 J=3,NJM1                                                 MAIN0288
      YYY=YV(J)/DJET                                                  MAIN0289
      TAU=VIS(NP,J)*V(NIM1,J)/DZN                                     MAIN0290
      CF=TAU*2./(DEN(1,2)*UIN*UIN)                                    MAIN0291
      ACF=0.5*(CF*RENO)                                               MAIN0292
      WRITE (6,426) J,YYY,TAU,CF,ACF                                  MAIN0293
      IF((J-2)/5*5.EQ.(J-2)) WRITE (6,422)                            MAIN0294
  407 CONTINUE                                                        MAIN0295
```


30

```
 FORTRAN IV G1  RELEASE 2.0             MAIN              DATE = 79037          23/48/10            PAGE 0007

                  C-----AVERAGE TRANSPORT PROPERTIES CALCULATIONS                            MAIN0296
   0246                 WRITE (6,424)                                                        MAIN0297
   0247                 DO 430 J=2,NJM1                                                      MAIN0298
   0248                 PR=CPP(NI,J)*VIS(NI,J)/COND(NI,J)                                    MAIN0299
   0249                 SC=VIS(NI,J)/(DEN(NI,J)*DIFF(NI,J))                                  MAIN0300
   0250                 PR=0.5*(PR+PRANDL)                                                   MAIN0301
   0251                 SC=0.5*(SC+SCHMIT)                                                   MAIN0302
   0252                 AVIS=0.5*(VIS(NI,J)+VIS(2,2))                                        MAIN0303
   0253                 ADEN=0.5*(DEN(NI,J)+DEN(2,2))                                        MAIN0304
   0254                 ACPP=0.5*(CPP(NI,J)+CPP(2,2))                                        MAIN0305
   0255                 ADIFF=0.5*(DIFF(NI,J)+DIFF(2,2))                                     MAIN0306
   0256                 ACOND=0.5*(COND(NI,J)+COND(2,2))                                     MAIN0307
   0257                 WRITE (6,423) J,PR,SC,AVIS,ADEN,ACPP,ADIFF,ACOND                     MAIN0308
   0258                 IF((J-1)/5*5.EQ.(J-1)) WRITE (6,422)                                 MAIN0309
   0259             430 CONTINUE                                                             MAIN0310
   0260                 STOP                                                                 MAIN0311
                  C                                                                          MAIN0312
                  C-----FORMAT STATEMENTS                                                    MAIN0313
   0261             210 FORMAT (1H0,9X,'PULJET',//,10X,'SIMULTANEOUS HEAT & MASS TRANSFER
                       1UNDER AN IMPINGING JET',///,5X,'SCALAR GRID SYSTEM:  X-,  Y-
                       2DIRECTION',/)
   0262             220 FORMAT(///,15X,'JET INLET CONDITIONS',/,                             MAIN0317
                       2   20X,'REYNOLDS NUMBER',T40,1PE11.3,/,                              MAIN0318
                       3   20X,'AVERAGE VELOCITY',T40,1PE11.3,/,                             MAIN0319
                       4   20X,'TEMPERATURE',T40,1PE11.3,/,                                  MAIN0320
                       5   20X,'PRESSURE',T40,1PE11.3,/,                                     MAIN0321
                       6   20X,'MASS FRACTION OF A',T40,1PE11.3,/,                           MAIN0322
                       7   20X,'MOLE FRACTION,A',T40,0PE11.3)                                MAIN0323
   0263             221 FORMAT(//,20X,'PRANDTL NO',T40,1PE11.3,/,                            MAIN0324
                       2   20X,'SCHMICT NO',T40,1PE11.3)                                     MAIN0325
   0264             222 FORMAT(///,8X,'CROSS FLOW INLET CONDITIONS',/,
                       2   20X,'REYNOLDS NUMBER',T40,1PE11.3,/,
                       3   20X,'AVERAGE VELOCITY',T40,1PE11.3,/,
                       4   20X,'TEMPERATURE',T40,1PE11.3,/,
                       5   20X,'PRESSURE',T40,1PE11.3,/,
                       6   20X,'MASS FRACTION OF A',T40,1PE11.3)
   0265             223 FORMAT(///,18X,'CROSS MASS FLOW-RATE IS',F8.2,1X,'% OF JET MASS FL
                       1OW RATE')
   0266             230 FORMAT(///,15X,'IMPINGEMENT WALL CONDITIONS',/,                      MAIN0326
                       2   20X,'TEMPERTURE',T40,1PE11.3,/,20X,'USUC/UIN',T40,0PE11.3)        MAIN0327
   0267             232 FORMAT(///,15X,'GEOMETRY OF SYSTEM',/,20X,'JET RADIUS',              MAIN0328
                       2        T40,1PE11.3,/,20X,'H/D RATIO',T40,1PE11.3,/,                 MAIN0329
                       3        20X,'NOZZLE FROM J',T40,I11,/,29X,'TO J',T40,I11,
                       4        /,20X,'IMPINGEMENT ANGLE',T40,0PF11.6)
   0268             250 FORMAT(///,15X,'PROGRAM CONDITIONS',/,                               MAIN0331
                       2   20X,'MAX ALLOW. ITER',T40,I11,/,                                  MAIN0332
                       3   20X,'MAX ALLOW. TIME',T40,1PE11.3,/,                              MAIN0333
                       4   20X,'MAX ALLOW. RESI',T40,1PE11.3)                                MAIN0334
   0269             260 FORMAT(///,15X,'JET MASS FLOW IN',T35,1PE15.6,/,                     MAIN0335
                       2   13X,'JET X-MOMENTUM IN',T35,1PE15.6,/,
                       3   13X,'JET Y-MOMENTUM IN',T35,1PE15.6)
   0270             261 FORMAT(///,8X,'CROSS-FLOW MASS FLOW IN',T35,1PE15.6,/,
                       2   6X,'CROSS-FLOW Y-MOMENTUM IN',T35,1PE15.6,///,
                       3   15X,'VARIABLE FIELD INITIALISED AS :')
```

```
FORTRAN IV G1  RELEASE 2.0              MAIN              DATE = 79037          23/48/10               PAGE 0008

 0271              280 FORMAT(1H ,/,8(1PE15.7))                                                   MAIN0338
 0272              310 FORMAT(1H1,4HITER,4X,95HI----------ABSOLUTE RESIDUAL SOURCE SUMS--
                      1-------I         I--FIELD VALUES AT MONITORING LOCATION(,I2,1H,,I2,
                      21H),3H--I,6X,'SPLIT RATE'/2X,2HNO,6X,4HUMOM,6X,4HVMOM,6X,4HMASS,6X
                      3,4HENER,6X,4HSPEC,11X,1HU,9X,1HV,9X,1HP,9X,1HT,9X,1HW,7X,5HALPHA,
                      44X,4HVINC,/)
 0273              311 FORMAT(1H ,I3,1X,1P5E10.3,6X,1P5E10.3,2X,0PF6.4,1X,1PE10.3)
 0274              402 FORMAT(1H1,/,10X,'TRANSFER COEFFICIENTS',//,1X,' J       R/D    WDIFFMAIN0344
                      2      WFLUX',8X,'HM1',8X,'SH1',9X,'HM',9X,'SH',                            MAIN0345
                      36X,'HFLUX',10X,'H',9X,'NU',9X,'ST',                                        MAIN0346
                      4/,130('-'))                                                                MAIN0347
 0275              403 FORMAT(' ',I2,F8.5,1X,F8.5,9(1PE11.3))                                     MAIN0348
 0276              420 FORMAT(//,5X,'OVERALL MASS EVAPOTATION =',1PE15.6,/,                       MAIN0349
                      25X,'OVERALL MASS OUTFLOW =',1PE15.6,/,5X,'NET MASS ACCUMUL. =',            MAIN0350
                      3 1PE15.6,//,5X,'OUTPUT PUNCH =',L3,//)                                     MAIN0351
 0277              422 FORMAT(' ')                                                                MAIN0352
 0278              423 FORMAT(' ',I3,1X,8(1PE11.4))                                               MAIN0353
 0279              424 FORMAT(1H1,20X,'AVERAGE TRANSPORT PROPERTIES',/,                            MAIN0354
                      1              3X,'J',9X,'PR',9X,'SC',8X,'VIS',8X,'DEN',9X,'CP',7X          MAIN0355
                      2              ,'DIFF',10X,'K',/,2X,81('-'))                                MAIN0356
 0280              425 FORMAT(///,3X,'J',7X,'YV/D',8X,'TAU',9X,'CF',3X,'CF*REO/2',/,2X,           MAIN0357
                      2             46('-'))                                                      MAIN0358
 0281              426 FORMAT(' ',I3,1X,4(1PE11.4))                                               MAIN0359
 0282              600 FORMAT(10Z8)                                                               MAIN0360
 0283              602 FORMAT(' ',15X,5X,9A4,//)                                                  MAIN0361
 0284                  END                                                                        MAIN0362

 *OPTIONS IN EFFECT*  NOTERM,ID,EBCDIC,SOURCE,NOLIST,NODECK,LOAD,NOMAP,NOTEST
 *OPTIONS IN EFFECT*  NAME = MAIN     , LINECNT =       56
 *STATISTICS*     SOURCE STATEMENTS =       284,PROGRAM SIZE =     11276
 *STATISTICS*  NO DIAGNOSTICS GENERATED
```

```
FORTRAN IV G1  RELEASE 2.0            MAIN              DATE = 79037          23/48/10              PAGE 0001

                C--BLOCK DATA--------------------------------------------------------------DATA0001
 0001                 BLOCK DATA                                                          DATA0002
 0002                 COMMON                                                              DATA0003
                     1/UVEL/RESORU,NSWPU,URFU,DXEPU(22),DXPWU(22),SEWU(22)
                     1/VVEL/RESORV,NSWPV,URFV,DYNPV(22),DYPSV(22),SNSV(22),YCV(22)
                     1/PCOR/RESORM,NSWPP,URFP,DU(20,20),DV(20,20),IPREF,JPREF
                     1/TEMP/RESORT,NSWPT,URFT                                             DATA0007
                     1/SPEC/RESORW,NSWPW,URFW                                             DATA0008
 0003                 COMMON /MOLEWT/WTA,WTB                                              DATA0009
                     1/FLUPR2/CONDA1,CONDA2,CONDA3,CONDB1,CONDB2,CONDB3,                  DATA0010
                     2VISA1,VISA2,VISA3,VISB1,VISB2,VISB3,DIFFU,                          DATA0011
                     3CPA1,CPA2,CPA3,CPB1,CPB2,CPB3                                       DATA0012
                     1/PROB1/RE,TIN,PIN,TWALL,WIN,FLOWIN,FLOWEV,                          DATA0013
                     2        ISTEP,JSTEP,ISTP1,JSTP1,ISTM1,JSTM1                         DATA0014
                     3         ,JNOZ,JNOZP1,JNOZM1
 0004                 COMMON                                                              DATA0015
                     1/ALL/IT,JT,NI,NJ,NIM1,NJM1,GREAT                                    DATA0016
                     1/VAPP/ANTON1,ANTON2,ANTON3                                          DATA0017
                     1/PGM/PUNIN,PUNOUT,TIMAX,MAXIT,SORMAX,INDPRI                         DATA0018
 0005                 COMMON /DIFFUS/DIFF1,DIFF2,DIFF3,DIFF4,DIFF5                        DATA0019
 0006                 COMMON /SUCTON/USUC,SUCR                                            DATA0020
 0007                 COMMON/ANGLE/THETA
 0008                 COMMON/CROSS/PCNTCR,DELTIN,DELWIN
 0009                 LOGICAL PUNIN,PUNOUT                                                DATA0021
                C---- LENGTH        M                                                     DATA0022
                C---- VELOCITY      M/S                                                   DATA0023
                C---- TEMPT         K                                                     DATA0024
                C---- SPECIES.      MASS FRACTION OF SPECIES A                            DATA0025
                C---- PRESSURE      N/M**2                                                DATA0026
                C---- DENSITY       KG/M**3                                               DATA0027
                C---- DIFFUSITY     M**2/S                                                DATA0028
                C---- SPECI.HEAT    J/KG/K                                                DATA0029
                C---- THERM.CONDU   W/M/K                                                 DATA0030
                C---- VISCOSITY,    KG/M/S                                                DATA0031
                C---- MOLE.WT       G/MOLE                                                DATA0032
                C-------M   METER                                                         DATA0033
                C-------KG  KILOGRAM                                                      DATA0034
                C-------G   GRAM                                                          DATA0035
                C-------S   SEC.                                                          DATA0036
                C-------N   NEWTON                                                        DATA0037
                C-------J   JOULE                                                         DATA0038
                C-------W   WATT                                                          DATA0039
                C--------------------------------------------------------------------------DATA0040
                C------PROGRAM- AND PRINTOUT-CONTROL DATA                                 DATA0041
 0010                 DATA ISTEP,GREAT/2,1.E30/                                           DATA0042
 0011                 DATA NSWPU,NSWPV,NSWPP,NSWPT,NSWPW/3,3,5,3,3/                       DATA0043
                     &     ,IT,JT,IPREF,JPREF/20,50,2,24/
                     3     ,URFU,URFV,URFP,URFT,URFW/0.2,0.25,0.5,0.9,0.9/
                     4     ,PUNIN,PUNOUT/.TRUE.,.TRUE./
                     5     ,MAXIT,TIMAX,SORMAX,INDPRI/200,900.,0.015,101/
                C                                                                         DATA0048
                C------PHYSICAL DATA                                                      DATA0049
                C     BINARY MIXTURE OF WATER VAP (A)  AND  AIR (B)                       DATA0050
 0012                 DATA WTA,WTB/18.02,28.97/                                           DATA0051
```

```
FORTRAN IV G1  RELEASE 2.0              BLK DATA          DATE = 79037        23/48/10              PAGE 0002
                     1      ,ANTON1,ANTON2,ANTON3/23.365186,3919.884,-42.061625/        DATA0052
   0013                DATA VISA1,VISA2,VISA3/0.99354E-6,0.27067E-7,0.88906E-11/         DATA0053
   0014                DATA VISB1,VISB2,VISB3/0.25641E-5,0.60198E-7,-0.23723E-10/        DATA0054
   0015                DATA CPA1,CPA2,CPA3/0.18241E4,0.21976,0.23487E-3/                 DATA0055
   0016                DATA CPB1,CPB2,CPB3/0.10256E4,-0.17317,0.36146E-3/                DATA0056
   0017                DATA CONDA1,CONDA2,CONDA3/0.86868E-2,0.11318E-4,0.85793E-7/       DATA0057
   0018                DATA CONDB1,CONDB2,CONDB3/0.38793E-3,0.95425E-4,-0.30699E-7/      DATA0058
   0019                DATA DIFF1,DIFF2,DIFF3/0.2794E-4,-0.1306E-6,0.4016E-9/            DATA0059
   0020                DATA DIFF4,DIFF5/-0.1057E-3,0.335E-6/                             DATA0060
                 C                                                                       DATA0061
                 C-----PROBLEM SPECIFICATION                                             DATA0062
   0021                DATA PIN/101325.0/                                                DATA0063
   0022                DATA SUCR/0.0/                                                    DATA0064
   0023                DATA THETA/0.00/
   0024                DATA RE,TIN,TWALL,WIN/1000.,450.,350.,0.1/
   0025                DATA PCNTCR,DELTIN,DELWIN/0.10,0.00,0.00/
   0026                END                                                               DATA0066

 *OPTIONS IN EFFECT*  NOTERM,ID,EBCDIC,SOURCE,NOLIST,NODECK,LOAD,NOMAP,NOTEST
 *OPTIONS IN EFFECT*  NAME = BLK DATA, LINECNT =       56
 *STATISTICS*  NO DIAGNOSTICS GENERATED
```

```
FORTRAN IV G1  RELEASE 2.0              MAIN            DATE = 79037        23/48/10            PAGE 0001
                  C--GRID---------------------------------------------------------------GRID0001
                  C--GRID DISTRIBUTION CALCULATIONS ------------------------------------GRID0002
0001                    SUBROUTINE GRID(JNOZ,JSTEP,RSMALL,HDRATO)
0002                    COMMON                                                          GRID0004
                       1/ALL/IT,JT,NI,NJ,NIM1,NJM1,GREAT                               GRID0005
                       1/GEOM/X(22),Y(22),DXEP(22),DXPW(22),DYNP(22),
                       2      DYPS(22),SNS(22),SEW(22),XU(22),YV(22)
0003                    COMMON/ANGLE/THETA
0004                    DIMENSION DDX(19)
                  C-----------GRID   20*50
0005                    DATA DDX/1.,2.,4.,8.,16.,32.,64.,128.,64.,32.,16.,8.,4.,2.,1.,  GRID0011
                       2          0.5,0.5,0.25,0.18/                                    GRID0012
0006                    NI=20
0007                    NJ=20
0008                    NIM1=NI-1                                                       GRID0016
0009                    JNOZ=14
0010                    JSTEP=33
0011                    RSMALL=1.6E-03
0012                    HDRATO=3.
0013                    DY=2.0E-03
0014                    Y(1)=-0.5*DY
0015                    DO 6 I=2,NJ
0016                  6 Y(I)=Y(I-1)+DY
0017                    SUM=0.0                                                         GRID0035
0018                    DJP=HDRATO*2.*RSMALL                                            GRID0036
0019                    DO 30 I=1,NIM1
0020               30   SUM=SUM+DDX(I)                                                  GRID0038
0021                    SUM = SUM-0.5*(DDX(1)+DDX(NIM1))
0022                    DX=DJP/SUM                                                      GRID0040
0023                    X(1)=-DDX(1)*DX*0.5                                             GRID0041
0024                    DO 40 I=2,NI                                                    GRID0042
0025               40   X(I)=X(I-1)+DX*DDX(I-1)                                         GRID0043
0026                    RETURN                                                          GRID0044
0027                    END                                                             GRID0045

 *OPTIONS IN EFFECT*  NOTERM,ID,EBCDIC,SOURCE,NOLIST,NODECK,LOAD,NOMAP,NOTEST
 *OPTIONS IN EFFECT*  NAME = GRID    , LINECNT =       56
 *STATISTICS*    SOURCE STATEMENTS =       27,PROGRAM SIZE =       864
 *STATISTICS*  NO DIAGNOSTICS GENERATED
```

```
FORTRAN IV G1 RELEASE 2.0          MAIN          DATE = 79037          23/48/10          PAGE 0001

               C--INIT---------------------------------------------------------------INIT0001
               C--GEOMETRICAL QUANTITIES CALCULATIONS -------------------------------INIT0002
      0001           SUBROUTINE INIT                                                 INIT0003
               C                                                                     INIT0004
               CHAPTER  0  0  0  0  0  0  0  0  PRELIMINARIES  0  0  0  0  0  0  0  0 INIT0005
               C                                                                     INIT0006
      0002           COMMON                                                          INIT0007
                    1/UVEL/RESORU,NSWPU,URFU,DXEPU(22),DXPWU(22),SEWU(22)
                    1/VVEL/RESORV,NSWPV,URFV,DYNPV(22),DYPSV(22),SNSV(22),YCV(22)
                    1/ALL/IT,JT,NI,NJ,NIM1,NJM1,GREAT                                INIT0010
                    1/PROB1/RE,TIN,PIN,TWALL,WIN,FLOWIN,FLOWEV,                      INIT0011
                    2       ISTEP,JSTEP,ISTP1,JSTP1,ISTM1,JSTM1                      INIT0012
                    3       ,JNOZ,JNOZP1,JNOZM1
      0003           COMMON                                                          INIT0013
                    1/GEOM/X(22),Y(22),DXEP(22),DXPW(22),DYNP(22),
                    2       DYPS(22),SNS(22),SEW(22),XU(22),YV(22)
               C                                                                     INIT0016
               CHAPTER  1  1  1  1  1  CALCULATE GEOMETRICAL QUANTITIES  1  1  1  1  1 INIT0017
               C                                                                     INIT0018
      0004           DXPW(1)=0.0                                                     INIT0022
      0005           DXEP(NI)=0.0                                                    INIT0023
      0006           DO 101 I=1,NIM1                                                 INIT0024
      0007           DXEP(I)=X(I+1)-X(I)                                             INIT0025
      0008       101 DXPW(I+1)=DXEP(I)                                               INIT0026
      0009           DYPS(1)=0.0                                                     INIT0027
      0010           DYNP(NJ)=0.0                                                    INIT0028
      0011           DO 102 J=1,NJM1                                                 INIT0029
      0012           DYNP(J)=Y(J+1)-Y(J)                                             INIT0030
      0013       102 DYPS(J+1)=DYNP(J)                                               INIT0031
      0014           SEW(1)=0.0                                                      INIT0032
      0015           SEW(NI)=0.0                                                     INIT0033
      0016           DO 103 I=2,NIM1                                                 INIT0034
      0017       103 SEW(I)=0.5*(DXEP(I)+DXPW(I))                                    INIT0035
      0018           SNS(1)=0.0                                                      INIT0036
      0019           SNS(NJ)=0.0                                                     INIT0037
      0020           DO 104 J=2,NJM1                                                 INIT0038
      0021       104 SNS(J)=0.5*(DYNP(J)+DYPS(J))                                    INIT0039
      0022           XU(1)=0.0                                                       INIT0040
      0023           DO 105 I=2,NI                                                   INIT0041
      0024       105 XU(I)=0.5*(X(I)+X(I-1))                                         INIT0042
      0025           DXPWU(1)=0.0                                                    INIT0043
      0026           DXPWU(2)=0.0                                                    INIT0044
      0027           DXEPU(1)=0.0                                                    INIT0045
      0028           DXEPU(NI)=0.0                                                   INIT0046
      0029           DO 106 I=2,NIM1                                                 INIT0047
      0030           DXEPU(I)=XU(I+1)-XU(I)                                          INIT0048
      0031       106 DXPWU(I+1)=DXEPU(I)                                             INIT0049
      0032           SEWU(1)=0.0                                                     INIT0050
      0033           SEWU(2)=0.0                                                     INIT0051
      0034           SEWU(NI)=0.                                                     INIT0052
      0035           DO 107 I=3,NIM1                                                 INIT0053
      0036       107 SEWU(I)=0.5*(DXEPU(I)+DXPWU(I))                                 INIT0054
      0037           YV(1)=0.0                                                       INIT0055
      0038           DO 108 J=2,NJ                                                   INIT0057
```

```
0039                 YV(J) = 0.5*(Y(J)+Y(J-1))
0040             108 YCV(J) = 0.5*(YV(J)+YV(J-1))
0041                 DYPSV(1)=0.0                                  INIT0061
0042                 DYPSV(2)=0.0                                  INIT0062
0043                 DYNPV(NJ)=0.0                                 INIT0063
0044                 DO 109 J=2,NJM1                               INIT0064
0045                 DYNPV(J)=YV(J+1)-YV(J)                        INIT0065
0046             109 DYPSV(J+1)=DYNPV(J)                           INIT0066
0047                 SNSV(1)=0.0                                   INIT0067
0048                 SNSV(2)=0.0                                   INIT0068
0049                 SNSV(NJ)=0.0                                  INIT0069
0050                 DO 110 J=3,NJM1                               INIT0070
0051             110 SNSV(J)=0.5*(DYNPV(J)+DYPSV(J))               INIT0071
               C                                                   INIT0072
0052                 RETURN                                        INIT0073
0053                 END                                           INIT0074

 *OPTIONS IN EFFECT*  NOTERM,ID,EBCDIC,SOURCE,NOLIST,NODECK,LOAD,NOMAP,NOTEST
 *OPTIONS IN EFFECT*  NAME = INIT    , LINECNT =       56
 *STATISTICS*    SOURCE STATEMENTS =         53,PROGRAM SIZE =      1286
 *STATISTICS*  NO DIAGNOSTICS GENERATED
```

```
FORTRAN IV G1  RELEASE 2.0          MAIN          DATE = 79037          14/58/32          PAGE 0001

                C--PROPS-----------------------------------------------------PROP0001
                C--FLUID.PROPERTIES CALCULATIONS -----------------------------PROP0002
 0001                 SUBROUTINE PROPS                                        PROP0003
                CHAPTER  0  0  0  0  0  0  0  0   PRELIMINARIES  0  0  0  0  0  0  0  0  PROP0004
                C                                                             PROP0005
 0002                COMMON                                                   PROP0006
                    1/ALL/IT,JT,NI,NJ,NIM1,NJM1,GREAT                         PROP0007
                    1/VAR/U(20,20),V(20,20),P(20,20),PP(20,20),T(20,20),W(20,20)
                    1/FLUPR/RHOA,RHOB,RATIO,CPA,CPB,CPDEL,                    PROP0009
                    2        DEN(20,20),VIS(20,20),CPP(20,20),DIFF(20,20),COND(20,20)
 0003                COMMON                                                   PROP0011
                    1/FLUPR2/CONDA1,CONDA2,CONDA3,CONDB1,CONDB2,CONDB3,       PROP0012
                    2VISA1,VISA2,VISA3,VISB1,VISB2,VISB3,DIFFU,               PROP0013
                    3CPA1,CPA2,CPA3,CPB1,CPB2,CPB3                            PROP0014
                    1/PROBI/RE,TIN,PIN,TWALL,WIN,FLOWIN,FLOWEV,               PROP0015
                    2        ISTEP,JSTEP,ISTP1,JSTP1,ISTM1,JSTM1              PROP0016
                    3        ,JNOZ,JNOZP1,JNOZM1
 0004                COMMON/HEAT/CPPDEL(20,20)
 0005                COMMON /DIFFUS/DIFF1,DIFF2,DIFF3,DIFF4,DIFF5             PROP0018
 0006                COMMON /MOLEWT/WTA,WTB                                   PROP0019
 0007                DATA GAS/8314.2/                                         PROP0020
                C                                                             PROP0021
                C------CP OF WATER WATER VAP ASSUMED CONST UNDER 100'C        PROP0022
                C------CP OF AIR ASSUMED CONST                                PROP0023
 0008                DO 110 I=1,NI                                            PROP0024
 0009                DO 100 J=1,NJM1
 0010                Q=T(I,J)                                                 PROP0026
 0011                TT=Q*Q                                                   PROP0027
 0012                YA=W(I,J)/(W(I,J)+(1.-W(I,J))/RATIO)                     PROP0028
 0013                YB=1.-YA                                                 PROP0029
 0014                CPA=CPA1+CPA2*Q+CPA3*TT                                  PROP0030
 0015                CPPDEL(I,J)=CPA-CPB                                      PROP0031
 0016                VISA=VISA1+VISA2*Q+VISA3*TT                              PROP0032
 0017                VISB=VISB1+VISB2*Q+VISB3*TT                              PROP0033
 0018                IF(VISB.GT.0.00) GO TO 52
 0019                WRITE(6,51) I,J,Q,VISB
 0020             51 FORMAT(10X,'I=',I3,'J=',I3,'T(I,J)=',F7.3,'VISB=',F10.3)
 0021             52 CONTINUE
 0022                CONDA=CONDA1+CONDA2*Q+CONDA3*TT                          PROP0034
 0023                CONDB=CONDB1+CONDB2*Q+CONDB3*TT                          PROP0035
 0024                DIFF(I,J)=DIFF1+DIFF2*Q+DIFF3*TT                         PROP0036
 0025                IF(Q.GT.521.) DIFF(I,J)=DIFF4+DIFF5*Q                    PROP0037
 0026                DIFF(I,J)=DIFF(I,J)*101325./(P(I,J)+PIN)                 PROP0038
 0027                AVEM=1./(W(I,J)/WTA+(1.-W(I,J))/WTB)                     PROP0039
 0028                DEN(I,J)=(P(I,J)+PIN)*AVEM/(GAS*Q)                       PROP0040
 0029                CONST=1.126*SQRT(VISA/VISB)                              PROP0041
 0030                PHIAB=(1.+CONST)*(1.+CONST)/3.6022                       PROP0042
 0031                PHIBA=(1.+1./CONST)*(1.+1./CONST)/4.5674                 PROP0043
 0032                VIS(I,J)=VISA/(1.+YB*PHIAB/YA)+VISB/(1.+YA*PHIBA/YB)     PROP0044
 0033                A=1.+155./Q                                              PROP0045
 0034                B=1.+411./Q                                              PROP0046
 0035                C=1.+120./Q                                              PROP0047
 0036                CONST=SQRT(1.428*(VISA/VISB)*B/C)                        PROP0048
 0037                PHIAB=(1.+CONST)*(1.+CONST)*A/(4.*B)                     PROP0049
```

```
                PHIBA=(1.+1./CONST)*(1.+1./CONST)*A/(4.*C)                 PROP0050
                COND(I,J)=CONDA/(1.+PHIAB*YB/YA)+CONDB/(1.+PHIBA*YA/YB)    PROP0051
                CPP(I,J)=W(I,J)*CPA+(1.-W(I,J))*CPB                        PROP0052
           100  CONTINUE                                                   PROP0053
                VIS(I,NJ)=VIS(I,NJM1)                                      PROP0059
                DEN(I,NJ)=DEN(I,NJM1)                                      PROP0060
                DIFF(I,NJ)=DIFF(I,NJM1)                                    PROP0061
                CPP(I,NJ)=CPP(I,NJM1)                                      PROP0062
                COND(I,NJ)=COND(I,NJM1)                                    PROP0063
           110  CONTINUE                                                   PROP0064
                RETURN                                                     PROP0065
                END                                                        PROP0066

 *OPTIONS IN EFFECT*  NOTERM,ID,EBCDIC,SOURCE,NOLIST,NODECK,LOAD,NOMAP,NOTEST
 *OPTIONS IN EFFECT*  NAME = PROPS    , LINECNT =       56
 *STATISTICS*     SOURCE STATEMENTS =       49,PROGRAM SIZE =      1902
 *STATISTICS*  NO DIAGNOSTICS GENERATED
```


30

```
FORTRAN IV G1   RELEASE 2.0              MAIN            DATE = 79037        23/48/10            PAGE 0001

                   C--CALCU-----------------------------------------------------------------CALCU001
                   C--SOLUTION OF U EQUATION -----------------------------------------------CALCU002
  0001                   SUBROUTINE CALCU                                                  CALCU003
                   C                                                                       CALCU004
                   CHAPTER  0  0  0  0  0  0  0  0  PRELIMINARIES  0  0  0  0  0  0  0  0  CALCU005
                   C                                                                       CALCU006
  0002                   COMMON NITER
  0003                   COMMON SPLIT(200)
  0004                   COMMON CNIV(200)
  0005                   COMMON HEDU(9),HEDV(9),HEDP(9),HEDT(9),HEDW(9),HEDVIS(9),
                        1       HEDDEN(9),HEDCP(9),HEDDIF(9),HEDCON(9)
  0006                   COMMON                                                            CALCU007
                        1/UVEL/RESORU,NSWPU,URFU,DXEPU(22),DXPWU(22),SEWU(22)
                        1/PCOR/RESORM,NSWPP,URFP,DU(20,20),DV(20,20),IPREF,JPREF
                        1/ALL/IT,JT,NI,NJ,NIM1,NJM1,GREAT                                  CALCU010
                        1/VAR/U(20,20),V(20,20),P(20,20),PP(20,20),T(20,20),W(20,20)
  0007                   COMMON                                                            CALCU012
                        1/GEOM/X(22),Y(22),DXEP(22),DXPW(22),DYNP(22),
                        2      DYPS(22),SNS(22),SEW(22),XU(22),YV(22)
                        1/FLUPR/RHOA,RHOB,RATIO,CPA,CPB,CPDEL,                             CALCU015
                        2      DEN(20,20),VIS(20,20),CPP(20,20),DIFF(20,20),COND(20,20)
  0008                   COMMON                                                            CALCU017
                        1/PROB1/RE,TIN,PIN,TWALL,WIN,FLOWIN,FLOWEV,                        CALCU018
                        2      ISTEP,JSTEP,ISTP1,JSTP1,ISTM1,JSTM1                         CALCU019
                        3      ,JNOZ,JNOZP1,JNOZM1
                        1/COEF/AP(20,20),AN(20,20),AS(20,20),AE(20,20),AW(20,20),
                        2      SU(20,20),SP(20,20)
  0009                   GRAVTY=9.807                                                      CALCU022
                   C                                                                       CALCU023
                   CHAPTER  1  1  1  1  1  1  ASSEMBLY OF COEFFICIENTS  1  1  1  1  1  1  1CALCU024
                   C                                                                       CALCU025
  0010                   DO 101 J=2,NJM1                                                   CALCU026
  0011                   DELUE = 0.0
  0012                   AREAEW = SNS(J)*0.01
  0013                   DO 100 I=3,NIM1                                                   CALCU029
  0014                   DENIJ=DEN(I,J)                                                    CALCU030
                   C-----COMPUTE AREAS AND VOLUME                                          CALCU031
  0015                   AREAN = DXPW(I)*0.01
  0016                   AREAS = DXPW(I)*0.01
  0017                   VOL = AREAEW*DXPW(I)
                   C-----CALCULATE CONVECTION COEFFICIENTS                                 CALCU035
  0018                   GN=0.5*(DEN(I,J+1)+DENIJ)*V(I,J+1)                                CALCU036
  0019                   GNW=0.5*(DEN(I-1,J)+DEN(I-1,J+1))*V(I-1,J+1)                      CALCU037
  0020                   GS=0.5*(DEN(I,J-1)+DENIJ)*V(I,J)                                  CALCU038
  0021                   GSW=0.5*(DEN(I-1,J)+DEN(I-1,J-1))*V(I-1,J)                        CALCU039
  0022                   GE=0.5*(DEN(I+1,J)+DENIJ)*U(I+1,J)                                CALCU040
  0023                   GP=0.5*(DENIJ+DEN(I-1,J))*U(I,J)                                  CALCU041
  0024                   GW=0.5*(DEN(I-1,J)+DEN(I-2,J))*U(I-1,J)                           CALCU042
  0025                   CN=0.5*(GN+GNW)*AREAN                                             CALCU043
  0026                   CS=0.5*(GS+GSW)*AREAS                                             CALCU044
  0027                   CE=0.5*(GE+GP)*AREAEW                                             CALCU045
  0028                   CW=0.5*(GP+GW)*AREAEW                                             CALCU046
                   C-----CALCULATE DIFFUSION COEFFICIENTS                                  CALCU047
  0029                   VISN=0.25*(VIS(I,J)+VIS(I,J+1)+VIS(I-1,J)+VIS(I-1,J+1))           CALCU048
```

```
      VISS=0.25*(VIS(I,J)+VIS(I,J-1)+VIS(I-1,J)+VIS(I-1,J-1))           CALCU049
      DN=VISN*AREAN/DYNP(J)                                             CALCU050
      DS=VISS*AREAS/DYPS(J)                                             CALCU051
      DE=VIS(I,J)*AREAEW/DXEPU(I)                                       CALCU052
      DW=VIS(I-1,J)*AREAEW/DXPWU(I)                                     CALCU053
C-----CALCULATE COEFFICIENTS OF SOURCE TERMS                             CALCU054
      SMP=CN-CS+CE-CW                                                   CALCU055
      CP=AMAX1(0.0,SMP)                                                 CALCU056
      CPO=CP                                                            CALCU057
C-----ASSEMBLE MAIN COEFFICIENTS                                         CALCU058
      AN(I,J)=AMAX1(ABS(0.5*CN),DN)-0.5*CN                              CALCU059
      AS(I,J)=AMAX1(ABS(0.5*CS),DS)+0.5*CS                              CALCU060
      AE(I,J)=AMAX1(ABS(0.5*CE),DE)-0.5*CE                              CALCU061
      AW(I,J)=AMAX1(ABS(0.5*CW),DW)+0.5*CW                              CALCU062
      DU(I,J)=AREAEW                                                    CALCU063
      SU(I,J)=CPO*U(I,J)+DU(I,J)*(P(I-1,J)-P(I,J))                      CALCU064
      SP(I,J)=-CP                                                       CALCU065
      DRDXE = 0.5*((DEN(I+1,J)+DEN(I,J))-(DEN(I,J)+DEN(I-1,J)))/SEW(I)
      DRDYE = 0.5*((DEN(I,J+1)+DEN(I,J))-(DEN(I,J)+DEN(I,J-1)))/SNS(J)
      DELUW = DELUE
      DELUE=0.5*(U(I+1,J)+U(I-1,J))*DRDXE+0.5*(V(I,J+1)+V(I,J))*DRDYE
      DELUE = DELUE*VIS(I,J)/DEN(I,J)
      ALPHA=0.3333*(DELUW-DELUE)*0.01
      SU(I,J) = SU(I,J)+ALPHA*SNS(J)
      SU(I,J)=SU(I,J)+SNS(J)*DXPW(I)*GRAVTY*0.5
     1         *(DEN(I,J)+DEN(I-1,J))*0.01
  100 CONTINUE                                                          CALCU085
  101 CONTINUE                                                          CALCU086
C                                                                       CALCU087
CHAPTER  2  2  2  2  2  2  2  PROBLEM MODIFICATIONS  2  2  2  2  2  2  2CALCU088
C                                                                       CALCU089
      CALL MODU                                                         CALCU090
C                                                                       CALCU091
CHAPTER  3  FINAL COEFF. ASSEMBLY AND RESIDUAL SOURCE CALCULATION  3  3 CALCU092
C                                                                       CALCU093
      RESORU=0.0                                                        CALCU094
      DO 300 I=3,NIM1                                                   CALCU095
      DO 301 J=2,NJM1                                                   CALCU096
      AP(I,J)=AN(I,J)+AS(I,J)+AE(I,J)+AW(I,J)-SP(I,J)                   CALCU097
      DU(I,J)=DU(I,J)/AP(I,J)                                           CALCU098
      RESOR=AN(I,J)*U(I,J+1)+AS(I,J)*U(I,J-1)+AE(I,J)*U(I+1,J)          CALCU099
     1     +AW(I,J)*U(I-1,J)-AP(I,J)*U(I,J)+SU(I,J)                     CALCU100
      VOL = SNS(J)*DXPW(I)*0.01
      SORVOL=GREAT*VOL                                                  CALCU102
      IF(-SP(I,J).GT.0.5*SORVOL)  RESOR=RESOR/SORVOL                    CALCU103
      RESORU=RESORU+ABS(RESOR)                                          CALCU104
C-----UNDER-RELAXATION                                                  CALCU105
      AP(I,J)=AP(I,J)/URFU                                              CALCU106
      SU(I,J)=SU(I,J)+(1.-URFU)*AP(I,J)*U(I,J)                          CALCU107
      DU(I,J)=DU(I,J)*URFU                                              CALCU108
  301 CONTINUE                                                          CALCU109
  300 CONTINUE                                                          CALCU110
C                                                                       CALCU111
CHAPTER  4  4  4  SOLUTION OF DIFFERENCE EQUATION  4  4  4  4  4  4  4  CALCU112
```

```
FORTRAN IV G1  RELEASE 2.0             CALCU              DATE = 79037         23/48/10          PAGE 0003
                  C                                                                    CALCU113
 0071             400 CALL LOSILV(3,2,NI,NJ,IT,JT,U,NSWPU,0.)
 0072                 RETURN                                                           CALCU115
 0073                 END                                                              CALCU116

  *OPTIONS IN EFFECT*  NOTERM,ID,EBCDIC,SOURCE,NOLIST,NODECK,LOAD,NOMAP,NOTEST
  *OPTIONS IN EFFECT*  NAME = CALCU    , LINECNT =       56
  *STATISTICS*     SOURCE STATEMENTS =        73,PROGRAM SIZE =       2570
  *STATISTICS*  NO DIAGNOSTICS GENERATED
```

```
FORTRAN IV G1  RELEASE 2.0            MAIN             DATE = 79037          23/48/10                PAGE 0001

                 C--CALCV-------------------------------------------------------------------CALCV001
                 C--SOLUTION OF V EQUATION -------------------------------------------------CALCV002
 0001                  SUBROUTINE CALCV                                                     CALCV003
                 C                                                                          CALCV004
                 CHAPTER  0  0  0  0  0  0  0  0  PRELIMINARIES  0  0  0  0  0  0  0  0     CALCV005
                 C                                                                          CALCV006
 0002                  COMMON NITER
 0003                  COMMON                                                               CALCV007
                      1/VVEL/RESORV,NSWPV,URFV,DYNPV(22),DYPSV(22),SNSV(22),YCV(22)
                      1/PCOR/RESORM,NSWPP,URFP,DU(20,20),DV(20,20),IPREF,JPREF
                      1/ALL/IT,JT,NI,NJ,NIM1,NJM1,GREAT                                     CALCV010
                      1/GEOM/X(22),Y(22),DXEP(22),DXPW(22),DYNP(22),
                      2        DYPS(22),SNS(22),SEW(22),XU(22),YV(22)
 0004                  COMMON                                                               CALCV013
                      1/VAR/U(20,20),V(20,20),P(20,20),PP(20,20),T(20,20),W(20,20)
                      1/FLUPR/RHOA,RHOB,RATIO,CPA,CPB,CPDEL,                                CALCV015
                      2        DEN(20,20),VIS(20,20),CPP(20,20),DIFF(20,20),COND(20,20)
                      1/PROB1/RE,TIN,PIN,TWALL,WIN,FLOWIN,FLOWEV,                           CALCV017
                      2        ISTEP,JSTEP,ISTP1,JSTP1,ISTM1,JSTM1                          CALCV018
                      3        ,JNOZ,JNOZP1,JNOZM1
 0005                  COMMON                                                               CALCV019
                      1/COEF/AP(20,20),AN(20,20),AS(20,20),AE(20,20),AW(20,20),
                      2        SU(20,20),SP(20,20)
                 C                                                                          CALCV022
                 CHAPTER  1  1  1  1  1  1  ASSEMBLY OF COEFFICIENTS  1  1  1  1  1  1  1CALCV023
                 C                                                                          CALCV024
 0006                  DO 100 I=2,NIM1                                                      CALCV025
 0007                  DELUN = 0.0
 0008                  DO 101 J = 3,NJM1
 0009                  AREAEW = DYPS(J)*0.01
 0010                  DENIJ=DEN(I,J)                                                       CALCV029
                 C-----COMPUTE AREAS AND VOLUME                                             CALCV030
 0011                  AREAN = SEW(I)*0.01
 0012                  AREAS = SEW(I)*0.01
 0013                  VOL = AREAEW*SEW(I)
                 C-----CALCULATE CONVECTION COEFFICIENTS                                    CALCV034
 0014                  GN=0.5*(DEN(I,J+1)+DENIJ)*V(I,J+1)                                   CALCV035
 0015                  GP=0.5*(DENIJ+DEN(I,J-1))*V(I,J)                                     CALCV036
 0016                  GS=0.5*(DEN(I,J-1)+DEN(I,J-2))*V(I,J-1)                              CALCV037
 0017                  GE=0.5*(DEN(I+1,J)+DENIJ)*U(I+1,J)                                   CALCV038
 0018                  GSE=0.5*(DEN(I,J-1)+DEN(I+1,J-1))*U(I+1,J-1)                         CALCV039
 0019                  GW=0.5*(DENIJ+DEN(I-1,J))*U(I,J)                                     CALCV040
 0020                  GSW=0.5*(DEN(I,J-1)+DEN(I-1,J-1))*U(I,J-1)                           CALCV041
 0021                  CN=0.5*(GN+GP)*AREAN                                                 CALCV042
 0022                  CS=0.5*(GP+GS)*AREAS                                                 CALCV043
 0023                  CE=0.5*(GE+GSE)*AREAEW                                               CALCV044
 0024                  CW=0.5*(GW+GSW)*AREAEW                                               CALCV045
                 C-----CALCULATE DIFFUSION COEFFICIENTS                                     CALCV046
 0025                  VISE=0.25*(VIS(I,J)+VIS(I+1,J)+VIS(I,J-1)+VIS(I+1,J-1))              CALCV047
 0026                  VISW=0.25*(VIS(I,J)+VIS(I-1,J)+VIS(I,J-1)+VIS(I-1,J-1))              CALCV048
 0027                  DN=VIS(I,J)*AREAN/DYNPV(J)                                           CALCV049
 0028                  DS=VIS(I,J-1)*AREAS/DYPSV(J)                                         CALCV050
 0029                  DE=VISE*AREAEW/DXEP(I)                                               CALCV051
 0030                  DW=VISW*AREAEW/DXPW(I)                                               CALCV052
```

```
FORTRAN IV G1  RELEASE 2.0             CALCV              DATE = 79037        23/48/10              PAGE 0002
             C-----CALCULATE COEFFICIENTS OF SOURCE TERMS                                     CALCV053
 0031              SMP=CN-CS+CE-CW                                                            CALCV054
 0032              CP=AMAX1(0.0,SMP)                                                          CALCV055
 0033              CPO=CP
             C-----ASSEMBLE MAIN COEFFICIENTS                                                 CALCV057
 0034              AN(I,J)=AMAX1(ABS(0.5*CN),DN)-0.5*CN                                       CALCV058
 0035              AE(I,J)=AMAX1(ABS(0.5*CE),DE)-0.5*CE                                       CALCV059
 0036              AS(I,J)=AMAX1(ABS(0.5*CS),DS)+0.5*CS                                       CALCV060
 0037              AW(I,J)=AMAX1(ABS(0.5*CW),DW)+0.5*CW                                       CALCV061
 0038              DV(I,J)=SEW(I)*0.01
 0039              SU(I,J)=CPO*V(I,J)+SEW(I)*(P(I,J-1)-P(I,J))*0.01
 0040              SP(I,J) = -CPO
 0041              DRDXN=0.5*((DEN(I+1,J)+DEN(I,J))-(DEN(I,J)+DEN(I-1,J)))/SEW(I)
 0042              DRDYN=0.5*((DEN(I,J+1)+DEN(I,J))-(DEN(I,J)+DEN(I,J-1)))/SNS(J)
 0043              DELUS = DELUN
 0044              DELUN=0.5*((U(I+1,J)+U(I,J))*DRDXN+(V(I,J+1)+V(I,J))*DRDYN)
 0045              DELUN = DELUN*VIS(I,J)/DEN(I,J)
 0046              ALPHA=0.3333*(DELUS-DELUN)*0.01
 0047              SU(I,J) = SU(I,J)+ALPHA*SEW(I)
 0048          101 CONTINUE                                                                   CALCV085
 0049          100 CONTINUE
             CHAPTER  2  2  2  2  2  2  2  PROBLEM MODIFICATIONS  2  2  2  2  2  2  2CALCV088
             C                                                                                CALCV089
 0050              CALL MODV                                                                  CALCV090
             C                                                                                CALCV091
             CHAPTER  3  FINAL COEFF. ASSEMBLY AND RESIDUAL SOURCE CALCULATION  3  3 CALCV092
             C                                                                                CALCV093
 0051              RESORV=0.0                                                                 CALCV094
 0052              DO 300 I=2,NIM1                                                            CALCV095
 0053              DO 301 J=3,NJM1                                                            CALCV096
 0054              AP(I,J)=AN(I,J)+AS(I,J)+AE(I,J)+AW(I,J)-SP(I,J)                            CALCV097
 0055              DV(I,J)=DV(I,J)/AP(I,J)                                                    CALCV098
 0056              RESOR=AN(I,J)*V(I,J+1)+AS(I,J)*V(I,J-1)+AE(I,J)*V(I+1,J)                   CALCV099
                  1     +AW(I,J)*V(I-1,J)-AP(I,J)*V(I,J)+SU(I,J)                              CALCV100
 0057              VOL=DYPS(J)*SEW(I)*0.01
 0058              SORVOL=GREAT*VOL                                                           CALCV102
 0059              IF(-SP(I,J).GT.0.5*SORVOL)  RESOR=RESOR/SORVOL                             CALCV103
 0060              RESORV=RESORV+ABS(RESOR)                                                   CALCV104
             C-----UNDER-RELAXATION                                                           CALCV105
 0061              AP(I,J)=AP(I,J)/URFV                                                       CALCV106
 0062              SU(I,J)=SU(I,J)+(1.-URFV)*AP(I,J)*V(I,J)                                   CALCV107
 0063              DV(I,J)=DV(I,J)*URFV                                                       CALCV108
 0064          301 CONTINUE                                                                   CALCV109
 0065          300 CONTINUE                                                                   CALCV110
             C                                                                                CALCV111
             CHAPTER  4  4  4  SOLUTION OF DIFFERENCE EQUATION  4  4  4  4  4  4  4  CALCV112
             C                                                                                CALCV113
 0066          400 CALL LOSILV(2,3,NI,NJ,IT,JT,V,NSWPV,1.)
 0067              RETURN                                                                     CALCV115
 0068              END                                                                        CALCV116

 *OPTIONS IN EFFECT*  NOTERM,ID,EBCDIC,SOURCE,NOLIST,NODECK,LOAD,NOMAP,NOTEST
 *OPTIONS IN EFFECT*  NAME = CALCV    , LINECNT =       56
 *STATISTICS*     SOURCE STATEMENTS =       68,PROGRAM SIZE =      2332
```

```
FORTRAN IV G1   RELEASE 2.0          CALCV          DATE = 79037          23/48/10          PAGE 0003
   *STATISTICS*  NO DIAGNOSTICS GENERATED
```

30

```
FORTRAN IV G1  RELEASE 2.0            MAIN            DATE = 79037          23/48/10            PAGE 0001

                 C--CALCP-------------------------------------------------------------CALCP001
                 C--SOLUTION OF P EQUATION -------------------------------------------CALCP002
 0001                  SUBROUTINE CALCP                                                CALCP003
                 C                                                                     CALCP004
                 CHAPTER  0  0  0  0  0  0  0  0  PRELIMINARIES  0  0  0  0  0  0  0  0  CALCP005
                 C                                                                     CALCP006
 0002                  COMMON NITER
 0003                  COMMON                                                          CALCP007
                      1/PCOR/RESORM,NSWPP,URFP,DU(20,20),DV(20,20),IPREF,JPREF
                      1/ALL/IT,JT,NI,NJ,NIM1,NJM1,GREAT                                CALCP009
                      1/VAR/U(20,20),V(20,20),P(20,20),PP(20,20),T(20,20),W(20,20)
                      1/GEOM/X(22),Y(22),DXEP(22),DXPW(22),DYNP(22),
                      2      DYPS(22),SNS(22),SEW(22),XU(22),YV(22)
 0004                  COMMON                                                          CALCP013
                      1/FLUPR/RHOA,RHOB,RATIO,CPA,CPB,CPDEL,                           CALCP014
                      2      DEN(20,20),VIS(20,20),CPP(20,20),DIFF(20,20),COND(20,20)
                      1/COEF/AP(20,20),AN(20,20),AS(20,20),AE(20,20),AW(20,20),
                      2      SU(20,20),SP(20,20)
                 C                                                                     CALCP018
                 CHAPTER  1  1  1  1  1  1  ASSEMBLY OF COEFFICIENTS  1  1  1  1  1  1  1CALCP019
                 C                                                                     CALCP021
 0005                  RESORM=0.                                                       CALCP020
 0006                  DO 101 J=2,NJM1                                                 CALCP022
 0007                  AREAEW = SNS(J)*0.01
 0008                  DO 100 I=2,NIM1                                                 CALCP024
 0009                  DENIJ=DEN(I,J)                                                  CALCP025
 0010                  PP(I,J)=0.0                                                     CALCP026
                 C-----COMPUTE AREAS AND VOLUME                                        CALCP027
 0011                  AREAN = SEW(I)*0.01
 0012                  AREAS = SEW(I)*0.01
 0013                  VOL = AREAEW*SEW(I)
                 C-----CALCULATE COEFFICIENTS                                          CALCP031
 0014                  DENN=0.5*(DENIJ+DEN(I,J+1))                                     CALCP032
 0015                  DENS=0.5*(DENIJ+DEN(I,J-1))                                     CALCP033
 0016                  DENE=0.5*(DENIJ+DEN(I+1,J))                                     CALCP034
 0017                  DENW=0.5*(DENIJ+DEN(I-1,J))                                     CALCP035
 0018                  AN(I,J)=DENN*AREAN*DV(I,J+1)                                    CALCP036
 0019                  AS(I,J)=DENS*AREAS*DV(I,J)                                      CALCP037
 0020                  AE(I,J)=DENE*AREAEW*DU(I+1,J)                                   CALCP038
 0021                  AW(I,J)=DENW*AREAEW*DU(I,J)                                     CALCP039
                 C-----CALCULATE SOURCE TERMS                                          CALCP040
 0022                  CN=DENN*V(I,J+1)*AREAN                                          CALCP041
 0023                  CS=DENS*V(I,J)*AREAS                                            CALCP042
 0024                  CE=DENE*U(I+1,J)*AREAEW                                         CALCP043
 0025                  CW=DENW*U(I,J)*AREAEW                                           CALCP044
 0026                  SMP=CN-CS+CE-CW                                                 CALCP045
 0027                  SP(I,J)=0.0                                                     CALCP046
 0028                  SU(I,J)=-SMP                                                    CALCP047
                 C-----COMPUTE SUM OF ABSOLUTE MASS SOURCES                            CALCP048
 0029                  RESORM=RESORM+ABS(SMP)                                          CALCP049
 0030              100 CONTINUE                                                        CALCP050
 0031              101 CONTINUE                                                        CALCP051
                 C                                                                     CALCP052
                 CHAPTER  2  2  2  2  2  2  2  PROBLEM MODIFICATIONS  2  2  2  2  2  2  2CALCP053
```

```
FORTRAN IV G1  RELEASE 2.0          CALCP           DATE = 79037          23/48/10                    PAGE 0002
                  C                                                                       CALCP054
                  C       CALL MODP                                                       CALCP055
                  C                                                                       CALCP056
                  CHAPTER  3  3  3  3  3  FINAL COEFFICIENT ASSEMBLY  3  3  3  3  3  3  3 CALCP057
                  C                                                                       CALCP058
 0032                     DO 300 I=2,NIM1                                                 CALCP059
 0033                     DO 301 J=2,NJM1                                                 CALCP060
 0034                301  AP(I,J)=AN(I,J)+AS(I,J)+AE(I,J)+AW(I,J)-SP(I,J)                 CALCP061
 0035                300  CONTINUE                                                        CALCP062
                  C                                                                       CALCP063
                  CHAPTER  4  4  4  4  4  SOLUTION OF DIFFERENCE EQUATIONS  4  4  4  4  4 CALCP064
                  C                                                                       CALCP065
 0036                400  CALL LOSILV(2,2,NI,NJ,IT,JT,PP,NSWPP,0.)
                  C                                                                       CALCP067
                  CHAPTER  5  5  5  5  CORRECT VELOCITIES AND PRESSURE  5  5  5  5  5  5  CALCP068
                  C                                                                       CALCP069
                  C-----VELOCITIES                                                        CALCP070
                  C-----PRESSURES (WITH PROVISION FOR UNDER-RELAXATION)                   CALCP071
 0037                     PPREF=PP(IPREF,JPREF)                                           CALCP072
 0038                     DO 500 I=2,NIM1                                                 CALCP073
 0039                     DO 501 J=2,NJM1                                                 CALCP074
 0040                     IF(I.NE.2) U(I,J)=U(I,J)+DU(I,J)*(PP(I-1,J)-PP(I,J))            CALCP075
 0041                     V(I,J) = V(I,J)+DV(I,J)*(PP(I,J-1)-PP(I,J))
 0042                     P(I,J)=P(I,J)+URFP*(PP(I,J)-PPREF)                              CALCP077
 0043                501  CONTINUE                                                        CALCP078
 0044                500  CONTINUE                                                        CALCP079
 0045                     RETURN                                                          CALCP080
 0046                     END                                                             CALCP081

 *OPTIONS IN EFFECT*  NOTERM,ID,EBCDIC,SOURCE,NOLIST,NODECK,LOAD,NOMAP,NOTEST
 *OPTIONS IN EFFECT*  NAME = CALCP    , LINECNT =       56
 *STATISTICS*    SOURCE STATEMENTS =          46,PROGRAM SIZE =      1572
 *STATISTICS*  NO DIAGNOSTICS GENERATED
```

```
                C--CALCT-------------------------------------------------------CALCT001
                C--SOLUTION OF TEMPERATURE EQUATION ---------------------------CALCT002
 0001                 SUBROUTINE CALCT                                         CALCT003
                C                                                              CALCT004
                CHAPTER  0  0  0  0  0  0  0  PRELIMINARIES  0  0  0  0  0  0  0  CALCT005
                C                                                              CALCT006
 0002                COMMON NITER
 0003                COMMON                                                    CALCT007
                    1/TEMP/RESORT,NSWPT,URFT                                   CALCT008
                    1/ALL/IT,JT,NI,NJ,NIM1,NJM1,GREAT                          CALCT009
                    1/VAR/U(20,20),V(20,20),P(20,20),PP(20,20),T(20,20),W(20,20)
                    1/GEOM/X(22),Y(22),DXEP(22),DXPW(22),DYNP(22),
                    2       DYPS(22),SNS(22),SEW(22),XU(22),YV(22)
 0004                COMMON                                                    CALCT013
                    1/FLUPR/RHOA,RHOB,RATIO,CPA,CPB,CPDEL,                     CALCT014
                    2       DEN(20,20),VIS(20,20),CPP(20,20),DIFF(20,20),COND(20,20)
                    1/PROB1/RE,TIN,PIN,TWALL,WIN,FLOWIN,FLOWEV,                CALCT016
                    2       ISTEP,JSTEP,ISTP1,JSTP1,ISTM1,JSTM1                CALCT017
                    3       ,JNOZ,JNOZP1,JNOZM1
 0005                COMMON                                                    CALCT018
                    1/COEF/AP(20,20),AN(20,20),AS(20,20),AE(20,20),AW(20,20),
                    2       SU(20,20),SP(20,20)
 0006                COMMON/HEAT/CPPDEL(20,20)
                C                                                              CALCT022
                CHAPTER  1  1  1  1  1  1  ASSEMBLY OF COEFFICIENTS  1  1  1  1  1  1  CALCT023
                C                                                              CALCT024
 0007                DO 101 J=2,NJM1                                           CALCT025
 0008                AREAEW = SNS(J)*0.01
 0009                DO 100 I=2,NIM1                                           CALCT027
 0010                DENIJ=DEN(I,J)                                            CALCT028
                C-----COMPUTE AREAS VOLUME                                     CALCT029
 0011                AREAN = SEW(I)*0.01
 0012                AREAS = SEW(I)*0.01
 0013                VOL=AREAEW*SEW(I)                                         CALCT032
 0014                CPDEL=CPPDEL(I,J)                                         CALCT033
                C-----CALCULATE CONVECTION COEFFICIENTS                        CALCT034
 0015                GN=0.5*(DENIJ+DEN(I,J+1))*V(I,J+1)                        CALCT035
 0016                GS=0.5*(DENIJ+DEN(I,J-1))*V(I,J)                          CALCT036
 0017                GE=0.5*(DENIJ+DEN(I+1,J))*U(I+1,J)                        CALCT037
 0018                GW=0.5*(DENIJ+DEN(I-1,J))*U(I,J)                          CALCT038
 0019                CN=GN*AREAN                                               CALCT039
 0020                CS=GS*AREAS                                               CALCT040
 0021                CE=GE*AREAEW                                              CALCT041
 0022                CW=GW*AREAEW                                              CALCT042
                C-----CALCULATE DIFFUSION COEFFICIENTS                         CALCT043
 0023                GAM=COND(I,J)/CPP(I,J)                                    CALCT044
 0024                GAMN=0.5*(GAM+COND(I,J+1) /CPP(I,J+1))                    CALCT045
 0025                GAMS=0.5*(GAM+COND(I,J-1)/CPP(I,J-1))                     CALCT046
 0026                GAME=0.5*(GAM+COND(I+1,J)/CPP(I+1,J))                     CALCT047
 0027                GAMW=0.5*(GAM+COND(I-1,J)/CPP(I-1,J))                     CALCT048
 0028                DN=GAMN*AREAN/DYNP(J)                                     CALCT049
 0029                DS=GAMS*AREAS/DYPS(J)                                     CALCT050
 0030                DE=GAME*AREAEW/DXEP(I)                                    CALCT051
 0031                DW=GAMW*AREAEW/DXPW(I)                                    CALCT052
```

```
C-----SOURCE TERMS
      SMP=CN-CS+CE-CW
      CP=AMAX1(0.0,SMP)
      CPO=CP
C-----ASSEMBLE MAIN COEFFICIENTS
      AN(I,J)=AMAX1(ABS(0.5*CN),DN)-0.5*CN
      AS(I,J)=AMAX1(ABS(0.5*CS),DS)+0.5*CS
      AE(I,J)=AMAX1(ABS(0.5*CE),DE)-0.5*CE
      AW(I,J)=AMAX1(ABS(0.5*CW),DW)+0.5*CW
      SU(I,J)=CPO*T(I,J)
      DELZ=DXEP(I)
      IF(I.EQ.NIM1) DELZ=DELZ*0.5
      DTZ1=(T(I+1,J)-T(I,J))/DELZ
      DTZ2=(T(I,J)-T(I,J-1))/DXPW(I)
      DTR1=(T(I,J+1)-T(I,J))/DYNP(J)
      DTR2=(T(I,J)-T(I,J-1))/DYPS(J)
      DWZ1=(W(I+1,J)-W(I,J))/DELZ
      DWZ2=(W(I,J)-W(I,J-1))/DXPW(I)
      DWR1=(W(I,J+1)-W(I,J))/DYNP(J)
      DWR2=(W(I,J)-W(I,J-1))/DYPS(J)
      DTZ=0.5*(DTZ1+DTZ2)
      DTR=0.5*(DTR1+DTR2)
      DWZ=0.5*(DWZ1+DWZ2)
      DWR=0.5*(DWR1+DWR2)
      WTERM=(DWZ*DTZ+DWR*DTR)*VOL*DENIJ*DIFF(I,J)*CPDEL/CPP(I,J)
      DCPZ1=(CPP(I,J)-CPP(I+1,J))/(CPP(I+1,J)*CPP(I,J)*DELZ)
      DCPZ2=(CPP(I-1,J)-CPP(I,J))/(CPP(I,J)*CPP(I-1,J)*DXPW(I))
      DCPR1=(CPP(I,J)-CPP(I,J+1))/(CPP(I,J)*CPP(I,J+1)*DYNP(J))
      DCPR2=(CPP(I,J-1)-CPP(I,J))/(CPP(I,J)*CPP(I,J-1)*DYPS(J))
      DCPZ=0.5*(DCPZ1+DCPZ2)
      DCPR=0.5*(DCPR1+DCPR2)
      CPTERM=(DCPR*DTR+DCPZ*DTZ)*VOL*COND(I,J)
      SU(I,J)=SU(I,J)+WTERM-CPTERM
      SP(I,J)=-CP
  100 CONTINUE
  101 CONTINUE
C
CHAPTER  2  2  2  2  2  2  PROBLEM MODIFICATIONS  2  2  2  2  2  2
C
      CALL MODT
CHAPTER 3 FINAL COEFFICIENT ASSEMBLY AND RESIDUAL SOURCE CALCULATION 3
C
      RESORT=0.0
      DO 300 I=2,NIM1
      DO 301 J=2,NJM1
      AP(I,J)=AN(I,J)+AS(I,J)+AE(I,J)+AW(I,J)-SP(I,J)
      RESOR=AN(I,J)*T(I,J+1)+AS(I,J)*T(I,J-1)+AE(I,J)*T(I+1,J)
     1      +AW(I,J)*T(I-1,J)-AP(I,J)*T(I,J)+SU(I,J)
      VOL = SNS(J)*SEW(I)*0.01
      SORVOL=GREAT*VOL
      IF(-SP(I,J).GT.0.5*SORVOL) RESOR=RESOR/SORVOL
      RESORT=RESORT+ABS(RESOR)
C-----UNDER-RELAXATION
      AP(I,J)=AP(I,J)/URFT
```

```
0077          SU(I,J)=SU(I,J)+(1.0-URFT)*AP(I,J)*T(I,J)                    CALCT107
0078      301 CONTINUE                                                       CALCT108
0079      300 CONTINUE                                                       CALCT109
        C                                                                    CALCT110
        CHAPTER  4  4  4  4  4  SOLUTION OF DIFFERENCE EQUATIONS  4  4  4  4  4 CALCT111
        C                                                                    CALCT112
0080      400 CALL LOSILV(2,2,NI,NJ,IT,JT,T,NSWPT,0.)
0081          RETURN                                                         CALCT114
0082          END                                                            CALCT115

 *OPTIONS IN EFFECT*  NOTERM,ID,EBCDIC,SOURCE,NOLIST,NODECK,LOAD,NOMAP,NOTEST
 *OPTIONS IN EFFECT*  NAME = CALCT    , LINECNT =       56
 *STATISTICS*    SOURCE STATEMENTS =        82,PROGRAM SIZE =      2818
 *STATISTICS*  NO DIAGNOSTICS GENERATED
```

```
             C--CALCW-------------------------------------------------------CALCW001
             C--SOLUTION OF SPECIES EQUATION -------------------------------CALCW002
 0001              SUBROUTINE CALCW                                          CALCW003
             C                                                               CALCW004
             CHAPTER  0  0  0  0  0  0  0  PRELIMINARIES  0  0  0  0  0  0  0 CALCW005
             C                                                               CALCW006
 0002              COMMON NITER
 0003              COMMON                                                    CALCW007
                  1/SPEC/RESORW,NSWPW,URFW                                   CALCW008
                  1/ALL/IT,JT,NI,NJ,NIM1,NJM1,GREAT                          CALCW009
                  1/VAR/U(20,20),V(20,20),P(20,20),PP(20,20),T(20,20),W(20,20)
                  1/GEOM/X(22),Y(22),DXEP(22),DXPW(22),DYNP(22),
                  2      DYPS(22),SNS(22),SEW(22),XU(22),YV(22)
 0004              COMMON                                                    CALCW013
                  1/FLUPR/RHOA,RHOB,RATIO,CPA,CPB,CPDEL,                     CALCW014
                  2      DEN(20,20),VIS(20,20),CPP(20,20),DIFF(20,20),COND(20,20)
                  1/PROB1/RE,TIN,PIN,TWALL,WIN,FLOWIN,FLOWEV,                CALCW016
                  2      ISTEP,JSTEP,ISTP1,JSTP1,ISTM1,JSTM1                 CALCW017
                  3      ,JNOZ,JNOZP1,JNOZM1
 0005              COMMON                                                    CALCW018
                  1/COEF/AP(20,20),AN(20,20),AS(20,20),AE(20,20),AW(20,20),
                  2      SU(20,20),SP(20,20)
             C                                                               CALCW021
             CHAPTER  1  1  1  1  1  1  ASSEMBLY OF COEFFICIENTS  1  1  1  1  1  1 CALCW022
             C                                                               CALCW023
 0006              DO 101 J=2,NJM1                                           CALCW024
 0007              AREAEW = SNS(J)*0.01
 0008              DO 100 I=2,NIM1                                           CALCW026
 0009              DENIJ=DEN(I,J)                                            CALCW027
             C-----COMPUTE AREAS VOLUME                                      CALCW028
 0010              AREAN = SEW(I)*0.01
 0011              AREAS = SEW(I)*0.01
 0012              VOL=AREAEW*SEW(I)                                         CALCW031
             C-----CALCULATE CONVECTION COEFFICIENTS                         CALCW032
 0013              GN=0.5*(DENIJ+DEN(I,J+1))*V(I,J+1)                        CALCW033
 0014              GS=0.5*(DENIJ+DEN(I,J-1))*V(I,J)                          CALCW034
 0015              GE=0.5*(DENIJ+DEN(I+1,J))*U(I+1,J)                        CALCW035
 0016              GW=0.5*(DENIJ+DEN(I-1,J))*U(I,J)                          CALCW036
 0017              CN=GN*AREAN                                               CALCW037
 0018              CS=GS*AREAS                                               CALCW038
 0019              CE=GE*AREAEW                                              CALCW039
 0020              CW=GW*AREAEW                                              CALCW040
             C-----CALCULATE DIFFUSION COEFFICIENTS                          CALCW041
 0021              GAM=DIFF(I,J)*DENIJ                                       CALCW042
 0022              GAMN=0.5*(GAM+DIFF(I,J+1)*DEN(I,J+1))                     CALCW043
 0023              GAMS=0.5*(GAM+DIFF(I,J-1)*DEN(I,J-1))                     CALCW044
 0024              GAME=0.5*(GAM+DIFF(I+1,J)*DEN(I+1,J))                     CALCW045
 0025              GAMW=0.5*(GAM+DIFF(I-1,J)*DEN(I-1,J))                     CALCW046
 0026              DN=GAMN*AREAN/DYNP(J)                                     CALCW047
 0027              DS=GAMS*AREAS/DYPS(J)                                     CALCW048
 0028              DE=GAME*AREAEW/DXEP(I)                                    CALCW049
 0029              DW=GAMW*AREAEW/DXPW(I)                                    CALCW050
             C-----SOURCE TERMS                                              CALCW051
 0030              SMP=CN-CS+CE-CW                                           CALCW052
```

```
FORTRAN IV G1  RELEASE 2.0             CALCW              DATE = 79037          23/48/10              PAGE 0002
 0031                 CP=AMAX1(0.0,SMP)
 0032                 CPO=CP                                                                     CALCW054
            C-----ASSEMBLE MAIN COEFFICIENTS                                                     CALCW055
 0033                 AN(I,J)=AMAX1(ABS(0.5*CN),DN)-0.5*CN                                       CALCW056
 0034                 AS(I,J)=AMAX1(ABS(0.5*CS),DS)+0.5*CS                                       CALCW057
 0035                 AE(I,J)=AMAX1(ABS(0.5*CE),DE)-0.5*CE                                       CALCW058
 0036                 AW(I,J)=AMAX1(ABS(0.5*CW),DW)+0.5*CW                                       CALCW059
 0037                 SU(I,J)=CPO*W(I,J)                                                         CALCW060
 0038                 SP(I,J)=-CP                                                                CALCW061
 0039             100 CONTINUE                                                                   CALCW062
 0040             101 CONTINUE                                                                   CALCW063
            C                                                                                    CALCW064
            CHAPTER  2  2  2  2  2  2  PROBLEM MODIFICATIONS  2  2  2  2  2  2                   CALCW065
            C                                                                                    CALCW066
 0041                 CALL  MODW                                                                 CALCW067
            CHAPTER 3 FINAL COEFFICIENT ASSEMBLY AND RESIDUAL SOURCE CALCULATION 3               CALCW068
            C                                                                                    CALCW069
 0042                 RESORW=0.0                                                                 CALCW070
 0043                 DO 300 I=2,NIM1                                                            CALCW071
 0044                 DO 301 J=2,NJM1                                                            CALCW072
 0045                 AP(I,J)=AN(I,J)+AS(I,J)+AE(I,J)+AW(I,J)-SP(I,J)                            CALCW073
 0046                 RESOR=AN(I,J)*W(I,J+1)+AS(I,J)*W(I,J-1)+AE(I,J)*W(I+1,J)                   CALCW074
                    1       +AW(I,J)*W(I-1,J)-AP(I,J)*W(I,J)+SU(I,J)                             CALCW075
 0047                 VOL = SEW(I)*SNS(J)*0.01
 0048                 SORVOL=GREAT*VOL                                                           CALCW077
 0049                 IF(-SP(I,J).GT.0.5*SORVOL) RESOR=RESOR/SORVOL                              CALCW078
 0050                 RESORW=RESORW+ABS(RESOR)                                                   CALCW079
            C-----UNDER-RELAXATION                                                               CALCW080
 0051                 AP(I,J)=AP(I,J)/URFW                                                       CALCW081
 0052                 SU(I,J)=SU(I,J)+(1.0-URFW)*AP(I,J)*W(I,J)                                  CALCW082
 0053             301 CONTINUE                                                                   CALCW083
 0054             300 CONTINUE                                                                   CALCW084
            C                                                                                    CALCW085
 0055             400 CALL LOSILV(2,2,NI,NJ,IT,JT,W,NSWPW,0.)
            CHAPTER  4  4  4  4  4  SOLUTION OF DIFFERENCE EQUATIONS  4  4  4  4  4              CALCW086
            C                                                                                    CALCW087
 0056                 RETURN                                                                     CALCW089
 0057                 END                                                                        CALCW090

   *OPTIONS IN EFFECT*  NOTERM,ID,EBCDIC,SOURCE,NOLIST,NODECK,LOAD,NOMAP,NOTEST
   *OPTIONS IN EFFECT*  NAME = CALCW   , LINECNT =       56
   *STATISTICS*    SOURCE STATEMENTS =       57,PROGRAM SIZE =      1952
   *STATISTICS*  NO DIAGNOSTICS GENERATED
```

```
FORTRAN IV G1   RELEASE 2.0                 MAIN                  DATE = 79037            23/48/10                PAGE 0001
                       C PROMOD------------------------------------------------------------------------MOD00001
                       C--ITERATIVE BOUNDARY CONDITIONS CALCULATIONS -------------------------------MOD00002
 0001                        SUBROUTINE PROMOD                                                         MOD00003
                       C                                                                               MOD00004
                       CHAPTER  0  0  0  0  0  0  0  PRELIMINARIES  0  0  0  0  0  0  0  0  0         MOD00005
                       C
 0002                        COMMON NITER
 0003                        COMMON SPLIT(200)
 0004                        COMMON CNIV(200)
 0005                        COMMON                                                                    MOD00007
                            1/ALL/IT,JT,NI,NJ,NIM1,NJM1,GREAT                                          MOD00008
                            1/VAR/U(20,20),V(20,20),P(20,20),PP(20,20),T(20,20),W(20,20)
                            1/GEOM/X(22),Y(22),DXEP(22),DXPW(22),DYNP(22),
                            2        DYPS(22),SNS(22),SEW(22),XU(22),YV(22)
                            1/PGM/PUNIN,PUNOUT,TIMAX,MAXIT,SORMAX,INDPRI                               MOD00012
 0006                        COMMON                                                                    MOD00013
                            1/FLUPR/RHOA,RHOB,RATIO,CPA,CPB,CPDEL,                                     MOD00014
                            2          DEN(20,20),VIS(20,20),CPP(20,20),DIFF(20,20),COND(20,20)
                            1/PROB1/RE,TIN,PIN,TWALL,WIN,FLOWIN,FLOWEV,                                MOD00016
                            2          ISTEP,JSTEP,ISTP1,JSTP1,ISTM1,JSTM1                             MOD00017
                            3          ,JNOZ,JNOZP1,JNOZM1
                            1/COEF/AP(20,20),AN(20,20),AS(20,20),AE(20,20),AW(20,20),
                            2          SU(20,20),SP(20,20)
 0007                        COMMON                                                                    MOD00020
                            1/VVEL/RESORV,NSWPV,URFV,DYNPV(22),DYPSV(22),SNSV(22),YCV(22)
 0008                        COMMON /SUCTON/USUC,SUCR                                                  MOD00022
 0009                        COMMON/ANGLE/THETA
                       C                                                                               MOD00023
                       CHAPTER  2  2  2  2  2  2  2  2  U MOMENTUM  2  2  2  2  2  2  2  2  2          MOD00024
 0010                        ENTRY MODU                                                                MOD00025
                       C-----CONFINEMENT WALL                                                          MOD00026
                       C-----IMPINGEMENT WALL                                                          MOD00027
 0011                        FLOWEV=0.0                                                                MOD00028
 0012                        DO 210 J=2,NJM1                                                           MOD00029
 0013                        U(NI,J)=-DIFF(NI,J)*(W(NI,J)-W(NIM1,J))/(XU(NI)-X(NIM1))                   MOD00030
                            2          /(1.-W(NI,J))                                                   MOD00031
 0014                        U(NI,J)=U(NI,J)+USUC                                                      MOD00032
 0015                        FLOWEV=FLOWEV-DEN(NI,J)*SNS(J)*0.01*U(NI,J)
 0016                    210 CONTINUE                                                                  MOD00034
 0017                        U(NI,1)=0.0
                       C-----OUTFLOW REGION                                                            MOD00037
 0018                        DO 212 I=2,NI                                                             MOD00038
 0019                    212 U(I,NJ)=U(I,NJM1)                                                         MOD00041
 0020                        RETURN                                                                    MOD00042
                       C                                                                               MOD00043
                       CHAPTER  3  3  3  3  3  3  3  3  V MOMENTUM  3  3  3  3  3  3  3  3  3          MOD00044
                       C                                                                               MOD00045
 0021                        ENTRY MODV                                                                MOD00046
                       C-----CONFINEMENT WALL                                                          MOD00047
 0022                        DO 305 J=2,NJ
 0023                        AW(2,J) = 0.0
 0024                        SP(2,J) = SP(2,J)-0.5*(VIS(2,J)+VIS(2,J-1))/X(2)*DYPS(J)*0.01
 0025                    305 CONTINUE
                       C-----IMPINGEMENT WALL                                                          MOD00053
```

```
              XPP=XU(NI)-X(NIM1)                                    MOD00048
              DO 311 J=2,NJ
              AE(NIM1,J)=0.0                                        MOD00055
              SP(NIM1,J)=SP(NIM1,J)-0.5*(VIS(NIM1,J)+VIS(NIM1,J-1))/XPP  MOD00056
             1*DYPS(J)*0.01
         311 CONTINUE                                               MOD00058
      C-----OUTFLOW REGION                                          MOD00060
              ARDENT=0.0                                            MOD00061
              FLOWL = 0.0
              FLOWR = 0.0
              DO 312 I=2,NIM1
              V(I,NJ)=V(I,NJM1)
              ARDENR = 0.5*(DEN(I,NJ)+DEN(I,NJM1))*SEW(I)*0.01
              ARDENT=ARDENT+ARDENR
              FLOWR = FLOWR+ARDENR*V(I,NJ)
         312 CONTINUE
              FLOW=FLOWR
              SPLIT(NITER)=1.234
              VINC = (FLOWIN+FLOWEV-FLOW)/ARDENT
              CNIV(NITER)=VINC
              DO 313 I=2,NIM1
              V(I,NJ)=V(I,NJ)+VINC
         313 CONTINUE
              RETURN                                                MOD00072
      C                                                             MOD00073
      CHAPTER  5  5  5  5  5  5  5  THERMAL ENERGY  5  5  5  5  5  5  5  5  5 MOD00074
      C                                                             MOD00075
              ENTRY MODT                                            MOD00076
      C-----CONFINEMENT WALL                                        MOD00077
              XP=X(ISTEP)-XU(ISTEP)                                 MOD00078
              DO 501 J=2,NJ
              TMULT = -COND(1,J)/(CPP(1,J)*XP)
              TAREA = TMULT*SNS(J)*0.01
              SU(ISTEP,J) = SU(ISTEP,J)[illegible]REA*TIN
              SP(ISTEP,J) = SP(ISTEP,J)+TAREA
              AW(ISTEP,J) = 0.0
         501 CONTINUE
      C-----INPINGEMENT WALL                                        MOD00085
              XP=XU(NI)-X(NIM1)                                     MOD00086
              DO 510 J=2,NJ                                         MOD00087
              TMULT=-COND(NI,J)/(CPP(NI,J)*XP)                      MOD00088
              TAREA = TMULT*SNS(J)*0.01
              SU(NIM1,J)=SU(NIM1,J)-TAREA*TWALL                     MOD00090
              SP(NIM1,J)=SP(NIM1,J)+TAREA                           MOD00091
         510 AE(NIM1,J)=0.0                                         MOD00092
      C-----OUTFLOW REGION                                          MOD00094
              DO 511 I=2,NIM1                                       MOD00095
         511 T(I,NJ)=T(I,NJM1)                                      MOD00098
              RETURN                                                MOD00099
      C                                                             MOD00100
      C                                                             MOD00101
              ENTRY MODW                                            MOD00102
      C-----CONFINEMENT WALL                                        MOD00103
              DO 605 J=2,NJ
```

```
FORTRAN IV G1  RELEASE 2.0            PROMOD              DATE = 79037         23/48/10              PAGE 0003

            W(1,J) = W(2,J)
        605 AW(2,J) = 0.0
      C-----IMPINGEMENT WALL                                                       MOD00107
            XP=XU(NI)-X(NIM1)                                                      MOD00108
            DO 610 J=2,NJ                                                          MOD00109
            PSTT=PST(T(NI,J))                                                      MOD00110
            W(NI,J)=PSTT/(PSTT+(P(NIM1,J)+PIN-PSTT)*RATIO)                         MOD00111
            TMULT=-DIFF(NI,J)*DEN(NI,J)/XP                                         MOD00112
            TAREA = TMULT*SNS(J)*0.01
            SU(NIM1,J)=SU(NIM1,J)-TAREA*W(NI,J)                                    MOD00114
            SP(NIM1,J)=SP(NIM1,J)+TAREA                                            MOD00115
            AE(NIM1,J)=0.0                                                         MOD00116
        610 CONTINUE                                                               MOD00117
      C-----OUTFLOW REGION                                                         MOD00119
            DO 613 I=2,NI                                                          MOD00120
        613 W(I,NJ)=W(I,NJM1)                                                      MOD00123
            RETURN                                                                 MOD00124
            END                                                                    MOD00125

  *OPTIONS IN EFFECT*  NOTERM,ID,EBCDIC,SOURCE,NOLIST,NODECK,LOAD,NOMAP,NOTEST
  *OPTIONS IN EFFECT*  NAME = PROMOD   , LINECNT =        56
  *STATISTICS*    SOURCE STATEMENTS =        84,PROGRAM SIZE =      3244
  *STATISTICS*  NO DIAGNOSTICS GENERATED
```

```
FORTRAN IV G1  RELEASE 2.0                MAIN              DATE = 79037          23/48/10              PAGE 0001
                     C--LISOLV-------------------------------------------------------------
                     C--TDMA OF LINE-BY-LINE SOLUTION ------------------------------------LISOLV01
 0001                      SUBROUTINE LISOLV(ISTART,JSTART,NI,NJ,IT,JT,PHI,NSW,CAGE)  ----LISOLV02
                     CHAPTER  0  0  0  0  0  0  0  0  PRELIMINARIES  0  0  0  0  0  0  0  0  LISOLV04
                     C
 0002                      DIMENSION PHI(IT,JT),A(21),B(21),C(21),D(21)                     LISOLV05
 0003                      COMMON NITER
 0004                      COMMON
                          1/COEF/AP(20,20),AN(20,20),AS(20,20),AE(20,20),AW(20,20),         LISOLV07
                          2      SU(20,20),SP(20,20)
 0005                      LOGICAL SKIP
 0006                      LOGICAL LEND
 0007                      SKIP=.FALSE.
 0008                      LEND=.FALSE.
 0009                      NIM1=NI-1
 0010                      NJM1=NJ-1                                                        LISOLV10
 0011                      ISTM1=ISTART-1
                     C
                     C                                                                      LISOLV13
 0012                      A(ISTM1)=0.0                                                     LISOLV14
                     C-----COMMENCE S-N SWEEP
 0013                      DO 100 J=JSTART,NJM1
 0014                      C(ISTM1)=PHI(ISTM1,J)
                     C-----COMMENCE W-E TRAVERSE
 0015                      DO 101 I=ISTART,NIM1
                     C-----ASSEMBLE TDMA COEFFICIENTS
 0016                      A(I)=AE(I,J)
 0017                      B(I)=AW(I,J)
 0018                      C(I)=AN(I,J)*PHI(I,J+1)+AS(I,J)*PHI(I,J-1)+SU(I,J)
 0019                      D(I)=AP(I,J)
 0020                      IF((D(I)-B(I)*A(I-1)).EQ.0.) SKIP=.TRUE.
 0021                      IF(.NOT.SKIP) GO TO 50
 0022                      WRITE(6,199) SKIP,I,J
 0023                  199 FORMAT(5X,'SKIP =',L2,'ON I=',I2,',J=',I2)
 0024                      LEND=.TRUE.
 0025                      GO TO 108
                     C-----CALCULATE COEFFICIENTS OF RECURENCE FORMULA
 0026                   50 TERM=1./(D(I)-B(I)*A(I-1))
 0027                      A(I)=A(I)*TERM
 0028                      C(I)=(C(I)+B(I)*C(I-1))*TERM
 0029                      IF(.NOT.LEND) GO TO 108
 0030                      A(I-1)=A(I)
 0031                      C(I-1)=C(I)
 0032                      LEND=.FALSE.
 0033                  108 SKIP=.FALSE.
 0034                  101 CONTINUE
                     C     OBTAIN NEW PHI'S
 0035                      DO 102 II=ISTART,NIM1
 0036                      I=NI+ISTM1-II
 0037                  102 PHI(I,J)=A(I)*PHI(I+1,J)+C(I)
 0038                  100 CONTINUE
 0039                      RETURN
 0040                      END
```

```
FORTRAN IV G1  RELEASE 2.0            LISOLV            DATE = 79037         23/48/10            PAGE 0002

   *OPTIONS IN EFFECT*  NOTERM,ID,EBCDIC,SOURCE,NOLIST,NODECK,LOAD,NOMAP,NOTEST
   *OPTIONS IN EFFECT*  NAME = LISOLV  , LINECNT =       56
   *STATISTICS*     SOURCE STATEMENTS =       40,PROGRAM SIZE =      1700
   *STATISTICS*  NO DIAGNOSTICS GENERATED
```

30

```
FORTRAN IV G1  RELEASE 2.0            MAIN              DATE = 79037           23/48/10              PAGE 0001

                    C--LISOLV------------------------------------------------------------LISOLV01
                    C--TDMA OF LINE-BY-LINE SOLUTION ------------------------------------LISOLV02
 0001                     SUBROUTINE LOSILV(ISTART,JSTART,NI,NJ,IT,JT,PHI,NSW,CAGE)
                    CHAPTER  0  0  0  0  0  0  0  0  PRELIMINARIES  0  0  0  0  0  0  0  0  LISOLV04
  -                 C                                                                    LISOLV05
 0002                     DIMENSION PHI(IT,JT),A(21),B(21),C(21),D(21)
 0003                     COMMON NITER
 0004                     COMMON                                                         LISOLV07
                         1/COEF/AP(20,20),AN(20,20),AS(20,20),AE(20,20),AW(20,20),
                         2        SU(20,20),SP(20,20)
 0005                     LOGICAL SKIP
 0006                     LOGICAL LEND
 0007                     SKIP=.FALSE.
 0008                     LEND=.FALSE.
 0009                     NIM1=NI-1                                                      LISOLV10
 0010                     NJM1=NJ-1                                                      LISOLV11
 0011                     JSTM1=JSTART-1                                                 LISOLV12
                    C                                                                    LISOLV13
                    C                                                                    LISOLV14
 0012                     A(JSTM1)=0.0                                                   LISOLV15
                    C-----COMMENCE W-E SWEEP                                             LISOLV16
 0013                     DO 100 I=ISTART,NIM1                                           LISOLV17
 0014                     C(JSTM1)=PHI(I,JSTM1)                                          LISOLV18
                    C-----COMMENCE S-N TRAVERSE                                          LISOLV19
 0015                     DO 101 J=JSTART,NJM1                                           LISOLV20
                    C-----ASSEMBLE TDMA COEFFICIENTS                                     LISOLV21
 0016                     A(J)=AN(I,J)                                                   LISOLV22
 0017                     B(J)=AS(I,J)                                                   LISOLV23
 0018                     C(J)=AE(I,J)*PHI (I+1,J)+AW(I,J)*PHI (I-1,J)+SU(I,J)           LISOLV24
 0019                     D(J)=AP(I,J)                                                   LISOLV25
 0020                     IF((D(J)-B(J)*A(J-1)).EQ.0.) SKIP=.TRUE.
 0021                     IF(.NOT.SKIP) GO TO 50
 0022                     WRITE(6,199) SKIP,I,J
 0023                 199 FORMAT(5X,'SKIP =',L2,'ON I=',I2,',J=',I2)
 0024                     LEND=.TRUE.
 0025                     GO TO 108
                    C-----CALCULATE COEFFICIENTS OF RECURRENCE FORMULA                   LISOLV26
 0026                  50 TERM=1./(D(J)-B(J)*A(J-1))
 0027                     A(J)=A(J)*TERM                                                 LISOLV28
 0028                     C(J)=(C(J)+B(J)*C(J-1))*TERM
 0029                     IF(.NOT.LEND) GO TO 108
 0030                     A(J-1)=A(J)
 0031                     C(J-1)=C(J)
 0032                     LEND=.FALSE.
 0033                 108 SKIP=.FALSE.
 0034                 101 CONTINUE
                    C-----OBTAIN NEW PHI'S                                               LISOLV30
 0035                     DO 102 JJ=JSTART,NJM1                                          LISOLV31
 0036                     J=NJ+JSTM1-JJ                                                  LISOLV32
 0037                 102 PHI(I,J)=A(J)*PHI(I,J+1)+C(J)                                  LISOLV33
 0038                 100 CONTINUE                                                       LISOLV34
 0039                     RETURN                                                         LISOLV35
 0040                     END                                                            LISOLV36
```

```
FORTRAN IV G1  RELEASE 2.0            LOSILV            DATE = 79037        23/48/10           PAGE 0002

 *OPTIONS IN EFFECT*  NOTERM,ID,EBCDIC,SOURCE,NOLIST,NODECK,LOAD,NOMAP,NOTEST
 *OPTIONS IN EFFECT*  NAME = LOSILV   , LINECNT =        56
 *STATISTICS*    SOURCE STATEMENTS =          40,PROGRAM SIZE =      1708
 *STATISTICS*  NO DIAGNOSTICS GENERATED
```

30

```
FORTRAN IV G1  RELEASE 2.0            MAIN                DATE = 79037        23/48/10            PAGE 0001
                   C-- PST ------------------------------------------------------------------PST00001
                   C--SATURATED VAPOR PRESSURE CALCULATION ---------------------------------PST00002
 0001                    FUNCTION PST(TEMP)                                                 PST00003
 0002                    COMMON /VAPP/ANTON1,ANTON2,ANTON3                                  PST00004
 0003                    PST=ANTON1-ANTON2/(TEMP+ANTON3)                                    PST00005
 0004                    PST=EXP(PST)                                                       PST00006
 0005                    RETURN                                                             PST00007
 0006                    END                                                                PST00008

  *OPTIONS IN EFFECT*  NOTERM,ID,EBCDIC,SOURCE,NOLIST,NODECK,LOAD,NOMAP,NOTEST
  *OPTIONS IN EFFECT*  NAME = PST      , LINECNT =        56
  *STATISTICS*     SOURCE STATEMENTS =          6,PROGRAM SIZE =       342
  *STATISTICS*  NO DIAGNOSTICS GENERATED
```

```
      C--PRINT------------------------------------------------------PRINT001
      C--PRINTING SUBPROGRAM -----------------------------------------PRINT002
            SUBROUTINE PRINT(ISTART,JSTART,NI,NJ,IT,JT,X,Y,PHI,HEAD)   PRINT003
            DIMENSION PHI(IT,JT),X(IT),Y(JT),HEAD(9),STORE(50)         PRINT004
        105 FORMAT(4H  I=,2X,'1',9X,'2',9X,'3',9X,'4',9X,'5',9X,'6',9X,'7',9X
           1      ,'8',9X,'9',8X,'10',8X,'11',10X,'Y =')
        106 FORMAT(4H  I=,' 12',8X,'13',8X,'14',8X,'15',8X,'16',8X,'17',8X,
           1      '18',8X,'19',8X,'20',8X,'21',8X,'22',10X,'Y =')
        107 FORMAT(4H  I=,' 23',8X,'24',8X,'25',8X,'26',10X,'Y =')
        165 FORMAT(4H  I=,2X,'3',9X,'4',9X,'5',9X,'6',9X,'7',9X,'8',
           1      9X,'9',8X,'10',8X,'11',8X,'12',8X,'13',10X,'Y =')
        166 FORMAT(4H  I=,' 14',8X,'15',8X,'16',8X,'17',8X,'18',8X,'19',
           1      8X,'  Y =')
            NIM1=NI-1
            NJM1=NJ-1
            ISKIP=1                                                    PRINT011
            JSKIP=1                                                    PRINT012
            WRITE(6,110)HEAD                                           PRINT013
            ISTA = ISTART-11
        100 CONTINUE                                                   PRINT015
            ISTA = ISTA+11
            IEND = ISTA+10
            IF(ISTA.EQ.14) IEND=NIM1
            IEND=MIN0(NI,IEND)                                         PRINT018
            IF(ISTA.EQ.1) WRITE(6,105)
            IF(ISTA.EQ.3) WRITE(6,165)
            IF(ISTA.EQ.12) WRITE(6,106)
            IF(ISTA.EQ.14) WRITE(6,166)
            IF(ISTA.EQ.23) WRITE(6,107)
            WRITE(6,112)                                               PRINT021
            IF(ISTA.EQ.3) GO TO 44
            IF(ISTA.EQ.14) GO TO 44
            DO 101 JJ=JSTART,NJ,JSKIP                                  PRINT022
            J=JSTART+NJ-JJ                                             PRINT023
            DO 120 I=ISTA,IEND                                         PRINT024
            A=PHI(I,J)                                                 PRINT025
            IF(ABS(A).LT.1.E-20) A=0.0                                 PRINT026
        120 STORE(I)=A                                                 PRINT027
        101 WRITE(6,113)  J,(STORE(I),I=ISTA,IEND,ISKIP),Y(J)          PRINT028
            WRITE(6,115)
            WRITE(6,114) (X(I),I=ISTA,IEND,ISKIP)                      PRINT029
            IF(IEND.LT.NI)GO TO 100                                    PRINT031
            RETURN                                                     PRINT032
         44 DO 161 JJ=JSTART,NJM1,JSKIP
            J=JSTART+NJM1-JJ
            DO 126 I=ISTA,IEND
            A=PHI(I,J)
            IF(ABS(A).LT.1.E-20) A=0.0
        126 STORE(I)=A
        161 WRITE(6,113)  J,(STORE(I),I=ISTA,IEND,ISKIP),Y(J)
            WRITE(6,115)
            WRITE(6,114) (X(I),I=ISTA,IEND,ISKIP)
            IF(IEND.LT.NIM1) GO TO 100
            RETURN
```

```
FORTRAN IV G1  RELEASE 2.0            PRINT              DATE = 79037          23/48/10                PAGE 0002

               110 FORMAT(1H1,///,1X,20(2H*-),7X,9A4,7X,20(2H-*))                              PRINT033
               112 FORMAT(3H  J)                                                               PRINT034
               113 FORMAT(1H ,I3,1P11E10.3,0PF10.4)
               114 FORMAT(4H X= ,11F10.7)
               115 FORMAT(' ')
                   END                                                                         PRINT037

  *OPTIONS IN EFFECT*  NOTERM,ID,EBCDIC,SOURCE,NOLIST,NODECK,LOAD,NOMAP,NOTEST
  *OPTIONS IN EFFECT*  NAME = PRINT    , LINECNT =        56
  *STATISTICS*    SOURCE STATEMENTS =        54,PROGRAM SIZE =      2446
  *STATISTICS*  NO DIAGNOSTICS GENERATED

  *STATISTICS*  NO DIAGNOSTICS THIS STEP
```

```
F64-LEVEL LINKAGE EDITOR OPTIONS SPECIFIED SIZE=(95K,14K)
          VARIABLE OPTIONS USED -   SIZE=(97280,14336)
          SYSPRINT DEFAULT BLOCKING USED   1 - 1
****MAIN      DOES NOT EXIST BUT HAS BEEN ADDED TO DATA SET.
AUTHORIZATION CODE IS         0.
```

APPENDIX B

LISTING OF COMPUTER OUTPUT

```
PULJET

SIMULTANEOUS HEAT & MASS TRANSFER UNDER AN IMPINGING JET

SCALAR GRID SYSTEM:  X-,  Y-      DIRECTION

-1.2537872E-05  1.2537872E-05  6.2069300E-05  1.6299234E-04  3.6359811E-04  7.6481001E-04  1.5672338E-03  3.1720814E-03
 6.3817762E-03  7.9866238E-03  8.7890476E-03  9.1902576E-03  9.3908608E-03  9.4911605E-03  9.5413104E-03  9.5663853E-03
 9.5789209E-03  9.5914565E-03  9.5977224E-03  9.6022338E-03

-1.5873094E-03  1.5873094E-03  4.7619268E-03  7.9365447E-03  1.1111163E-02  1.4285780E-02  1.6153201E-02  1.7251685E-02
 1.7897852E-02  1.8277947E-02  1.8501531E-02  1.8633053E-02  1.8710416E-02  1.8787779E-02  1.8942509E-02  1.9174606E-02
 1.9400702E-02  1.9638799E-02  1.9870896E-02  2.0025626E-02  2.0180356E-02  2.0257719E-02  2.0335082E-02  2.0412445E-02
 2.0489808E-02  2.0567171E-02  2.0721901E-02  2.0876631E-02  2.1108728E-02  2.1340825E-02  2.1572921E-02  2.1805018E-02
 2.1959748E-02  2.2037111E-02  2.2191841E-02  2.2389177E-02  2.2586513E-02  2.2783849E-02  2.2981185E-02  2.3178522E-02
 2.3544680E-02  2.3910839E-02  2.4276998E-02  2.5210708E-02  2.6144419E-02  2.9319037E-02  3.2493655E-02  3.5668273E-02
 3.8842890E-02  4.2017508E-02

      JET INLET CONDITIONS
           REYNOLDS NUMBER          1.000E+03
           AVERAGE VELOCITY         9.879E+00
           TEMPERATURE              4.500E+02
           PRESSURE                 1.013E+05
           MASS FRACTION OF A       1.000E-01
           MOLE FRACTION,A          0.152E+00

           PRANDTL NO               6.928E-01
           SCHMICT NO               6.261E-01

  CROSS FLOW INLET CONDITIONS
           REYNOLDS NUMBER          1.667E+02
           AVERAGE VELOCITY         4.803E-01
           TEMPERATURE              4.500E+02
           PRESSURE                 0.0
           MASS FRACTION OF A       1.000E-01

        CROSS MASS FLOW-RATE IS    10.00 % OF JET MASS FLOW RATE

      IMPINGEMENT WALL CONDITIONS
           TEMPERTURE               3.500E+02
           USUC/UIN                 0.0

      GEOMETRY OF SYSTEM
           JET RADIUS               1.600E-03
           H/D RATIO                3.000E+00
           NOZZLE FROM J                   14
                    TO J                   33
           IMPINGEMENT ANGLE        0.174532
```

```
PROGRAM CONDITIONS
        MAX ALLOW. ITER            200
        MAX ALLOW. TIME      9.000E+02
        MAX ALLOW. RESI      1.500E-02


     JET MASS FLOWIN          2.331540E-04
   JET X-MOMENTUM IN          2.731954E-03
   JET Y-MOMENTUM IN          8.418890E-05


  CROSS-FLOW MASS FLOW IN     3.474274E-05
CROSS-FLOW Y-MOMENTUM IN      1.677235E-05

   VARIABLE FIELD INITIALISED AS :
        MESSAGE DE PERFORATION:DATA# 163
```

ITER NO	I-----------ABSOLUTE RESIDUAL SOURCE SUMS---------I UMOM	VMOM	MASS	ENER	SPEC	I--FIELD VALUES AT MONITORING LOCATION(18,20)--I U	V	P	T	W	ALPHA	SPLIT RATE VINC
1	1.774E-02	1.236E-02	2.542E-02	1.060E-02	8.866E-03	-3.421E-02	-4.167E-01	7.227E+00	3.529E+02	2.965E-01	1.2340	6.054E-03
2	2.072E-02	1.274E-02	2.800E-02	8.908E-03	7.817E-03	-3.359E-02	-4.167E-01	7.186E+00	3.529E+02	2.965E-01	1.2340	3.198E-03
3	1.918E-02	1.210E-02	2.653E-02	8.908E-03	7.817E-03	-3.345E-02	-4.168E-01	7.166E+00	3.529E+02	2.965E-01	1.2340	4.312E-03
4	1.819E-02	1.191E-02	2.671E-02	8.908E-03	7.817E-03	-3.346E-02	-4.169E-01	7.147E+00	3.529E+02	2.965E-01	1.2340	3.937E-03
5	1.759E-02	1.188E-02	2.683E-02	8.908E-03	7.817E-03	-3.346E-02	-4.169E-01	7.128E+00	3.529E+02	2.965E-01	1.2340	4.129E-03
6	1.718E-02	1.188E-02	2.674E-02	8.908E-03	7.817E-03	-3.347E-02	-4.170E-01	7.108E+00	3.529E+02	2.965E-01	1.2340	4.129E-03
7	1.687E-02	1.187E-02	2.663E-02	8.908E-03	7.817E-03	-3.347E-02	-4.170E-01	7.089E+00	3.529E+02	2.965E-01	1.2340	4.126E-03
8	1.671E-02	1.180E-02	2.644E-02	8.908E-03	7.817E-03	-3.348E-02	-4.171E-01	7.068E+00	3.529E+02	2.965E-01	1.2340	4.126E-03
9	1.663E-02	1.171E-02	2.638E-02	8.908E-03	7.817E-03	-3.349E-02	-4.171E-01	7.047E+00	3.529E+02	2.965E-01	1.2340	4.123E-03
10	1.657E-02	1.165E-02	2.616E-02	8.908E-03	7.817E-03	-3.349E-02	-4.172E-01	7.026E+00	3.529E+02	2.965E-01	1.2340	4.123E-03
11	1.651E-02	1.166E-02	2.593E-02	8.908E-03	7.817E-03	-3.350E-02	-4.172E-01	7.004E+00	3.529E+02	2.965E-01	1.2340	4.129E-03
12	1.642E-02	1.171E-02	2.570E-02	7.959E-03	7.122E-03	-3.350E-02	-4.173E-01	6.981E+00	3.529E+02	2.965E-01	1.2340	4.126E-03
13	1.638E-02	1.177E-02	2.549E-02	7.959E-03	7.122E-03	-3.339E-02	-4.173E-01	6.955E+00	3.529E+02	2.965E-01	1.2340	4.272E-03
14	1.657E-02	1.192E-02	2.530E-02	7.959E-03	7.122E-03	-3.340E-02	-4.174E-01	6.931E+00	3.529E+02	2.965E-01	1.2340	3.983E-03
15	1.638E-02	1.204E-02	2.478E-02	7.959E-03	7.122E-03	-3.340E-02	-4.174E-01	6.907E+00	3.529E+02	2.965E-01	1.2340	4.123E-03
16	1.623E-02	1.218E-02	2.428E-02	7.959E-03	7.122E-03	-3.341E-02	-4.174E-01	6.884E+00	3.529E+02	2.965E-01	1.2340	4.123E-03
17	1.615E-02	1.234E-02	2.370E-02	7.959E-03	7.122E-03	-3.341E-02	-4.174E-01	6.861E+00	3.529E+02	2.965E-01	1.2340	4.123E-03
18	1.613E-02	1.251E-02	2.308E-02	7.959E-03	7.122E-03	-3.342E-02	-4.175E-01	6.839E+00	3.529E+02	2.965E-01	1.2340	4.123E-03
19	1.613E-02	1.267E-02	2.242E-02	7.959E-03	7.122E-03	-3.342E-02	-4.175E-01	6.817E+00	3.529E+02	2.965E-01	1.2340	4.126E-03
20	1.613E-02	1.284E-02	2.175E-02	7.959E-03	7.122E-03	-3.343E-02	-4.175E-01	6.795E+00	3.529E+02	2.965E-01	1.2340	4.123E-03
21	1.613E-02	1.300E-02	2.105E-02	7.959E-03	7.122E-03	-3.343E-02	-4.175E-01	6.774E+00	3.529E+02	2.965E-01	1.2340	4.123E-03
22	1.614E-02	1.316E-02	2.031E-02	7.351E-03	6.518E-03	-3.344E-02	-4.175E-01	6.753E+00	3.529E+02	2.965E-01	1.2340	4.123E-03
23	1.619E-02	1.330E-02	1.963E-02	7.351E-03	6.518E-03	-3.335E-02	-4.175E-01	6.731E+00	3.529E+02	2.965E-01	1.2340	4.250E-03
24	1.645E-02	1.343E-02	1.903E-02	7.351E-03	6.518E-03	-3.335E-02	-4.175E-01	6.711E+00	3.529E+02	2.965E-01	1.2340	4.002E-03
25	1.636E-02	1.351E-02	1.814E-02	7.351E-03	6.518E-03	-3.336E-02	-4.175E-01	6.691E+00	3.529E+02	2.965E-01	1.2340	4.119E-03
26	1.631E-02	1.359E-02	1.725E-02	7.351E-03	6.518E-03	-3.336E-02	-4.175E-01	6.674E+00	3.529E+02	2.965E-01	1.2340	4.110E-03
27	1.630E-02	1.366E-02	1.635E-02	7.351E-03	6.518E-03	-3.336E-02	-4.175E-01	6.657E+00	3.529E+02	2.965E-01	1.2340	4.113E-03
28	1.631E-02	1.367E-02	1.543E-02	7.351E-03	6.518E-03	-3.337E-02	-4.175E-01	6.642E+00	3.529E+02	2.965E-01	1.2340	4.123E-03
29	1.633E-02	1.367E-02	1.450E-02	7.351E-03	6.518E-03	-3.337E-02	-4.175E-01	6.628E+00	3.529E+02	2.965E-01	1.2340	4.110E-03
30	1.635E-02	1.364E-02	1.355E-02	7.351E-03	6.518E-03	-3.337E-02	-4.175E-01	6.615E+00	3.529E+02	2.965E-01	1.2340	4.113E-03
31	1.636E-02	1.357E-02	1.259E-02	7.351E-03	6.518E-03	-3.338E-02	-4.175E-01	6.603E+00	3.529E+02	2.965E-01	1.2340	4.110E-03
32	1.638E-02	1.348E-02	1.163E-02	7.159E-03	6.129E-03	-3.338E-02	-4.174E-01	6.593E+00	3.529E+02	2.965E-01	1.2340	4.116E-03
33	1.639E-02	1.337E-02	1.081E-02	7.159E-03	6.129E-03	-3.331E-02	-4.174E-01	6.581E+00	3.529E+02	2.965E-01	1.2340	4.217E-03
34	1.649E-02	1.327E-02	1.013E-02	7.159E-03	6.129E-03	-3.331E-02	-4.174E-01	6.574E+00	3.529E+02	2.965E-01	1.2340	4.100E-03
35	1.637E-02	1.312E-02	9.750E-03	7.159E-03	6.129E-03	-3.331E-02	-4.174E-01	6.565E+00	3.529E+02	2.965E-01	1.2340	4.048E-03
36	1.627E-02	1.296E-02	9.372E-03	7.159E-03	6.129E-03	-3.331E-02	-4.173E-01	6.559E+00	3.529E+02	2.965E-01	1.2340	4.109E-03
37	1.619E-02	1.281E-02	9.214E-03	7.159E-03	6.129E-03	-3.331E-02	-4.173E-01	6.556E+00	3.529E+02	2.965E-01	1.2340	4.106E-03
38	1.611E-02	1.263E-02	9.150E-03	7.159E-03	6.129E-03	-3.332E-02	-4.172E-01	6.552E+00	3.529E+02	2.965E-01	1.2340	4.106E-03
39	1.603E-02	1.245E-02	9.204E-03	7.159E-03	6.129E-03	-3.332E-02	-4.172E-01	6.549E+00	3.529E+02	2.965E-01	1.2340	4.106E-03
40	1.593E-02	1.224E-02	9.377E-03	7.159E-03	6.129E-03	-3.332E-02	-4.171E-01	6.548E+00	3.529E+02	2.965E-01	1.2340	4.106E-03
41	1.580E-02	1.200E-02	9.643E-03	7.159E-03	6.129E-03	-3.332E-02	-4.171E-01	6.548E+00	3.529E+02	2.965E-01	1.2340	4.109E-03
42	1.568E-02	1.176E-02	9.969E-03	7.148E-03	5.770E-03	-3.332E-02	-4.170E-01	6.549E+00	3.529E+02	2.965E-01	1.2340	4.106E-03
43	1.558E-02	1.149E-02	1.041E-02	7.148E-03	5.770E-03	-3.328E-02	-4.170E-01	6.549E+00	3.529E+02	2.965E-01	1.2340	4.207E-03
44	1.557E-02	1.121E-02	1.074E-02	7.148E-03	5.770E-03	-3.328E-02	-4.169E-01	6.550E+00	3.529E+02	2.965E-01	1.2340	4.096E-03
45	1.532E-02	1.094E-02	1.107E-02	7.148E-03	5.770E-03	-3.328E-02	-4.169E-01	6.553E+00	3.529E+02	2.965E-01	1.2340	4.093E-03
46	1.509E-02	1.065E-02	1.139E-02	7.148E-03	5.770E-03	-3.328E-02	-4.168E-01	6.557E+00	3.529E+02	2.965E-01	1.2340	4.100E-03
47	1.493E-02	1.035E-02	1.176E-02	7.148E-03	5.770E-03	-3.327E-02	-4.168E-01	6.562E+00	3.529E+02	2.965E-01	1.2340	4.100E-03

OVERALL MASS EVAPUTATION = -6.293779E-C6
OVERALL MASS OUTFLOW = 2.741902E-04
NET MASS ACCUMUL. = 0.0

OUTPUT PUNCH = T

J \ I=	1	2	3	4	5	6	7	8	9	10	11	Y =
50	0.0	0.0	-4.858E-05	-1.457E-04	-3.393E-04	-7.239E-04	-1.487E-03	-2.978E-03	-6.192E-03	-9.343E-03	-1.110E-02	0.0420
49	0.0	0.0	-4.858E-05	-1.457E-04	-3.392E-04	-7.244E-04	-1.489E-03	-2.979E-03	-6.179E-03	-9.326E-03	-1.108E-02	0.0388
48	0.0	0.0	-6.531E-05	-6.954E-04	-3.729E-03	-1.427E-02	-3.059E-02	-2.509E-02	-4.102E-02	-7.649E-02	-1.052E-01	0.0357
47	0.0	0.0	-4.251E-04	-4.367E-03	-2.191E-02	-7.221E-02	-1.281E-01	-6.256E-02	1.575E-02	-5.422E-02	-1.171E-01	0.0325
46	0.0	0.0	-1.780E-03	-1.749E-02	-8.091E-02	-2.354E-01	-4.167E-01	-3.956E-01	2.455E-01	1.664E-01	-4.344E-03	0.0293
45	0.0	0.0	-2.175E-03	-1.887E-02	-7.401E-02	-2.154E-01	-5.987E-01	-1.486E+00	1.097E+00	1.003E+00	4.743E-01	0.0261
44	0.0	0.0	6.143E-03	5.022E-02	1.617E-01	2.368E-01	2.406E-01	1.872E-01	2.879E+00	2.504E+00	1.454E+00	0.0252
43	0.0	0.0	7.366E-03	6.466E-02	2.400E-01	4.278E-01	6.961E-01	2.037E+00	4.235E+00	3.531E+00	2.108E+00	0.0243
42	0.0	0.0	1.517E-03	2.941E-02	2.300E-01	4.847E-01	8.109E-01	3.260E+00	5.364E+00	4.349E+00	2.648E+00	0.0239
41	0.0	0.0	3.072E-03	3.468E-02	2.036E-01	4.719E-01	7.332E-01	4.017E+00	6.044E+00	4.802E+00	2.927E+00	0.0235
40	0.0	0.0	3.841E-03	3.866E-02	1.920E-01	4.388E-01	5.168E-01	4.853E+00	6.729E+00	5.243E+00	3.213E+00	0.0232
39	0.0	0.0	2.474E-03	2.756E-02	1.523E-01	4.540E-01	4.273E-01	5.665E+00	7.236E+00	5.530E+00	3.396E+00	0.0230
38	0.0	0.0	3.250E-03	3.189E-02	1.441E-01	5.216E-01	6.251E-01	6.366E+00	7.573E+00	5.688E+00	3.492E+00	0.0228
37	0.0	0.0	4.536E-03	3.712E-02	1.203E-01	6.440E-01	2.073E+00	7.188E+00	7.880E+00	5.805E+00	3.562E+00	0.0226
36	0.0	0.0	1.066E-03	1.829E-03	-2.083E-02	6.232E-01	4.169E+00	8.099E+00	8.140E+00	5.867E+00	3.595E+00	0.0224
35	0.0	0.0	-1.734E-02	-1.186E-01	-2.829E-01	5.756E-02	5.557E+00	8.991E+00	8.334E+00	5.860E+00	3.581E+00	0.0222
34	0.0	0.0	5.721E-04	-2.100E-02	-1.102E-01	9.655E-01	6.850E+00	9.765E+00	8.432E+00	5.780E+00	3.524E+00	0.0220
33	0.0	6.869E-01	7.179E-01	7.661E-01	9.488E-01	3.573E+00	7.941E+00	1.025E+01	8.441E+00	5.679E+00	3.473E+00	0.0220
32	0.0	3.268E+00	3.371E+00	3.633E+00	4.349E+00	6.146E+00	9.013E+00	1.068E+01	8.414E+00	5.548E+00	3.417E+00	0.0218
31	0.0	6.643E+00	6.745E+00	6.969E+00	7.475E+00	8.590E+00	1.046E+01	1.131E+01	8.298E+00	5.260E+00	3.254E+00	0.0216
30	0.0	9.423E+00	9.605E+00	9.677E+00	1.004E+01	1.078E+01	1.189E+01	1.187E+01	8.003E+00	4.763E+00	2.920E+00	0.0213
29	0.0	1.161E+01	1.167E+01	1.180E+01	1.205E+01	1.249E+01	1.298E+01	1.216E+01	7.512E+00	4.096E+00	2.457E+00	0.0211
28	0.0	1.319E+01	1.325E+01	1.333E+01	1.347E+01	1.367E+01	1.368E+01	1.213E+01	6.818E+00	3.275E+00	1.899E+00	0.0209
27	0.0	1.392E+01	1.396E+01	1.402E+01	1.412E+01	1.421E+01	1.391E+01	1.181E+01	6.093E+00	2.527E+00	1.479E+00	0.0207
26	0.0	1.439E+01	1.441E+01	1.444E+01	1.448E+01	1.446E+01	1.388E+01	1.135E+01	5.442E+00	1.948E+00	1.195E+00	0.0206
25	0.0	1.452E+01	1.453E+01	1.455E+01	1.457E+01	1.447E+01	1.369E+01	1.088E+01	4.932E+00	1.557E+00	1.019E+00	0.0205
24	0.0	1.458E+01	1.459E+01	1.460E+01	1.459E+01	1.441E+01	1.349E+01	1.051E+01	4.594E+00	1.330E+00	8.668E-01	0.0204
23	0.0	1.458E+01	1.458E+01	1.458E+01	1.454E+01	1.428E+01	1.322E+01	1.010E+01	4.258E+00	1.126E+00	7.351E-01	0.0203
22	0.0	1.452E+01	1.451E+01	1.450E+01	1.441E+01	1.407E+01	1.289E+01	9.656E+00	3.928E+00	9.471E-01	6.219E-01	0.0203
21	0.0	1.439E+01	1.437E+01	1.433E+01	1.420E+01	1.378E+01	1.250E+01	9.179E+00	3.607E+00	7.931E-01	4.809E-01	0.0202
20	0.0	1.392E+01	1.390E+01	1.385E+01	1.370E+01	1.321E+01	1.182E+01	8.393E+00	3.128E+00	5.883E-01	3.401E-01	0.0200
19	0.0	1.319E+01	1.316E+01	1.308E+01	1.285E+01	1.224E+01	1.071E+01	7.214E+00	2.518E+00	3.746E-01	2.106E-01	0.0199
18	0.0	1.161E+01	1.156E+01	1.145E+01	1.120E+01	1.055E+01	8.997E+00	5.567E+00	1.854E+00	2.057E-01	9.958E-02	0.0196
17	0.0	9.423E+00	9.357E+00	9.216E+00	8.900E+00	8.185E+00	6.558E+00	3.486E+00	1.284E+00	1.176E-01	1.769E-02	0.0194
16	0.0	6.643E+00	6.560E+00	6.386E+00	6.025E+00	5.293E+00	3.647E+00	1.759E+00	1.013E+00	1.098E-01	-4.716E-02	0.0192
15	0.0	3.268E+00	3.156E+00	2.947E+00	2.565E+00	1.860E+00	6.044E-01	9.680E-01	9.138E-01	1.250E-01	-9.546E-02	0.0189
14	0.0	6.869E-01	5.194E-01	2.716E-01	1.607E-02	-1.172E-01	4.734E-03	8.698E-01	8.699E-01	1.441E-01	-1.204E-01	0.0188
13	0.0	0.0	8.340E-03	7.516E-03	-1.134E-01	-2.983E-01	5.747E-02	8.240E-01	8.497E-01	1.650E-01	-1.326E-01	0.0187
12	0.0	0.0	-1.124E-02	-5.400E-02	-1.656E-01	-3.435E-01	9.643E-02	7.949E-01	8.404E-01	1.856E-01	-1.383E-01	0.0186
11	0.0	0.0	-5.273E-03	-4.388E-02	-1.550E-01	-3.102E-01	1.379E-01	7.578E-01	8.244E-01	2.066E-01	-1.383E-01	0.0185
10	0.0	0.0	-1.239E-03	-1.329E-02	-6.560E-02	-1.770E-01	1.775E-01	7.013E-01	7.915E-01	2.274E-01	-1.337E-01	0.0183
9	0.0	0.0	2.838E-04	2.002E-03	3.039E-03	-2.703E-02	2.209E-01	6.228E-01	7.334E-01	2.466E-01	-1.276E-01	0.0179
8	0.0	0.0	4.469E-04	4.570E-03	2.299E-02	8.105E-02	2.555E-01	5.238E-01	6.406E-01	2.607E-01	-1.202E-01	0.0173
7	0.0	0.0	4.565E-04	4.949E-03	2.755E-02	1.161E-01	2.473E-01	4.058E-01	5.033E-01	2.585E-01	-1.159E-01	0.0162
6	0.0	0.0	4.512E-04	4.650E-03	2.377E-02	8.693E-02	1.727E-01	2.542E-01	3.008E-01	1.839E-01	-1.919E-01	0.0143
5	7.939E-03	0.0	2.897E-04	2.901E-03	1.404E-02	4.483E-02	6.984E-02	4.880E-02	-5.821E-02	-2.970E-01	-2.919E-01	0.0111
4	7.939E-03	0.0	-3.622E-05	-4.447E-04	-2.972E-03	-1.729E-02	-8.031E-02	-2.391E-01	-4.999E-01	-5.513E-01	-3.968E-01	0.0079
3	7.939E-03	0.0	-3.024E-04	-3.147E-03	-1.632E-02	-6.180E-02	-1.766E-01	-3.880E-01	-6.864E-01	-6.787E-01	-3.975E-01	0.0048
2	7.939E-03	0.0	5.072E-03	1.211E-02	1.553E-02	-7.351E-03	-9.795E-02	-2.757E-01	-5.348E-01	-5.263E-01	-2.091E-01	0.0016
1	7.939E-03	0.0	0.0	0.0	0.0	0.0	0.0	0.0	0.0	0.0	0.0	-0.0016
X=	0.0	0.0	0.0000376	0.0001128	0.0002633	0.0005642	0.0011660	0.0023697	0.0047769	0.0071842	0.0083878	

J \ I=	12	13	14	15	16	17	18	19	20	21	22	Y =
50	-1.298E-02	-1.484E-02	-1.490E-02	-1.475E-02	-1.466E-02	-1.460E-02	-1.457E-02	-1.454E-02	-1.453E-02	4.202E-02		
49	-1.298E-02	-1.484E-02	-1.490E-02	-1.475E-02	-1.466E-02	-1.460E-02	-1.457E-02	-1.454E-02	-1.453E-02	3.884E-02		
48	-1.053E-01	-6.470E-02	-3.149E-02	-2.040E-02	-1.710E-02	-1.609E-02	-1.564E-02	-1.548E-02	-1.544E-02	3.567E-02		
47	-1.347E-01	-9.620E-02	-4.714E-02	-2.731E-02	-2.100E-02	-1.903E-02	-1.815E-02	-1.784E-02	-1.778E-02	3.249E-02		
46	[illegible]	[illegible]	[illegible]	[illegible]	[illegible]	[illegible]	[illegible]	[illegible]	[illegible]	[illegible]		

46	[illegible]	[illegible]	[illegible]	[illegible]	[illegible]	[illegible]	[illegible]	[illegible]	[illegible]	[illegible]
45	9.527E-02	-7.483E-02	-8.085E-02	-5.193E-02	-3.720E-02	-3.173E-02	-2.913E-02	-2.817E-02	-2.798E-02	2.614E-02
44	6.873E-01	2.475E-01	4.980E-02	-1.170E-02	-2.897E-02	-3.394E-02	-3.594E-02	-3.643E-02	-3.643E-02	2.521E-02
43	1.040E+00	4.017E-01	8.716E-02	-1.149E-02	-3.353E-02	-3.831E-02	-3.983E-02	-4.000E-02	-3.993E-02	2.428E-02
42	1.376E+00	6.144E-01	2.103E-01	4.007E-02	-1.663E-02	-3.423E-02	-4.174E-02	-4.393E-02	-4.416E-02	2.391E-02
41	1.533E+00	7.016E-01	2.574E-01	6.055E-02	-9.597E-03	-3.233E-02	-4.225E-02	-4.526E-02	-4.563E-02	2.354E-02
40	1.702E+00	7.766E-01	2.695E-01	5.409E-02	-1.493E-02	-3.542E-02	-4.390E-02	-4.629E-02	-4.653E-02	2.318E-02
39	1.824E+00	8.635E-01	3.329E-01	8.648E-02	-2.773E-03	-3.171E-02	-4.433E-02	-4.819E-02	-4.867E-02	2.298E-02
38	1.890E+00	9.133E-01	3.654E-01	1.014E-01	2.174E-03	-3.044E-02	-4.474E-02	-4.913E-02	-4.969E-02	2.278E-02
37	1.944E+00	9.695E-01	4.149E-01	1.144E-01	4.712E-03	-3.034E-02	-4.550E-02	-5.010E-02	-5.069E-02	2.259E-02
36	1.975E+00	1.003E+00	3.868E-01	1.017E-01	1.044E-03	-3.119E-02	-4.515E-02	-4.937E-02	-4.989E-02	2.239E-02
35	1.956E+00	9.014E-01	3.219E-01	8.158E-02	-4.023E-03	-3.177E-02	-4.388E-02	-4.757E-02	-4.802E-02	2.219E-02
34	1.883E+00	8.520E-01	3.153E-01	8.686E-02	6.711E-04	-2.910E-02	-4.263E-02	-4.698E-02	-4.756E-02	2.204E-02
33	1.886E+00	8.869E-01	3.269E-01	7.068E-02	-1.191E-02	-3.517E-02	-4.431E-02	-4.665E-02	-4.687E-02	2.196E-02
32	1.842E+00	8.688E-01	3.221E-01	7.880E-02	-4.798E-03	-3.135E-02	-4.284E-02	-4.630E-02	-4.673E-02	2.181E-02
31	1.699E+00	7.764E-01	2.779E-01	6.561E-02	-8.186E-03	-3.200E-02	-4.239E-02	-4.555E-02	-4.593E-02	2.157E-02
30	1.504E+00	6.645E-01	2.138E-01	3.654E-02	-1.891E-02	-3.542E-02	-4.227E-02	-4.418E-02	-4.436E-02	2.134E-02
29	1.232E+00	5.138E-01	1.350E-01	4.276E-03	-2.972E-02	-3.839E-02	-4.161E-02	-4.230E-02	-4.229E-02	2.111E-02
28	9.495E-01	3.668E-01	7.221E-02	-1.550E-02	-3.459E-02	-3.890E-02	-4.035E-02	-4.055E-02	-4.048E-02	2.088E-02
27	7.371E-01	2.481E-01	5.799E-03	-4.743E-02	-4.687E-02	-4.294E-02	-4.026E-02	-3.895E-02	-3.864E-02	2.072E-02
26	5.887E-01	1.635E-01	-2.417E-02	-5.291E-02	-4.647E-02	-4.163E-02	-3.886E-02	-3.764E-02	-3.736E-02	2.057E-02
25	5.024E-01	1.092E-01	-6.050E-02	-7.068E-02	-5.246E-02	-4.333E-02	-3.861E-02	-3.676E-02	-3.638E-02	2.049E-02
24	4.213E-01	5.669E-02	-9.028E-02	-8.177E-02	-5.581E-02	-4.402E-02	-3.806E-02	-3.579E-02	-3.535E-02	2.041E-02
23	3.465E-01	7.105E-03	-1.161E-01	-8.961E-02	-5.750E-02	-4.393E-02	-3.725E-02	-3.478E-02	-3.431E-02	2.034E-02
22	2.786E-01	-3.891E-02	-1.398E-01	-9.582E-02	-5.847E-02	-4.357E-02	-3.637E-02	-3.377E-02	-3.329E-02	2.026E-02
21	1.860E-01	-1.035E-01	-1.749E-01	-1.017E-01	-5.778E-02	-4.201E-02	-3.477E-02	-3.229E-02	-3.184E-02	2.018E-02
20	7.478E-02	-1.595E-01	-1.826E-01	-1.003E-01	-5.701E-02	-4.090E-02	-3.327E-02	-3.057E-02	-3.009E-02	2.003E-02
19	-3.471E-02	-2.178E-01	-1.963E-01	-9.432E-02	-5.137E-02	-3.709E-02	-3.071E-02	-2.859E-02	-2.821E-02	1.987E-02
18	-1.292E-01	-2.445E-01	-1.850E-01	-8.688E-02	-4.781E-02	-3.463E-02	-2.865E-02	-2.662E-02	-2.627E-02	1.964E-02
17	-1.927E-01	-2.573E-01	-1.717E-01	-7.648E-02	-4.227E-02	-3.135E-02	-2.653E-02	-2.494E-02	-2.466E-02	1.941E-02
16	-2.324E-01	-2.584E-01	-1.555E-01	-6.758E-02	-3.800E-02	-2.884E-02	-2.486E-02	-2.355E-02	-2.332E-02	1.917E-02
15	-2.504E-01	-2.469E-01	-1.419E-01	-6.467E-02	-3.702E-02	-2.796E-02	-2.390E-02	-2.253E-02	-2.229E-02	1.894E-02
14	-2.587E-01	-2.426E-01	-1.330E-01	-6.108E-02	-3.562E-02	-2.715E-02	-2.331E-02	-2.199E-02	-2.175E-02	1.879E-02
13	-2.630E-01	-2.456E-01	-1.228E-01	-4.863E-02	-2.871E-02	-2.386E-02	-2.209E-02	-2.162E-02	-2.154E-02	1.871E-02
12	-2.682E-01	-2.498E-01	-1.121E-01	-4.190E-02	-2.623E-02	-2.278E-02	-2.157E-02	-2.124E-02	-2.117E-02	1.863E-02
11	-2.745E-01	-2.494E-01	-1.049E-01	-4.388E-02	-2.764E-02	-2.306E-02	-2.113E-02	-2.050E-02	-2.038E-02	1.850E-02
10	-2.762E-01	-2.377E-01	-9.339E-02	-4.156E-02	-2.642E-02	-2.188E-02	-1.992E-02	-1.927E-02	-1.915E-02	1.828E-02
9	-2.613E-01	-2.068E-01	-7.455E-02	-3.435E-02	-2.291E-02	-1.952E-02	-1.805E-02	-1.757E-02	-1.748E-02	1.790E-02
8	-2.241E-01	-1.585E-01	-5.501E-02	-2.674E-02	-1.900E-02	-1.673E-02	-1.576E-02	-1.544E-02	-1.538E-02	1.725E-02
7	-1.798E-01	-1.071E-01	-3.923E-02	-2.062E-02	-1.548E-02	-1.397E-02	-1.331E-02	-1.309E-02	-1.305E-02	1.615E-02
6	-1.725E-01	-7.865E-02	-3.047E-02	-1.640E-02	-1.237E-02	-1.116E-02	-1.063E-02	-1.046E-02	-1.043E-02	1.429E-02
5	-1.820E-01	-6.975E-02	-2.622E-02	-1.323E-02	-9.476E-03	-8.352E-03	-7.869E-03	-7.712E-03	-7.685E-03	1.111E-02
4	-2.061E-01	-6.166E-02	-2.030E-02	-9.339E-03	-6.372E-03	-5.519E-03	-5.161E-03	-5.049E-03	-5.031E-03	7.937E-03
3	-1.751E-01	-3.705E-02	-1.259E-02	-7.228E-03	-5.913E-03	-5.559E-03	-5.416E-03	-5.374E-03	-5.367E-03	4.762E-03
2	1.244E-03	-2.323E-02	-2.653E-02	-2.342E-02	-2.042E-02	-1.858E-02	-1.737E-02	-1.645E-02	-1.591E-02	1.587E-03
1	0.0	0.0	0.0	0.0	0.0	0.0	0.0	0.0	0.0	-1.587E-03
X=	0.0089897	0.0092906	0.0094410	0.0095162	0.0095538	0.0095727	0.0095852	0.0095946	0.0096000	

--*-*-*-*-*-*-*-*-*-*-*-*-*-*-*-*-*-   VVVVVVVVVVVVVVVVVVVVVVVVVVVVVVVVVVVVVVVVVV   -*-*-*-*-*-*-*-*-*-*-*-*-*-*-*-*-*-*-*-

J \ I=	1	2	3	4	5	6	7	8	9	10	11	Y =
50	0.0	-2.671E-02	-1.466E-01	-3.730E-01	-7.698E-01	-1.321E+00	-1.507E+00	5.461E-01	7.036E+00	9.459E+00	1.028E+01	0.0404
49	0.0	-3.081E-02	-1.507E-01	-3.771E-01	-7.739E-01	-1.325E+00	-1.511E+00	5.418E-01	7.031E+00	9.454E+00	1.028E+01	0.0373
48	0.0	-3.631E-02	-1.772E-01	-4.408E-01	-8.841E-01	-1.410E+00	-1.495E+00	5.258E-01	6.985E+00	9.379E+00	1.028E+01	0.0341
47	0.0	-7.218E-02	-3.435E-01	-8.107E-01	-1.414E+00	-1.702E+00	-1.320E+00	6.341E-01	6.893E+00	9.214E+00	1.020E+01	0.0309
46	0.0	-2.225E-01	-1.006E+00	-2.149E+00	-3.044E+00	-2.657E+00	-1.263E+00	1.483E+00	6.789E+00	8.764E+00	9.735E+00	0.0277
45	0.0	-3.412E-01	-1.462E+00	-2.902E+00	-4.009E+00	-3.966E+00	-2.777E+00	3.688E+00	6.711E+00	7.862E+00	8.448E+00	0.0257
44	0.0	-1.887E-01	-9.150E-01	-2.210E+00	-3.776E+00	-3.960E+00	-2.818E+00	4.733E+00	6.566E+00	7.046E+00	7.259E+00	0.0247
43	0.0	-6.145E-02	-4.199E-01	-1.453E+00	-3.370E+00	-3.670E+00	-2.094E+00	5.328E+00	6.375E+00	6.278E+00	6.111E+00	0.0241
42	0.0	-4.607E-02	-2.841E-01	-9.643E-01	-3.060E+00	-3.472E+00	-1.349E+00	5.650E+00	6.221E+00	5.760E+00	5.337E+00	0.0237
41	0.0	-1.675E-02	-1.302E-01	-5.531E-01	-2.733E+00	-3.313E+00	-3.485E-01	5.960E+00	6.032E+00	5.189E+00	4.489E+00	0.0234
40	0.0	1.202E-02	2.025E-04	-2.658E-01	-2.502E+00	-3.276E+00	6.679E-01	6.181E+00	5.857E+00	4.713E+00	3.781E+00	0.0231
39	0.0	2.500E-02	6.600E-02	-1.022E-01	-2.304E+00	-3.285E+00	1.527E+00	6.311E+00	5.717E+00	4.362E+00	3.265E+00	0.0229
38	0.0	4.204E-02	1.411E-01	4.494E-02	-2.057E+00	-3.251E+00	2.469E+00	6.411E+00	5.562E+00	4.001E+00	2.739E+00	0.0227
37	0.0	6.582E-02	2.265E-01	1.538E-01	-1.713E+00	-2.783E+00	3.308E+00	6.469E+00	5.391E+00	3.632E+00	2.208E+00	0.0225
36	0.0	7.136E-02	2.283E-01	1.236E-01	-1.291E+00	-1.620E+00	3.953E+00	6.474E+00	5.204E+00	3.259E+00	1.675E+00	0.0223
35	0.0	-9.823E-03	-9.078E-03	-6.926E-02	-1.092E+00	-1.189E-02	4.456E+00	6.428E+00	5.022E+00	2.924E+00	1.197E+00	0.0221
34	0.0	-8.125E-03	-4.273E-02	-1.390E-01	-6.778E-01	1.122E+00	4.737E+00	6.364E+00	4.893E+00	2.704E+00	8.779E-01	0.0220
33	1.211E-01	8.714E-02	3.078E-02	5.935E-04	3.334E-01	1.964E+00	4.960E+00	6.279E+00	4.759E+00	2.490E+00	5.668E-01	0.0219
32	5.762E-01	6.169E-01	7.046E-01	9.195E-01	1.488E+00	2.885E+00	5.230E+00	6.099E+00	4.528E+00	2.146E+00	5.533E-02	0.0217
31	1.171E+00	1.244E+00	1.393E+00	1.701E+00	2.348E+00	3.605E+00	5.397E+00	5.810E+00	4.234E+00	1.758E+00	-5.498E-01	0.0215
30	1.661E+00	1.749E+00	1.924E+00	2.267E+00	2.919E+00	4.032E+00	5.396E+00	5.440E+00	3.919E+00	1.400E+00	-1.100E+00	0.0212
29	2.047E+00	2.140E+00	2.319E+00	2.654E+00	3.258E+00	4.223E+00	5.240E+00	4.995E+00	3.587E+00	1.082E+00	-1.576E+00	0.0210
28	2.327E+00	2.397E+00	2.542E+00	2.835E+00	3.385E+00	4.227E+00	4.994E+00	4.570E+00	3.299E+00	8.590E-01	-1.883E+00	0.0208
27	2.455E+00	2.528E+00	2.669E+00	2.939E+00	3.431E+00	4.150E+00	4.726E+00	4.203E+00	3.067E+00	7.245E-01	-2.075E+00	0.0206
26	2.537E+00	2.596E+00	2.721E+00	2.971E+00	3.420E+00	4.040E+00	4.484E+00	3.919E+00	2.897E+00	6.541E-01	-2.193E+00	0.0205
25	2.560E+00	2.622E+00	2.744E+00	2.980E+00	3.392E+00	3.940E+00	4.305E+00	3.728E+00	2.787E+00	6.240E-01	-2.260E+00	0.0205
24	2.572E+00	2.633E+00	2.752E+00	2.975E+00	3.347E+00	3.821E+00	4.114E+00	3.538E+00	2.682E+00	5.989E-01	-2.318E+00	0.0204
23	2.572E+00	2.632E+00	2.747E+00	2.953E+00	3.280E+00	3.685E+00	3.915E+00	3.350E+00	2.581E+00	5.788E-01	-2.368E+00	0.0203
22	2.560E+00	2.621E+00	2.729E+00	2.911E+00	3.192E+00	3.532E+00	3.709E+00	3.166E+00	2.485E+00	5.631E-01	-2.411E+00	0.0202
21	2.537E+00	2.579E+00	2.661E+00	2.810E+00	3.031E+00	3.285E+00	3.391E+00	2.897E+00	2.349E+00	5.390E-01	-2.467E+00	0.0201
20	2.455E+00	2.494E+00	2.557E+00	2.653E+00	2.781E+00	2.927E+00	2.955E+00	2.559E+00	2.185E+00	5.138E-01	-2.534E+00	0.0199
19	2.327E+00	2.330E+00	2.338E+00	2.356E+00	2.389E+00	2.437E+00	2.399E+00	2.160E+00	2.012E+00	4.948E-01	-2.612E+00	0.0198
18	2.047E+00	2.034E+00	2.008E+00	1.961E+00	1.894E+00	1.838E+00	1.743E+00	1.819E+00	1.852E+00	4.819E-01	-2.700E+00	0.0195
17	1.661E+00	1.630E+00	1.572E+00	1.474E+00	1.342E+00	1.214E+00	1.154E+00	1.603E+00	1.738E+00	4.699E-01	-2.780E+00	0.0193
16	1.171E+00	1.120E+00	1.035E+00	9.165E-01	7.768E-01	5.824E-01	7.886E-01	1.528E+00	1.651E+00	4.455E-01	-2.850E+00	0.0191
15	5.762E-01	5.458E-01	4.948E-01	4.252E-01	3.236E-01	1.781E-01	8.427E-01	1.521E+00	1.587E+00	4.140E-01	-2.900E+00	0.0189
14	0.0	2.759E-02	1.122E-01	2.274E-01	2.700E-01	1.967E-01	9.219E-01	1.520E+00	1.552E+00	3.893E-01	-2.926E+00	0.0187
13	0.0	4.434E-02	1.102E-01	1.629E-01	2.192E-01	2.381E-01	9.676E-01	1.519E+00	1.529E+00	3.694E-01	-2.942E+00	0.0187
12	0.0	1.284E-02	4.945E-02	8.300E-02	1.543E-01	3.106E-01	1.025E+00	1.520E+00	1.501E+00	3.397E-01	-2.964E+00	0.0186
11	0.0	-1.227E-02	-4.288E-02	-5.106E-02	5.884E-02	4.381E-01	1.115E+00	1.525E+00	1.455E+00	2.855E-01	-3.004E+00	0.0184
10	0.0	-2.236E-02	-9.209E-02	-1.587E-01	-5.763E-02	6.119E-01	1.245E+00	1.535E+00	1.383E+00	1.892E-01	-3.074E+00	0.0181
9	0.0	-1.856E-02	-8.083E-02	-1.567E-01	-1.131E-01	8.216E-01	1.416E+00	1.559E+00	1.278E+00	2.313E-02	-3.186E+00	0.0176
8	0.0	-8.228E-03	-3.321E-02	-5.056E-02	5.351E-02	1.075E+00	1.612E+00	1.601E+00	1.139E+00	-2.581E-01	-3.333E+00	0.0167
7	0.0	9.762E-03	5.530E-02	1.722E-01	4.906E-01	1.401E+00	1.809E+00	1.660E+00	9.868E-01	-7.205E-01	-3.482E+00	0.0152
6	0.0	4.000E-02	1.900E-01	4.929E-01	1.021E+00	1.762E+00	1.981E+00	1.708E+00	8.625E-01	-1.506E+00	-3.387E+00	0.0127
5	0.0	6.441E-02	3.061E-01	7.277E-01	1.345E+00	1.893E+00	1.923E+00	1.565E+00	5.461E-01	-1.486E+00	-2.794E+00	0.0095
4	0.0	6.134E-02	2.883E-01	6.729E-01	1.191E+00	1.555E+00	1.501E+00	1.219E+00	4.743E-01	-1.070E+00	-1.784E+00	0.0063
3	0.0	3.558E-02	1.674E-01	3.932E-01	7.086E-01	9.478E-01	9.443E-01	8.261E-01	4.770E-01	-3.446E-01	-6.334E-01	0.0032
2	0.0	4.638E-01	4.639E-01	4.651E-01	4.676E-01	4.721E-01	4.799E-01	4.904E-01	4.906E-01	4.803E-01	4.726E-01	0.0
X=	-0.0000125	0.0000125	0.0000627	0.0001630	0.0003636	0.0007648	0.0015672	0.0031721	0.0063818	0.0079866	0.0087890	

J \ I=	12	13	14	15	16	17	18	19	20	21	22	Y =
50	8.812E+00	5.291E+00	2.853E+00	1.554E+00	8.946E-01	5.630E-01	2.306E-01	6.409E-02	0.0	4.043E-02		
49	8.808E+00	5.288E+00	2.849E+00	1.550E+00	8.906E-01	5.590E-01	2.265E-01	5.999E-02	0.0	3.726E-02		
48	9.260E+00	5.982E+00	3.303E+00	1.814E+00	1.046E+00	6.577E-01	2.670E-01	7.078E-02	0.0	3.408E-02		
47	9.717E+00	7.025E+00	4.124E+00	2.328E+00	1.360E+00	8.604E-01	3.515E-01	9.354E-02	0.0	3.091E-02		
46	9.727E+00	7.932E+00	5.120E+00	3.027E+00	1.808E+00	1.157E+00	4.776E-01	1.279E-01	0.0	2.773E-02		
45	[illegible]	[illegible]	[illegible]	[illegible]	[illegible]	[illegible]	[illegible]	[illegible]	[illegible]	[illegible]		

45	[illegible]	[illegible]	[illegible]	[illegible]	[illegible]	[illegible]	[illegible]	[illegible]	[illegible]	[illegible]
44	7.292E+00	6.819E+00	5.228E+00	3.398E+00	2.120E+00	1.384E+00	5.834E-01	1.582E-01	0.0	2.474E-02
43	5.909E+00	5.513E+00	4.418E+00	3.022E+00	1.943E+00	1.288E+00	5.516E-01	1.510E-01	0.0	2.409E-02
42	4.986E+00	4.564E+00	3.630E+00	2.484E+00	1.597E+00	1.059E+00	4.531E-01	1.240E-01	0.0	2.373E-02
41	3.978E+00	3.509E+00	2.706E+00	1.812E+00	1.151E+00	7.571E-01	3.215E-01	8.757E-02	0.0	2.336E-02
40	3.115E+00	2.580E+00	1.927E+00	1.304E+00	8.393E-01	5.569E-01	2.385E-01	6.532E-02	0.0	2.308E-02
39	2.487E+00	1.899E+00	1.304E+00	8.450E-01	5.343E-01	3.514E-01	1.490E-01	4.058E-02	0.0	2.288E-02
38	1.849E+00	1.194E+00	6.341E-01	3.343E-01	1.906E-01	1.192E-01	4.790E-02	1.265E-02	0.0	2.269E-02
37	1.211E+00	4.792E-01	-1.302E-01	-2.300E-01	-1.785E-01	-1.268E-01	-5.811E-02	-1.648E-02	0.0	2.249E-02
36	5.736E-01	-3.173E-01	-8.558E-01	-7.486E-01	-5.183E-01	-3.537E-01	-1.558E-01	-4.330E-02	0.0	2.229E-02
35	-4.448E-02	-9.871E-01	-1.402E+00	-1.143E+00	-7.799E-01	-5.298E-01	-2.324E-01	-6.446E-02	0.0	2.211E-02
34	-4.461E-01	-1.397E+00	-1.744E+00	-1.404E+00	-9.645E-01	-6.589E-01	-2.911E-01	-8.106E-02	0.0	2.200E-02
33	-8.374E-01	-1.826E+00	-2.131E+00	-1.657E+00	-1.110E+00	-7.479E-01	-3.250E-01	-8.967E-02	0.0	2.188E-02
32	-1.465E+00	-2.519E+00	-2.738E+00	-2.080E+00	-1.386E+00	-9.317E-01	-4.044E-01	-1.115E-01	0.0	2.169E-02
31	-2.177E+00	-3.274E+00	-3.372E+00	-2.528E+00	-1.682E+00	-1.132E+00	-4.915E-01	-1.356E-01	0.0	2.146E-02
30	-2.825E+00	-3.955E+00	-3.898E+00	-2.863E+00	-1.889E+00	-1.266E+00	-5.474E-01	-1.507E-01	0.0	2.122E-02
29	-3.379E+00	-4.525E+00	-4.285E+00	-3.070E+00	-2.000E+00	-1.332E+00	-5.725E-01	-1.570E-01	0.0	2.099E-02
28	-3.753E+00	-4.892E+00	-4.498E+00	-3.166E+00	-2.047E+00	-1.360E+00	-5.827E-01	-1.596E-01	0.0	2.080E-02
27	-4.005E+00	-5.133E+00	-4.600E+00	-3.164E+00	-2.018E+00	-1.331E+00	-5.659E-01	-1.542E-01	0.0	2.064E-02
26	-4.169E+00	-5.272E+00	-4.639E+00	-3.145E+00	-1.991E+00	-1.308E+00	-5.542E-01	-1.508E-01	0.0	2.053E-02
25	-4.271E+00	-5.354E+00	-4.646E+00	-3.108E+00	-1.955E+00	-1.281E+00	-5.411E-01	-1.470E-01	0.0	2.045E-02
24	-4.364E+00	-5.424E+00	-4.634E+00	-3.055E+00	-1.908E+00	-1.246E+00	-5.245E-01	-1.421E-01	0.0	2.037E-02
23	-4.451E+00	-5.482E+00	-4.603E+00	-2.990E+00	-1.854E+00	-1.206E+00	-5.061E-01	-1.369E-01	0.0	2.030E-02
22	-4.532E+00	-5.527E+00	-4.553E+00	-2.913E+00	-1.794E+00	-1.163E+00	-4.865E-01	-1.313E-01	0.0	2.022E-02
21	-4.641E+00	-5.572E+00	-4.435E+00	-2.778E+00	-1.698E+00	-1.099E+00	-4.583E-01	-1.236E-01	0.0	2.010E-02
20	-4.759E+00	-5.584E+00	-4.262E+00	-2.602E+00	-1.569E+00	-1.007E+00	-4.168E-01	-1.118E-01	0.0	1.995E-02
19	-4.872E+00	-5.543E+00	-3.998E+00	-2.383E+00	-1.425E+00	-9.115E-01	-3.762E-01	-1.008E-01	0.0	1.975E-02
18	-4.956E+00	-5.439E+00	-3.696E+00	-2.146E+00	-1.265E+00	-8.039E-01	-3.294E-01	-8.784E-02	0.0	1.952E-02
17	-5.001E+00	-5.297E+00	-3.405E+00	-1.938E+00	-1.133E+00	-7.176E-01	-2.930E-01	-7.799E-02	0.0	1.929E-02
16	-5.017E+00	-5.131E+00	-3.137E+00	-1.758E+00	-1.023E+00	-6.463E-01	-2.634E-01	-7.002E-02	0.0	1.906E-02
15	-5.012E+00	-4.994E+00	-2.942E+00	-1.619E+00	-9.322E-01	-5.856E-01	-2.372E-01	-6.281E-02	0.0	1.887E-02
14	-5.004E+00	-4.908E+00	-2.834E+00	-1.542E+00	-8.814E-01	-5.512E-01	-2.221E-01	-5.861E-02	0.0	1.875E-02
13	-4.998E+00	-4.843E+00	-2.759E+00	-1.502E+00	-8.623E-01	-5.410E-01	-2.190E-01	-5.797E-02	0.0	1.867E-02
12	-4.988E+00	-4.744E+00	-2.663E+00	-1.460E+00	-8.440E-01	-5.318E-01	-2.163E-01	-5.743E-02	0.0	1.857E-02
11	-4.969E+00	-4.568E+00	-2.520E+00	-1.385E+00	-8.022E-01	-5.060E-01	-2.059E-01	-5.470E-02	0.0	1.839E-02
10	-4.923E+00	-4.270E+00	-2.314E+00	-1.266E+00	-7.315E-01	-4.609E-01	-1.873E-01	-4.972E-02	0.0	1.809E-02
9	-4.819E+00	-3.812E+00	-2.042E+00	-1.113E+00	-6.421E-01	-4.043E-01	-1.642E-01	-4.355E-02	0.0	1.757E-02
8	-4.611E+00	-3.209E+00	-1.718E+00	-9.368E-01	-5.411E-01	-3.408E-01	-1.385E-01	-3.674E-02	0.0	1.670E-02
7	-4.224E+00	-2.542E+00	-1.355E+00	-7.392E-01	-4.267E-01	-2.686E-01	-1.091E-01	-2.892E-02	0.0	1.522E-02
6	-3.414E+00	-1.743E+00	-8.910E-01	-4.751E-01	-2.705E-01	-1.689E-01	-6.805E-02	-1.794E-02	0.0	1.270E-02
5	-2.227E+00	-8.380E-01	-3.502E-01	-1.631E-01	-8.521E-02	-5.065E-02	-1.930E-02	-4.901E-03	0.0	9.524E-03
4	-7.265E-01	2.142E-02	1.072E-01	8.455E-02	5.657E-02	3.813E-02	1.654E-02	4.565E-03	0.0	6.349E-03
3	7.044E-01	5.272E-01	3.253E-01	1.898E-01	1.126E-01	7.172E-02	2.942E-02	7.853E-03	0.0	3.175E-03
2	4.681E-01	4.657E-01	4.645E-01	4.638E-01	4.635E-01	4.633E-01	4.632E-01	4.631E-01	0.0	0.0
X=	0.0091903	0.0093909	0.0094912	0.0095413	0.0095664	0.0095789	0.0095915	0.0095977	0.0096022	

--*-*-*-*-*-*-*-*-*-*-*-*-*-*-*-*-*- PPPPPPPPPPPPPPPPPPPPPPPPPPPPPPPPPPPPP -*-*-*-*-*-*-*-*-*-*-*-*-*-*-*-*-*-*-*

J \ I=	1	2	3	4	5	6	7	8	9	10	11	Y =
50	0.0	0.0	0.0	0.0	0.0	0.0	0.0	0.0	0.0	0.0	0.0	0.0420
49	0.0	-1.359E+01	-1.359E+01	-1.359E+01	-1.359E+01	-1.359E+01	-1.358E+01	-1.357E+01	-1.364E+01	-1.384E+01	-1.401E+01	0.0388
48	0.0	-1.372E+01	-1.372E+01	-1.372E+01	-1.372E+01	-1.372E+01	-1.370E+01	-1.369E+01	-1.351E+01	-1.343E+01	-1.344E+01	0.0357
47	0.0	-1.390E+01	-1.390E+01	-1.390E+01	-1.390E+01	-1.389E+01	-1.385E+01	-1.383E+01	-1.316E+01	-1.249E+01	-1.228E+01	0.0325
46	0.0	-1.461E+01	-1.461E+01	-1.462E+01	-1.462E+01	-1.464E+01	-1.454E+01	-1.450E+01	-1.184E+01	-9.373E+00	-8.530E+00	0.0293
45	0.0	-1.881E+01	-1.882E+01	-1.882E+01	-1.883E+01	-1.895E+01	-1.953E+01	-1.870E+01	-7.961E+00	-1.544E+00	1.068E+00	0.0261
44	0.0	-2.167E+01	-2.166E+01	-2.167E+01	-2.182E+01	-2.241E+01	-2.420E+01	-2.195E+01	-5.516E+00	4.123E+00	8.651E+00	0.0252
43	0.0	-2.201E+01	-2.199E+01	-2.200E+01	-2.209E+01	-2.247E+01	-2.399E+01	-2.174E+01	-2.725E+00	8.752E+00	1.478E+01	0.0243
42	0.0	-2.149E+01	-2.148E+01	-2.146E+01	-2.149E+01	-2.172E+01	-2.240E+01	-2.082E+01	-1.431E+00	1.097E+01	1.788E+01	0.0239
41	0.0	-2.126E+01	-2.125E+01	-2.124E+01	-2.125E+01	-2.128E+01	-2.108E+01	-1.927E+01	-1.983E-01	1.281E+01	2.042E+01	0.0235
40	0.0	-2.105E+01	-2.105E+01	-2.104E+01	-2.106E+01	-2.100E+01	-2.018E+01	-1.709E+01	6.302E-01	1.359E+01	2.161E+01	0.0232
39	0.0	-2.091E+01	-2.090E+01	-2.089E+01	-2.087E+01	-2.100E+01	-2.062E+01	-1.592E+01	1.104E+00	1.402E+01	2.219E+01	0.0230
38	0.0	-2.077E+01	-2.076E+01	-2.076E+01	-2.077E+01	-2.114E+01	-2.170E+01	-1.463E+01	1.493E+00	1.421E+01	2.242E+01	0.0228
37	0.0	-2.061E+01	-2.060E+01	-2.060E+01	-2.060E+01	-2.124E+01	-2.255E+01	-1.327E+01	1.797E+00	1.416E+01	2.230E+01	0.0226
36	0.0	-2.036E+01	-2.036E+01	-2.037E+01	-2.029E+01	-2.036E+01	-2.197E+01	-1.182E+01	2.017E+00	1.386E+01	2.181E+01	0.0224
35	0.0	-2.004E+01	-2.006E+01	-2.006E+01	-1.987E+01	-1.849E+01	-2.024E+01	-1.028E+01	2.080E+00	1.323E+01	2.092E+01	0.0222
34	0.0	-2.013E+01	-2.004E+01	-1.988E+01	-1.972E+01	-1.788E+01	-1.856E+01	-9.090E+00	2.002E+00	1.252E+01	1.998E+01	0.0220
33	0.0	-2.015E+01	-2.008E+01	-1.994E+01	-1.964E+01	-1.845E+01	-1.808E+01	-8.294E+00	2.195E+00	1.233E+01	1.953E+01	0.0220
32	0.0	-2.051E+01	-2.042E+01	-2.028E+01	-1.981E+01	-1.860E+01	-1.668E+01	-6.806E+00	2.390E+00	1.171E+01	1.837E+01	0.0218
31	0.0	-2.002E+01	-1.994E+01	-1.974E+01	-1.912E+01	-1.739E+01	-1.407E+01	-4.850E+00	2.419E+00	1.042E+01	1.635E+01	0.0216
30	0.0	-1.790E+01	-1.784E+01	-1.764E+01	-1.700E+01	-1.512E+01	-1.121E+01	-2.963E+00	2.462E+00	9.053E+00	1.417E+01	0.0213
29	0.0	-1.426E+01	-1.425E+01	-1.414E+01	-1.366E+01	-1.201E+01	-8.179E+00	-1.204E+00	2.551E+00	7.738E+00	1.188E+01	0.0211
28	0.0	-9.406E+00	-9.564E+00	-9.710E+00	-9.574E+00	-8.420E+00	-5.314E+00	8.698E-02	2.571E+00	6.566E+00	9.725E+00	0.0209
27	0.0	-6.756E+00	-6.808E+00	-6.877E+00	-6.808E+00	-5.953E+00	-3.348E+00	1.033E+00	2.733E+00	5.964E+00	8.431E+00	0.0207
26	0.0	-3.738E+00	-3.872E+00	-4.027E+00	-4.104E+00	-3.659E+00	-1.766E+00	1.596E+00	2.800E+00	5.497E+00	7.425E+00	0.0206
25	0.0	-2.485E+00	-2.546E+00	-2.670E+00	-2.796E+00	-2.512E+00	-8.936E-01	1.984E+00	2.908E+00	5.327E+00	6.938E+00	0.0205
24	0.0	-1.143E+00	-1.210E+00	-1.346E+00	-1.539E+00	-1.422E+00	-6.948E-02	2.343E+00	3.017E+00	5.194E+00	6.573E+00	0.0204
23	0.0	2.105E-01	1.222E-01	-6.107E-02	-3.481E-01	-3.972E-01	7.044E-01	2.676E+00	3.126E+00	5.087E+00	6.260E+00	0.0203
22	0.0	1.562E+00	1.435E+00	1.168E+00	7.627E-01	5.526E-01	1.426E+00	2.982E+00	3.235E+00	5.001E+00	5.992E+00	0.0203
21	0.0	2.995E+00	2.750E+00	2.379E+00	1.899E+00	1.624E+00	2.362E+00	3.460E+00	3.422E+00	4.938E+00	5.770E+00	0.0202
20	0.0	4.963E+00	4.731E+00	4.282E+00	3.611E+00	3.099E+00	3.506E+00	3.936E+00	3.616E+00	4.833E+00	5.448E+00	0.0200
19	0.0	6.847E+00	6.444E+00	5.807E+00	5.008E+00	4.422E+00	4.637E+00	4.454E+00	3.843E+00	4.769E+00	5.205E+00	0.0199
18	0.0	7.502E+00	7.206E+00	6.697E+00	6.015E+00	5.524E+00	5.589E+00	4.890E+00	4.053E+00	4.717E+00	5.008E+00	0.0196
17	0.0	7.430E+00	7.170E+00	6.764E+00	6.291E+00	6.083E+00	6.117E+00	5.189E+00	4.214E+00	4.700E+00	4.898E+00	0.0194
16	0.0	6.808E+00	6.627E+00	6.387E+00	6.173E+00	6.258E+00	6.338E+00	5.359E+00	4.341E+00	4.715E+00	4.857E+00	0.0192
15	0.0	5.995E+00	5.997E+00	6.000E+00	6.017E+00	6.175E+00	6.368E+00	5.436E+00	4.432E+00	4.748E+00	4.865E+00	0.0189
14	0.0	5.946E+00	5.975E+00	5.979E+00	5.985E+00	6.146E+00	6.335E+00	5.465E+00	4.481E+00	4.784E+00	4.859E+00	0.0188
13	0.0	5.888E+00	5.969E+00	6.002E+00	6.005E+00	6.132E+00	6.304E+00	5.475E+00	4.512E+00	4.814E+00	4.845E+00	0.0187
12	0.0	6.007E+00	6.003E+00	6.011E+00	6.015E+00	6.118E+00	6.262E+00	5.480E+00	4.549E+00	4.844E+00	4.849E+00	0.0186
11	0.0	6.029E+00	6.020E+00	6.012E+00	6.007E+00	6.090E+00	6.196E+00	5.488E+00	4.605E+00	4.881E+00	4.875E+00	0.0185
10	0.0	5.981E+00	5.979E+00	5.973E+00	5.963E+00	6.022E+00	6.094E+00	5.492E+00	4.683E+00	4.929E+00	4.921E+00	0.0183
9	0.0	5.892E+00	5.892E+00	5.892E+00	5.889E+00	5.917E+00	5.949E+00	5.485E+00	4.780E+00	4.979E+00	4.980E+00	0.0179
8	0.0	5.794E+00	5.795E+00	5.797E+00	5.799E+00	5.803E+00	5.780E+00	5.448E+00	4.875E+00	5.011E+00	5.021E+00	0.0173
7	0.0	5.680E+00	5.682E+00	5.684E+00	5.686E+00	5.675E+00	5.614E+00	5.371E+00	4.911E+00	4.986E+00	5.004E+00	0.0162
6	0.0	5.517E+00	5.519E+00	5.521E+00	5.522E+00	5.512E+00	5.464E+00	5.279E+00	4.842E+00	4.869E+00	4.923E+00	0.0143
5	0.0	5.653E+00	5.654E+00	5.655E+00	5.656E+00	5.647E+00	5.597E+00	5.416E+00	5.047E+00	5.121E+00	5.195E+00	0.0111
4	0.0	6.255E+00	6.255E+00	6.256E+00	6.256E+00	6.250E+00	6.210E+00	6.071E+00	5.952E+00	6.068E+00	6.164E+00	0.0079
3	0.0	6.922E+00	6.922E+00	6.922E+00	6.922E+00	6.922E+00	6.896E+00	6.823E+00	6.925E+00	7.074E+00	7.130E+00	0.0048
2	0.0	7.232E+00	7.231E+00	7.230E+00	7.229E+00	7.228E+00	7.220E+00	7.202E+00	7.425E+00	7.622E+00	7.646E+00	0.0016
1	0.0	0.0	0.0	0.0	0.0	0.0	0.0	0.0	0.0	0.0	0.0	-0.0016
X=	-0.0000125	0.0000125	0.0000627	0.0001630	0.0003636	0.0007648	0.0015672	0.0031721	0.0063818	0.0079866	0.0087890	

J \ I=	12	13	14	15	16	17	18	19	20	21	22	Y =
50	0.0	0.0	0.0	0.0	0.0	0.0	0.0	0.0	0.0	4.202E-02		
49	-1.409E+01	-1.411E+01	1411E+01	-1.411E+01	-1.411E+01	-1.411E+01	-1.411E+01	-1.411E+01	0.0	3.884E-02		
48	-1.347E+01	-1.347E+01	-1.347E+01	-1.347E+01	-1.348E+01	-1.348E+01	-1.348E+01	-1.348E+01	0.0	3.567E-02		
47	-1.224E+01	-1.223E+01	-1.223E+01	-1.223E+01	-1.223E+01	-1.223E+01	-1.223E+01	-1.223E+01	0.0	3.249E-02		
46	-8.362E+00	-8.332E+00	-8.333E+00	-8.335E+00	-8.336E+00	-8.337E+00	-8.338E+00	-8.338E+00	0.0	2.932E-02		

46	[illegible]	[illegible]	[illegible]	[illegible]	[illegible]	[illegible]	[illegible]	[illegible]	0.0	[illegible]
45	1.874E+00	2.085E+00	2.130E+00	2.135E+00	2.134E+00	2.133E+00	2.131E+00	2.130E+00	0.0	2.614E-02
44	1.009E+01	1.041E+01	1.045E+01	1.046E+01	1.046E+01	1.046E+01	1.047E+01	1.047E+01	0.0	2.521E-02
43	1.694E+01	1.755E+01	1.767E+01	1.770E+01	1.771E+01	1.771E+01	1.771E+01	1.771E+01	0.0	2.428E-02
42	2.043E+01	2.117E+01	2.129E+01	2.133E+01	2.134E+01	2.135E+01	2.135E+01	2.136E+01	0.0	2.391E-02
41	2.331E+01	2.411E+01	2.424E+01	2.427E+01	2.428E+01	2.429E+01	2.430E+01	2.430E+01	0.0	2.354E-02
40	2.481E+01	2.579E+01	2.599E+01	2.603E+01	2.605E+01	2.606E+01	2.606E+01	2.607E+01	0.0	2.318E-02
39	2.552E+01	2.656E+01	2.678E+01	2.682E+01	2.684E+01	2.685E+01	2.686E+01	2.687E+01	0.0	2.298E-02
38	2.583E+01	2.691E+01	2.714E+01	2.719E+01	2.721E+01	2.722E+01	2.724E+01	2.724E+01	0.0	2.278E-02
37	2.570E+01	2.678E+01	2.702E+01	2.708E+01	2.710E+01	2.712E+01	2.713E+01	2.714E+01	0.0	2.259E-02
36	2.515E+01	2.622E+01	2.650E+01	2.655E+01	2.658E+01	2.659E+01	2.660E+01	2.661E+01	0.0	2.239E-02
35	2.422E+01	2.536E+01	2.560E+01	2.565E+01	2.567E+01	2.567E+01	2.568E+01	2.569E+01	0.0	2.219E-02
34	2.332E+01	2.442E+01	2.462E+01	2.465E+01	2.467E+01	2.468E+01	2.469E+01	2.469E+01	0.0	2.204E-02
33	2.272E+01	2.372E+01	2.392E+01	2.398E+01	2.400E+01	2.401E+01	2.402E+01	2.403E+01	0.0	2.196E-02
32	2.151E+01	2.253E+01	2.274E+01	2.278E+01	2.280E+01	2.281E+01	2.282E+01	2.282E+01	0.0	2.181E-02
31	1.940E+01	2.039E+01	2.058E+01	2.063E+01	2.064E+01	2.065E+01	2.066E+01	2.066E+01	0.0	2.157E-02
30	1.690E+01	1.780E+01	1.798E+01	1.803E+01	1.804E+01	1.805E+01	1.805E+01	1.806E+01	0.0	2.134E-02
29	1.430E+01	1.511E+01	1.529E+01	1.533E+01	1.534E+01	1.535E+01	1.535E+01	1.535E+01	0.0	2.111E-02
28	1.186E+01	1.260E+01	1.276E+01	1.279E+01	1.280E+01	1.280E+01	1.280E+01	1.280E+01	0.0	2.088E-02
27	1.024E+01	1.091E+01	1.110E+01	1.115E+01	1.116E+01	1.116E+01	1.116E+01	1.115E+01	0.0	2.072E-02
26	9.020E+00	9.635E+00	9.761E+00	9.780E+00	9.782E+00	9.782E+00	9.781E+00	9.779E+00	0.0	2.057E-02
25	8.315E+00	8.900E+00	9.109E+00	9.159E+00	9.164E+00	9.163E+00	9.160E+00	9.158E+00	0.0	2.049E-02
24	7.828E+00	8.382E+00	8.559E+00	8.594E+00	8.596E+00	8.594E+00	8.590E+00	8.588E+00	0.0	2.041E-02
23	7.391E+00	7.908E+00	8.064E+00	8.092E+00	8.092E+00	8.089E+00	8.085E+00	8.082E+00	0.0	2.034E-02
22	7.000E+00	7.479E+00	7.627E+00	7.650E+00	7.648E+00	7.645E+00	7.640E+00	7.636E+00	0.0	2.026E-02
21	6.659E+00	7.102E+00	7.251E+00	7.267E+00	7.262E+00	7.257E+00	7.252E+00	7.249E+00	0.0	2.018E-02
20	6.232E+00	6.523E+00	6.570E+00	6.576E+00	6.571E+00	6.567E+00	6.562E+00	6.558E+00	0.0	2.003E-02
19	5.812E+00	6.058E+00	6.116E+00	6.115E+00	6.108E+00	6.103E+00	6.099E+00	6.096E+00	0.0	1.987E-02
18	5.447E+00	5.552E+00	5.561E+00	5.558E+00	5.552E+00	5.548E+00	5.544E+00	5.541E+00	0.0	1.964E-02
17	5.193E+00	5.256E+00	5.261E+00	5.254E+00	5.249E+00	5.245E+00	5.242E+00	5.240E+00	0.0	1.941E-02
16	5.049E+00	5.077E+00	5.075E+00	5.068E+00	5.063E+00	5.060E+00	5.057E+00	5.056E+00	0.0	1.917E-02
15	4.981E+00	4.962E+00	4.957E+00	4.954E+00	4.950E+00	4.948E+00	4.945E+00	4.943E+00	0.0	1.894E-02
14	4.972E+00	4.980E+00	4.972E+00	4.968E+00	4.964E+00	4.962E+00	4.959E+00	4.957E+00	0.0	1.879E-02
13	4.973E+00	5.051E+00	5.027E+00	5.007E+00	5.001E+00	4.998E+00	4.997E+00	4.996E+00	0.0	1.871E-02
12	4.966E+00	5.045E+00	5.028E+00	5.016E+00	5.011E+00	5.010E+00	5.009E+00	5.009E+00	0.0	1.863E-02
11	4.960E+00	4.999E+00	4.997E+00	4.994E+00	4.991E+00	4.989E+00	4.988E+00	4.987E+00	0.0	1.850E-02
10	4.958E+00	4.964E+00	4.960E+00	4.956E+00	4.953E+00	4.952E+00	4.950E+00	4.950E+00	0.0	1.828E-02
9	4.966E+00	4.951E+00	4.943E+00	4.939E+00	4.937E+00	4.936E+00	4.935E+00	4.935E+00	0.0	1.790E-02
8	4.984E+00	4.967E+00	4.961E+00	4.958E+00	4.957E+00	4.956E+00	4.955E+00	4.955E+00	0.0	1.725E-02
7	4.980E+00	4.970E+00	4.967E+00	4.965E+00	4.964E+00	4.964E+00	4.964E+00	4.963E+00	0.0	1.615E-02
6	4.933E+00	4.934E+00	4.933E+00	4.932E+00	4.932E+00	4.931E+00	4.931E+00	4.931E+00	0.0	1.429E-02
5	5.214E+00	5.219E+00	5.218E+00	5.217E+00	5.217E+00	5.217E+00	5.216E+00	5.216E+00	0.0	1.111E-02
4	6.189E+00	6.195E+00	6.194E+00	6.193E+00	6.193E+00	6.193E+00	6.193E+00	6.192E+00	0.0	7.937E-03
3	7.144E+00	7.147E+00	7.146E+00	7.146E+00	7.145E+00	7.145E+00	7.145E+00	7.145E+00	0.0	4.762E-03
2	7.647E+00	7.650E+00	7.653E+00	7.654E+00	7.654E+00	7.654E+00	7.655E+00	7.655E+00	0.0	1.587E-03
1	0.0	0.0	0.0	0.0	0.0	0.0	0.0	0.0	0.0	-1.587E-03
X=	0.0091503	0.0093509	0.0094912	0.0095413	0.0095664	0.0095789	0.0095915	0.0095977	0.0096022	

J	I = 1	2	3	4	5	6	7	8	9	10	11	Y =
50	4.500E+02	4.500E+02	4.500E+02	4.499E+02	4.499E+02	4.497E+02	4.494E+02	4.487E+02	4.472E+02	4.451E+02	4.377E+02	0.0420
49	4.500E+02	4.500E+02	4.500E+02	4.499E+02	4.499E+02	4.497E+02	4.494E+02	4.487E+02	4.472E+02	4.451E+02	4.377E+02	0.0388
48	4.500E+02	4.500E+02	4.500E+02	4.499E+02	4.498E+02	4.497E+02	4.494E+02	4.488E+02	4.472E+02	4.452E+02	4.390E+02	0.0357
47	4.500E+02	4.500E+02	4.500E+02	4.499E+02	4.498E+02	4.496E+02	4.493E+02	4.489E+02	4.472E+02	4.454E+02	4.410E+02	0.0325
46	4.500E+02	4.500E+02	4.499E+02	4.498E+02	4.496E+02	4.493E+02	4.491E+02	4.489E+02	4.472E+02	4.455E+02	4.427E+02	0.0293
45	4.500E+02	4.500E+02	4.499E+02	4.498E+02	4.495E+02	4.492E+02	4.490E+02	4.489E+02	4.471E+02	4.455E+02	4.438E+02	0.0261
44	4.500E+02	4.500E+02	4.499E+02	4.498E+02	4.496E+02	4.492E+02	4.490E+02	4.489E+02	4.469E+02	4.451E+02	4.436E+02	0.0252
43	4.500E+02	4.500E+02	4.499E+02	4.499E+02	4.496E+02	4.493E+02	4.491E+02	4.489E+02	4.465E+02	4.446E+02	4.432E+02	0.0243
42	4.500E+02	4.500E+02	4.500E+02	4.499E+02	4.497E+02	4.493E+02	4.491E+02	4.489E+02	4.461E+02	4.440E+02	4.427E+02	0.0239
41	4.500E+02	4.500E+02	4.500E+02	4.499E+02	4.497E+02	4.493E+02	4.491E+02	4.489E+02	4.457E+02	4.436E+02	4.422E+02	0.0235
40	4.500E+02	4.500E+02	4.500E+02	4.499E+02	4.497E+02	4.494E+02	4.495E+02	4.489E+02	4.452E+02	4.430E+02	4.417E+02	0.0232
39	4.500E+02	4.500E+02	4.500E+02	4.499E+02	4.497E+02	4.494E+02	4.498E+02	4.488E+02	4.447E+02	4.424E+02	4.412E+02	0.0230
38	4.500E+02	4.500E+02	4.500E+02	4.499E+02	4.497E+02	4.494E+02	4.498E+02	4.488E+02	4.443E+02	4.419E+02	4.408E+02	0.0228
37	4.500E+02	4.500E+02	4.500E+02	4.499E+02	4.498E+02	4.494E+02	4.498E+02	4.487E+02	4.438E+02	4.413E+02	4.403E+02	0.0226
36	4.500E+02	4.500E+02	4.500E+02	4.499E+02	4.498E+02	4.495E+02	4.498E+02	4.486E+02	4.433E+02	4.407E+02	4.398E+02	0.0224
35	4.500E+02	4.500E+02	4.500E+02	4.499E+02	4.498E+02	4.495E+02	4.499E+02	4.484E+02	4.426E+02	4.399E+02	4.392E+02	0.0222
34	4.500E+02	4.500E+02	4.500E+02	4.499E+02	4.498E+02	4.499E+02	4.500E+02	4.483E+02	4.419E+02	4.391E+02	4.386E+02	0.0220
33	4.500E+02	4.500E+02	4.500E+02	4.500E+02	4.499E+02	4.500E+02	4.500E+02	4.482E+02	4.413E+02	4.385E+02	4.382E+02	0.0220
32	4.500E+02	4.500E+02	4.500E+02	4.500E+02	4.500E+02	4.500E+02	4.500E+02	4.480E+02	4.407E+02	4.379E+02	4.378E+02	0.0218
31	4.500E+02	4.500E+02	4.500E+02	4.500E+02	4.500E+02	4.500E+02	4.500E+02	4.478E+02	4.397E+02	4.368E+02	4.369E+02	0.0216
30	4.500E+02	4.500E+02	4.500E+02	4.500E+02	4.500E+02	4.500E+02	4.500E+02	4.474E+02	4.381E+02	4.351E+02	4.357E+02	0.0213
29	4.500E+02	4.500E+02	4.500E+02	4.500E+02	4.500E+02	4.500E+02	4.499E+02	4.468E+02	4.363E+02	4.331E+02	4.345E+02	0.0211
28	4.500E+02	4.500E+02	4.500E+02	4.500E+02	4.500E+02	4.500E+02	4.499E+02	4.461E+02	4.342E+02	4.307E+02	4.335E+02	0.0209
27	4.500E+02	4.500E+02	4.500E+02	4.500E+02	4.500E+02	4.500E+02	4.499E+02	4.453E+02	4.323E+02	4.285E+02	4.327E+02	0.0207
26	4.500E+02	4.500E+02	4.500E+02	4.500E+02	4.500E+02	4.500E+02	4.498E+02	4.445E+02	4.307E+02	4.268E+02	4.321E+02	0.0206
25	4.500E+02	4.500E+02	4.500E+02	4.500E+02	4.500E+02	4.500E+02	4.498E+02	4.438E+02	4.294E+02	4.259E+02	4.318E+02	0.0205
24	4.500E+02	4.500E+02	4.500E+02	4.500E+02	4.500E+02	4.500E+02	4.497E+02	4.432E+02	4.286E+02	4.252E+02	4.316E+02	0.0204
23	4.500E+02	4.500E+02	4.500E+02	4.500E+02	4.500E+02	4.500E+02	4.496E+02	4.426E+02	4.279E+02	4.247E+02	4.314E+02	0.0203
22	4.500E+02	4.500E+02	4.500E+02	4.500E+02	4.500E+02	4.500E+02	4.496E+02	4.420E+02	4.271E+02	4.242E+02	4.312E+02	0.0203
21	4.300E+02	4.500E+02	4.500E+02	4.500E+02	4.500E+02	4.500E+02	4.495E+02	4.413E+02	4.264E+02	4.238E+02	4.309E+02	0.0202
20	4.500E+02	4.500E+02	4.500E+02	4.500E+02	4.500E+02	4.500E+02	4.493E+02	4.400E+02	4.254E+02	4.232E+02	4.306E+02	0.0200
19	4.500E+02	4.500E+02	4.500E+02	4.500E+02	4.500E+02	4.500E+02	4.489E+02	4.381E+02	4.241E+02	4.229E+02	4.305E+02	0.0199
18	4.500E+02	4.500E+02	4.500E+02	4.500E+02	4.500E+02	4.499E+02	4.482E+02	4.353E+02	4.227E+02	4.227E+02	4.304E+02	0.0196
17	4.500E+02	4.500E+02	4.500E+02	4.500E+02	4.500E+02	4.498E+02	4.465E+02	4.316E+02	4.215E+02	4.227E+02	4.303E+02	0.0194
16	4.500E+02	4.500E+02	4.500E+02	4.500E+02	4.499E+02	4.494E+02	4.429E+02	4.286E+02	4.209E+02	4.226E+02	4.302E+02	0.0192
15	4.500E+02	4.500E+02	4.500E+02	4.498E+02	4.492E+02	4.478E+02	4.373E+02	4.271E+02	4.205E+02	4.224E+02	4.300E+02	0.0189
14	4.500E+02	4.499E+02	4.496E+02	4.487E+02	4.470E+02	4.457E+02	4.361E+02	4.266E+02	4.202E+02	4.222E+02	4.299E+02	0.0188
13	4.500E+02	4.499E+02	4.494E+02	4.483E+02	4.465E+02	4.452E+02	4.361E+02	4.264E+02	4.201E+02	4.221E+02	4.298E+02	0.0187
12	4.500E+02	4.499E+02	4.493E+02	4.481E+02	4.463E+02	4.449E+02	4.361E+02	4.262E+02	4.200E+02	4.222E+02	4.296E+02	0.0186
11	4.500E+02	4.493E+02	4.492E+02	4.480E+02	4.461E+02	4.447E+02	4.361E+02	4.261E+02	4.199E+02	4.224E+02	4.294E+02	0.0185
10	4.500E+02	4.499E+02	4.493E+02	4.482E+02	4.464E+02	4.447E+02	4.360E+02	4.257E+02	4.197E+02	4.224E+02	4.291E+02	0.0183
9	4.500E+02	4.499E+02	4.495E+02	4.487E+02	4.471E+02	4.447E+02	4.357E+02	4.252E+02	4.193E+02	4.222E+02	4.286E+02	0.0179
8	4.500E+02	4.499E+02	4.496E+02	4.491E+02	4.479E+02	4.445E+02	4.351E+02	4.244E+02	4.186E+02	4.215E+02	4.274E+02	0.0173
7	4.500E+02	4.499E+02	4.496E+02	4.490E+02	4.478E+02	4.438E+02	4.341E+02	4.231E+02	4.175E+02	4.204E+02	4.253E+02	0.0162
6	4.500E+02	4.499E+02	4.495E+02	4.486E+02	4.469E+02	4.427E+02	4.325E+02	4.216E+02	4.157E+02	4.193E+02	4.206E+02	0.0143
5	4.500E+02	4.499E+02	4.493E+02	4.482E+02	4.460E+02	4.411E+02	4.307E+02	4.199E+02	4.137E+02	4.172E+02	4.132E+02	0.0111
4	4.500E+02	4.498E+02	4.492E+02	4.479E+02	4.453E+02	4.399E+02	4.296E+02	4.198E+02	4.112E+02	4.111E+02	4.026E+02	0.0079
3	4.500E+02	4.499E+02	4.493E+02	4.482E+02	4.460E+02	4.414E+02	4.335E+02	4.245E+02	4.114E+02	4.008E+02	3.906E+02	0.0048
2	4.500E+02	4.500E+02	4.498E+02	4.496E+02	4.489E+02	4.473E+02	4.435E+02	4.392E+02	4.319E+02	4.195E+02	4.061E+02	0.0016
1	4.500E+02	4.500E+02	4.500E+02	4.500E+02	4.500E+02	4.500E+02	4.500E+02	4.500E+02	4.500E+02	4.500E+02	4.500E+02	-0.0016
X =	-0.0000125	0.0000125	0.0000627	0.0001630	0.0003636	0.0007648	0.0015672	0.0031721	0.0063818	0.0079866	0.0087890	

J	I = 12	13	14	15	16	17	18	19	20	21	22	Y =
50	4.116E+02	3.830E+02	3.673E+02	3.593E+02	3.553E+02	3.533E+02	3.514E+02	3.504E+02	3.500E+02	4.202E-02		
49	4.116E+02	3.830E+02	3.673E+02	3.593E+02	3.553E+02	3.533E+02	3.514E+02	3.504E+02	3.500E+02	3.884E-02		
48	4.153E+02	3.851E+02	3.683E+02	3.599E+02	3.557E+02	3.535E+02	3.514E+02	3.504E+02	3.500E+02	3.567E-02		
47	4.217E+02	3.902E+02	3.711E+02	3.614E+02	3.565E+02	3.541E+02	3.516E+02	3.504E+02	3.500E+02	3.249E-02		
46	4.298E+02	3.985E+02	[illegible]	[illegible]	[illegible]	[illegible]	[illegible]	[illegible]	[illegible]	[illegible]		

45	4.373E+02	4.103E+02	3.831E+02	3.680E+02	3.603E+02	3.564E+02	3.526E+02	3.507E+02	3.500E+02	2.614E-02
44	4.418E+02	4.225E+02	3.927E+02	3.735E+02	3.635E+02	3.585E+02	3.534E+02	3.509E+02	3.500E+02	2.521E-02
43	4.420E+02	4.267E+02	3.966E+02	3.758E+02	3.648E+02	3.593E+02	3.538E+02	3.510E+02	3.500E+02	2.428E-02
42	4.417E+02	4.303E+02	4.007E+02	3.786E+02	3.665E+02	3.603E+02	3.542E+02	3.511E+02	3.500E+02	2.391E-02
41	4.413E+02	4.314E+02	4.021E+02	3.795E+02	3.670E+02	3.607E+02	3.543E+02	3.511E+02	3.500E+02	2.354E-02
40	4.409E+02	4.322E+02	4.031E+02	3.801E+02	3.674E+02	3.609E+02	3.544E+02	3.512E+02	3.500E+02	2.318E-02
39	4.406E+02	4.332E+02	4.049E+02	3.814E+02	3.682E+02	3.614E+02	3.546E+02	3.512E+02	3.500E+02	2.298E-02
38	4.403E+02	4.336E+02	4.058E+02	3.820E+02	3.686E+02	3.617E+02	3.547E+02	3.513E+02	3.500E+02	2.278E-02
37	4.400E+02	4.340E+02	4.067E+02	3.827E+02	3.690E+02	3.619E+02	3.548E+02	3.513E+02	3.500E+02	2.259E-02
36	4.396E+02	4.335E+02	4.060E+02	3.822E+02	3.687E+02	3.617E+02	3.548E+02	3.513E+02	3.500E+02	2.239E-02
35	4.391E+02	4.320E+02	4.042E+02	3.810E+02	3.680E+02	3.613E+02	3.546E+02	3.512E+02	3.500E+02	2.219E-02
34	4.387E+02	4.314E+02	4.036E+02	3.807E+02	3.678E+02	3.612E+02	3.545E+02	3.512E+02	3.500E+02	2.204E-02
33	4.385E+02	4.312E+02	4.032E+02	3.803E+02	3.675E+02	3.610E+02	3.545E+02	3.512E+02	3.500E+02	2.196E-02
32	4.381E+02	4.308E+02	4.030E+02	3.802E+02	3.675E+02	3.610E+02	3.544E+02	3.512E+02	3.500E+02	2.181E-02
31	4.375E+02	4.300E+02	4.021E+02	3.797E+02	3.672E+02	3.608E+02	3.544E+02	3.512E+02	3.500E+02	2.157E-02
30	4.369E+02	4.287E+02	4.008E+02	3.788E+02	3.666E+02	3.604E+02	3.542E+02	3.511E+02	3.500E+02	2.134E-02
29	4.363E+02	4.270E+02	3.989E+02	3.775E+02	3.659E+02	3.600E+02	3.540E+02	3.511E+02	3.500E+02	2.111E-02
28	4.359E+02	4.254E+02	3.971E+02	3.764E+02	3.652E+02	3.595E+02	3.539E+02	3.510E+02	3.500E+02	2.088E-02
27	4.355E+02	4.239E+02	3.954E+02	3.752E+02	3.645E+02	3.591E+02	3.537E+02	3.510E+02	3.500E+02	2.072E-02
26	4.353E+02	4.227E+02	3.941E+02	3.744E+02	3.640E+02	3.588E+02	3.536E+02	3.509E+02	3.500E+02	2.057E-02
25	4.351E+02	4.218E+02	3.931E+02	3.738E+02	3.637E+02	3.586E+02	3.535E+02	3.509E+02	3.500E+02	2.049E-02
24	4.349E+02	4.209E+02	3.921E+02	3.731E+02	3.633E+02	3.583E+02	3.534E+02	3.509E+02	3.500E+02	2.041E-02
23	4.347E+02	4.199E+02	3.910E+02	3.724E+02	3.629E+02	3.581E+02	3.533E+02	3.509E+02	3.500E+02	2.034E-02
22	4.345E+02	4.189E+02	3.899E+02	3.718E+02	3.625E+02	3.578E+02	3.532E+02	3.508E+02	3.500E+02	2.026E-02
21	4.340E+02	4.172E+02	3.883E+02	3.708E+02	3.619E+02	3.575E+02	3.530E+02	3.508E+02	3.500E+02	2.018E-02
20	4.334E+02	4.151E+02	3.863E+02	3.697E+02	3.613E+02	3.571E+02	3.529E+02	3.508E+02	3.500E+02	2.003E-02
19	4.324E+02	4.123E+02	3.840E+02	3.684E+02	3.605E+02	3.566E+02	3.527E+02	3.507E+02	3.500E+02	1.987E-02
18	4.312E+02	4.092E+02	3.816E+02	3.671E+02	3.598E+02	3.561E+02	3.525E+02	3.507E+02	3.500E+02	1.964E-02
17	4.299E+02	4.063E+02	3.796E+02	3.660E+02	3.592E+02	3.558E+02	3.523E+02	3.506E+02	3.500E+02	1.941E-02
16	4.286E+02	4.036E+02	3.780E+02	3.651E+02	3.587E+02	3.554E+02	3.522E+02	3.506E+02	3.500E+02	1.917E-02
15	4.275E+02	4.015E+02	3.768E+02	3.644E+02	3.583E+02	3.552E+02	3.521E+02	3.506E+02	3.500E+02	1.894E-02
14	4.268E+02	4.004E+02	3.762E+02	3.641E+02	3.581E+02	3.551E+02	3.521E+02	3.505E+02	3.500E+02	1.879E-02
13	4.264E+02	3.998E+02	3.759E+02	3.640E+02	3.580E+02	3.550E+02	3.520E+02	3.505E+02	3.500E+02	1.871E-02
12	4.259E+02	3.989E+02	3.755E+02	3.638E+02	3.579E+02	3.550E+02	3.520E+02	3.505E+02	3.500E+02	1.863E-02
11	4.249E+02	3.974E+02	3.747E+02	3.633E+02	3.576E+02	3.548E+02	3.519E+02	3.505E+02	3.500E+02	1.850E-02
10	4.232E+02	3.947E+02	3.734E+02	3.626E+02	3.572E+02	3.545E+02	3.518E+02	3.505E+02	3.500E+02	1.828E-02
9	4.204E+02	3.910E+02	3.715E+02	3.616E+02	3.566E+02	3.542E+02	3.517E+02	3.504E+02	3.500E+02	1.790E-02
8	4.157E+02	3.862E+02	3.690E+02	3.603E+02	3.559E+02	3.537E+02	3.515E+02	3.504E+02	3.500E+02	1.725E-02
7	4.089E+02	3.810E+02	3.662E+02	3.588E+02	3.550E+02	3.531E+02	3.513E+02	3.503E+02	3.500E+02	1.615E-02
6	3.992E+02	3.751E+02	3.631E+02	3.571E+02	3.540E+02	3.525E+02	3.510E+02	3.503E+02	3.500E+02	1.429E-02
5	3.877E+02	3.688E+02	3.598E+02	3.553E+02	3.530E+02	3.519E+02	3.508E+02	3.502E+02	3.500E+02	1.111E-02
4	3.760E+02	3.626E+02	3.565E+02	3.535E+02	3.520E+02	3.513E+02	3.505E+02	3.501E+02	3.500E+02	7.937E-03
3	3.686E+02	3.589E+02	3.545E+02	3.525E+02	3.515E+02	3.509E+02	3.504E+02	3.501E+02	3.500E+02	4.762E-03
2	3.856E+02	3.615E+02	3.462E+02	3.391E+02	3.370E+02	3.378E+02	3.430E+02	3.472E+02	3.500E+02	1.587E-03
1	4.500E+02	4.500E+02	4.500E+02	4.500E+02	4.500E+02	4.500E+02	4.500E+02	4.500E+02	3.500E+02	-1.587E-03
X=	0.0091903	0.0093909	0.0094912	0.0095413	0.0095664	0.0095789	0.0095915	0.0095977	0.0096022	

J \ I=	1	2	3	4	5	6	7	8	9	10	11	Y =
50	1.031E-01	1.031E-01	1.031E-01	1.031E-01	1.031E-01	1.031E-01	1.031E-01	1.032E-01	1.062E-01	1.106E-01	1.263E-01	0.0420
49	1.031E-01	1.031E-01	1.031E-01	1.031E-01	1.031E-01	1.031E-01	1.031E-01	1.032E-01	1.063E-01	1.107E-01	1.263E-01	0.0388
48	1.031E-01	1.031E-01	1.031E-01	1.031E-01	1.031E-01	1.031E-01	1.031E-01	1.031E-01	1.063E-01	1.104E-01	1.235E-01	0.0357
47	1.031E-01	1.031E-01	1.031E-01	1.031E-01	1.031E-01	1.031E-01	1.030E-01	1.027E-01	1.062E-01	1.100E-01	1.193E-01	0.0325
46	1.030E-01	1.030E-01	1.030E-01	1.030E-01	1.030E-01	1.030E-01	1.029E-01	1.027E-01	1.062E-01	1.097E-01	1.156E-01	0.0293
45	1.030E-01	1.030E-01	1.030E-01	1.030E-01	1.030E-01	1.029E-01	1.028E-01	1.027E-01	1.063E-01	1.097E-01	1.133E-01	0.0261
44	1.030E-01	1.030E-01	1.030E-01	1.030E-01	1.030E-01	1.029E-01	1.027E-01	1.027E-01	1.069E-01	1.105E-01	1.135E-01	0.0252
43	1.029E-01	1.029E-01	1.029E-01	1.030E-01	1.029E-01	1.029E-01	1.027E-01	1.027E-01	1.076E-01	1.115E-01	1.145E-01	0.0243
42	1.029E-01	1.029E-01	1.029E-01	1.029E-01	1.029E-01	1.028E-01	1.027E-01	1.027E-01	1.084E-01	1.127E-01	1.156E-01	0.0239
41	1.029E-01	1.029E-01	1.029E-01	1.029E-01	1.029E-01	1.028E-01	1.027E-01	1.027E-01	1.092E-01	1.137E-01	1.165E-01	0.0235
40	1.029E-01	1.029E-01	1.029E-01	1.029E-01	1.029E-01	1.028E-01	1.019E-01	1.027E-01	1.102E-01	1.149E-01	1.176E-01	0.0232
39	1.029E-01	1.029E-01	1.029E-01	1.029E-01	1.029E-01	1.028E-01	1.013E-01	1.028E-01	1.112E-01	1.162E-01	1.186E-01	0.0230
38	1.027E-01	1.027E-01	1.027E-01	1.028E-01	1.029E-01	1.028E-01	1.012E-01	1.029E-01	1.121E-01	1.172E-01	1.195E-01	0.0228
37	1.026E-01	1.026E-01	1.026E-01	1.026E-01	1.029E-01	1.028E-01	1.011E-01	1.030E-01	1.131E-01	1.184E-01	1.205E-01	0.0226
36	1.023E-01	1.023E-01	1.023E-01	1.025E-01	1.029E-01	1.029E-01	1.009E-01	1.032E-01	1.143E-01	1.198E-01	1.216E-01	0.0224
35	1.019E-01	1.019E-01	1.019E-01	1.022E-01	1.028E-01	1.026E-01	1.006E-01	1.034E-01	1.158E-01	1.214E-01	1.229E-01	0.0222
34	1.010E-01	1.010E-01	1.010E-01	1.014E-01	1.025E-01	1.011E-01	1.002E-01	1.037E-01	1.173E-01	1.230E-01	1.241E-01	0.0220
33	1.000E-01	1.001E-01	1.003E-01	1.007E-01	1.015E-01	1.004E-01	1.001E-01	1.039E-01	1.184E-01	1.242E-01	1.249E-01	0.0220
32	1.000E-01	1.000E-01	1.000E-01	1.000E-01	1.001E-01	1.000E-01	1.001E-01	1.042E-01	1.196E-01	1.255E-01	1.259E-01	0.0218
31	1.000E-01	1.000E-01	1.000E-01	1.000E-01	1.000E-01	1.000E-01	1.001E-01	1.048E-01	1.219E-01	1.280E-01	1.277E-01	0.0216
30	1.000E-01	1.000E-01	1.000E-01	1.000E-01	1.000E-01	1.000E-01	1.001E-01	1.057E-01	1.251E-01	1.315E-01	1.302E-01	0.0213
29	1.000E-01	1.000E-01	1.000E-01	1.000E-01	1.000E-01	1.000E-01	1.002E-01	1.069E-01	1.289E-01	1.356E-01	1.327E-01	0.0211
28	1.000E-01	1.000E-01	1.000E-01	1.000E-01	1.000E-01	1.000E-01	1.002E-01	1.084E-01	1.334E-01	1.406E-01	1.348E-01	0.0209
27	1.000E-01	1.000E-01	1.000E-01	1.000E-01	1.000E-01	1.000E-01	1.003E-01	1.101E-01	1.375E-01	1.451E-01	1.364E-01	0.0207
26	1.000E-01	1.000E-01	1.000E-01	1.000E-01	1.000E-01	1.000E-01	1.005E-01	1.119E-01	1.409E-01	1.486E-01	1.375E-01	0.0206
25	1.000E-01	1.000E-01	1.000E-01	1.000E-01	1.000E-01	1.000E-01	1.006E-01	1.134E-01	1.435E-01	1.503E-01	1.380E-01	0.0205
24	1.000E-01	1.000E-01	1.000E-01	1.000E-01	1.000E-01	1.000E-01	1.007E-01	1.146E-01	1.451E-01	1.516E-01	1.384E-01	0.0204
23	1.000E-01	1.000E-01	1.000E-01	1.000E-01	1.000E-01	1.000E-01	1.009E-01	1.159E-01	1.467E-01	1.527E-01	1.388E-01	0.0203
22	1.000E-01	1.000E-01	1.000E-01	1.000E-01	1.000E-01	1.000E-01	1.011E-01	1.173E-01	1.483E-01	1.537E-01	1.392E-01	0.0203
21	1.000E-01	1.000E-01	1.000E-01	1.000E-01	1.000E-01	1.000E-01	1.013E-01	1.188E-01	1.498E-01	1.545E-01	1.396E-01	0.0202
20	1.000E-01	1.000E-01	1.000E-01	1.000E-01	1.000E-01	1.000E-01	1.017E-01	1.215E-01	1.520E-01	1.556E-01	1.401E-01	0.0200
19	1.000E-01	1.000E-01	1.000E-01	1.000E-01	1.000E-01	1.001E-01	1.026E-01	1.255E-01	1.547E-01	1.562E-01	1.405E-01	0.0199
18	1.000E-01	1.000E-01	1.000E-01	1.000E-01	1.000E-01	1.002E-01	1.044E-01	1.315E-01	1.575E-01	1.565E-01	1.407E-01	0.0196
17	1.000E-01	1.000E-01	1.000E-01	1.000E-01	1.001E-01	1.007E-01	1.085E-01	1.393E-01	1.599E-01	1.565E-01	1.409E-01	0.0194
16	1.000E-01	1.000E-01	1.000E-01	1.001E-01	1.006E-01	1.024E-01	1.169E-01	1.456E-01	1.612E-01	1.568E-01	1.412E-01	0.0192
15	1.000E-01	1.000E-01	1.003E-01	1.013E-01	1.038E-01	1.085E-01	1.297E-01	1.486E-01	1.621E-01	1.572E-01	1.414E-01	0.0189
14	1.000E-01	1.014E-01	1.039E-01	1.081E-01	1.124E-01	1.154E-01	1.320E-01	1.495E-01	1.626E-01	1.576E-01	1.416E-01	0.0188
13	1.073E-01	1.074E-01	1.082E-01	1.107E-01	1.145E-01	1.174E-01	1.321E-01	1.499E-01	1.628E-01	1.578E-01	1.416E-01	0.0187
12	1.107E-01	1.108E-01	1.112E-01	1.127E-01	1.160E-01	1.188E-01	1.321E-01	1.501E-01	1.630E-01	1.577E-01	1.417E-01	0.0186
11	1.139E-01	1.140E-01	1.142E-01	1.151E-01	1.175E-01	1.201E-01	1.821E-01	1.504E-01	1.632E-01	1.574E-01	1.418E-01	0.0185
10	1.164E-01	1.165E-01	1.166E-01	1.170E-01	1.185E-01	1.207E-01	1.322E-01	1.510E-01	1.636E-01	1.573E-01	1.421E-01	0.0183
9	1.180E-01	1.181E-01	1.181E-01	1.183E-01	1.190E-01	1.207E-01	1.326E-01	1.520E-01	1.644E-01	1.578E-01	1.433E-01	0.0179
8	1.190E-01	1.191E-01	1.191E-01	1.192E-01	1.196E-01	1.209E-01	1.333E-01	1.535E-01	1.658E-01	1.593E-01	1.459E-01	0.0173
7	1.194E-01	1.195E-01	1.195E-01	1.196E-01	1.198E-01	1.212E-01	1.347E-01	1.558E-01	1.682E-01	1.618E-01	1.514E-01	0.0162
6	1.191E-01	1.193E-01	1.193E-01	1.193E-01	1.196E-01	1.216E-01	1.368E-01	1.589E-01	1.720E-01	1.647E-01	1.622E-01	0.0143
5	1.183E-01	1.184E-01	1.184E-01	1.185E-01	1.190E-01	1.224E-01	1.395E-01	1.622E-01	1.767E-01	1.697E-01	1.785E-01	0.0111
4	1.163E-01	1.164E-01	1.164E-01	1.165E-01	1.173E-01	1.225E-01	1.415E-01	1.624E-01	1.815E-01	1.829E-01	2.005E-01	0.0079
3	1.119E-01	1.119E-01	1.119E-01	1.120E-01	1.128E-01	1.181E-01	1.332E-01	1.518E-01	1.793E-01	2.021E-01	2.209E-01	0.0048
2	1.030E-01	1.030E-01	1.030E-01	1.031E-01	1.036E-01	1.057E-01	1.126E-01	1.210E-01	1.353E-01	1.595E-01	1.822E-01	0.0016
1	1.180E-01	1.000E-01	1.000E-01	1.000E-01	1.000E-01	1.000E-01	1.000E-01	1.000E-01	1.000E-01	1.000E-01	1.000E-01	-0.0016
X=	-0.0000125	0.0000125	0.0000627	0.0001630	0.0003636	0.0007648	0.0015672	0.0031721	0.0063818	0.0079866	0.0087890	

J \ I=	12	13	14	15	16	17	18	19	20	21	22	Y =
50	1.794E-01	2.358E-01	2.673E-01	2.834E-01	2.915E-01	2.955E-01	2.995E-01	3.016E-01	3.023E-01	4.202E-02		
49	1.793E-01	2.358E-01	2.673E-01	2.834E-01	2.915E-01	2.955E-01	2.996E-01	3.016E-01	3.023E-01	3.884E-02		
48	1.718E-01	2.316E-01	2.651E-01	2.822E-01	2.908E-01	2.951E-01	2.994E-01	3.015E-01	3.023E-01	3.567E-02		
47	1.589E-01	2.214E-01	2.598E-01	2.792E-01	2.891E-01	2.940E-01	2.989E-01	3.014E-01	3.023E-01	3.249E-02		
46	[illegible]	[illegible]	[illegible]	[illegible]	[illegible]	[illegible]	[illegible]	[illegible]	[illegible]	[illegible]		

[illegible]	[illegible]	[illegible]	[illegible]	[illegible]	[illegible]	[illegible]	[illegible]	[illegible]	[illegible]	[illegible]
45	1.273E-01	1.820E-01	2.357E-01	2.660E-01	2.814E-01	2.892E-01	2.970E-01	3.008E-01	3.022E-01	2.614E-02
44	1.177E-01	1.582E-01	2.173E-01	2.552E-01	2.752E-01	2.852E-01	2.953E-01	3.004E-01	3.022E-01	2.521E-02
43	1.170E-01	1.498E-01	2.097E-01	2.507E-01	2.726E-01	2.836E-01	2.946E-01	3.002E-01	3.022E-01	2.428E-02
42	1.176E-01	1.428E-01	2.018E-01	2.455E-01	2.694E-01	2.816E-01	2.938E-01	3.000E-01	3.022E-01	2.391E-02
41	1.183E-01	1.405E-01	1.991E-01	2.437E-01	2.683E-01	2.809E-01	2.936E-01	2.999E-01	3.022E-01	2.354E-02
40	1.191E-01	1.387E-01	1.970E-01	2.425E-01	2.677E-01	2.805E-01	2.934E-01	2.998E-01	3.022E-01	2.318E-02
39	1.199E-01	1.367E-01	1.935E-01	2.400E-01	2.661E-01	2.795E-01	2.930E-01	2.997E-01	3.022E-01	2.298E-02
38	1.205E-01	1.358E-01	1.919E-01	2.388E-01	2.654E-01	2.790E-01	2.928E-01	2.997E-01	3.022E-01	2.278E-02
37	1.212E-01	1.351E-01	1.901E-01	2.375E-01	2.646E-01	2.786E-01	2.926E-01	2.996E-01	3.022E-01	2.259E-02
36	1.220E-01	1.360E-01	1.916E-01	2.386E-01	2.652E-01	2.789E-01	2.927E-01	2.997E-01	3.022E-01	2.239E-02
35	1.231E-01	1.392E-01	1.951E-01	2.408E-01	2.666E-01	2.798E-01	2.931E-01	2.998E-01	3.022E-01	2.219E-02
34	1.239E-01	1.405E-01	1.963E-01	2.415E-01	2.669E-01	2.800E-01	2.932E-01	2.998E-01	3.022E-01	2.204E-02
33	1.243E-01	1.408E-01	1.970E-01	2.422E-01	2.675E-01	2.803E-01	2.933E-01	2.998E-01	3.022E-01	2.196E-02
32	1.252E-01	1.415E-01	1.975E-01	2.425E-01	2.676E-01	2.804E-01	2.933E-01	2.998E-01	3.022E-01	2.181E-02
31	1.263E-01	1.434E-01	1.992E-01	2.435E-01	2.682E-01	2.808E-01	2.935E-01	2.999E-01	3.022E-01	2.157E-02
30	1.276E-01	1.460E-01	2.020E-01	2.454E-01	2.693E-01	2.815E-01	2.938E-01	3.000E-01	3.022E-01	2.134E-02
29	1.288E-01	1.496E-01	2.058E-01	2.479E-01	2.708E-01	2.825E-01	2.942E-01	3.001E-01	3.022E-01	2.111E-02
28	1.298E-01	1.530E-01	2.094E-01	2.502E-01	2.722E-01	2.833E-01	2.946E-01	3.002E-01	3.022E-01	2.088E-02
27	1.305E-01	1.560E-01	2.127E-01	2.524E-01	2.735E-01	2.842E-01	2.949E-01	3.003E-01	3.022E-01	2.072E-02
26	1.310E-01	1.584E-01	2.153E-01	2.540E-01	2.745E-01	2.848E-01	2.952E-01	3.003E-01	3.022E-01	2.057E-02
25	1.313E-01	1.601E-01	2.172E-01	2.553E-01	2.752E-01	2.853E-01	2.953E-01	3.004E-01	3.022E-01	2.049E-02
24	1.317E-01	1.619E-01	2.192E-01	2.565E-01	2.760E-01	2.857E-01	2.955E-01	3.004E-01	3.022E-01	2.041E-02
23	1.321E-01	1.639E-01	2.213E-01	2.578E-01	2.767E-01	2.862E-01	2.957E-01	3.005E-01	3.022E-01	2.034E-02
22	1.327E-01	1.660E-01	2.234E-01	2.591E-01	2.775E-01	2.867E-01	2.959E-01	3.006E-01	3.022E-01	2.026E-02
21	1.336E-01	1.693E-01	2.266E-01	2.610E-01	2.786E-01	2.874E-01	2.962E-01	3.006E-01	3.022E-01	2.018E-02
20	1.351E-01	1.737E-01	2.305E-01	2.633E-01	2.799E-01	2.882E-01	2.965E-01	3.007E-01	3.022E-01	2.003E-02
19	1.371E-01	1.791E-01	2.349E-01	2.657E-01	2.813E-01	2.891E-01	2.969E-01	3.008E-01	3.022E-01	1.987E-02
18	1.397E-01	1.852E-01	2.395E-01	2.682E-01	2.827E-01	2.900E-01	2.973E-01	3.009E-01	3.022E-01	1.964E-02
17	1.424E-01	1.910E-01	2.433E-01	2.703E-01	2.839E-01	2.907E-01	2.976E-01	3.010E-01	3.022E-01	1.941E-02
16	1.451E-01	1.962E-01	2.465E-01	2.721E-01	2.849E-01	2.914E-01	2.978E-01	3.011E-01	3.022E-01	1.917E-02
15	1.473E-01	2.001E-01	2.488E-01	2.734E-01	2.857E-01	2.918E-01	2.980E-01	3.011E-01	3.022E-01	1.894E-02
14	1.484E-01	2.022E-01	2.500E-01	2.740E-01	2.861E-01	2.921E-01	2.981E-01	3.011E-01	3.022E-01	1.879E-02
13	1.490E-01	2.034E-01	2.506E-01	2.743E-01	2.862E-01	2.922E-01	2.982E-01	3.012E-01	3.022E-01	1.871E-02
12	1.499E-01	2.053E-01	2.515E-01	2.748E-01	2.865E-01	2.923E-01	2.982E-01	3.012E-01	3.022E-01	1.863E-02
11	1.518E-01	2.086E-01	2.532E-01	2.757E-01	2.870E-01	2.927E-01	2.984E-01	3.012E-01	3.022E-01	1.850E-02
10	1.555E-01	2.141E-01	2.560E-01	2.773E-01	2.880E-01	2.933E-01	2.986E-01	3.013E-01	3.022E-01	1.828E-02
9	1.619E-01	2.218E-01	2.600E-01	2.795E-01	2.892E-01	2.941E-01	2.989E-01	3.014E-01	3.022E-01	1.790E-02
8	1.722E-01	2.313E-01	2.650E-01	2.822E-01	2.908E-01	2.950E-01	2.993E-01	3.015E-01	3.022E-01	1.725E-02
7	1.868E-01	2.417E-01	2.706E-01	2.852E-01	2.925E-01	2.961E-01	2.998E-01	3.016E-01	3.022E-01	1.615E-02
6	2.071E-01	2.535E-01	2.769E-01	2.886E-01	2.944E-01	2.973E-01	3.003E-01	3.017E-01	3.022E-01	1.429E-02
5	2.303E-01	2.661E-01	2.835E-01	2.922E-01	2.965E-01	2.986E-01	3.008E-01	3.018E-01	3.022E-01	1.111E-02
4	2.543E-01	2.786E-01	2.900E-01	2.957E-01	2.985E-01	2.999E-01	3.013E-01	3.020E-01	3.022E-01	7.937E-03
3	2.578E-01	2.777E-01	2.892E-01	2.952E-01	2.982E-01	2.997E-01	3.012E-01	3.020E-01	3.022E-01	4.762E-03
2	2.062E-01	2.417E-01	2.672E-01	2.824E-01	2.906E-01	2.948E-01	2.992E-01	3.014E-01	3.022E-01	1.587E-03
1	1.000E-01	1.000E-01	1.000E-01	1.000E-01	1.000E-01	1.000E-01	1.000E-01	1.000E-01	3.022E-01	-1.587E-03
X=	0.0091903	0.0093909	0.0094912	0.0095413	0.0095664	0.0095789	0.0095915	0.0095977	0.0096022	

- VIS VIS VIS VIS VIS VIS VIS VIS VIS -*

I=	1	2	3	4	5	6	7	8	9	10	11	Y =
50	2.334E-05	2.334E-05	2.334E-05	2.334E-05	2.333E-05	2.333E-05	2.331E-05	2.329E-05	2.318E-05	2.304E-05	2.254E-05	0.0420
49	2.334E-05	2.334E-05	2.334E-05	2.334E-05	2.333E-05	2.333E-05	2.331E-05	2.329E-05	2.318E-05	2.304E-05	2.254E-05	0.0388
48	2.334E-05	2.334E-05	2.334E-05	2.334E-05	2.333E-05	2.333E-05	2.331E-05	2.329E-05	2.318E-05	2.305E-05	2.263E-05	0.0357
47	2.334E-05	2.334E-05	2.334E-05	2.333E-05	2.333E-05	2.332E-05	2.331E-05	2.330E-05	2.319E-05	2.306E-05	2.276E-05	0.0325
46	2.334E-06	2.334E-05	2.334E-05	2.333E-05	2.332E-05	2.331E-05	2.331E-05	2.330E-05	2.319E-05	2.307E-05	2.288E-05	0.0293
45	2.334E-05	2.334E-05	2.334E-05	2.333E-05	2.332E-05	2.331E-05	2.330E-05	2.330E-05	2.318E-05	2.307E-05	2.296E-05	0.0261
44	2.334E-05	2.334E-05	2.334E-05	2.333E-05	2.332E-05	2.331E-05	2.330E-05	2.330E-05	2.316E-05	2.305E-05	2.295E-05	0.0252
43	2.334E-05	2.334E-05	2.334E-05	2.333E-05	2.333E-05	2.331E-05	2.331E-05	2.330E-05	2.314E-05	2.301E-05	2.292E-05	0.0243
42	2.334E-05	2.334E-05	2.334E-05	2.334E-05	2.333E-05	2.331E-05	2.331E-05	2.330E-05	2.311E-05	2.297E-05	2.288E-05	0.0239
41	2.334E-05	2.334E-05	2.334E-05	2.334E-05	2.333E-05	2.332E-05	2.331E-05	2.330E-05	2.309E-05	2.294E-05	2.285E-05	0.0235
40	2.334E-05	2.334E-05	2.334E-05	2.334E-05	2.333E-05	2.332E-05	2.334E-05	2.330E-05	2.305E-05	2.290E-05	2.281E-05	0.0232
39	2.334E-05	2.334E-05	2.334E-05	2.334E-05	2.333E-05	2.332E-05	2.335E-05	2.330E-05	2.302E-05	2.286E-05	2.278E-05	0.0230
38	2.334E-05	2.334E-05	2.334E-05	2.334E-05	2.333E-05	2.332E-05	2.336E-05	2.329E-05	2.299E-05	2.283E-05	2.275E-05	0.0228
37	2.335E-05	2.335E-05	2.334E-05	2.334E-05	2.333E-05	2.332E-05	2.336E-05	2.329E-05	2.296E-05	2.279E-05	2.272E-05	0.0226
36	2.335E-05	2.335E-05	2.335E-05	2.334E-05	2.333E-05	2.332E-05	2.336E-05	2.328E-05	2.292E-05	2.274E-05	2.269E-05	0.0224
35	2.335E-05	2.335E-05	2.335E-05	2.335E-05	2.333E-05	2.333E-05	2.337E-05	2.327E-05	2.287E-05	2.269E-05	2.264E-05	0.0222
34	2.337E-05	2.337E-05	2.337E-05	2.336E-05	2.334E-05	2.336E-05	2.338E-05	2.326E-05	2.282E-05	2.264E-05	2.260E-05	0.0220
33	2.338E-05	2.338E-05	2.338E-05	2.337E-05	2.336E-05	2.337E-05	2.338E-05	2.326E-05	2.279E-05	2.260E-05	2.258E-05	0.0220
32	2.338E-05	2.338E-05	2.338E-05	2.338E-05	2.338E-05	2.338E-05	2.338E-05	2.325E-05	2.275E-05	2.256E-05	2.255E-05	0.0218
31	2.338E-05	2.338E-05	2.338E-05	2.338E-05	2.338E-05	2.338E-05	2.338E-05	2.323E-05	2.268E-05	2.248E-05	2.249E-05	0.0216
30	2.338E-05	2.338E-05	2.338E-05	2.338E-05	2.338E-05	2.338E-05	2.338E-05	2.320E-05	2.257E-05	2.237E-05	2.241E-05	0.0213
29	2.338E-05	2.338E-05	2.338E-05	2.338E-05	2.338E-05	2.338E-05	2.338E-05	2.316E-05	2.245E-05	2.223E-05	2.233E-05	0.0211
28	2.338E-05	2.338E-05	2.338E-05	2.338E-05	2.338E-05	2.338E-05	2.337E-05	2.311E-05	2.231E-05	2.207E-05	2.226E-05	0.0209
27	2.338E-05	2.338E-05	2.338E-05	2.338E-05	2.338E-05	2.338E-05	2.337E-05	2.306E-05	2.218E-05	2.192E-05	2.220E-05	0.0207
26	2.338E-05	2.338E-05	2.338E-05	2.338E-05	2.338E-05	2.338E-05	2.337E-05	2.300E-05	2.207E-05	2.181E-05	2.217E-05	0.0206
25	2.338E-05	2.338E-05	2.338E-05	2.338E-05	2.338E-05	2.338E-05	2.336E-05	2.295E-05	2.198E-05	2.175E-05	2.215E-05	0.0205
24	2.338E-05	2.338E-05	2.338E-05	2.338E-05	2.338E-05	2.338E-05	2.336E-05	2.292E-05	2.193E-05	2.171E-05	2.213E-05	0.0204
23	2.338E-05	2.338E-05	2.338E-05	2.338E-05	2.338E-05	2.338E-05	2.336E-05	2.287E-05	2.188E-05	2.167E-05	2.212E-05	0.0203
22	2.338E-05	2.338E-05	2.338E-05	2.338E-05	2.338E-05	2.338E-05	2.335E-05	2.283E-05	2.183E-05	2.164E-05	2.211E-05	0.0203
21	2.338E-05	2.338E-05	2.338E-05	2.338E-05	2.338E-05	2.338E-05	2.334E-05	2.278E-05	2.178E-05	2.161E-05	2.209E-05	0.0202
20	2.338E-05	2.338E-05	2.338E-05	2.338E-05	2.338E-05	2.338E-05	2.333E-05	2.270E-05	2.171E-05	2.158E-05	2.208E-05	0.0200
19	2.338E-05	2.338E-05	2.338E-05	2.338E-05	2.338E-05	2.338E-05	2.330E-05	2.257E-05	2.162E-05	2.156E-05	2.206E-05	0.0199
18	2.338E-05	2.338E-05	2.338E-05	2.338E-05	2.338E-05	2.338E-05	2.325E-05	2.237E-05	2.153E-05	2.165E-05	2.206E-05	0.0196
17	2.338E-05	2.338E-05	2.338E-05	2.338E-05	2.338E-05	2.336E-05	2.313E-05	2.212E-05	2.145E-05	2.155E-05	2.205E-05	0.0194
16	2.338E-05	2.338E-05	2.338E-05	2.338E-05	2.337E-05	2.333E-05	2.287E-05	2.192E-05	2.141E-05	2.154E-05	2.204E-05	0.0192
15	2.338E-05	2.338E-05	2.338E-05	2.336E-05	2.330E-05	2.318E-05	2.248E-05	2.182E-05	2.138E-05	2.152E-05	2.203E-05	0.0189
14	2.338E-05	2.336E-05	2.331E-05	2.322E-05	2.309E-05	2.300E-05	2.240E-05	2.179E-05	2.137E-05	2.151E-05	2.203E-05	0.0188
13	2.328E-05	2.327E-05	2.324E-05	2.317E-05	2.305E-05	2.295E-05	2.240E-05	2.178E-05	2.136E-05	2.150E-05	2.202E-05	0.0187
12	2.323E-05	2.323E-05	2.320E-05	2.313E-05	2.301E-05	2.292E-05	2.240E-05	2.177E-05	2.135E-05	2.151E-05	2.201E-05	0.0186
11	2.319E-05	2.318E-05	2.316E-05	2.310E-05	2.299E-05	2.290E-05	2.240E-05	2.176E-05	2.135E-05	2.152E-05	2.201E-05	0.0185
10	2.316E-05	2.315E-05	2.313E-05	2.308E-05	2.299E-05	2.289E-05	2.239E-05	2.174E-05	2.133E-05	2.152E-05	2.199E-05	0.0183
9	2.313E-05	2.313E-05	2.311E-05	2.308E-05	2.301E-05	2.289E-05	2.237E-05	2.170E-05	2.131E-05	2.151E-05	2.195E-05	0.0179
8	2.312E-05	2.312E-05	2.310E-05	2.308E-05	2.303E-05	2.288E-05	2.234E-05	2.165E-05	2.126E-05	2.146E-05	2.187E-05	0.0173
7	2.312E-05	2.311E-05	2.310E-05	2.307E-05	2.302E-05	2.285E-05	2.228E-05	2.157E-05	2.118E-05	2.139E-05	2.171E-05	0.0162
6	2.312E-05	2.311E-05	2.310E-05	2.306E-05	2.299E-05	2.280E-05	2.219E-05	2.147E-05	2.107E-05	2.130E-05	2.139E-05	0.0143
5	2.313E-05	2.312E-05	2.310E-05	2.306E-05	2.296E-05	2.273E-05	2.209E-05	2.136E-05	2.092E-05	2.115E-05	2.088E-05	0.0111
4	2.316E-05	2.315E-05	2.312E-05	2.307E-05	2.296E-05	2.268E-05	2.201E-05	2.135E-05	2.076E-05	2.074E-05	2.018E-05	0.0079
3	2.322E-05	2.321E-05	2.319E-05	2.315E-05	2.305E-05	2.280E-05	2.228E-05	2.168E-05	2.080E-05	2.009E-05	1.945E-05	0.0048
2	2.334E-05	2.334E-05	2.333E-05	2.332E-05	2.329E-05	2.320E-05	2.295E-05	2.267E-05	2.219E-05	2.138E-05	2.055E-05	0.0016
1	2.338E-05	2.338E-05	2.338E-05	2.338E-05	2.338E-05	2.338E-05	2.338E-05	2.338E-05	2.338E-05	2.338E-05	2.338E-05	-0.0016
X=	-0.0000125	0.0000125	0.0000627	0.0001630	0.0003636	0.0007648	0.0015672	0.0031721	0.0063818	0.0079866	0.0087890	

I= J	12	13	14	15	16	17	18	19	20	21	22	Y =
50	2.081E-05	1.897E-05	1.797E-05	1.747E-05	1.722E-05	1.710E-05	1.697E-05	1.691E-05	1.689E-05	4.202E-02		
49	2.081E-05	1.897E-05	1.797E-05	1.747E-05	1.722E-05	1.710E-05	1.697E-05	1.691E-05	1.689E-05	3.884E-02		
48	2.105E-05	1.910E-05	1.804E-05	1.751E-05	1.724E-05	1.711E-05	1.698E-05	1.691E-05	1.689E-05	3.567E-02		
47	2.147E-05	1.943E-05	1.821E-05	1.760E-05	1.730E-05	1.714E-05	1.699E-05	1.692E-05	1.689E-05	3.249E-02		
46	[illegible]	[illegible]	[illegible]	[illegible]	[illegible]	[illegible]	[illegible]	[illegible]	[illegible]	[illegible]		

[illegible]	[illegible]	[illegible]	[illegible]	[illegible]	[illegible]	[illegible]	[illegible]	[illegible]	[illegible]
45	2.251E-05	2.072E-05	1.897E-05	1.801E-05	1.753E-05	1.729E-05	1.705E-05	1.693E-05	1.689E-05 2.614E-02
44	2.282E-05	2.151E-05	1.958E-05	1.836E-05	1.773E-05	1.742E-05	1.710E-05	1.695E-05	1.689E-05 2.521E-02
43	2.283E-05	2.179E-05	1.983E-05	1.850E-05	1.781E-05	1.747E-05	1.712E-05	1.695E-05	1.689E-05 2.428E-02
42	2.281E-05	2.203E-05	2.009E-05	1.868E-05	1.792E-05	1.753E-05	1.715E-05	1.696E-05	1.689E-05 2.391E-02
41	2.279E-05	2.210E-05	2.018E-05	1.873E-05	1.795E-05	1.755E-05	1.716E-05	1.696E-05	1.689E-05 2.354E-02
40	2.276E-05	2.216E-05	2.025E-05	1.877E-05	1.797E-05	1.757E-05	1.716E-05	1.696E-05	1.689E-05 2.318E-02
39	2.274E-05	2.222E-05	2.036E-05	1.885E-05	1.802E-05	1.760E-05	1.718E-05	1.697E-05	1.689E-05 2.298E-02
38	2.272E-05	2.225E-05	2.042E-05	1.889E-05	1.804E-05	1.761E-05	1.718E-05	1.697E-05	1.689E-05 2.276E-02
37	2.270E-05	2.227E-05	2.048E-05	1.894E-05	1.807E-05	1.763E-05	1.719E-05	1.697E-05	1.689E-05 2.259E-02
36	2.267E-05	2.224E-05	2.043E-05	1.890E-05	1.805E-05	1.762E-05	1.719E-05	1.697E-05	1.689E-05 2.239E-02
35	2.264E-05	2.214E-05	2.031E-05	1.883E-05	1.801E-05	1.759E-05	1.717E-05	1.697E-05	1.689E-05 2.219E-02
34	2.261E-05	2.210E-05	2.028E-05	1.881E-05	1.800E-05	1.758E-05	1.717E-05	1.697E-05	1.689E-05 2.204E-02
33	2.260E-05	2.209E-05	2.025E-05	1.878E-05	1.798E-05	1.757E-05	1.717E-05	1.696E-05	1.689E-05 2.196E-02
32	2.257E-05	2.206E-05	2.023E-05	1.878E-05	1.798E-05	1.757E-05	1.717E-05	1.696E-05	1.689E-05 2.181E-02
31	2.253E-05	2.201E-05	2.018E-05	1.875E-05	1.796E-05	1.756E-05	1.716E-05	1.696E-05	1.689E-05 2.157E-02
30	2.249E-05	2.192E-05	2.009E-05	1.869E-05	1.792E-05	1.754E-05	1.715E-05	1.696E-05	1.689E-05 2.134E-02
29	2.245E-05	2.181E-05	1.997E-05	1.860E-05	1.787E-05	1.751E-05	1.714E-05	1.696E-05	1.689E-05 2.111E-02
28	2.242E-05	2.170E-05	1.985E-05	1.853E-05	1.783E-05	1.748E-05	1.713E-05	1.695E-05	1.689E-05 2.088E-02
27	2.240E-05	2.160E-05	1.974E-05	1.846E-05	1.779E-05	1.745E-05	1.712E-05	1.695E-05	1.689E-05 2.072E-02
26	2.238E-05	2.152E-05	1.966E-05	1.841E-05	1.776E-05	1.743E-05	1.711E-05	1.695E-05	1.689E-05 2.057E-02
25	2.237E-05	2.146E-05	1.960E-05	1.837E-05	1.774E-05	1.742E-05	1.710E-05	1.695E-05	1.689E-05 2.049E-02
24	2.236E-05	2.140E-05	1.953E-05	1.833E-05	1.771E-05	1.741E-05	1.710E-05	1.695E-05	1.689E-05 2.041E-02
23	2.234E-05	2.134E-05	1.946E-05	1.829E-05	1.769E-05	1.739E-05	1.709E-05	1.694E-05	1.689E-05 2.034E-02
22	2.233E-05	2.127E-05	1.939E-05	1.825E-05	1.766E-05	1.737E-05	1.709E-05	1.694E-05	1.689E-05 2.026E-02
21	2.230E-05	2.116E-05	1.929E-05	1.819E-05	1.763E-05	1.735E-05	1.708E-05	1.694E-05	1.689E-05 2.018E-02
20	2.225E-05	2.102E-05	1.916E-05	1.811E-05	1.759E-05	1.733E-05	1.707E-05	1.694E-05	1.689E-05 2.003E-02
19	2.219E-05	2.084E-05	1.902E-05	1.803E-05	1.754E-05	1.730E-05	1.706E-05	1.693E-05	1.689E-05 1.987E-02
18	2.210E-05	2.064E-05	1.887E-05	1.795E-05	1.750E-05	1.727E-05	1.704E-05	1.693E-05	1.689E-05 1.964E-02
17	2.202E-05	2.045E-05	1.875E-05	1.789E-05	1.746E-05	1.725E-05	1.704E-05	1.693E-05	1.689E-05 1.941E-02
16	2.193E-05	2.027E-05	1.864E-05	1.783E-05	1.743E-05	1.723E-05	1.703E-05	1.693E-05	1.689E-05 1.917E-02
15	2.185E-05	2.014E-05	1.857E-05	1.779E-05	1.740E-05	1.721E-05	1.702E-05	1.693E-05	1.689E-05 1.894E-02
14	2.181E-05	2.008E-05	1.853E-05	1.777E-05	1.739E-05	1.720E-05	1.702E-05	1.692E-05	1.689E-05 1.879E-02
13	2.179E-05	2.004E-05	1.851E-05	1.776E-05	1.739E-05	1.720E-05	1.702E-05	1.692E-05	1.689E-05 1.871E-02
12	2.176E-05	1.998E-05	1.848E-05	1.775E-05	1.738E-05	1.720E-05	1.702E-05	1.692E-05	1.689E-05 1.863E-02
11	2.169E-05	1.987E-05	1.843E-05	1.772E-05	1.736E-05	1.719E-05	1.701E-05	1.692E-05	1.689E-05 1.850E-02
10	2.158E-05	1.970E-05	1.834E-05	1.767E-05	1.734E-05	1.717E-05	1.700E-05	1.692E-05	1.689E-05 1.828E-02
9	2.138E-05	1.946E-05	1.822E-05	1.761E-05	1.730E-05	1.715E-05	1.699E-05	1.692E-05	1.689E-05 1.790E-02
8	2.106E-05	1.915E-05	1.807E-05	1.752E-05	1.725E-05	1.712E-05	1.698E-05	1.692E-05	1.689E-05 1.725E-02
7	2.061E-05	1.882E-05	1.789E-05	1.743E-05	1.720E-05	1.708E-05	1.697E-05	1.691E-05	1.689E-05 1.615E-02
6	1.996E-05	1.845E-05	1.770E-05	1.732E-05	1.714E-05	1.705E-05	1.695E-05	1.691E-05	1.689E-05 1.429E-02
5	1.922E-05	1.805E-05	1.749E-05	1.721E-05	1.707E-05	1.701E-05	1.694E-05	1.690E-05	1.689E-05 1.111E-02
4	1.847E-05	1.766E-05	1.729E-05	1.710E-05	1.701E-05	1.697E-05	1.692E-05	1.690E-05	1.689E-05 7.937E-03
3	1.813E-05	1.752E-05	1.721E-05	1.707E-05	1.699E-05	1.696E-05	1.692E-05	1.690E-05	1.689E-05 4.762E-03
2	1.943E-05	1.802E-05	1.711E-05	1.666E-05	1.649E-05	1.647E-05	1.664E-05	1.679E-05	1.689E-05 1.587E-03
1	2.338E-05	2.338E-05	2.338E-05	2.338E-05	2.338E-05	2.338E-05	2.338E-05	2.338E-05	2.338E-05-1.587E-03
X=	0.0091903	0.0093909	0.0094912	0.0095413	0.0095664	0.0095789	0.0095915	0.0095977	0.0096022

- DEN DEN DEN DEN DEN DEN DEN DEN DEN -

J \ I=	1	2	3	4	5	6	7	8	9	10	11	Y =
50	7.383E-01	7.382E-01	7.383E-01	7.383E-01	7.385E-01	7.387E-01	7.392E-01	7.402E-01	7.416E-01	7.432E-01	7.490E-01	0.0420
49	7.383E-01	7.382E-01	7.383E-01	7.383E-01	7.385E-01	7.387E-01	7.392E-01	7.402E-01	7.416E-01	7.432E-01	7.490E-01	0.0388
48	7.383E-01	7.382E-01	7.383E-01	7.383E-01	7.385E-01	7.388E-01	7.393E-01	7.403E-01	7.416E-01	7.431E-01	7.479E-01	0.0357
47	7.383E-01	7.382E-01	7.383E-01	7.384E-01	7.386E-01	7.389E-01	7.394E-01	7.402E-01	7.415E-01	7.430E-01	7.464E-01	0.0325
46	7.384E-01	7.383E-01	7.384E-01	7.386E-01	7.389E-01	7.393E-01	7.397E-01	7.401E-01	7.415E-01	7.429E-01	7.450E-01	0.0293
45	7.384E-01	7.383E-01	7.384E-01	7.386E-01	7.390E-01	7.396E-01	7.400E-01	7.401E-01	7.416E-01	7.430E-01	7.443E-01	0.0261
44	7.384E-01	7.382E-01	7.383E-01	7.385E-01	7.389E-01	7.395E-01	7.399E-01	7.401E-01	7.418E-01	7.433E-01	7.445E-01	0.0252
43	7.384E-01	7.382E-01	7.383E-01	7.384E-01	7.388E-01	7.394E-01	7.398E-01	7.401E-01	7.421E-01	7.437E-01	7.449E-01	0.0243
42	7.384E-01	7.382E-01	7.383E-01	7.384E-01	7.388E-01	7.394E-01	7.398E-01	7.401E-01	7.425E-01	7.442E-01	7.454E-01	0.0239
41	7.384E-01	7.382E-01	7.383E-01	7.384E-01	7.387E-01	7.393E-01	7.397E-01	7.402E-01	7.428E-01	7.446E-01	7.457E-01	0.0235
40	7.384E-01	7.383E-01	7.383E-01	7.384E-01	7.387E-01	7.393E-01	7.395E-01	7.402E-01	7.432E-01	7.451E-01	7.462E-01	0.0232
39	7.384E-01	7.383E-01	7.383E-01	7.384E-01	7.387E-01	7.393E-01	7.393E-01	7.403E-01	7.436E-01	7.456E-01	7.466E-01	0.0230
38	7.385E-01	7.383E-01	7.384E-01	7.385E-01	7.387E-01	7.393E-01	7.393E-01	7.404E-01	7.439E-01	7.460E-01	7.469E-01	0.0228
37	7.385E-01	7.384E-01	7.384E-01	7.385E-01	7.387E-01	7.392E-01	7.393E-01	7.404E-01	7.443E-01	7.464E-01	7.473E-01	0.0226
36	7.386E-01	7.385E-01	7.386E-01	7.386E-01	7.386E-01	7.392E-01	7.394E-01	7.405E-01	7.448E-01	7.469E-01	7.477E-01	0.0224
35	7.388E-01	7.387E-01	7.387E-01	7.388E-01	7.387[illegible]-01	7.392E-01	7.394E-01	7.407E-01	7.453E-01	7.476E-01	7.482E-01	0.0222
34	7.392E-01	7.391E-01	7.391E-01	7.390E-01	7.388E-01	7.393E-01	7.395E-01	7.408E-01	7.459E-01	7.482E-01	7.487E-01	0.0220
33	7.396E-01	7.394E-01	7.394E-01	7.392E-01	7.390E-01	7.394E-01	7.395E-01	7.409E-01	7.463E-01	7.486E-01	7.490E-01	0.0220
32	7.396E-01	7.395E-01	7.395E-01	7.395E-01	7.395E-01	7.395E-01	7.395E-01	7.410E-01	7.468E-01	7.491E-01	7.493E-01	0.0218
31	7.396E-01	7.395E-01	7.395E-01	7.395E-01	7.395E-01	7.395E-01	7.395E-01	7.412E-01	7.477E-01	7.501E-01	7.501E-01	0.0216
30	7.396E-01	7.395E-01	7.395E-01	7.395E-01	7.395E-01	7.395E-01	7.396E-01	7.415E-01	7.489E-01	7.515E-01	7.510E-01	0.0213
29	7.396E-01	7.395E-01	7.395E-01	7.395E-01	7.395E-01	7.395E-01	7.396E-01	7.420E-01	7.504E-01	7.532E-01	7.520E-01	0.0211
28	7.396E-01	7.396E-01	7.396E-01	7.396E-01	7.396E-01	7.396E-01	7.396E-01	7.425E-01	7.521E-01	7.553E-01	7.529E-01	0.0209
27	7.396E-01	7.396E-01	7.396E-01	7.396E-01	7.396E-01	7.396E-01	7.397E-01	7.431E-01	7.538E-01	7.572E-01	7.536E-01	0.0207
26	7.396E-01	7.396E-01	7.396E-01	7.396E-01	7.396E-01	7.396E-01	7.397E-01	7.437E-01	7.552E-01	7.588E-01	7.541E-01	0.0206
25	7.396E-01	7.396E-01	7.396E-01	7.396E-01	7.396E-01	7.396E-01	7.398E-01	7.443E-01	7.562E-01	7.597E-01	7.544E-01	0.0205
24	7.396E-01	7.396E-01	7.396E-01	7.396E-01	7.396E-01	7.396E-01	7.398E-01	7.447E-01	7.569E-01	7.603E-01	7.546E-01	0.0204
23	7.396E-01	7.396E-01	7.396E-01	7.396E-01	7.396E-01	7.396E-01	7.398E-01	7.452E-01	7.576E-01	7.608E-01	7.549E-01	0.0203
22	7.396E-01	7.396E-01	7.396E-01	7.396E-01	7.396E-01	7.396E-01	7.399E-01	7.457E-01	7.583E-01	7.613E-01	7.551E-01	0.0203
21	7.396E-01	7.396E-01	7.396E-01	7.396E-01	7.396E-01	7.396E-01	7.400E-01	7.463E-01	7.589E-01	7.616E-01	7.553E-01	0.0202
20	7.396E-01	7.397E-01	7.397E-01	7.397E-01	7.397E-01	7.396E-01	7.401E-01	7.472E-01	7.599E-01	7.622E-01	7.555E-01	0.0200
19	7.396E-01	7.397E-01	7.397E-01	7.397E-01	7.397E-01	7.397E-01	7.403E-01	7.488E-01	7.611E-01	7.625E-01	7.557E-01	0.0199
18	7.396E-01	7.397E-01	7.397E-01	7.397E-01	7.397E-01	7.397E-01	7.407E-01	7.511E-01	7.623E-01	7.627E-01	7.558E-01	0.0196
17	7.396E-01	7.397E-01	7.397E-01	7.397E-01	7.397E-01	7.396E-01	7.418E-01	7.542E-01	7.634E-01	7.627E-01	7.559E-01	0.0194
16	7.396E-01	7.397E-01	7.397E-01	7.397E-01	7.396E-01	7.396E-01	7.443E-01	7.569E-01	7.640E-01	7.626E-01	7.560E-01	0.0192
15	7.396E-01	7.397E-01	7.396E-01	7.394E-01	7.394E-01	7.396E-01	7.485E-01	7.583E-01	7.644E-01	7.630E-01	7.561E-01	0.0189
14	7.396E-01	7.393E-01	7.387E-01	7.384E-01	7.393E-01	7.402E-01	7.495E-01	7.588E-01	7.647E-01	7.632E-01	7.562E-01	0.0188
13	7.365E-01	7.367E-01	7.372E-01	7.379E-01	7.393E-01	7.402E-01	7.495E-01	7.590E-01	7.648E-01	7.633E-01	7.564E-01	0.0187
12	7.351E-01	7.353E-01	7.361E-01	7.374E-01	7.391E-01	7.401E-01	7.495E-01	7.591E-01	7.649E-01	7.632E-01	7.567E-01	0.0186
11	7.338E-01	7.340E-01	7.350E-01	7.366E-01	7.387E-01	7.399E-01	7.495E-01	7.593E-01	7.650E-01	7.630E-01	7.570E-01	0.0185
10	7.327E-01	7.330E-01	7.338E-01	7.354E-01	7.378E-01	7.397E-01	7.497E-01	7.596E-01	7.652E-01	7.629E-01	7.573E-01	0.0183
9	7.321E-01	7.322E-01	7.329E-01	7.342E-01	7.365E-01	7.397E-01	7.500E-01	7.602E-01	7.656E-01	7.631E-01	7.579E-01	0.0179
8	7.317E-01	7.318E-01	7.323E-01	7.332E-01	7.350E-01	7.400E-01	7.506E-01	7.610E-01	7.662E-01	7.637E-01	7.587E-01	0.0173
7	7.315E-01	7.316E-01	7.321E-01	7.331E-01	7.350E-01	7.410E-01	7.518E-01	7.622E-01	7.673E-01	7.646E-01	7.603E-01	0.0162
6	7.316E-01	7.318E-01	7.324E-01	7.338E-01	7.365E-01	7.427E-01	7.536E-01	7.638E-01	7.689E-01	7.655E-01	7.641E-01	0.0143
5	7.319E-01	7.322E-01	7.331E-01	7.348E-01	7.383E-01	7.450E-01	7.556E-01	7.654E-01	7.708E-01	7.672E-01	7.708E-01	0.0111
4	7.328E-01	7.331E-01	7.341E-01	7.362E-01	7.401E-01	7.470E-01	7.569E-01	7.656E-01	7.734E-01	7.730E-01	7.817E-01	0.0079
3	7.346E-01	7.349E-01	7.358E-01	7.376E-01	7.408E-01	7.463E-01	7.535E-01	7.615E-01	7.739E-01	7.846E-01	7.969E-01	0.0048
2	7.384E-01	7.385E-01	7.387E-01	7.391E-01	7.399E-01	7.417E-01	7.452E-01	7.488E-01	7.554E-01	7.673E-01	7.828E-01	0.0016
1	7.396E-01	7.396E-01	7.396E-01	7.396E-01	7.396E-01	7.396E-01	7.396E-01	7.396E-01	7.396E-01	7.396E-01	7.396E-01	-0.0016
X=	-0.0000125	0.0000125	0.0000627	0.0001630	0.0003636	0.0007648	0.0015672	0.0031721	0.0063818	0.0079866	0.0087890	

J \ I=	12	13	14	15	16	17	18	19	20	21	22	Y =
50	7.734E-01	8.061E-01	8.267E-01	8.381E-01	8.439E-01	8.469E-01	8.500E-01	8.515E-01	8.522E-01	4.202E-02		
49	7.734E-01	8.061E-01	8.267E-01	8.381E-01	8.439E-01	8.469E-01	8.500E-01	8.515E-01	8.522E-01	3.884E-02		
48	7.696E-01	8.036E-01	8.254E-01	8.373E-01	8.435E-01	8.467E-01	8.499E-01	8.515E-01	8.522E-01	3.567E-02		
47	7.653E-01	7.974E-01	8.217E-01	8.352E-01	8.423E-01	8.459E-01	8.496E-01	8.514E-01	8.522E-01	3.249E-02		
46	[illegible]	7.877E-01	[illegible]	[illegible]	[illegible]	[illegible]	[illegible]	[illegible]	[illegible]	[illegible]		

[illegible]	[illegible]	[illegible]	[illegible]	[illegible]	[illegible]	[illegible]	[illegible]	[illegible]	[illegible]	[illegible]
45	7.495E-01	7.748E-01	8.061E-01	8.260E-01	8.369E-01	8.425E-01	8.483E-01	8.512E-01	8.522E-01	2.614E-02
44	7.459E-01	7.625E-01	7.943E-01	8.183E-01	8.322E-01	8.395E-01	8.470E-01	8.509E-01	8.522E-01	2.521E-02
43	7.458E-01	7.585E-01	7.898E-01	8.153E-01	8.303E-01	8.383E-01	8.466E-01	8.508E-01	8.522E-01	2.428E-02
42	7.462E-01	7.552E-01	7.850E-01	8.117E-01	8.280E-01	8.368E-01	8.460E-01	8.507E-01	8.522E-01	2.391E-02
41	7.465E-01	7.543E-01	7.835E-01	8.106E-01	8.273E-01	8.363E-01	8.458E-01	8.507E-01	8.523E-01	2.354E-02
40	7.468E-01	7.535E-01	7.824E-01	8.098E-01	8.268E-01	8.361E-01	8.457E-01	8.507E-01	8.523E-01	2.318E-02
39	7.471E-01	7.527E-01	7.804E-01	8.081E-01	8.257E-01	8.353E-01	8.454E-01	8.506E-01	8.523E-01	2.298E-02
38	7.473E-01	7.524E-01	7.795E-01	8.073E-01	8.251E-01	8.349E-01	8.452E-01	8.505E-01	8.523E-01	2.278E-02
37	7.476E-01	7.520E-01	7.784E-01	8.063E-01	8.245E-01	8.345E-01	8.450E-01	8.505E-01	8.523E-01	2.259E-02
36	7.479E-01	7.524E-01	7.791E-01	8.070E-01	8.249E-01	8.348E-01	8.451E-01	8.505E-01	8.523E-01	2.239E-02
35	7.483E-01	7.538E-01	7.811E-01	8.085E-01	8.259E-01	8.354E-01	8.454E-01	8.506E-01	8.523E-01	2.219E-02
34	7.487E-01	7.543E-01	7.817E-01	8.089E-01	8.261E-01	8.355E-01	8.455E-01	8.506E-01	8.523E-01	2.204E-02
33	7.488E-01	7.544E-01	7.822E-01	8.094E-01	8.265E-01	8.358E-01	8.456E-01	8.506E-01	8.523E-01	2.196E-02
32	7.491E-01	7.547E-01	7.825E-01	8.095E-01	8.266E-01	8.358E-01	8.456E-01	8.506E-01	8.522E-01	2.181E-02
31	7.496E-01	7.555E-01	7.833E-01	8.101E-01	8.269E-01	8.361E-01	8.457E-01	8.506E-01	8.522E-01	2.157E-02
30	7.501E-01	7.565E-01	7.848E-01	8.113E-01	8.277E-01	8.366E-01	8.458E-01	8.506E-01	8.522E-01	2.134E-02
29	7.506E-01	7.580E-01	7.869E-01	8.129E-01	8.287E-01	8.372E-01	8.461E-01	8.507E-01	8.522E-01	2.111E-02
28	7.509E-01	7.595E-01	7.889E-01	8.144E-01	8.297E-01	8.378E-01	8.464E-01	8.507E-01	8.522E-01	2.088E-02
27	7.512E-01	7.609E-01	7.908E-01	8.159E-01	8.306E-01	8.385E-01	8.466E-01	8.508E-01	8.522E-01	2.072E-02
26	7.514E-01	7.620E-01	7.923E-01	8.170E-01	8.313E-01	8.389E-01	8.468E-01	8.508E-01	8.522E-01	2.057E-02
25	7.515E-01	7.628E-01	7.935E-01	8.178E-01	8.318E-01	8.392E-01	8.469E-01	8.509E-01	8.522E-01	2.049E-02
24	7.517E-01	7.637E-01	7.947E-01	8.187E-01	8.324E-01	8.396E-01	8.471E-01	8.509E-01	8.522E-01	2.041E-02
23	7.519E-01	7.647E-01	7.960E-01	8.196E-01	8.329E-01	8.400E-01	8.472E-01	8.509E-01	8.522E-01	2.034E-02
22	7.521E-01	7.657E-01	7.973E-01	8.205E-01	8.335E-01	8.403E-01	8.474E-01	8.510E-01	8.522E-01	2.026E-02
21	7.524E-01	7.673E-01	7.993E-01	8.218E-01	8.343E-01	8.408E-01	8.476E-01	8.510E-01	8.522E-01	2.018E-02
20	7.529E-01	7.695E-01	8.018E-01	8.234E-01	8.353E-01	8.415E-01	8.478E-01	8.511E-01	8.522E-01	2.003E-02
19	7.537E-01	7.722E-01	8.047E-01	8.252E-01	8.364E-01	8.422E-01	8.481E-01	8.512E-01	8.522E-01	1.987E-02
18	7.547E-01	7.755E-01	8.077E-01	8.271E-01	8.375E-01	8.429E-01	8.484E-01	8.512E-01	8.522E-01	1.964E-02
17	7.559E-01	7.787E-01	8.103E-01	8.286E-01	8.384E-01	8.435E-01	8.487E-01	8.513E-01	8.522E-01	1.941E-02
16	7.570E-01	7.817E-01	8.124E-01	8.299E-01	8.392E-01	8.440E-01	8.489E-01	8.514E-01	8.522E-01	1.917E-02
15	7.581E-01	7.840E-01	8.140E-01	8.308E-01	8.397E-01	8.443E-01	8.490E-01	8.514E-01	8.522E-01	1.894E-02
14	7.588E-01	7.852E-01	8.149E-01	8.313E-01	8.400E-01	8.445E-01	8.491E-01	8.514E-01	8.522E-01	1.879E-02
13	7.592E-01	7.859E-01	8.152E-01	8.315E-01	8.401E-01	8.446E-01	8.491E-01	8.514E-01	8.522E-01	1.871E-02
12	7.598E-01	7.869E-01	8.157E-01	8.317E-01	8.402E-01	8.446E-01	8.491E-01	8.514E-01	8.522E-01	1.863E-02
11	7.607E-01	7.886E-01	8.167E-01	8.323E-01	8.406E-01	8.449E-01	8.492E-01	8.515E-01	8.522E-01	1.850E-02
10	7.622E-01	7.915E-01	8.183E-01	8.333E-01	8.412E-01	8.452E-01	8.494E-01	8.515E-01	8.522E-01	1.828E-02
9	7.647E-01	7.958E-01	8.208E-01	8.347E-01	8.420E-01	8.458E-01	8.496E-01	8.516E-01	8.522E-01	1.790E-02
8	7.688E-01	8.015E-01	8.241E-01	8.366E-01	8.431E-01	8.465E-01	8.499E-01	8.516E-01	8.522E-01	1.725E-02
7	7.754E-01	8.080E-01	8.279E-01	8.388E-01	8.444E-01	8.473E-01	8.503E-01	8.517E-01	8.522E-01	1.615E-02
6	7.856E-01	8.155E-01	8.324E-01	8.413E-01	8.459E-01	8.483E-01	8.506E-01	8.518E-01	8.522E-01	1.429E-02
5	7.989E-01	8.240E-01	8.372E-01	8.440E-01	8.475E-01	8.493E-01	8.511E-01	8.519E-01	8.522E-01	1.111E-02
4	8.133E-01	8.327E-01	8.420E-01	8.467E-01	8.491E-01	8.503E-01	8.515E-01	8.521E-01	8.522E-01	7.937E-03
3	8.281E-01	8.417E-01	8.470E-01	8.493E-01	8.505E-01	8.511E-01	8.518E-01	8.522E-01	8.522E-01	4.762E-03
2	8.137E-01	8.517E-01	8.773E-01	8.888E-01	8.904E-01	8.865E-01	8.710E-01	8.594E-01	8.522E-01	1.587E-03
1	7.396E-01	7.396E-01	7.396E-01	7.396E-01	7.396E-01	7.396E-01	7.396E-01	7.396E-01	7.396E-01	-1.587E-03
X=	0.0091903	0.0093909	0.0094912	0.0095413	0.0095664	0.0095789	0.0095915	0.0095977	0.0096022	

--*-*-*-*-*-*-*-*-*-*-*-*-*-*-*-*-*- CP CP CP CP CP CCCP CP CP CP CP CP -*

I= / J	1	2	3	4	5	6	7	8	9	10	11	Y =
50	1.113E+03	1.113E+03	1.113E+03	1.113E+03	1.113E+03	1.113E+03	1.113E+03	1.113E+03	1.116E+03	1.120E+03	1.134E+03	0.0420
49	1.113E+03	1.113E+03	1.113E+03	1.113E+03	1.113E+03	1.113E+03	1.113E+03	1.113E+03	1.116E+03	1.120E+03	1.134E+03	0.0388
48	1.113E+03	1.113E+03	1.113E+03	1.113E+03	1.113E+03	1.113E+03	1.113E+03	1.113E+03	1.116E+03	1.120E+03	1.132E+03	0.0357
47	1.113E+03	1.113E+03	1.113E+03	1.113E+03	1.113E+03	1.113E+03	1.113E+03	1.112E+03	1.116E+03	1.119E+03	1.128E+03	0.0325
46	1.113E+03	1.113E+03	1.113E+03	1.113E+03	1.113E+03	1.113E+03	1.113E+03	1.112E+03	1.116E+03	1.119E+03	1.124E+03	0.0293
45	1.113E+03	1.113E+03	1.113E+03	1.113E+03	1.113E+03	1.113E+03	1.112E+03	1.112E+03	1.116E+03	1.119E+03	1.122E+03	0.0261
44	1.113E+03	1.113E+03	1.113E+03	1.113E+03	1.113E+03	1.113E+03	1.112E+03	1.112E+03	1.116E+03	1.120E+03	1.122E+03	0.0252
43	1.113E+03	1.113E+03	1.113E+03	1.113E+03	1.113E+03	1.113E+03	1.112E+03	1.112E+03	1.117E+03	1.121E+03	1.123E+03	0.0243
42	1.113E+03	1.113E+03	1.113E+03	1.113E+03	1.113E+03	1.112E+03	1.112E+03	1.112E+03	1.118E+03	1.122E+03	1.124E+03	0.0239
41	1.113E+03	1.113E+03	1.113E+03	1.113E+03	1.113E+03	1.112E+03	1.112E+03	1.112E+03	1.118E+03	1.123E+03	1.125E+03	0.0235
40	1.113E+03	1.113E+03	1.113E+03	1.113E+03	1.113E+03	1.112E+03	1.112E+03	1.112E+03	1.119E+03	1.124E+03	1.126E+03	0.0232
39	1.113E+03	1.113E+03	1.113E+03	1.113E+03	1.113E+03	1.112E+03	1.111E+03	1.112E+03	1.120E+03	1.125E+03	1.127E+03	0.0230
38	1.112E+03	1.112E+03	1.112E+03	1.112E+03	1.113E+03	1.112E+03	1.111E+03	1.112E+03	1.121E+03	1.126E+03	1.128E+03	0.0228
37	1.112E+03	1.112E+03	1.112E+03	1.112E+03	1.113E+03	1.112E+03	1.111E+03	1.113E+03	1.122E+03	1.127E+03	1.129E+03	0.0226
36	1.112E+03	1.112E+03	1.112E+03	1.112E+03	1.113E+03	1.113E+03	1.111E+03	1.113E+03	1.123E+03	1.128E+03	1.130E+03	0.0224
35	1.112E+03	1.112E+03	1.112E+03	1.112E+03	1.112E+03	1.112E+03	1.110E+03	1.113E+03	1.125E+03	1.130E+03	1.131E+03	0.0222
34	1.111E+03	1.111E+03	1.111E+03	1.111E+03	1.112E+03	1.111E+03	1.110E+03	1.113E+03	1.126E+03	1.131E+03	1.132E+03	0.0220
33	1.110E+03	1.110E+03	1.110E+03	1.110E+03	1.111E+03	1.110E+03	1.110E+03	1.113E+03	1.127E+03	1.132E+03	1.133E+03	0.0220
32	1.110E+03	1.110E+03	1.110E+03	1.110E+03	1.110E+03	1.110E+03	1.110E+03	1.114E+03	1.128E+03	1.134E+03	1.134E+03	0.0218
31	1.110E+03	1.110E+03	1.110E+03	1.110E+03	1.110E+03	1.110E+03	1.110E+03	1.114E+03	1.130E+03	1.136E+03	1.136E+03	0.0216
30	1.110E+03	1.110E+03	1.110E+03	1.110E+03	1.110E+03	1.110E+03	1.110E+03	1.115E+03	1.133E+03	1.139E+03	1.138E+03	0.0213
29	1.110E+03	1.110E+03	1.110E+03	1.110E+03	1.110E+03	1.110E+03	1.110E+03	1.116E+03	1.137E+03	1.143E+03	1.140E+03	0.0211
28	1.110E+03	1.110E+03	1.110E+03	1.110E+03	1.110E+03	1.110E+03	1.110E+03	1.118E+03	1.141E+03	1.147E+03	1.142E+03	0.0209
27	1.110E+03	1.110E+03	1.110E+03	1.110E+03	1.110E+03	1.110E+03	1.110E+03	1.119E+03	1.145E+03	1.152E+03	1.144E+03	0.0207
26	1.110E+03	1.110E+03	1.110E+03	1.110E+03	1.110E+03	1.110E+03	1.110E+03	1.121E+03	1.148E+03	1.155E+03	1.145E+03	0.0206
25	1.110E+03	1.110E+03	1.110E+03	1.110E+03	1.110E+03	1.110E+03	1.110E+03	1.122E+03	1.150E+03	1.156E+03	1.145E+03	0.0205
24	1.110E+03	1.110E+03	1.110E+03	1.110E+03	1.110E+03	1.110E+03	1.110E+03	1.123E+03	1.152E+03	1.158E+03	1.145E+03	0.0204
23	1.110E+03	1.110E+03	1.110E+03	1.110E+03	1.110E+03	1.110E+03	1.111E+03	1.125E+03	1.153E+03	1.159E+03	1.146E+03	0.0203
22	1.110E+03	1.110E+03	1.110E+03	1.110E+03	1.110E+03	1.110E+03	1.111E+03	1.126E+03	1.155E+03	1.159E+03	1.146E+03	0.0203
21	1.110E+03	1.110E+03	1.110E+03	1.110E+03	1.110E+03	1.110E+03	1.111E+03	1.127E+03	1.156E+03	1.160E+03	1.147E+03	0.0202
20	1.110E+03	1.110E+03	1.110E+03	1.110E+03	1.110E+03	1.110E+03	1.111E+03	1.130E+03	1.158E+03	1.161E+03	1.147E+03	0.0200
19	1.110E+03	1.110E+03	1.110E+03	1.110E+03	1.110E+03	1.110E+03	1.112E+03	1.134E+03	1.160E+03	1.162E+03	1.147E+03	0.0199
18	1.110E+03	1.110E+03	1.110E+03	1.110E+03	1.110E+03	1.110E+03	1.114E+03	1.139E+03	1.163E+03	1.162E+03	1.148E+03	0.0196
17	1.110E+03	1.110E+03	1.110E+03	1.110E+03	1.110E+03	1.111E+03	1.118E+03	1.146E+03	1.165E+03	1.162E+03	1.148E+03	0.0194
16	1.110E+03	1.110E+03	1.110E+03	1.110E+03	1.110E+03	1.112E+03	1.126E+03	1.152E+03	1.166E+03	1.162E+03	1.148E+03	0.0192
15	1.110E+03	1.110E+03	1.110E+03	1.111E+03	1.113E+03	1.118E+03	1.137E+03	1.155E+03	1.167E+03	1.163E+03	1.148E+03	0.0189
14	1.110E+03	1.111E+03	1.114E+03	1.117E+03	1.122E+03	1.124E+03	1.140E+03	1.156E+03	1.168E+03	1.163E+03	1.148E+03	0.0188
13	1.117E+03	1.117E+03	1.118E+03	1.120E+03	1.124E+03	1.126E+03	1.140E+03	1.156E+03	1.168E+03	1.163E+03	1.148E+03	0.0187
12	1.120E+03	1.120E+03	1.120E+03	1.122E+03	1.125E+03	1.128E+03	1.140E+03	1.156E+03	1.168E+03	1.163E+03	1.148E+03	0.0186
11	1.123E+03	1.123E+03	1.123E+03	1.124E+03	1.126E+03	1.129E+03	1.140E+03	1.157E+03	1.168E+03	1.163E+03	1.148E+03	0.0185
10	1.125E+03	1.126E+03	1.126E+03	1.126E+03	1.127E+03	1.129E+03	1.140E+03	1.157E+03	1.169E+03	1.163E+03	1.149E+03	0.0183
9	1.127E+03	1.127E+03	1.127E+03	1.127E+03	1.128E+03	1.129E+03	1.140E+03	1.158E+03	1.169E+03	1.163E+03	1.150E+03	0.0179
8	1.128E+03	1.128E+03	1.128E+03	1.128E+03	1.128E+03	1.130E+03	1.141E+03	1.159E+03	1.171E+03	1.165E+03	1.152E+03	0.0173
7	1.128E+03	1.128E+03	1.128E+03	1.128E+03	1.129E+03	1.130E+03	1.142E+03	1.161E+03	1.173E+03	1.167E+03	1.157E+03	0.0162
6	1.128E+03	1.128E+03	1.128E+03	1.128E+03	1.128E+03	1.130E+03	1.144E+03	1.164E+03	1.176E+03	1.170E+03	1.167E+03	0.0143
5	1.127E+03	1.127E+03	1.127E+03	1.127E+03	1.128E+03	1.131E+03	1.146E+03	1.167E+03	1.180E+03	1.174E+03	1.182E+03	0.0111
4	1.125E+03	1.125E+03	1.125E+03	1.125E+03	1.126E+03	1.131E+03	1.148E+03	1.167E+03	1.185E+03	1.186E+03	1.202E+03	0.0079
3	1.121E+03	1.121E+03	1.121E+03	1.121E+03	1.122E+03	1.127E+03	1.141E+03	1.158E+03	1.183E+03	1.203E+03	1.220E+03	0.0048
2	1.113E+03	1.113E+03	1.113E+03	1.113E+03	1.113E+03	1.115E+03	1.122E+03	1.129E+03	1.143E+03	1.165E+03	1.185E+03	0.0016
1	1.110E+03	1.110E+03	1.110E+03	1.110E+03	1.110E+03	1.110E+03	1.110E+03	1.110E+03	1.110E+03	1.110E+03	1.110E+03	-0.0016
X=	-0.0000125	0.0000125	0.0000627	0.0001630	0.0003636	0.0007648	0.0015672	0.0031721	0.0063818	0.0079866	0.0087890	

I= / J	12	13	14	15	16	17	18	19	20	21	22	Y =
50	1.183E+03	1.233E+03	1.261E+03	1.275E+03	1.282E+03	1.285E+03	1.289E+03	1.290E+03	1.291E+03	4.202E-02		
49	1.183E+03	1.233E+03	1.261E+03	1.275E+03	1.282E+03	1.285E+03	1.289E+03	1.290E+03	1.291E+03	3.884E-02		
48	1.176E+03	1.229E+03	1.259E+03	1.274E+03	1.281E+03	1.285E+03	1.288E+03	1.290E+03	1.291E+03	3.567E-02		
47	1.164E+03	1.220E+03	1.254E+03	1.271E+03	1.280E+03	1.284E+03	1.288E+03	1.290E+03	1.291E+03	3.249E-02		
46	[illegible]	[illegible]	[illegible]	[illegible]	[illegible]	[illegible]	[illegible]	[illegible]	[illegible]	[illegible]		

46	[illegible]	[illegible]	[illegible]	[illegible]	[illegible]	[illegible]	[illegible]	[illegible]	[illegible]	[illegible]
45	1.135E+03	1.185E+03	1.233E+03	1.260E+03	1.273E+03	1.280E+03	1.286E+03	1.290E+03	1.291E+03	2.614E-02
44	1.126E+03	1.164E+03	1.217E+03	1.250E+03	1.268E+03	1.276E+03	1.285E+03	1.289E+03	1.291E+03	2.521E-02
43	1.126E+03	1.156E+03	1.210E+03	1.246E+03	1.265E+03	1.275E+03	1.284E+03	1.289E+03	1.291E+03	2.428E-02
42	1.126E+03	1.150E+03	1.203E+03	1.242E+03	1.263E+03	1.273E+03	1.284E+03	1.289E+03	1.291E+03	2.391E-02
41	1.127E+03	1.147E+03	1.201E+03	1.240E+03	1.262E+03	1.273E+03	1.283E+03	1.289E+03	1.291E+03	2.354E-02
40	1.128E+03	1.146E+03	1.199E+03	1.239E+03	1.261E+03	1.272E+03	1.283E+03	1.289E+03	1.291E+03	2.318E-02
39	1.128E+03	1.144E+03	1.196E+03	1.237E+03	1.260E+03	1.271E+03	1.283E+03	1.289E+03	1.291E+03	2.298E-02
38	1.129E+03	1.143E+03	1.194E+03	1.236E+03	1.259E+03	1.271E+03	1.283E+03	1.289E+03	1.291E+03	2.278E-02
37	1.130E+03	1.142E+03	1.192E+03	1.235E+03	1.258E+03	1.271E+03	1.283E+03	1.289E+03	1.291E+03	2.259E-02
36	1.130E+03	1.143E+03	1.194E+03	1.236E+03	1.259E+03	1.271E+03	1.283E+03	1.289E+03	1.291E+03	2.239E-02
35	1.131E+03	1.146E+03	1.197E+03	1.238E+03	1.260E+03	1.272E+03	1.283E+03	1.289E+03	1.291E+03	2.219E-02
34	1.132E+03	1.147E+03	1.198E+03	1.238E+03	1.260E+03	1.272E+03	1.283E+03	1.289E+03	1.291E+03	2.204E-02
33	1.132E+03	1.148E+03	1.199E+03	1.239E+03	1.261E+03	1.272E+03	1.283E+03	1.289E+03	1.291E+03	2.196E-02
32	1.133E+03	1.148E+03	1.199E+03	1.239E+03	1.261E+03	1.272E+03	1.283E+03	1.289E+03	1.291E+03	2.181E-02
31	1.134E+03	1.150E+03	1.201E+03	1.240E+03	1.262E+03	1.272E+03	1.283E+03	1.289E+03	1.291E+03	2.157E-02
30	1.135E+03	1.152E+03	1.203E+03	1.242E+03	1.263E+03	1.273E+03	1.284E+03	1.289E+03	1.291E+03	2.134E-02
29	1.137E+03	1.156E+03	1.207E+03	1.244E+03	1.264E+03	1.274E+03	1.284E+03	1.289E+03	1.291E+03	2.111E-02
28	1.137E+03	1.159E+03	1.210E+03	1.246E+03	1.265E+03	1.275E+03	1.284E+03	1.289E+03	1.291E+03	2.088E-02
27	1.138E+03	1.162E+03	1.213E+03	1.248E+03	1.266E+03	1.275E+03	1.285E+03	1.289E+03	1.291E+03	2.072E-02
26	1.139E+03	1.164E+03	1.215E+03	1.249E+03	1.267E+03	1.276E+03	1.285E+03	1.289E+03	1.291E+03	2.057E-02
25	1.139E+03	1.165E+03	1.217E+03	1.250E+03	1.268E+03	1.276E+03	1.285E+03	1.289E+03	1.291E+03	2.049E-02
24	1.139E+03	1.167E+03	1.218E+03	1.251E+03	1.268E+03	1.277E+03	1.285E+03	1.289E+03	1.291E+03	2.041E-02
23	1.140E+03	1.169E+03	1.220E+03	1.253E+03	1.269E+03	1.277E+03	1.285E+03	1.289E+03	1.291E+03	2.034E-02
22	1.140E+03	1.171E+03	1.222E+03	1.254E+03	1.270E+03	1.278E+03	1.285E+03	1.289E+03	1.291E+03	2.026E-02
21	1.141E+03	1.174E+03	1.225E+03	1.255E+03	1.271E+03	1.278E+03	1.286E+03	1.290E+03	1.291E+03	2.018E-02
20	1.142E+03	1.178E+03	1.229E+03	1.257E+03	1.272E+03	1.279E+03	1.286E+03	1.290E+03	1.291E+03	2.003E-02
19	1.144E+03	1.183E+03	1.232E+03	1.259E+03	1.273E+03	1.280E+03	1.286E+03	1.290E+03	1.291E+03	1.987E-02
18	1.147E+03	1.188E+03	1.236E+03	1.262E+03	1.274E+03	1.280E+03	1.287E+03	1.290E+03	1.291E+03	1.964E-02
17	1.149E+03	1.193E+03	1.240E+03	1.263E+03	1.275E+03	1.281E+03	1.287E+03	1.290E+03	1.291E+03	1.941E-02
16	1.152E+03	1.198E+03	1.243E+03	1.265E+03	1.276E+03	1.282E+03	1.287E+03	1.290E+03	1.291E+03	1.917E-02
15	1.154E+03	1.202E+03	1.245E+03	1.266E+03	1.277E+03	1.282E+03	1.287E+03	1.290E+03	1.291E+03	1.894E-02
14	1.155E+03	1.203E+03	1.246E+03	1.267E+03	1.277E+03	1.282E+03	1.287E+03	1.290E+03	1.291E+03	1.879E-02
13	1.155E+03	1.204E+03	1.246E+03	1.267E+03	1.277E+03	1.282E+03	1.287E+03	1.290E+03	1.291E+03	1.871E-02
12	1.156E+03	1.206E+03	1.247E+03	1.267E+03	1.277E+03	1.282E+03	1.287E+03	1.290E+03	1.291E+03	1.863E-02
11	1.158E+03	1.209E+03	1.248E+03	1.268E+03	1.278E+03	1.283E+03	1.288E+03	1.290E+03	1.291E+03	1.850E-02
10	1.161E+03	1.214E+03	1.251E+03	1.269E+03	1.279E+03	1.283E+03	1.288E+03	1.290E+03	1.291E+03	1.828E-02
9	1.167E+03	1.221E+03	1.254E+03	1.271E+03	1.280E+03	1.284E+03	1.288E+03	1.290E+03	1.291E+03	1.790E-02
8	1.176E+03	1.229E+03	1.259E+03	1.274E+03	1.281E+03	1.285E+03	1.288E+03	1.290E+03	1.291E+03	1.725E-02
7	1.190E+03	1.238E+03	1.264E+03	1.276E+03	1.283E+03	1.286E+03	1.289E+03	1.290E+03	1.291E+03	1.615E-02
6	1.208E+03	1.249E+03	1.269E+03	1.279E+03	1.284E+03	1.287E+03	1.289E+03	1.290E+03	1.291E+03	1.429E-02
5	1.228E+03	1.260E+03	1.275E+03	1.282E+03	1.286E+03	1.288E+03	1.290E+03	1.291E+03	1.291E+03	1.111E-02
4	1.250E+03	1.271E+03	1.280E+03	1.285E+03	1.288E+03	1.289E+03	1.290E+03	1.291E+03	1.291E+03	7.937E-03
3	1.252E+03	1.269E+03	1.280E+03	1.285E+03	1.287E+03	1.289E+03	1.290E+03	1.291E+03	1.291E+03	4.762E-03
2	1.206E+03	1.237E+03	1.258E+03	1.272E+03	1.279E+03	1.283E+03	1.287E+03	1.290E+03	1.291E+03	1.587E-03
1	1.110E+03	1.110E+03	1.110E+03	1.110E+03	1.110E+03	1.110E+03	1.110E+03	1.110E+03	1.110E+03	-1.587E-03
X=	0.0091903	0.0093909	0.0094912	0.0095413	0.0095664	0.0095789	0.0095915	0.0095977	0.0096022	

30

- DIF DIF DIF DIF DIF DIF DIF DIF DIF -

J \ I=	1	2	3	4	5	6	7	8	9	10	11	Y =
50	5.049E-05	5.050E-05	5.049E-05	5.049E-05	5.047E-05	5.043E-05	5.036E-05	5.021E-05	4.985E-05	4.937E-05	4.772E-05	0.0420
49	5.049E-05	5.050E-05	5.049E-05	5.049E-05	5.047E-05	5.043E-05	5.036E-05	5.021E-05	4.985E-05	4.937E-05	4.772E-05	0.0388
48	5.049E-05	5.050E-05	5.049E-05	5.048E-05	5.046E-05	5.043E-05	5.035E-05	5.022E-05	4.985E-05	4.940E-05	4.802E-05	0.0357
47	5.049E-05	5.050E-05	5.049E-05	5.048E-05	5.045E-05	5.041E-05	5.034E-05	5.025E-05	4.986E-05	4.944E-05	4.845E-05	0.0325
46	5.049E-05	5.050E-05	5.048E-05	5.046E-05	5.041E-05	5.035E-05	5.031E-05	5.026E-05	4.986E-05	4.947E-05	4.884E-05	0.0293
45	5.049E-05	5.050E-05	5.048E-05	5.045E-05	5.040E-05	5.032E-05	5.027E-05	5.026E-05	4.984E-05	4.946E-05	4.908E-05	0.0261
44	5.049E-05	5.050E-05	5.049E-05	5.046E-05	5.041E-05	5.033E-05	5.028E-05	5.026E-05	4.978E-05	4.937E-05	4.904E-05	0.0252
43	5.049E-05	5.050E-05	5.049E-05	5.047E-05	5.042E-05	5.034E-05	5.029E-05	5.026E-05	4.970E-05	4.926E-05	4.893E-05	0.0243
42	5.049E-05	5.050E-05	5.049E-05	5.048E-05	5.043E-05	5.035E-05	5.030E-05	5.026E-05	4.960E-05	4.913E-05	4.881E-05	0.0239
41	5.049E-05	5.050E-05	5.050E-05	5.048E-05	5.043E-05	5.035E-05	5.031E-05	5.025E-05	4.951E-05	4.902E-05	4.872E-05	0.0235
40	5.049E-05	5.050E-05	5.050E-05	5.048E-05	5.044E-05	5.036E-05	5.039E-05	5.024E-05	4.940E-05	4.889E-05	4.869E-05	0.0232
39	5.049E-05	5.050E-05	5.050E-05	5.048E-05	5.044E-05	5.036E-05	5.045E-05	5.023E-05	4.929E-05	4.875E-05	4.848E-05	0.0230
38	5.049E-05	5.050E-05	5.050E-05	5.048E-05	5.044E-05	5.037E-05	5.045E-05	5.021E-05	4.920E-05	4.864E-05	4.839E-05	0.0228
37	5.049E-05	5.050E-05	5.050E-05	5.048E-05	5.045E-05	5.037E-05	5.046E-05	5.019E-05	4.908E-05	4.851E-05	4.829E-05	0.0226
36	5.049E-05	5.050E-05	5.049E-05	5.048E-05	5.045E-05	5.038E-05	5.046E-05	5.017E-05	4.895E-05	4.837E-05	4.817E-05	0.0224
35	5.049E-05	5.050E-05	5.049E-05	5.048E-05	5.045E-05	5.039E-05	5.048E-05	5.014E-05	4.880E-05	4.820E-05	4.804E-05	0.0222
34	5.049E-05	5.050E-05	5.050E-05	5.049E-05	5.046E-05	5.047E-05	5.049E-05	5.011E-05	4.864E-05	4.802E-05	4.790E-05	0.0220
33	5.049E-05	5.050E-05	5.050E-05	5.050E-05	5.048E-05	5.050E-05	5.050E-05	5.008E-05	4.852E-05	4.790E-05	4.782E-05	0.0220
32	5.049E-05	5.050E-05	5.050E-05	5.050E-05	5.050E-05	5.050E-05	5.050E-05	5.005E-05	4.839E-05	4.776E-05	4.772E-05	0.0218
31	5.049E-05	5.050E-05	5.050E-05	5.050E-05	5.050E-05	5.050E-05	5.049E-05	4.998E-05	4.815E-05	4.751E-05	4.753E-05	0.0216
30	5.049E-05	5.050E-05	5.050E-05	5.050E-05	5.050E-05	5.050E-05	5.049E-05	4.989E-05	4.781E-05	4.714E-05	4.726E-05	0.0213
29	5.049E-05	5.050E-05	5.050E-05	5.050E-05	5.050E-05	5.050E-05	5.048E-05	4.977E-05	4.741E-05	4.670E-05	4.700E-05	0.0211
28	5.049E-05	5.050E-05	5.050E-05	5.050E-05	5.050E-05	5.050E-05	5.047E-05	4.960E-05	4.695E-05	4.619E-05	4.678E-05	0.0209
27	5.049E-05	5.050E-05	5.050E-05	5.050E-05	5.050E-05	5.050E-05	5.046E-05	4.942E-05	4.653E-05	4.571E-05	4.661E-05	0.0207
26	5.049E-05	5.050E-05	5.050E-05	5.050E-05	5.050E-05	5.050E-05	5.045E-05	4.924E-05	4.618E-05	4.534E-05	4.649E-05	0.0206
25	[illegible]	5.050E-05	5.049E-05	5.049E-05	5.050E-05	5.049E-05	5.044E-05	4.907E-05	4.591E-05	4.516E-05	4.643E-05	0.0205
24	5.049E-05	5.049E-05	5.049E-05	5.049E-05	5.049E-05	5.049E-05	5.043E-05	4.895E-05	4.575E-05	4.502E-05	4.637E-05	0.0204
23	5.049E-05	5.049E-05	5.049E-05	5.049E-05	5.049E-05	5.049E-05	5.041E-05	4.881E-05	4.558E-05	4.490E-05	4.633E-05	0.0203
22	5.049E-05	5.049E-05	5.049E-05	5.049E-05	5.049E-05	5.049E-05	5.039E-05	4.867E-05	4.542E-05	4.480E-05	4.628E-05	0.0203
21	5.049E-05	5.049E-05	5.049E-05	5.049E-05	5.049E-05	5.049E-05	5.037E-05	4.850E-05	4.527E-05	4.472E-05	4.623E-05	0.0202
20	5.049E-05	5.049E-05	5.049E-05	5.049E-05	5.049E-05	5.049E-05	5.033E-05	4.823E-05	4.505E-05	4.460E-05	4.617E-05	0.0200
19	5.049E-05	5.049E-05	5.049E-05	5.049E-05	5.049E-05	5.049E-05	5.025E-05	4.781E-05	4.477E-05	4.453E-05	4.614E-05	0.0199
18	5.049E-05	5.049E-05	5.049E-05	5.049E-05	5.049E-05	5.048E-05	5.008E-05	4.719E-05	4.449E-05	4.450E-05	4.611E-05	0.0196
17	5.049E-05	5.049E-05	5.049E-05	5.049E-05	5.049E-05	5.045E-05	4.969E-05	4.638E-05	4.425E-05	4.449E-05	4.609E-05	0.0194
16	5.049E-05	5.049E-05	5.049E-05	5.049E-05	5.046E-05	5.036E-05	4.888E-05	4.573E-05	4.411E-05	4.447E-05	4.607E-05	0.0192
15	5.049E-05	5.049E-05	5.048E-05	5.045E-05	5.031E-05	5.000E-05	4.762E-05	4.541E-05	4.402E-05	4.443E-05	4.604E-05	0.0189
14	5.049E-05	5.047E-05	5.040E-05	5.019E-05	4.981E-05	4.951E-05	4.736E-05	4.531E-05	4.397E-05	4.438E-05	4.601E-05	0.0188
13	5.049E-05	5.046E-05	5.035E-05	5.011E-05	4.970E-05	4.939E-05	4.736E-05	4.526E-05	4.394E-05	4.437E-05	4.599E-05	0.0187
12	5.049E-05	5.046E-05	5.033E-05	5.006E-05	4.963E-05	4.933E-05	4.736E-05	4.523E-05	4.393E-05	4.438E-05	4.596E-05	0.0186
11	5.049E-05	5.046E-05	5.031E-05	5.004E-05	4.960E-05	4.929E-05	4.735E-05	4.519E-05	4.391E-05	4.442E-05	4.592E-05	0.0185
10	5.049E-05	5.046E-05	5.033E-05	5.008E-05	4.967E-05	4.928E-05	4.733E-05	4.513E-05	4.386E-05	4.448E-05	4.585E-05	0.0183
9	5.049E-05	5.047E-05	5.037E-05	5.018E-05	4.982E-05	4.928E-05	4.727E-05	4.501E-05	4.378E-05	4.438E-05	4.573E-05	0.0179
8	5.049E-05	5.047E-05	5.041E-05	5.027E-05	5.000E-05	4.923E-05	4.715E-05	4.484E-05	4.364E-05	4.424E-05	4.549E-05	0.0173
7	5.049E-05	5.047E-05	5.040E-05	5.026E-05	4.998E-05	4.907E-05	4.692E-05	4.458E-05	4.341E-05	4.402E-05	4.503E-05	0.0162
6	5.049E-05	5.047E-05	5.037E-05	5.018E-05	4.978E-05	4.882E-05	4.658E-05	4.425E-05	4.306E-05	4.378E-05	4.406E-05	0.0143
5	5.049E-05	5.046E-05	5.033E-05	5.008E-05	4.957E-05	4.848E-05	4.620E-05	4.391E-05	4.264E-05	4.335E-05	4.255E-05	0.0111
4	5.049E-05	5.045E-05	5.031E-05	5.001E-05	4.942E-05	4.821E-05	4.594E-05	4.388E-05	4.214E-05	4.212E-05	4.045E-05	0.0079
3	5.049E-05	5.046E-05	5.033E-05	5.008E-05	4.958E-05	4.854E-05	4.679E-05	4.487E-05	4.218E-05	4.011E-05	3.820E-05	0.0048
2	5.049E-05	5.048E-05	5.045E-05	5.039E-05	5.025E-05	4.988E-05	4.900E-05	4.804E-05	4.644E-05	4.383E-05	4.113E-05	0.0016
1	5.049E-05	5.049E-05	5.049E-05	5.049E-05	5.049E-05	5.049E-05	5.049E-05	5.049E-05	5.049E-05	5.049E-05	5.049E-05	-0.0016
X=	-0.0000125	0.0000125	0.0000627	0.0001630	0.0003636	0.0007648	0.0015672	0.0031721	0.0063818	0.0079806	0.0087890	

J \ I=	12	13	14	15	16	17	18	19	20	21	22	Y =
50	4.222E-05	3.684E-05	3.416E-05	3.287E-05	3.225E-05	3.194E-05	3.164E-05	3.148E-05	3.143E-05	4.202E-02		
49	4.222E-05	3.684E-05	3.416E-05	3.287E-05	3.225E-05	3.194E-05	3.164E-05	3.148E-05	3.143E-05	3.884E-02		
48	4.298E-05	3.721E-05	3.433E-05	3.296E-05	3.229E-05	3.197E-05	3.165E-05	3.149E-05	3.143E-05	3.567E-02		
47	4.430E-05	3.813E-05	3.478E-05	3.319E-05	3.242E-05	3.205E-05	3.168E-05	3.150E-05	3.143E-05	3.249E-02		
46	[illegible]	[illegible]	[illegible]	[illegible]	[illegible]	[illegible]	[illegible]	[illegible]	[illegible]	[illegible]		

45	4.762E-05	4.197E-05	3.685E-05	3.426E-05	3.301E-05	3.241E-05	3.182E-05	3.153E-05	3.143E-05	2.614E-02
44	4.862E-05	4.444E-05	3.858E-05	3.519E-05	3.353E-05	3.273E-05	3.194E-05	3.156E-05	3.143E-05	2.521E-02
43	4.867E-05	4.533E-05	3.930E-05	3.557E-05	3.374E-05	3.286E-05	3.199E-05	3.157E-05	3.143E-05	2.428E-02
42	4.859E-05	4.609E-05	4.008E-05	3.605E-05	3.401E-05	3.302E-05	3.206E-05	3.159E-05	3.143E-05	2.391E-02
41	4.852E-05	4.632E-05	4.034E-05	3.620E-05	3.410E-05	3.307E-05	3.208E-05	3.159E-05	3.143E-05	2.354E-02
40	4.843E-05	4.651E-05	4.054E-05	3.631E-05	3.415E-05	3.310E-05	3.209E-05	3.159E-05	3.143E-05	2.318E-02
39	4.834E-05	4.671E-05	4.085E-05	3.654E-05	3.429E-05	3.319E-05	3.212E-05	3.160E-05	3.143E-05	2.298E-02
38	4.828E-05	4.680E-05	4.106E-05	3.665E-05	3.435E-05	3.323E-05	3.214E-05	3.161E-05	3.143E-05	2.278E-02
37	4.820E-05	4.689E-05	4.125E-05	3.677E-05	3.442E-05	3.327E-05	3.215E-05	3.161E-05	3.143E-05	2.259E-02
36	4.812E-05	4.679E-05	4.110E-05	3.668E-05	3.437E-05	3.324E-05	3.214E-05	3.161E-05	3.143E-05	2.239E-02
35	4.801E-05	4.645E-05	4.075E-05	3.648E-05	3.425E-05	3.317E-05	3.211E-05	3.160E-05	3.143E-05	2.219E-02
34	4.792E-05	4.632E-05	4.064E-05	3.642E-05	3.423E-05	3.315E-05	3.211E-05	3.160E-05	3.143E-05	2.204E-02
33	4.787E-05	4.628E-05	4.057E-05	3.635E-05	3.418E-05	3.312E-05	3.210E-05	3.160E-05	3.143E-05	2.196E-02
32	4.778E-05	4.621E-05	4.051E-05	3.633E-05	3.417E-05	3.312E-05	3.210E-05	3.160E-05	3.143E-05	2.181E-02
31	4.766E-05	4.602E-05	4.036E-05	3.624E-05	3.413E-05	3.309E-05	3.209E-05	3.159E-05	3.143E-05	2.157E-02
30	4.753E-05	4.576E-05	4.009E-05	3.608E-05	3.403E-05	3.304E-05	3.206E-05	3.159E-05	3.143E-05	2.134E-02
29	4.740E-05	4.540E-05	3.973E-05	3.586E-05	3.391E-05	3.296E-05	3.204E-05	3.158E-05	3.143E-05	2.111E-02
28	4.731E-05	4.504E-05	3.940E-05	3.567E-05	3.380E-05	3.289E-05	3.201E-05	3.158E-05	3.143E-05	2.088E-02
27	4.723E-05	4.473E-05	3.908E-05	3.547E-05	3.369E-05	3.283E-05	3.198E-05	3.157E-05	3.143E-05	2.072E-02
26	4.717E-05	4.448E-05	3.884E-05	3.533E-05	3.361E-05	3.278E-05	3.196E-05	3.157E-05	3.143E-05	2.057E-02
25	4.714E-05	4.431E-05	3.866E-05	3.523E-05	3.355E-05	3.274E-05	3.195E-05	3.156E-05	3.143E-05	2.049E-02
24	4.710E-05	4.411E-05	3.847E-05	3.512E-05	3.349E-05	3.270E-05	3.193E-05	3.156E-05	3.143E-05	2.041E-02
23	4.706E-05	4.391E-05	3.827E-05	3.500E-05	3.343E-05	3.267E-05	3.192E-05	3.155E-05	3.143E-05	2.034E-02
22	4.700E-05	4.369E-05	3.807E-05	3.489E-05	3.337E-05	3.263E-05	3.190E-05	3.155E-05	3.143E-05	2.026E-02
21	4.690E-05	4.336E-05	3.777E-05	3.473E-05	3.328E-05	3.257E-05	3.188E-05	3.154E-05	3.143E-05	2.018E-02
20	4.676E-05	4.292E-05	3.741E-05	3.454E-05	3.317E-05	3.251E-05	3.186E-05	3.154E-05	3.143E-05	2.003E-02
19	4.656E-05	4.237E-05	3.700E-05	3.433E-05	3.305E-05	3.244E-05	3.183E-05	3.153E-05	3.143E-05	1.987E-02
18	4.630E-05	4.174E-05	3.659E-05	3.411E-05	3.294E-05	3.236E-05	3.180E-05	3.152E-05	3.143E-05	1.964E-02
17	4.602E-05	4.117E-05	3.624E-05	3.393E-05	3.284E-05	3.230E-05	3.178E-05	3.152E-05	3.143E-05	1.941E-02
16	4.573E-05	4.064E-05	3.595E-05	3.379E-05	3.276E-05	3.225E-05	3.176E-05	3.151E-05	3.143E-05	1.917E-02
15	4.550E-05	4.025E-05	3.574E-05	3.368E-05	3.270E-05	3.222E-05	3.174E-05	3.151E-05	3.143E-05	1.894E-02
14	4.536E-05	4.004E-05	3.564E-05	3.362E-05	3.267E-05	3.220E-05	3.173E-05	3.151E-05	3.143E-05	1.879E-02
13	4.527E-05	3.992E-05	3.559E-05	3.360E-05	3.266E-05	3.219E-05	3.173E-05	3.151E-05	3.143E-05	1.871E-02
12	4.516E-05	3.975E-05	3.552E-05	3.357E-05	3.264E-05	3.218E-05	3.173E-05	3.150E-05	3.143E-05	1.863E-02
11	4.496E-05	3.945E-05	3.539E-05	3.350E-05	3.260E-05	3.216E-05	3.172E-05	3.150E-05	3.143E-05	1.850E-02
10	4.460E-05	3.896E-05	3.516E-05	3.339E-05	3.253E-05	3.212E-05	3.170E-05	3.150E-05	3.143E-05	1.828E-02
9	4.400E-05	3.826E-05	3.484E-05	3.322E-05	3.244E-05	3.206E-05	3.168E-05	3.149E-05	3.143E-05	1.790E-02
8	4.305E-05	3.740E-05	3.443E-05	3.301E-05	3.232E-05	3.199E-05	3.165E-05	3.148E-05	3.143E-05	1.725E-02
7	4.169E-05	3.648E-05	3.397E-05	3.277E-05	3.219E-05	3.190E-05	3.162E-05	3.148E-05	3.143E-05	1.615E-02
6	3.980E-05	3.546E-05	3.346E-05	3.251E-05	3.204E-05	3.181E-05	3.158E-05	3.147E-05	3.143E-05	1.429E-02
5	3.76[illegible]E-05	3.440E-05	3.293E-05	3.223E-05	3.188E-05	3.171E-05	3.154E-05	3.145E-05	3.143E-05	1.111E-02
4	3.562E-05	3.339E-05	3.242E-05	3.196E-05	3.173E-05	3.161E-05	3.150E-05	3.144E-05	3.143E-05	7.937E-03
3	3.436E-05	3.280E-05	3.212E-05	3.180E-05	3.164E-05	3.156E-05	3.148E-05	3.144E-05	3.143E-05	4.762E-03
2	3.730E-05	3.320E-05	3.086E-05	2.983E-05	2.954E-05	2.964E-05	3.039E-05	3.101E-05	3.143E-05	1.587E-03
1	5.049E-05	5.049E-05	5.049E-05	5.049E-05	5.049E-05	5.049E-05	5.049E-05	5.049E-05	5.049E-05	-1.587E-03
X=	0.0091503	0.0093909	0.0094912	0.0095413	0.0095664	0.0095789	0.0095915	0.0095977	0.0096022	

- CON CON CON CONCCON CON CON CON CON -

J \ I=	1	2	3	4	5	6	7	8	9	10	11	Y =
50	3.746E-02	3.746E-02	3.746E-02	3.745E-02	3.745E-02	3.744E-02	3.741E-02	3.737E-02	3.725E-02	3.710E-02	3.656E-02	0.0420
49	3.746E-02	3.746E-02	3.746E-02	3.745E-02	3.745E-02	3.744E-02	3.741E-02	3.737E-02	3.725E-02	3.710E-02	3.656E-02	0.0388
48	3.746E-02	3.746E-02	3.746E-02	3.745E-02	3.745E-02	3.744E-02	3.741E-02	3.737E-02	3.726E-02	3.711E-02	3.666E-02	0.0357
47	3.746E-02	3.746E-02	3.746E-02	3.745E-02	3.744E-02	3.743E-02	3.741E-02	3.738E-02	3.726E-02	3.713E-02	3.681E-02	0.0325
46	3.746E-02	3.746E-02	3.745E-02	3.745E-02	3.743E-02	3.741E-02	3.740E-02	3.738E-02	3.726E-02	3.714E-02	3.693E-02	0.0293
45	3.746E-02	3.746E-02	3.745E-02	3.744E-02	3.743E-02	3.740E-02	3.739E-02	3.738E-02	3.725E-02	3.713E-02	3.701E-02	0.0261
44	3.746E-02	3.746E-02	3.745E-02	3.745E-02	3.743E-02	3.740E-02	3.739E-02	3.738E-02	3.723E-02	3.711E-02	3.700E-02	0.0252
43	3.746E-02	3.746E-02	3.745E-02	3.745E-02	3.743E-02	3.741E-02	3.739E-02	3.738E-02	3.721E-02	3.707E-02	3.697E-02	0.0243
42	3.746E-02	3.746E-02	3.746E-02	3.745E-02	3.743E-02	3.741E-02	3.739E-02	3.738E-02	3.718E-02	3.703E-02	3.693E-02	0.0239
41	3.746E-02	3.746E-02	3.746E-02	3.745E-02	3.744E-02	3.741E-02	3.740E-02	3.738E-02	3.715E-02	3.700E-02	3.690E-02	0.0235
40	3.746E-02	3.746E-02	3.746E-02	3.745E-02	3.744E-02	3.741E-02	3.742E-02	3.738E-02	3.712E-02	3.695E-02	3.686E-02	0.0232
39	3.746E-02	3.746E-02	3.746E-02	3.745E-02	3.744E-02	3.741E-02	3.744E-02	3.737E-02	3.708E-02	3.691E-02	3.682E-02	0.0230
38	3.746E-02	3.746E-02	3.746E-02	3.745E-02	3.744E-02	3.742E-02	3.744E-02	3.737E-02	3.705E-02	3.687E-02	3.679E-02	0.0228
37	3.746E-02	3.746E-02	3.746E-02	3.745E-02	3.744E-02	3.742E-02	3.744E-02	3.736E-02	3.701E-02	3.683E-02	3.676E-02	0.0226
36	3.746E-02	3.746E-02	3.746E-02	3.745E-02	3.744E-02	3.742E-02	3.744E-02	3.736E-02	3.697E-02	3.678E-02	3.672E-02	0.0224
35	3.746E-02	3.746E-02	3.745E-02	3.745E-02	3.744E-02	3.742E-02	3.745E-02	3.735E-02	3.692E-02	3.672E-02	3.667E-02	0.0222
34	3.746E-02	3.746E-02	3.746E-02	3.745E-02	3.744E-02	3.745E-02	3.745E-02	3.734E-02	3.687E-02	3.667E-02	3.663E-02	0.0220
33	3.746E-02	3.746E-02	3.746E-02	3.745E-02	3.745E-02	3.745E-02	3.745E-02	3.733E-02	3.683E-02	3.662E-02	3.660E-02	0.0220
32	3.746E-02	3.746E-02	3.746E-02	3.746E-02	3.746E-02	3.746E-02	3.745E-02	3.732E-02	3.679E-02	3.658E-02	3.657E-02	0.0218
31	3.746E-02	3.746E-02	3.746E-02	3.746E-02	3.746E-02	3.746E-02	3.745E-02	3.730E-02	3.671E-02	3.649E-02	3.650E-02	0.0216
30	3.746E-02	3.746E-02	3.746E-02	3.746E-02	3.746E-02	3.746E-02	3.745E-02	3.727E-02	3.659E-02	3.636E-02	3.641E-02	0.0213
29	3.746E-02	3.746E-02	3.746E-02	3.746E-02	3.746E-02	3.746E-02	3.745E-02	3.723E-02	3.646E-02	3.621E-02	3.632E-02	0.0211
28	3.746E-02	3.746E-02	3.746E-02	3.746E-02	3.746E-02	3.746E-02	3.745E-02	3.718E-02	3.630E-02	3.603E-02	3.624E-02	0.0209
27	3.746E-02	3.746E-02	3.746E-02	3.746E-02	3.746E-02	3.746E-02	3.745E-02	3.712E-02	3.615E-02	3.586E-02	3.618E-02	0.0207
26	3.746E-02	3.746E-02	3.746E-02	3.746E-02	3.746E-02	3.746E-02	3.744E-02	3.706E-02	3.602E-02	3.572E-02	3.614E-02	0.0206
25	3.746E-02	3.746E-02	3.746E-02	3.746E-02	3.746E-02	3.746E-02	3.744E-02	3.701E-02	3.593E-02	3.565E-02	3.611E-02	0.0205
24	3.746E-02	3.746E-02	3.746E-02	3.746E-02	3.746E-02	3.746E-02	3.744E-02	3.697E-02	3.587E-02	3.560E-02	3.609E-02	0.0204
23	3.746E-02	3.746E-02	3.746E-02	3.746E-02	3.746E-02	3.746E-02	3.743E-02	3.693E-02	3.581E-02	3.555E-02	3.608E-02	0.0203
22	3.746E-02	3.746E-02	3.746E-02	3.746E-02	3.746E-02	3.746E-02	3.743E-02	3.688E-02	3.575E-02	3.552E-02	3.606E-02	0.0203
21	3.746E-02	3.746E-02	3.746E-02	3.746E-02	3.746E-02	3.746E-02	3.742E-02	3.682E-02	3.569E-02	3.549E-02	3.604E-02	0.0202
20	3.746E-02	3.746E-02	3.746E-02	3.746E-02	3.746E-02	3.746E-02	3.741E-02	3.673E-02	3.561E-02	3.544E-02	3.602E-02	0.0200
19	3.746E-02	3.746E-02	3.746E-02	3.746E-02	3.746E-02	3.745E-02	3.738E-02	3.659E-02	3.551E-02	3.542E-02	3.601E-02	0.0199
18	3.746E-02	3.746E-02	3.746E-02	3.746E-02	3.746E-02	3.745E-02	3.733E-02	3.638E-02	3.540E-02	3.540E-02	3.600E-02	0.0196
17	3.746E-02	3.746E-02	3.746E-02	3.746E-02	3.745E-02	3.744E-02	3.721E-02	3.610E-02	3.531E-02	3.540E-02	3.599E-02	0.0194
16	3.746E-02	3.746E-02	3.746E-02	3.746E-02	3.745E-02	3.742E-02	3.695E-02	3.586E-02	3.525E-02	3.539E-02	3.599E-02	0.0192
15	3.746E-02	3.746E-02	3.745E-02	3.744E-02	3.740E-02	3.731E-02	3.653E-02	3.574E-02	3.522E-02	3.538E-02	3.598E-02	0.0189
14	3.746E-02	3.745E-02	3.743E-02	3.737E-02	3.725E-02	3.715E-02	3.644E-02	3.570E-02	3.520E-02	3.536E-02	3.597E-02	0.0188
13	3.746E-02	3.745E-02	3.742E-02	3.734E-02	3.721E-02	3.711E-02	3.644E-02	3.569E-02	3.519E-02	3.535E-02	3.596E-02	0.0187
12	3.746E-02	3.745E-02	3.741E-02	3.733E-02	3.719E-02	3.709E-02	3.644E-02	3.568E-02	3.518E-02	3.536E-02	3.595E-02	0.0186
11	3.746E-02	3.745E-02	3.741E-02	3.732E-02	3.716E-02	3.708E-02	3.644E-02	3.566E-02	3.517E-02	3.537E-02	3.593E-02	0.0185
10	3.746E-02	3.745E-02	3.741E-02	3.734E-02	3.720E-02	3.708E-02	3.643E-02	3.564E-02	3.516E-02	3.538E-02	3.591E-02	0.0183
9	3.746E-02	3.746E-02	3.743E-02	3.737E-02	3.725E-02	3.708E-02	3.641E-02	3.560E-02	3.512E-02	3.536E-02	3.586E-02	0.0179
8	3.746E-02	3.746E-02	3.744E-02	3.740E-02	3.731E-02	3.706E-02	3.636E-02	3.553E-02	3.507E-02	3.530E-02	3.578E-02	0.0173
7	3.746E-02	3.746E-02	3.744E-02	3.739E-02	3.730E-02	3.701E-02	3.629E-02	3.544E-02	3.498E-02	3.522E-02	3.560E-02	0.0162
6	3.746E-02	3.746E-02	3.743E-02	3.736E-02	3.724E-02	3.693E-02	3.617E-02	3.531E-02	3.484E-02	3.512E-02	3.523E-02	0.0143
5	3.746E-02	3.745E-02	3.741E-02	3.733E-02	3.717E-02	3.681E-02	3.603E-02	3.518E-02	3.467E-02	3.495E-02	3.463E-02	0.0111
4	3.746E-02	3.745E-02	3.741E-02	3.731E-02	3.712E-02	3.673E-02	3.594E-02	3.517E-02	3.446E-02	3.445E-02	3.374E-02	0.0079
3	3.746E-02	3.745E-02	3.741E-02	3.733E-02	3.717E-02	3.684E-02	3.624E-02	3.555E-02	3.449E-02	3.360E-02	3.274E-02	0.0048
2	3.746E-02	3.746E-02	3.745E-02	3.743E-02	3.738E-02	3.727E-02	3.699E-02	3.667E-02	3.612E-02	3.515E-02	3.407E-02	0.0016
1	3.746E-02	3.746E-02	3.746E-02	3.746E-02	3.746E-02	3.746E-02	3.746E-02	3.746E-02	3.746E-02	3.746E-02	3.746E-02	-0.0016
X=	-0.0000125	0.0000125	0.0000627	0.0001630	0.0003636	0.0007648	0.0015672	0.0031721	0.0063818	0.0079866	0.0087890	

J \ I=	12	13	14	15	16	17	18	19	20	21	22	Y =
50	3.450E-02	3.208E-02	3.070E-02	3.000E-02	2.964E-02	2.946E-02	2.928E-02	2.919E-02	2.916E-02	4.202E-02		
49	3.450E-02	3.208E-02	3.070E-02	3.000E-02	2.964E-02	2.946E-02	2.928E-02	2.919E-02	2.916E-02	3.884E-02		
48	3.481E-02	3.226E-02	3.079E-02	3.004E-02	2.967E-02	2.948E-02	2.929E-02	2.920E-02	2.916E-02	3.567E-02		
47	3.532E-02	3.270E-02	3.104E-02	3.018E-02	2.974E-02	2.953E-02	2.931E-02	2.920E-02	2.916E-02	3.249E-02		
46	[illegible]	3.341E-02	3.145E-02	3.040E-02	2.987E-02	2.961E-02	2.934E-02	2.921E-02	2.916E-02	2.932E-02		

45	3.653E-02	3.440E-02	3.209E-02	3.076E-02	3.008E-02	2.974E-02	2.939E-02	2.922E-02	2.916E-02	2.614E-02
44	3.687E-02	3.538E-02	3.291E-02	3.125E-02	3.037E-02	2.992E-02	2.947E-02	2.924E-02	2.916E-02	2.521E-02
43	3.688E-02	3.571E-02	3.324E-02	3.145E-02	3.048E-02	2.999E-02	2.950E-02	2.925E-02	2.916E-02	2.420E-02
42	3.686E-02	3.599E-02	3.359E-02	3.169E-02	3.063E-02	3.008E-02	2.954E-02	2.926E-02	2.916E-02	2.391E-02
41	3.683E-02	3.608E-02	3.371E-02	3.177E-02	3.068E-02	3.011E-02	2.955E-02	2.926E-02	2.916E-02	2.354E-02
40	3.680E-02	3.614E-02	3.379E-02	3.182E-02	3.070E-02	3.013E-02	2.956E-02	2.927E-02	2.916E-02	2.318E-02
39	3.677E-02	3.622E-02	3.394E-02	3.194E-02	3.078E-02	3.018E-02	2.957E-02	2.927E-02	2.916E-02	2.298E-02
38	3.675E-02	3.625E-02	3.401E-02	3.199E-02	3.081E-02	3.020E-02	2.958E-02	2.927E-02	2.916E-02	2.278E-02
37	3.673E-02	3.628E-02	3.410E-02	3.205E-02	3.085E-02	3.022E-02	2.959E-02	2.928E-02	2.916E-02	2.259E-02
36	3.670E-02	3.624E-02	3.403E-02	3.201E-02	3.082E-02	3.021E-02	2.959E-02	2.927E-02	2.916E-02	2.239E-02
35	3.666E-02	3.612E-02	3.388E-02	3.190E-02	3.076E-02	3.017E-02	2.957E-02	2.927E-02	2.916E-02	2.219E-02
34	3.663E-02	3.608E-02	3.384E-02	3.188E-02	3.074E-02	3.016E-02	2.957E-02	2.927E-02	2.916E-02	2.204E-02
33	3.662E-02	3.606E-02	3.380E-02	3.184E-02	3.072E-02	3.014E-02	2.956E-02	2.927E-02	2.916E-02	2.196E-02
32	3.659E-02	3.604E-02	3.378E-02	3.183E-02	3.071E-02	3.014E-02	2.956E-02	2.927E-02	2.916E-02	2.181E-02
31	3.655E-02	3.597E-02	3.371E-02	3.179E-02	3.069E-02	3.012E-02	2.955E-02	2.927E-02	2.916E-02	2.157E-02
30	3.650E-02	3.587E-02	3.359E-02	3.171E-02	3.064E-02	3.009E-02	2.954E-02	2.926E-02	2.916E-02	2.134E-02
29	3.646E-02	3.574E-02	3.343E-02	3.159E-02	3.057E-02	3.005E-02	2.952E-02	2.926E-02	2.916E-02	2.111E-02
28	3.642E-02	3.561E-02	3.328E-02	3.149E-02	3.051E-02	3.001E-02	2.951E-02	2.925E-02	2.916E-02	2.088E-02
27	3.640E-02	3.549E-02	3.314E-02	3.139E-02	3.045E-02	2.997E-02	2.949E-02	2.925E-02	2.916E-02	2.072E-02
26	3.638E-02	3.539E-02	3.303E-02	3.132E-02	3.041E-02	2.995E-02	2.948E-02	2.925E-02	2.916E-02	2.057E-02
25	3.636E-02	3.533E-02	3.295E-02	3.127E-02	3.038E-02	2.992E-02	2.947E-02	2.924E-02	2.916E-02	2.049E-02
24	3.635E-02	3.525E-02	3.286E-02	3.121E-02	3.034E-02	2.990E-02	2.946E-02	2.924E-02	2.916E-02	2.041E-02
23	3.633E-02	3.517E-02	3.277E-02	3.115E-02	3.031E-02	2.988E-02	2.945E-02	2.924E-02	2.916E-02	2.034E-02
22	3.632E-02	3.509E-02	3.267E-02	3.109E-02	3.027E-02	2.986E-02	2.944E-02	2.924E-02	2.916E-02	2.026E-02
21	3.628E-02	3.496E-02	3.253E-02	3.101E-02	3.022E-02	2.983E-02	2.943E-02	2.923E-02	2.916E-02	2.018E-02
20	3.623E-02	3.478E-02	3.236E-02	3.091E-02	3.016E-02	2.979E-02	2.942E-02	2.923E-02	2.916E-02	2.003E-02
19	3.616E-02	3.456E-02	3.216E-02	3.080E-02	3.010E-02	2.975E-02	2.940E-02	2.923E-02	2.916E-02	1.987E-02
18	3.607E-02	3.430E-02	3.196E-02	3.068E-02	3.003E-02	2.971E-02	2.938E-02	2.922E-02	2.916E-02	1.964E-02
17	3.597E-02	3.406E-02	3.178E-02	3.058E-02	2.998E-02	2.968E-02	2.937E-02	2.922E-02	2.916E-02	1.941E-02
16	3.586E-02	3.383E-02	3.164E-02	3.051E-02	2.993E-02	2.965E-02	2.936E-02	2.921E-02	2.916E-02	1.917E-02
15	3.578E-02	3.366E-02	3.153E-02	3.045E-02	2.990E-02	2.962E-02	2.935E-02	2.921E-02	2.916E-02	1.894E-02
14	3.573E-02	3.357E-02	3.148E-02	3.042E-02	2.988E-02	2.961E-02	2.934E-02	2.921E-02	2.916E-02	1.879E-02
13	3.569E-02	3.352E-02	3.146E-02	3.041E-02	2.988E-02	2.961E-02	2.934E-02	2.921E-02	2.916E-02	1.871E-02
12	3.565E-02	3.344E-02	3.142E-02	3.039E-02	2.987E-02	2.960E-02	2.934E-02	2.921E-02	2.916E-02	1.863E-02
11	3.558E-02	3.331E-02	3.135E-02	3.035E-02	2.984E-02	2.959E-02	2.933E-02	2.921E-02	2.916E-02	1.850E-02
10	3.544E-02	3.308E-02	3.123E-02	3.028E-02	2.981E-02	2.957E-02	2.933E-02	2.921E-02	2.916E-02	1.828E-02
9	3.521E-02	3.276E-02	3.106E-02	3.019E-02	2.975E-02	2.953E-02	2.931E-02	2.920E-02	2.916E-02	1.790E-02
8	3.484E-02	3.235E-02	3.085E-02	3.007E-02	2.968E-02	2.949E-02	2.929E-02	2.920E-02	2.916E-02	1.725E-02
7	3.428E-02	3.190E-02	3.060E-02	2.994E-02	2.961E-02	2.944E-02	2.927E-02	2.919E-02	2.916E-02	1.615E-02
6	3.345E-02	3.138E-02	3.032E-02	2.979E-02	2.952E-02	2.939E-02	2.925E-02	2.919E-02	2.916E-02	1.429E-02
5	3.247E-02	3.083E-02	3.003E-02	2.963E-02	2.943E-02	2.933E-02	2.923E-02	2.918E-02	2.916E-02	1.111E-02
4	3.145E-02	3.028E-02	2.974E-02	2.947E-02	2.934E-02	2.927E-02	2.921E-02	2.917E-02	2.916E-02	7.937E-03
3	3.086E-02	3.000E-02	2.959E-02	2.940E-02	2.930E-02	2.925E-02	2.920E-02	2.917E-02	2.916E-02	4.762E-03
2	3.243E-02	3.041E-02	2.910E-02	2.847E-02	2.826E-02	2.828E-02	2.865E-02	2.896E-02	2.916E-02	1.587E-03
1	3.746E-02	3.746E-02	3.746E-02	3.746E-02	3.746E-02	3.746E-02	3.746E-02	3.746E-02	3.746E-02	-1.587E-03
X=	0.0091903	0.0093909	0.0094912	0.0095413	0.0095664	0.0095789	0.0095915	0.0095977	0.0096022	

TRANSFER COEFFICIENTS

J	R/D	WDIFF	WFLUX	HM1	SH1	HM	SH	HFLUX	H	NU	ST
2	-5.32970	0.36410	1.000E-04	2.067E-03	5.300E+00	4.749E-02	4.076E+00	-2.388E+04	-2.388E+02	-2.040E+01	-2.942E-02
3	-4.33753	0.36410	1.000E-04	6.971E-04	1.788E+00	1.602E-02	1.375E+00	1.287E+03	1.287E+01	1.099E+00	1.585E-03
4	-3.34556	0.36411	1.000E-04	6.535E-04	1.676E+00	1.501E-02	1.289E+00	1.741E+03	1.741E+01	1.487E+00	2.144E-03
5	-2.35350	0.36411	1.000E-04	9.981E-04	2.560E+00	2.293E-02	1.968E+00	2.606E+03	2.606E+01	2.227E+00	3.211E-03
6	-1.36143	0.36412	1.000E-04	1.354E-03	3.473E+00	3.111E-02	2.670E+00	3.504E+03	3.504E+01	2.993E+00	4.317E-03
7	-0.77786	0.36412	1.000E-04	1.695E-03	4.346E+00	3.893E-02	3.342E+00	4.357E+03	4.357E+01	3.722E+00	5.368E-03
8	-0.43458	0.36412	1.000E-04	1.997E-03	5.122E+00	4.588E-02	3.938E+00	5.112E+03	5.112E+01	4.367E+00	6.298E-03
9	-0.23266	0.36412	1.000E-04	2.270E-03	5.822E+00	5.216E-02	4.477E+00	5.772E+03	5.772E+01	4.931E+00	7.111E-03
10	-0.11388	0.36412	1.000E-04	2.487E-03	6.377E+00	5.713E-02	4.904E+00	6.282E+03	6.282E+01	5.367E+00	7.740E-03
11	-0.04401	0.36412	1.000E-04	2.648E-03	6.790E+00	6.083E-02	5.221E+00	6.648E+03	6.648E+01	5.679E+00	8.190E-03
12	-0.00291	0.36412	1.000E-04	2.750E-03	7.052E+00	6.318E-02	5.423E+00	6.872E+03	6.872E+01	5.871E+00	8.466E-03
13	0.02127	0.36412	1.000E-04	2.797E-03	7.174E+00	6.427E-02	5.517E+00	6.965E+03	6.965E+01	5.951E+00	8.581E-03
14	0.04545	0.36412	1.000E-04	2.825E-03	7.246E+00	6.492E-02	5.572E+00	7.018E+03	7.018E+01	5.996E+00	8.646E-03
15	0.09380	0.36412	1.000E-04	2.895E-03	7.425E+00	6.652E-02	5.710E+00	7.188E+03	7.188E+01	6.141E+00	8.856E-03
16	0.16633	0.36412	1.000E-04	3.029E-03	7.768E+00	6.959E-02	5.973E+00	7.527E+03	7.527E+01	6.430E+00	9.273E-03
17	0.23886	0.36411	1.000E-04	3.203E-03	8.215E+00	7.360E-02	6.318E+00	7.974E+03	7.974E+01	6.812E+00	9.824E-03
18	0.31139	0.36411	1.000E-04	3.412E-03	8.749E+00	7.838E-02	6.728E+00	8.507E+03	8.507E+01	7.268E+00	1.048E-02
19	0.38392	0.36411	1.000E-04	3.664E-03	9.397E+00	8.418E-02	7.226E+00	9.158E+03	9.158E+01	7.824E+00	1.128E-02
20	0.43227	0.36411	1.000E-04	3.908E-03	1.002E+01	8.979E-02	7.707E+00	9.784E+03	9.784E+01	8.359E+00	1.205E-02
21	0.48063	0.36410	1.000E-04	4.136E-03	1.061E+01	9.503E-02	8.157E+00	1.037E+04	1.037E+02	8.859E+00	1.278E-02
22	0.50480	0.36410	1.000E-04	4.324E-03	1.109E+01	9.935E-02	8.528E+00	1.085E+04	1.085E+02	9.269E+00	1.337E-02
23	0.52898	0.36409	1.000E-04	4.456E-03	1.143E+01	1.024E-01	8.789E+00	1.119E+04	1.119E+02	9.557E+00	1.378E-02
24	0.55315	0.36409	1.000E-04	4.591E-03	1.177E+01	1.055E-01	9.055E+00	1.153E+04	1.153E+02	9.850E+00	1.420E-02
25	0.57733	0.36409	1.000E-04	4.726E-03	1.212E+01	1.086E-01	9.320E+00	1.187E+04	1.187E+02	1.014E+01	1.462E-02
26	0.60151	0.36408	1.000E-04	4.853E-03	1.245E+01	1.115E-01	9.571E+00	1.220E+04	1.220E+02	1.042E+01	1.502E-02
27	0.64986	0.36407	1.000E-04	5.019E-03	1.287E+01	1.153E-01	9.899E+00	1.262E+04	1.262E+02	1.078E+01	1.555E-02
28	0.69821	0.36406	1.000E-04	5.259E-03	1.349E+01	1.208E-01	1.037E+01	1.323E+04	1.323E+02	1.130E+01	1.630E-02
29	0.77074	0.36404	1.000E-04	5.494E-03	1.409E+01	1.262E-01	1.084E+01	1.381E+04	1.381E+02	1.180E+01	1.702E-02
30	0.84327	0.36403	1.000E-04	5.764E-03	1.478E+01	1.324E-01	1.137E+01	1.449E+04	1.449E+02	1.238E+01	1.785E-02
31	0.91580	0.36401	1.000E-04	5.967E-03	1.530E+01	1.371E-01	1.177E+01	1.498E+04	1.498E+02	1.280E+01	1.846E-02
32	0.98833	0.36399	1.000E-04	6.072E-03	1.557E+01	1.395E-01	1.198E+01	1.522E+04	1.522E+02	1.301E+01	1.876E-02
33	1.03669	0.36398	1.000E-04	6.090E-03	1.562E+01	1.399E-01	1.201E+01	1.526E+04	1.526E+02	1.304E+01	1.880E-02
34	1.06086	0.36398	1.000E-04	6.180E-03	1.585E+01	1.420E-01	1.219E+01	1.551E+04	1.551E+02	1.325E+01	1.911E-02
35	1.10921	0.36397	1.000E-04	6.240E-03	1.600E+01	1.434E-01	1.231E+01	1.566E+04	1.566E+02	1.338E+01	1.929E-02
36	1.17088	0.36397	1.000E-04	6.483E-03	1.663E+01	1.490E-01	1.279E+01	1.629E+04	1.629E+02	1.391E+01	2.006E-02
37	1.23255	0.36396	1.000E-04	6.586E-03	1.689E+01	1.513E-01	1.299E+01	1.653E+04	1.653E+02	1.413E+01	2.037E-02
38	1.29422	0.36396	1.000E-04	6.457E-03	1.656E+01	1.484E-01	1.273E+01	1.616E+04	1.616E+02	1.381E+01	1.991E-02
39	1.35589	0.36397	1.000E-04	6.324E-03	1.622E+01	1.453E-01	1.247E+01	1.582E+04	1.582E+02	1.352E+01	1.949E-02
40	1.41755	0.36397	1.000E-04	6.047E-03	1.551E+01	1.389E-01	1.193E+01	1.509E+04	1.509E+02	1.289E+01	1.859E-02
41	1.53198	0.36398	1.000E-04	5.929E-03	1.520E+01	1.362E-01	1.169E+01	1.482E+04	1.482E+02	1.266E+01	1.825E-02
42	1.64640	0.36400	1.000E-04	5.738E-03	1.472E+01	1.318E-01	1.132E+01	1.433E+04	1.433E+02	1.224E+01	1.766E-02
43	1.76083	0.36403	1.000E-04	5.187E-03	1.330E+01	1.192E-01	1.023E+01	1.289E+04	1.289E+02	1.101E+01	1.588E-02
44	2.05261	0.36408	1.000E-04	4.732E-03	1.214E+01	1.087E-01	9.333E+00	1.174E+04	1.174E+02	1.003E+01	1.447E-02
45	2.34440	0.36414	1.000E-04	3.634E-03	9.319E+00	8.348E-02	7.166E+00	8.893E+03	8.893E+01	7.598E+00	1.096E-02
46	3.33646	0.36421	1.000E-04	2.824E-03	7.241E+00	6.487E-02	5.568E+00	6.886E+03	6.886E+01	5.883E+00	8.483E-03
47	4.32853	0.36424	1.000E-04	2.308E-03	5.919E+00	5.302E-02	4.551E+00	5.632E+03	5.632E+01	4.812E+00	6.939E-03
48	5.32060	0.36424	1.000E-04	2.005E-03	5.142E+00	4.606E-02	3.953E+00	4.901E+03	4.901E+01	4.187E+00	6.038E-03
49	6.31267	0.36425	1.000E-04	1.880E-03	4.838E+00	4.334E-02	3.720E+00	4.636E+03	4.636E+01	3.961E+00	5.712E-03

J	YV/D	TAU	CF	CF*RED/2
3	9.9207E-01	5.8858E-02	1.6336E-03	2.5830E-02
4	1.9841E+00	3.4215E-02	9.4964E-04	1.5015E-02
5	2.9762E+00	-3.6727E-02	-1.0194E-03	-1.6118E-02
6	3.9683E+00	-1.3449E-01	-3.7327E-03	-5.9019E-02
7	4.7561E+00	-2.1677E-01	-6.0166E-03	-9.5131E-02
8	5.2195E+00	-2.7536E-01	-7.6428E-03	-1.2084E-01
9	5.4921E+00	-3.2641E-01	-9.0596E-03	-1.4324E-01
10	5.6525E+00	-3.7264E-01	-1.0343E-02	-1.6353E-01
11	5.7468E+00	-4.0994E-01	-1.1378E-02	-1.7990E-01
12	5.8023E+00	-4.3040E-01	-1.1946E-02	-1.8888E-01
13	5.8349E+00	-4.3443E-01	-1.2058E-02	-1.9065E-01
14	5.8591E+00	-4.3923E-01	-1.2191E-02	-1.9276E-01
15	5.8954E+00	-4.7077E-01	-1.3066E-02	-2.0660E-01
16	5.9558E+00	-5.2475E-01	-1.4565E-02	-2.3029E-01
17	6.0283E+00	-5.8448E-01	-1.6222E-02	-2.5650E-01
18	6.1009E+00	-6.5835E-01	-1.8273E-02	-2.8892E-01
19	6.1734E+00	-7.5519E-01	-2.0960E-02	-3.3141E-01
20	6.2338E+00	-8.3792E-01	-2.3257E-02	-3.6772E-01
21	6.2822E+00	-9.2600E-01	-2.5701E-02	-4.0638E-01
22	6.3184E+00	-9.8410E-01	-2.7314E-02	-4.3187E-01
23	6.3426E+00	-1.0258E+00	-2.8472E-02	-4.5018E-01
24	6.3668E+00	-1.0653E+00	-2.9569E-02	-4.6752E-01
25	6.3910E+00	-1.1015E+00	-3.0572E-02	-4.8339E-01
26	6.4152E+00	-1.1299E+00	-3.1360E-02	-4.9584E-01
27	6.4514E+00	-1.1560E+00	-3.2085E-02	-5.0731E-01
28	6.4998E+00	-1.1961E+00	-3.3198E-02	-5.2490E-01
29	6.5602E+00	-1.1767E+00	-3.2661E-02	-5.1642E-01
30	6.6327E+00	-1.1292E+00	-3.1340E-02	-4.9553E-01
31	6.7053E+00	-1.0162E+00	-2.8206E-02	-4.4597E-01
32	6.7778E+00	-8.3557E-01	-2.3192E-02	-3.6669E-01
33	6.8382E+00	-6.7204E-01	-1.8653E-02	-2.9492E-01
34	6.8745E+00	-6.0754E-01	-1.6862E-02	-2.6662E-01
35	6.9108E+00	-4.8305E-01	-1.3407E-02	-2.1198E-01
36	6.9658E+00	-3.2451E-01	-9.0070E-03	-1.4241E-01
37	7.0275E+00	-1.2354E-01	-3.4289E-03	-5.4216E-02
38	7.0891E+00	9.4790E-02	2.6309E-03	4.1598E-02
39	7.1508E+00	3.0416E-01	8.4419E-03	1.3348E-01
40	7.2125E+00	4.8955E-01	1.3588E-02	2.1484E-01
41	7.3005E+00	6.5632E-01	1.8216E-02	2.8803E-01
42	7.4149E+00	9.2916E-01	2.5789E-02	4.0776E-01
43	7.5293E+00	1.1315E+00	3.1405E-02	4.9656E-01
44	7.7325E+00	1.1858E+00	3.2911E-02	5.2037E-01
45	8.0242E+00	1.3328E+00	3.6991E-02	5.8488E-01
46	8.6602E+00	9.5875E-01	2.6611E-02	4.2075E-01
47	9.6582E+00	7.0104E-01	1.9458E-02	3.0765E-01
48	1.0650E+01	5.3044E-01	1.4723E-02	2.3278E-01
49	1.1642E+01	4.4959E-01	1.2479E-02	1.9730E-01

AVERAGE TRANSPORT PROPERTIES

J	PR	SC	VIS	DEN	CP	DIFF	K.
2	7.2024E-01	6.2838E-01	2.0115E-05	7.9535E-01	1.2018E+03	4.0954E-05	3.3309E-02
3	7.2024E-01	6.2838E-01	2.0115E-05	7.9535E-01	1.2018E+03	4.0954E-05	3.3309E-02
4	7.2024E-01	6.2838E-01	2.0115E-05	7.9535E-01	1.2018E+03	4.0954E-05	3.3309E-02
5	7.2024E-01	6.2838E-01	2.0115E-05	7.9535E-01	1.2018E+03	4.0954E-05	3.3309E-02
6	7.2024E-01	6.2838E-01	2.0115E-05	7.9535E-01	1.2018E+03	4.0954E-05	3.3309E-02
7	7.2024E-01	6.2838E-01	2.0115E-05	7.9535E-01	1.2018E+03	4.0954E-05	3.3309E-02
8	7.2024E-01	6.2838E-01	2.0115E-05	7.9535E-01	1.2018E+03	4.0954E-05	3.3309E-02
9	7.2024E-01	6.2838E-01	2.0115E-05	7.9535E-01	1.2018E+03	4.0954E-05	3.3309E-02
10	7.2024E-01	6.2838E-01	2.0115E-05	7.9535E-01	1.2018E+03	4.0954E-05	3.3309E-02
11	7.2024E-01	6.2838E-01	2.0115E-05	7.9535E-01	1.2018E+03	4.0954E-05	3.3309E-02
12	7.2024E-01	6.2838E-01	2.0115E-05	7.9535E-01	1.2018E+03	4.0954E-05	3.3309E-02
13	7.2024E-01	6.2838E-01	2.0115E-05	7.9535E-01	1.2018E+03	4.0954E-05	3.3309E-02
14	7.2024E-01	6.2838E-01	2.0115E-05	7.9535E-01	1.2018E+03	4.0954E-05	3.3309E-02
15	7.2024E-01	6.2838E-01	2.0115E-05	7.9535E-01	1.2018E+03	4.0954E-05	3.3309E-02
16	7.2024E-01	6.2838E-01	2.0115E-05	7.9535E-01	1.2018E+03	4.0954E-05	3.3309E-02
17	7.2024E-01	6.2838E-01	2.0115E-05	7.9535E-01	1.2018E+03	4.0954E-05	3.3309E-02
18	7.2024E-01	6.2838E-01	2.0115E-05	7.9535E-01	1.2018E+03	4.0954E-05	3.3309E-02
19	7.2024E-01	6.2838E-01	2.0115E-05	7.9535E-01	1.2018E+03	4.0954E-05	3.3309E-02
20	7.2024E-01	6.2838E-01	2.0115E-05	7.9535E-01	1.2018E+03	4.0954E-05	3.3309E-02
21	7.2024E-01	6.2838E-01	2.0115E-05	7.9535E-01	1.2018E+03	4.0954E-05	3.3309E-02
22	7.2024E-01	6.2838E-01	2.0115E-05	7.9535E-01	1.2018E+03	4.0954E-05	3.3309E-02
23	7.2024E-01	6.2838E-01	2.0115E-05	7.9535E-01	1.2018E+03	4.0954E-05	3.3309E-02
24	7.2024E-01	6.2838E-01	2.0115E-05	7.9536E-01	1.2018E+03	4.0954E-05	3.3309E-02
25	7.2024E-01	6.2838E-01	2.0115E-05	7.9536E-01	1.2018E+03	4.0954E-05	3.3309E-02
26	7.2024E-01	6.2838E-01	2.0115E-05	7.9536E-01	1.2018E+03	4.0954E-05	3.3309E-02
27	7.2024E-01	6.2838E-01	2.0115E-05	7.9536E-01	1.2018E+03	4.0954E-05	3.3309E-02
28	7.2024E-01	6.2838E-01	2.0115E-05	7.9536E-01	1.2017E+03	4.0954E-05	3.3309E-02
29	7.2024E-01	6.2838E-01	2.0115E-05	7.9536E-01	1.2017E+03	4.0954E-05	3.3309E-02
30	7.2024E-01	6.2838E-01	2.0115E-05	7.9536E-01	1.2017E+03	4.0954E-05	3.3309E-02
31	7.2024E-01	6.2838E-01	2.0115E-05	7.9536E-01	1.2017E+03	4.0954E-05	3.3309E-02
32	7.2023E-01	6.2838E-01	2.0115E-05	7.9537E-01	1.2017E+03	4.0954E-05	3.3309E-02
33	7.2023E-01	6.2838E-01	2.0115E-05	7.9537E-01	1.2017E+03	4.0954E-05	3.3309E-02
34	7.2023E-01	6.2838E-01	2.0115E-05	7.9537E-01	1.2017E+03	4.0954E-05	3.3309E-02
35	7.2023E-01	6.2838E-01	2.0115E-05	7.9537E-01	1.2017E+03	4.0954E-05	3.3309E-02
36	7.2023E-01	6.2838E-01	2.0115E-05	7.9537E-01	1.2017E+03	4.0954E-05	3.3309E-02
37	7.2023E-01	6.2838E-01	2.0115E-05	7.9537E-01	1.2017E+03	4.0954E-05	3.3309E-02
38	7.2023E-01	6.2838E-01	2.0115E-05	7.9537E-01	1.2017E+03	4.0954E-05	3.3309E-02
39	7.2023E-01	6.2838E-01	2.0115E-05	7.9537E-01	1.2017E+03	4.0954E-05	3.3309E-02
40	7.2023E-01	6.2838E-01	2.0115E-05	7.9537E-01	1.2017E+03	4.0954E-05	3.3309E-02
41	7.2023E-01	6.2838E-01	2.0115E-05	7.9537E-01	1.2017E+03	4.0954E-05	3.3309E-02
42	7.2024E-01	6.2838E-01	2.0115E-05	7.9536E-01	1.2017E+03	4.0954E-05	3.3309E-02
43	7.2024E-01	6.2838E-01	2.0115E-05	7.9536E-01	1.2017E+03	4.0954E-05	3.3309E-02
44	7.2024E-01	6.2838E-01	2.0115E-05	7.9536E-01	1.2018E+03	4.0954E-05	3.3309E-02
45	7.2024E-01	6.2838E-01	2.0115E-05	7.9535E-01	1.2018E+03	4.0954E-05	3.3309E-02
46	7.2025E-01	6.2837E-01	2.0115E-05	7.9534E-01	1.2018E+03	4.0954E-05	3.3309E-02
47	7.2025E-01	6.2837E-01	2.0115E-05	7.9534E-01	1.2018E+03	4.0954E-05	3.3309E-02
48	7.2025E-01	6.2837E-01	2.0115E-05	7.9534E-01	1.2018E+03	4.0954E-05	3.3309E-02
49	7.2025E-01	6.2837E-01	2.0115E-05	7.9534E-01	1.2018E+03	4.0954E-05	3.3309E-02

APPENDIX C

Code Listing of Computer Runs

Run code	H/D	M	θ ()
127	4	0.1	0
128	4	0.125	0
130	4	0.167	0
133	4	0.25	0
135	3	0.1	0
136	3	0.125	0
141	3	0.167	0
145	3	0	0
146	4	0	0
147	2	0	0
149	2	0.1	0
152	2	0.125	0
159	3	0.1	5
165	3	0.1	10
167	3	0.1	-5
172	3	0.1	-10
179	3	0.1	30
203	3	1.0	-30
208	4	1.0	0
209	3	2.0	-30
213	3	no jet	
214	4	2.0	0
218	3	10	30
223	3	2	30
226	3	0.7	30
229	3	0.5	30
232	3	0.5	30
234	3	2.0	-45
236	3	0.4	-30
246	3	0.1	-45
250	4	0	0